A treatment for SCI: From regeneration and plasticity to rehabilitative training

By

Zacnicte May

A thesis submitted in partial fulfillment of the requirements for the degree of

Doctor of Philosophy

Neuroscience
University of Alberta

Thesis Abstract

Spinal cord injury (SCI) is an extremely debilitating condition, leading to sensory and motor dysfunction below the injury. Presently, there are few effective treatments for SCI. This is in part due to the immense complexity of SCI pathophysiology. Thus, combined research approaches are required, but translating individual approaches, let alone combined ones poses a great challenge. In my thesis, I study different aspects of SCI that should be considered for combined treatments, including cell grafting to promote regeneration of injured spinal axons (Chapters 1 and 2), plasticity of injured and spared systems (Chapter 3), and rehabilitative training (Chapter 4 and Appendices). Chapters 1 and 2 address cell grafting and an associated challenge, i.e. tumour formation. This is a risk especially when grafting stem cell and stem cell-derived cells and can possibly be eliminated given modifications in cell culture protocols. Chapter 3 shows that descending reticulospinal axons form new connections with propriospinal interneurons, adding to the multiplicity of known recovery mechanisms post-SCI. The multiplicity of known recovery mechanisms provides opportunity for numerous possible targets to promote recovery. Chapter 4 demonstrated that pre-injury task-specific training impacts post-SCI recovery, advising that pre-injury variables deserve careful consideration in experimental design, clinical application, and reusing the same animals in multiple scientific studies. Understanding these different aspects of SCI will inform future combinatory treatments. For example, a combinatory treatment can be envisioned where cells are injected in the cavity commonly formed in the injured spinal cord, creating a bridge for growing axons. Then, to promote neuronal rewiring, soma of descending systems could be infused with growth factors and drawn to appropriate synaptic targets with chemoattractants. Lastly, these plastic mechanisms could be consolidated through rehabilitative training.

Preface

This thesis is an original work by Zacnicte May. The research project, of which this thesis is a part, received research ethics approval from the University of Alberta Research Ethics Board, Project Name "Repairing the Injured Spinal Cord", ID AUP00000254, Legacy study No. HS 354, Expiration date June 17, 2017. Chapters 1 and 2 are the result of research collaborations with Professor Jeff Biernaskie at the University of Calgary, Professor Molly S. Shoichet at the University of Toronto, and Professor Wolfram Tetzlaff at the University of British Colombia. Chapter 4 is the result of a research collaboration with Professor David S. K. Magnuson at the University of Louisville in Louisville, Kentucky, USA.

The chapters and appendices of this thesis have been published as follows:

Chapter 1: May, Z., Kumar, R., Führmann, T., Tam, R., Vulic, K., Forero, J., Lucas Osma, A., Fenrich, K. K., Assinck, P., Lee, M. J., Moulson, A., Shoichet, M. S., Tetzlaff, W., Biernaskie, J., & Fouad, K. (2017). Adult skin-derived precursor Schwann cell grafts form growths in the injured spinal cord of Fischer rats. *Manuscript submitted for publication*.

Chapter 2: May, Z., Torres-Espín, A., Lucas Osma, A., Batty, N., Raposo, P., Fenrich, K., Stykel, M., Führmann, T., Shoichet, M. S., Biernaskie, J., & Fouad, K. (2017). Immune rejection is not the main factor involved in post-transplantational loss of skin-derived precursor Schwann cells into the injured rat spinal cord. *Manuscript in preparation*.

Chapter 3: May, Z., Fenrich, K. K., Dahlby, J., Batty, N. J., Torres-Espín, A., & Fouad,

K. (2017). Following complete disruption of the reticulospinal tract, new collaterals to interneurons parallel locomotor recovery. *Manuscript submitted for publication*.

Chapter 4: May, Z., Fouad, K., Shum-Siu, A., & Magnuson, D. S. K. (2015). Challenges of animal models in SCI research: Effects of pre-injury task-specific training in adult rats before lesion. *Behavioural Brain Research, 291*, 26–35. https://doi.org/10.1016/j.bbr.2015.04.058

Appendix 1: Fenrich, K. K., May, Z., Hurd, C., Boychuk, C. E., Kowalczewski, J., Bennett, D. J., … Fouad, K. (2015). Improved single pellet grasping using automated *ad libitum* full-time training robot. *Behavioural Brain Research*, *281*, 137–148. https://doi.org/10.1016/j.bbr.2014.11.048

Appendix 2: Fenrich, K. K., May, Z., Torres-Espín, A., Forero, J., Bennett, D. J., & Fouad, K. (2016). Single pellet grasping following cervical spinal cord injury in adult rat using an automated full-time training robot. *Behavioural Brain Research*, *299*, 59–71. https://doi.org/10.1016/j.bbr.2015.11.020

I was responsible for the majority of data collection and analysis, as well as the manuscript composition. Romana Vavrek provided technical assistance and helped with data collection. Dr. Karim Fouad was the supervisory author and was involved with concept formation, surgical procedures, manuscript composition, and incomparably excellent mentorship.

Table of Contents

1. Introduction

1.1 Introduction to SCI

The spinal cord contains white matter tracts carrying afferent sensory and efferent motor signals between the brain and rest of the body. Spinal grey matter contains interneuron networks and motor neurons responsible for movement generation and motor sensory integration. When a spinal cord injury (SCI) occurs, neurons can no longer communicate with networks located below the injury, resulting in partial to complete loss of sensory and motor function often leading to paralysis. Paralysis affecting all four limbs is called tetraplegia or quadriplegia and paralysis affecting the lower limbs is called paraplegia (Kirshblum et al., 2011; Maynard et al., 1997). According to standards established by the American Spinal Injury Association (ASIA), cases of SCI can be classified as functionally complete or functionally incomplete (Kirshblum et al., 2011). In functionally complete SCI there is a complete absence of sensory and motor function below the level of injury, while in functionally incomplete injuries, some sensation and movement are possible (Kirshblum et al., 2011). Based on this functional classification system, incomplete tetraplegia is the most frequently reported SCI type followed by incomplete paraplegia, complete paraplegia, and complete tetraplegia (National SCI Database, 2016). Notably, functionally complete SCI is rarely anatomically complete. In other words, complete destruction of tissue at the injury epicenter is uncommon. Instead, varying amounts of spared white matter often persist, especially in the periphery of the spinal cord (Kakulas, 1984; Kakulas, 1999). SCI can result from non-traumatic and traumatic events. Non-traumatic SCI is internal damage of the spinal cord, possibly caused by congenital diseases, neurodegenerative diseases, inflammatory diseases, vascular problems, and spinal cord compression by tumours or stenosis

(van den Berg et al., 2010). Traumatic SCI, on the other hand, is damage to the spinal cord resulting from over-stretching of the spinal cord or mechanical forces applied to the spinal cord. The leading causes of trauma to the spinal cord worldwide are motor vehicle collisions and falls, accounting for nearly equal percentages of injuries (van den berg et al., 2010).

It is estimated there are 4,300 new cases of SCI every year and 86,000 people who are living with SCI in Canada today (Farry & Baxter, 2010). The distribution of incidence rates as a factor of age is bimodal, with a peak in adolescents and young adults and another in older adults (≥ 70 years; Farry & Baxter, 2010). Furthermore, incidences of non-traumatic SCI increase with advancing age (Farry & Baxter, 2010). Thus, incidence and prevalence rates of SCI are expected to increase with the aging of the Canadian population. Incidence and prevalence rates are expected to rise to 5,300 cases and 121,000 cases respectively by the year 2030 (Farry & Baxter, 2010). Estimated lifetime costs for living with SCI range from $1,115,312 to $4,729,788 US dollars depending on the age at time of injury and severity of injury (National SCI Database, 2016). In addition to the financial burden, the life expectancy of individuals with SCI is significantly below that of persons without SCI (National SCI Database, 2016). Compared to the normative population, individuals with SCI have a lower quality of life, as evaluated by measures of physical pain, social function, mental health, overall health and other biopsychosocial variables (Westgren & Levi, 1998). It is clear that SCI is a prevailing and growing national concern with powerful financial and personal ramifications. Unfortunately, there is a relative absence of effective treatments for SCI.

1.2 The Pathophysiology of SCI

The pathophysiology of SCI is highly complex (reviewed in Hagg & Oudega, 2006;

Oyinbo, 2011), involving primary and secondary mechanisms of injury. Primary mechanisms of injury develop in the acute phase post-SCI (seconds to minutes after injury) and secondary mechanisms develop in the sub-acute (minutes to weeks after injury) and chronic phase post-SCI (months to years after injury; Oyinbo, 2011). Primary SCI is damage to spinal tissue due to the initial impact, resulting in immediate spinal shock, ischemia, and cell death (Oyinbo, 2011). Secondary SCI is further spread of the damage as a consequence of a biochemical cascade and pathological changes initiated by the primary SCI (Tator & Fehlings, 1991). Mechanisms of secondary damage include ischemia, glutamatergic excitotoxicity, inflammation and free radical production, down-regulation of growth and survival factors, expression of growth-inhibitory molecules, and cavitation at the site of initial impact, which can lead to further cell death over weeks and even months after the initial injury (Hagg & Oudega, 2006; Oyinbo, 2011). Below is an expanded description of the major pathophysiological mechanisms after SCI.

1.2.1 Spinal shock

When a SCI is severe, immediately after injury there is usually a period distinguished by flaccid motor paralysis and loss of sensation and spinal reflexes below the level of injury. This period is called spinal shock (Dittuno et al., 2004). Spinal reflexes gradually return, but may be greatly exaggerated (Dittuno et al., 2004). Several mechanisms contribute to spinal shock, such as slight hyperpolarization of the resting membrane potential of motor neurons (Li et al., 2007), reduced muscle spindle excitability (D'Amico et al., 2014; Hunt et al., 1963), increased pre-synaptic inhibition of primary afferents (Quevedo et al., 1993), and the disappearance of voltage-gated persistent inward currents (PICs) of Ca2+ and Na+ in motor neurons (D'Amico et al., 2014; Murray et al., 2010). PICs are of critical importance, because they amplify synaptic input

(Lee & Heckman, 2000), enabling sustained muscle contractions. PICs are facilitated by brainstem descending serotonergic/5-HT input (Li et al., 2007). Removal of brainstem-derived serotonin after SCI leaves motor neurons in a state of low excitability with small PICs (Li et al., 2004), consistent with spinal shock. Over the course of weeks, however, motor neurons increase expression of spontaneously active 5-HT_{2C} receptor isoforms, restoring large PICs that elicit sustained muscles contractions (Murray et al., 2010). These mechanisms lead to both improvements in motor function and the development of spasticity (Maynard et al., 1990), which is characterized by increases in muscle tone with velocity-sensitive resistance to passive stretch, as well as muscle spasms, clonus (i.e., spasms with regular contractions and relaxations), and hyperreflexia (Nielsen et al., 2007).

1.2.2 Secondary Damage

SCI pathophysiology includes apoptosis (programmed cell death) of neurons and oligodendrocytes at the site of injury (Crowe et al., 1997; Liu et al., 1997), with rapid grey matter atrophy and extended degeneration of white matter tracts (Ek et al., 2010). Furthermore, endothelial cells making up the walls of blood vessels die off, causing impaired blood flow to the surrounding tissue and contributing to ischemia (Balentine, 1978). Ischemia is associated with the production of reactive oxygen species, free radicals and peroxides, resulting in further cell damage (Demopoulos et al., 1980). Moreover, the release of intracellular glutamate from the breakdown of neurons initiates a spreading excitotoxic cascade through the hyper-activation of AMPA, kainite, and metabotropic glutamate receptor types (Abraham et al., 2001; Li & Stys, 2000; Park et al., 2004).

1.2.3 Inflammation

The blood-brain barrier is a selective semipermeable membrane formed by tight junctions between endothelial cells in the CNS microvasculature (Janzer & Raff, 1987). The blood-brain barrier separates circulating blood from the CNS, protecting brain and spinal cord from neurotoxins, macromolecules, and polar molecules in blood that may disrupt neural function (Abbott et al., 2010). SCI damages the blood-brain barrier, causing a massive infiltration of inflammatory cells, including neutrophils, monocytes/macrophages, lymphocytes in addition to microglial (immune cells of the CNS) activation (Fleming et al., 2006). The inflammatory response post-SCI is extremely complex and has both detrimental and beneficial effects. For example, subpopulations of macrophages and microglia promote tissue repair after CNS damage (Kigerl, et al., 2009) and B and T lymphocytes release brain-derived neurotrophic factor (BDNF), suggesting a role in neuroprotection (Donnelly & Popovich, 2007; Kerschensteiner et al., 1999). However, neutrophils, macrophages, and microglia also produce cytokines and reactive oxygen species, contributing to tissue damage (Carlson et al., 1998; Ding et al., 1988; Donnelly & Popovich, 2007), and SCI triggers pathological lymphocyte autoantibody production (Ankeny et al., 2006; Donnelly & Popovich, 2007). Microglia activation and cytokine release lead not only to neuronal but also to oligodendrocyte apoptosis (D'Souza et al., 1995; Shuman et al., 1997), resulting in chronic progressive demyelination (Totoiu & Keirstead, 2005) and abnormal signal transmission in the spinal cord (James et al., 2011).

1.2.4 Downregulation of growth promoters

Plasticity is an umbrella term that describes lasting changes to the nervous system that occur throughout an organism's life, even into adulthood. Neural plasticity is triggered by experience-dependent stimulation, such as nervous system injury. Injury-induced plasticity

includes axon collateral sprouting (i.e., extension of collaterals from the main axon shaft of injured or spared neurons; Fouad et al., 2001), cortical map reorganization (Girgis et al., 2007; Krajacic et al., 2009), synaptic changes of descending axons (van den Brand et al., 2012) and intraspinal circuitry (Martinez et al., 2012; Singh et al., 2011), and changes in motor neuron properties (Murray et al., 2010). Axonal growth is a broad term that may refer to axon collateral sprouting or axonal regeneration. In contrast to collateral sprouting, regeneration describes the re-growth from the severed end of an injured axon (Cafferty et al., 2008). Central nervous system (CNS) axons have a limited growth capacity in adult mammals (Cajal, 1914; Huebner & Strittmatter, 2010). One explanation for limited axonal growth is that spinal axons retract from the site of SCI (Seif et al., 2007). Axonal dieback has been attributed to a decline in growth factors (Herrera et al., 2009) and second messenger molecules following injury (Pearse et al., 2004), which is supported by the finding that treatment with growth factors reduces axonal dieback (Guest et al., 1997). The following are examples of growth and survival molecules down-regulated post-SCI: vascular endothelial growth factor (Herrera et al., 2009), neurotrophin-3 (NT-3; Ying et al., 2008), brain-derived neurotrophic factor (BDNF; Gomez-Pinilla et al., 2012; Ying et al., 2005; Ying et al., 2008) and the intracellular second messenger molecule cAMP (Pearse et al., 2004). BDNF promotes axonal growth by acting on the TrkB receptor and increasing cAMP levels intracellularly. cAMP activates phosphokinase A (PKA) and exchange protein directly activated by cAMP (EPAC), the two of which independently activate cAMP response element-binding protein (CREB), a major player in neurite outgrowth (Delghandi et al., 2005; Stiles et al., 2014). Endogenous cAMP levels decrease dramatically after birth, coinciding with a loss in axon regenerative capacity in mature neurons (Cai et al., 2001; Spencer & Filbin, 2004). As a result, it has been hypothesized that a decrease in neuronal cAMP levels mediates

the developmental loss in the ability of neuronal axons to regenerate. In support of this hypothesis, blocking the cAMP signalling pathway through inhibition of PKA abolishes the improved regenerative capacity of embryonic neurons *in vitro* (Cai et al., 2001; Spencer & Filbin, 2004). Further, inhibition of PKA prevents spontaneous regeneration of transected rat neonatal neurons *in vivo* (Cai et al., 2001; Spencer & Filbin, 2004).

In addition to the cAMP signalling pathway, mammalian target of rapamycin (mTOR) and Rho enzyme/Rho-associated protein kinase (ROCK) pathways are differentially regulated with aging. mTOR is a serine/threonine kinase that contributes to normal neuronal development by promoting neuronal survival and differentiation, axonal growth, dendritic arborisation, and synaptogenesis (Swiech et al., 2008; Takei & Nawa, 2014). In the adult brain, mTOR activity declines but is still important for synaptic plasticity (Swiech et al., 2008). After SCI, mTOR activity declines further, causing a loss in the growth capacity of axons (Liu et al., 2010).

1.2.5 Upregulation of growth inhibitors

Another obstacle to axonal growth is the upregulation of various growth inhibitors after SCI. Activation of the Rho/ROCK pathway has an inhibitory effect on axon regeneration, triggering growth cone collapse (Wahl et al., 2000). The Rho/ROCK signalling pathway is upregulated after SCI (Forgione & Fehlings, 2014), consistent with the growth-inhibiting environment of the injured CNS. Furthermore, myelin associated proteins found in CNS white matter: reticulon-4A (NOGO-A), myelin associated glycoprotein (MAG), and oligodendrocyte myelin glycoprotein (OMpg; Akbik et al., 2012). NOGO-A, MAG, and OMpg restrict neurite outgrowth *in vitro* (Chen et al., 2000; McKerracher et al., 1994; Wang et al., 2002) and are involved in restricting axonal growth *in vivo* (Cafferty et al., 2010). In line with the inhibitory

properties of myelin-associated proteins, contact with oligodendrocytes elicits the collapse of neuronal growth cones (Bandtlow et al., 1990; Caroni & Schwab, 1988). The inhibitory properties of oligodendrocytes are more pronounced post-SCI. When oligodendrocytes undergo apoptosis as a result of injury, myelin degenerates, exposing an abundance of inhibitors that microglia are slow to clear (Filbin, 2003; Vargas & Barres, 2007). A second class of growth-inhibitory molecules are chondroitin sulfate proteoglycans (CSPGs), which are widely expressed in perineuronal nets, and act as specialized ECM structures responsible for synaptic stabilization in the adult CNS (Deepa et al., 2006; Massey et al., 2006; Siebert et al., 2014). After SCI, astrocytes undergo a process called reactive astrogliosis; astrocytes become hypertrophic and increase production of CSPGs, leading to the formation of a glial scar. CSPGs are composed of a protein core and a glycosaminoglycan (GAG) side chain (Fawcett & Asher, 1999). Treatment with chondroitinase ABC (ChABC), an enzyme that degrades CSPG GAG chains, increases neurite outgrowth *in vitro* (Zuo et al., 1998) and axonal regeneration in *in vivo* SCI models (Bradbury et al., 2010; Massey et al., 2008; Yick et al., 2000). Fibroblasts are also found within the glial scar and express high levels of axon repellent protein semaphorin3A (sema3A), contributing to the inhibitory nature of the scar (De Winter et al., 2002; Pasterkamp et al., 1999). Sema3A is also expressed in spinal motor neurons, some cortical neurons, and neurons in the spinal trigeminal nucleus of the medulla (Hashimoto et al., 2004). Cortical and spinal trigeminal nucleus neurons upregulate sema3A after SCI, further hindering growth (Hashimoto et al., 2004). In fact, inhibition of sema3A in rats with SCI causes enhanced regeneration of injured axons (Kaneko et al., 2006). In summary, there appear to be redundant amounts of axon growth inhibitors, including Rho/ROCK, myelin associated inhibitors, CSPGs, and semaphorins.

1.2.6 Cavitation

Another challenge to axonal growth and contributor to damage spread is cavitation at the site of a SCI (Fitch et al., 1999; Guest et al., 2005; Hill et al., 2001). As macrophages and microglia clear cellular debris, a fluid-filled cavity forms at the lesion site and is surrounded by glial scar (Fitch et al., 1999). The fluid-filled cavity presents yet another challenge for neurons to regenerate by eliminating an extracellular matrix over which axons can grow. Further, the absence of extracellular matrix attachment molecules will induce anoikis of some surviving cells; anoikis is a type of apoptosis caused by disruption of normal interactions between cells and the extracellular matrix, as well as neighbouring cells (Frisch & Francis, 1994). Anoikis is often studied by completely detaching cells from the extracellular matrix *in vitro* (Frisch & Francis; Koda et al., 2008), but anoikis is also important *in vivo.* Cells in living tissue require very specific interactions with extracellular matrix components and the wrong type of extracellular matrix will cause the same effect as complete detachment (Gilmore, 2005). Anoikis is likely one of the reasons why the fluid-filled cavity can enlarge over time, damaging the spinal cord further and causing new neurological deficits (Siddall & Loeser, 2001). Chronic pain is a typical deficit but sensory and motor function may also be affected (Siddall & Loeser, 2001).

In summary, the spinal cord response to injury involves both immediate (primary) and delayed (secondary) effects. Immediately after injury, there is cell death at the site impact, impaired blood flow, and spinal shock (Oyinbo, 2011). Continued vascular dysfunction, excitatory neurotransmitter accumulation in extracellular space from necrotic cell death, inflammation, free radical production, downregulation of growth supportive molecules, upregulation of growth-inhibitory factors, and cavitation cause secondary damage and prohibit regenerative processes (Hagg & Oudega, 2006; Oyinbo, 2011).

1.4 SCI treatment approaches

Different SCI treatment approaches attempt to target different aspects of SCI pathophysiology. Interventions in the acute phase post-SCI are intended for neuroprotection to prevent the spread of secondary damage by limiting neuronal death and demyelination. Anti-inflammatory drugs (e.g., methylprednisolone), anti-ischemia treatments, excitotoxicity limiting treatments, and anti-apoptotic agents are examples of neuroprotective strategies (Bracken et al., 1992; Tsai & Tator, 2005). In the chronic SCI setting, repair strategies promote regeneration and re-myelination of injured axons, collateral sprouting from injured or spared axons, and neural plasticity. For example, a therapeutic strategy targeting regeneration and re-myelination of injured axons is grafting SCs into the site of a SCI (Bunge, 1975; Bunge, 2016; Richardson et al., 1980; Thuret et al., 2006). Other repair strategies potentiate axon collateral sprouting onto new synaptic targets post-SCI to create new circuits for information flow (Bareyre et al., 2004; Fouad et al., 2001; van den Brand et al., 2012; Vavrek et al., 2006). Lastly, rehabilitation training is one of the most effective repair strategies used to enhance neural plasticity and functional recovery in animal models (Fouad & Tetzlaff, 2012) and humans (Behrman & Harkema, 2000; Harkema, 2001). I will focus on SCI treatment approaches for repair in the expanded description below. Regeneration, collateral sprouting (i.e., extension of collaterals from a main axon), and rehabilitation will be explored.

1.4.1 Axonal regeneration of descending pathways

Descending pathways: Motor descending pathways in the spinal cord include the corticospinal (CST; Lawrence & Kuypers, 1968a; van den Brand et al., 2012), reticulospinal (RtST), vestibulospinal, and rubrospinal tracts (Goulding, 2009; Lawrence & Kuypers, 1968b).

Of these tracts, this thesis will focus on the CST and RtST, the main tracts responsible for motor output generation. The CST is the main pathway responsible for the control of fine forelimb movements (Lawrence & Kuypers, 1968a), and the RtST is the main pathway involved in driving central pattern generator (CPG) networks within the spinal cord that trigger locomotion (Goulding, 2009; Lawrence & Kuypers, 1968b).

A SCI disrupts connections between motor descending pathways and spinal centers controlling movement. Re-establishing connectivity is challenging due to the low regenerative capacity of adult mammalian neurons in the CNS (Cajal, 1914; Huebner & Strittmatter, 2010). For example, studies have found that CST and RtST axons will not regrow across a SCI into the spinal cord caudal to the injury without treatment (Tuszynski & Steward, 2012; Vavrek et al., 2007). Therefore, one of the first treatments for SCI was to promote the regeneration of axons in the CNS (Richardson et al., 1980; Tuszynski & Steward, 2012). Regeneration promoting treatments are varied and include cell transplantation into the SCI site, increasing levels of growth-promoting molecules, and decreasing levels of growth-inhibitory molecules, often in combination.

Cell transplantation: Cells are grafted into the injured spinal cord for various therapeutic effects, such as neuroprotection, cell replacement, remyelination, and axon growth enhancement. Some of the most investigated cell types for transplantation are Schwann cells (SCs; Bunge 1975; Bunge, 2016; Richardson et al., 1980; Thuret et al., 2006), olfactory ensheathing glial cells (OEGs; Granger et al., 2012), neural stem cells (Cusimano et al., 2012), embryonic stem cells (Lu et al., 2012), and bone marrow stem cells (Pastor et al., 2011; Ritfeld & Oudega, 2014; Tetzlaff et al., 2011). Cavity formation is common in chronic SCI, presenting an obstacle for

regenerating axons. One strategy to overcome this obstacle is to transplant cells into the SCI cavity to provide a substrate for growing axons. However, cell grafts on their own are generally thought to be insufficient to enable long-distance regeneration, making additional treatments necessary (Oudega & Xu, 2006; Oudega et al., 2012).

Growth-promoting molecules: Pro-regenerative treatments may involve various growth-associated molecules, such as the second messenger cAMP, the protein kinase mTOR, and BDNF and NT-3 neurotrophic factors. Delivery of growth-associated molecules has only limited efficacy, as this approach addresses a single obstacle to regeneration (i.e., injury associated decline in growth promoting molecules; Gomez-Pinilla et al., 2012; Herrera et al., 2009; Ying et al., 2005; Ying et al., 2008; Pearse et al., 2004). Axons stimulated by growth-promoting molecules still cannot grow over the cystic cavity that frequently occurs after SCI (Fitch et al., 1999; Guest et al., 2005; Hill et al., 2001). Thus, cell transplantation to fill the cavity together with delivery of growth-promoting molecules act in a complimentary manner to support regeneration. For example, cAMP elevation in combination with SC grafts results in regeneration of injured raphespinal axons after SCI (Pearse et al., 2004), and forced expression of mTOR through inhibition of its negative regulator PTEN, enhances survival and neurite outgrowth of dopamine neuron grafts in a model of Parkinson's disease (Zhang et al., 2012). Axons can be drawn to grafts with neurotrophic factors that have chemotactic or attractive properties. For instance, BDNF and NT-3 infusion into the spinal cord promotes descending axon regeneration into cell grafts in rats, which is not found with the graft alone (Blesch et al., 2002; Xu et al., 1995).

Targeting growth inhibitors: Other regeneration-promoting treatments deal with growth-

inhibitory molecules in the injured spinal cord. A major growth inhibitor is NOGO-A, a large molecule in CNS myelin. NOGO-A is divided into three domains; a large N-terminal domain and small C-terminal domain located intracellularly and a short 66 amino acid extracellular loop (GrandPré et al., 2000; McGee & Strittmatter, 2003). Studies support the role of NOGO-A in restricting axonal regeneration. NOGO-A exerts its inhibitory effects independently through its large N-terminal and 66 amino acid domains *in vitro* (Fournier et al., 2001). Further, monoclonal antibodies against NOGO-A allow a small percentage of damaged axons to regenerate *in vivo* (Bregman et al., 1995; Filbin, 2003; Schnell & Schwab, 1990; Schnell & Schwab, 1993). Few axons regenerate probably because other myelin-associated inhibitors (i.e., MAG and OMpg) are unaffected by NOGO-A specific antibodies. The 66 amino acid domain of NOGO-A, MAG, and OMpg act via the Nogo-66 receptor (NgR; Domeniconi et al., 2002; Filbin, 2003; Fournier et al., 2001; Wang et al., 2002); thus, inhibiting NgR activity is a broad way of targeting myelin-mediated inhibition of axonal growth. Consistent with this, NgR antagonists promote axonal regeneration of greater numbers of axons *in vivo* than NOGO-A specific antibodies (Bregman et al., 1995; Filbin, 2003; GrandPré et al., 2002; Schnell & Schwab, 1990; Schnell & Schwab, 1993). CSPGs are a different category of growth-inhibitory molecules. CSPGs can be removed through enzymatic degradation with ChABC (Zuo et al., 1998). ChABC enhances the pro-regenerative effects of cell grafts following lesions to the CNS. Fouad et al. (2005) found that a combination of SC and OEG grafts with ChABC treatment enhanced axonal regeneration in rats with SCI. Studies by different laboratories have also reported combined use of cell grafts, growth factors, and ChABC has a synergistic positive effect on axon growth after SCI (Karimi-Abdolrezaee et al., 2010). The Rho/ROCK intracellular signalling pathway has been implicated in the inhibitory effects of both myelin-associated proteins (Lingor et al., 2008) and CSPGs

(Dergham et al., 2002; Forgione & Fehlings, 2014). Therefore, a more targeted way to deal with growth-inhibitors is to inhibit the Rho/ROCK pathway directly. In line with this, inhibition of Rho or ROCK stimulates axon regeneration in adult mice with SCI (Dergham et al., 2002), and ROCK inhibition together with neurotrophic factor delivery have an additive pro-regenerative effect on retinal ganglion neurons in an optic crush model (Lingor et al., 2008).

Limitations: Many challenges with regeneration-promoting therapies are unresolved. The first is that treatment effects are generally very moderate and not robust/reliable. Even with combination treatments RtST axon regeneration is limited and CST regeneration has only been reported in exceptional cases (Liu et al., 2010; Tuszynski & Steward, 2012; Vavrek et al., 2007). Another challenge is that grafted cell survival in the SCI area is poor; as little as 1% (Enomoto et al., 2013). Also, there are a few studies that have reported stem cell and stem cell-derived cells have the capacity to form harmful growths after transplantation for reasons that are not entirely understood (Brederlau et al., 2006; Dressel et al., 2008; Itakura et al., 2015; Jeong et al., 2011). Another challenge is that neurotrophic factors may cause inappropriate growth of nociceptive axons, leading to hyperalgesia (Romero et al., 2000). Chronic exposure to neurotrophic factors post-SCI may also lead to spasticity-like symptoms (Fouad et al., 2013). Also, many treatments that enhance axonal regeneration have a limited or no effect on motor recovery, possibly because regenerated axons do not synapse with the appropriate targets (Zhang et al., 2014). For example, experiments have failed to replicate the findings of GrandPré et al. (2002), where NgR antagonism greatly enhanced axon regeneration after SCI in mice (Steward et al., 2008). Lastly, inhibition of glial scar synthesis in the acute phase post-SCI has been associated with increased tissue damage, showing the scar plays an important role in tissue repair early after injury (Rolls et al., 2008; Shechter et al., 2011). These issues need to be carefully addressed before any of

these therapies are translated to the clinic.

1.4.2 Collateral sprouting

Intervention types: In addition to regeneration of injured CNS axons, promoting synaptic rearrangements of descending axons with spinal targets is a major treatment approach. Descending tracts can, for example, form new connections with lumbar-projecting propriospinal interneurons (PrINs) after SCI; thus, creating new circuits through which supraspinal signals can be relayed to targets caudal to the injury site. Indeed, even the injured CST with its limited regenerative capacity has been shown to sprout post-SCI and make connections with PrINs (Bareyre et al., 2004; Fouad et al., 2001; van den Brand et al., 2012; Vavrek et al., 2006). The RtST has also been suggested to form relays with PrINs after SCI (Filli et al., 2014). New connections between descending spinal tracts and PrINs (i.e., PrIN relays) happen spontaneously after injury (Bareyre et al., 2004; Filli et al., 2014), suggesting a possible treatment venue is to potentiate this plasticity. PrINs are promising as new synaptic targets, given the responsiveness of PrINs to regeneration-promoting treatments (Blesch & Tuszynski, 2009). Out of 21 neuronal populations, PrINs regenerated in greatest numbers with a combination therapy of SC/OEG grafts and ChABC in rats with SCI (Vavrek et al., 2007). Enhancing the regeneration of PrINs post-SCI provides new pathways for information flow from supraspinal centers. A second way to increase rewiring is to enhance axon collateral sprouting of descending systems rostral (Girgis et al., 2007; Krajacic et al., 2009; Schnell et al., 1994; Vavrek et al., 2006) and caudal (Weidner et al., 2001) to a SCI. One method to achieve this goal is the administration of neurotrophic factors post-SCI (Schnell et al., 1994; Vavrek et al., 2006). Administration of NT-3 rostral to a SCI increases sprouting of the injured CST (Schnell et al., 1994). Further, application of BDNF to the

cortex enhances sprouting of the injured CST and increases the number of contacts between collaterals and PrIN soma (Vavrek et al., 2006). BDNF is upregulated in response to increases in neuronal activity levels (Weishaupt et al., 2012), such as exercise (Ying et al., 2005) and electrical stimulation (Wenjin et al., 2011). In fact, exercise restores levels of BDNF and NT-3 and encourages synaptic plasticity in adult rats post-SCI (Ying et al., 2005). Also, chronic electrical stimulation of the motor cortex ipsilateral to damage of one half of the CST causes robust sprouting of spared CST axons (Carmel et al., 2010). Lastly, upregulating plasticity-enhancing transcriptional programs can enhance axon collateral sprouting. For example, overexpression of the transcription factor Sox2 enhances injured CST collateral sprouting in adult mice with acute and chronic SCI (Wang et al., 2015).

Immune activation: A small but thought-provoking area of research is exploring the role of immune activation in collateral sprouting. Neurotrophic factor induced collateral sprouting is well established in the scientific literature, but some studies suggest immune activation is needed for this effect. NT-3 effectively induces sprouting of spared CST axons after unilateral CST lesion in immunocompetent but not immunosuppressed rats (Chen et al., 2008). Tellingly, NT-3 induces collateral sprouting in rats with chronic CST injury given systemic injections of lipopolysaccharide (LPS) but not in control rats (Chen et al., 2008). Similarly, BDNF without injury does not increase sprouting (Vavrek et al., 2006). Given that LPS molecules are found on the membrane of Gram-negative bacteria, LPS causes a strong immune response. Therefore, the finding that CNS injury in combination with LPS enhances collateral sprouting suggests that activating the immune system is a possible venue of maximizing sprouting post-SCI, especially in a chronic setting.

Limitations: Collateral sprouting may not result in functional improvements post-SCI and, hence, is not an end goal in itself. Increased collateral sprouting and contact formation with inappropriate targets could, in fact, have detrimental effects. For instance, Sox2 overexpression enhanced CST sprouting, but significantly reduced forelimb placement ability on a horizontal ladder task in mice with cervical SCI (Wang et al., 2015). Further, ChABC treatment after cervical SCI enhances CST sprouting, but only improves manual function when combined with rehabilitation training (García-Alías et al., 2009). Finally, chronic overexpression of the growth-promoting factor BDNF can trigger spasticity after SCI (Fouad et al., 2013). BDNF is also strongly associated with increased pain (reviewed in Garraway & Huie, 2016; Garraway et al., 2003; Kerr et al., 1999; Yajima et al., 2005). While promoting reorganization of the system can contribute to functional recovery, further study of collateral sprouting is required. Broad unwanted effects of collateral sprouting enhancing treatments need to be carefully assessed, and techniques to increase the specificity of new connections must be explored.

1.4.3 Rehabilitation training

An approach to promote neural plasticity and fine tune connections is to combine axon growth-promoting interventions with rehabilitative training. Rehabilitative training alone enhances neural plasticity and improves functional outcome measures after damage to the adult mammalian CNS. For example, body-weight supported treadmill training post-SCI improves walking ability in rats (Singh et al., 2011), cats (Barbeau & Rossignol, 1987), and humans (Behrman & Harkema, 2000; Harkema, 2001; Hornby et al., 2005). Anatomically, rehabilitation causes cortical map reorganization and sprouting of spared systems, creating new routes of communication after SCI (Girgis et al., 2007). Some studies have shown rehabilitative training

amplifies the growth-promoting effects of individual treatments. For instance, sema3A inhibition enhances axonal regeneration but has a limited effect on motor recovery, possibly because regenerated axons fail to synapse with the appropriate neuronal targets (Zhang et al., 2014). However, combination of sema3A inhibition with extensive treadmill training results in the restoration of hindlimb motor function (Zhang et al., 2014). Following cervical SCI in rats, BDNF overexpression in the motor cortex does not improve forelimb function, while BDNF overexpression together with rehabilitative training significantly improves motor performance (Weishaupt et al., 2013). Taken together, rehabilitative training is a useful component in combined treatments to enhance neural plasticity and consolidate functional synaptic connections and eliminate redundant ones after SCI.

1.4.4 Combined treatments

Given the large number of mechanisms in SCI pathophysiology, it is generally agreed upon that there will not be a single treatment (magic bullet) to cure SCI. As mentioned before, pre-clinical data has revealed that combined treatments have beneficial effects above and beyond those of single treatments addressing only one growth inhibitory challenge. For example, Schwann cell (SC) and olfactory ensheathing glia (OEG) transplantation in combination with ChABC result in the regeneration of injured axons to the caudal spinal cord (Fouad et al., 2005; Vavrek et al., 2007). In a different study, BDNF, NT-3 and SC grafts promoted descending axon regeneration after SCI (Xu et al., 1995). Injured CNS axon regeneration has also been demonstrated after elevation of cAMP with rolipram, a drug that prevents cAMP hydrolysis, and db-cAMP, a cAMP analogue, together with SC grafts (Pearse et al., 2004). There are challenges, however, with the application of combination therapies. First, combination therapies are difficult

to coordinate and need many control groups. Second, many challenges with individual treatments for SCI are unresolved. These challenges need to be carefully resolved before the field moves forward with each of the individual treatments for SCI, let alone a combination treatment.

In conclusion, various treatments are used to promote axonal growth. Strategies to enhance regeneration of injured axons include cell transplantation into the SCI cavity, upregulation of growth-promoting molecules, and downregulation of growth inhibitory molecules, often in combination. Sprouting of axons onto new synaptic targets can be promoted with neurotrophic factor delivery, exercise, electrical stimulation, and possibly by activating the immune system. Rehabilitation training can increase neural plasticity and help fine tune connections. Due to the immense complexity of SCI inhibitory milieu and mechanisms underlying repair processes post-SCI, a combination treatment will likely be most effective in promoting recovery. Before a combination treatment is tested, however, we must understand the individual components of combination treatments. As such, the focus of my thesis will be the study of some of the different aspects of SCI that must be understood in order to design effective treatments for SCI: Chapters 1 and 2 (Cell grafts), Chapter 3 (Plasticity), Chapter 4 (Rehabilitation).

1.5 Chapter Background

1.5.1 Chapters 1 and 2

In some cases of SCI no bridge exists for axonal regeneration, as a common feature of SCI pathophysiology is cavitation at the injury epicenter (Fitch et al., 1999; Guest et al., 2005; Hill et al., 2001). A solution for this is to transplant cells into the SCI cavity, thereby bridging the injury. The high number of clinical trials employing cell grafts for the treatment of SCI

worldwide reflects the large amount of scientific and public interest in transplantation strategies for repair (clinical trials.gov). A search on clinicaltrials.gov on April 2nd, 2017, returned 47 results, using the search terms "spinal cord injury" and "transplant"; 7 of these results were not cell transplantation studies, transplanted cells for the treatment of injuries besides SCI, or were non-interventional observational studies. The remaining 40 clinical trials assessed the safety and efficacy of grafting various cell types into the injured human spinal cord, namely nerve-derived SCs, umbilical cord stem cells, neural stem cells, adipose tissue derived stem cells, oligodendrocyte progenitor cells, and OEGs (clinicaltrials.gov). Most of these are also the major cell types researched in animal models of SCI: bone marrow stem cells (Pastor et al., 2011; Ritfeld & Oudega, 2014), SCs (Bunge, 1975; Bunge, 2016; Richardson et al., 1980), embryonic stem cells (Lu et al., 2012), neural stem cells (Cusimano et al., 2012), and OEGs (Granger et al., 2012). Of these cell types, SCs have the longest history of pre-clinical research. In 1975, Richard Bunge proposed that SCs could be used to repair the injured CNS, given that SCs allow axonal regeneration in the PNS. SCs are absent in the CNS, where axons are myelinated by oligodendrocytes (Bunge, 1968). Hence, it was hypothesized that transplantation of peripheral nerve SCs into the lesioned CNS would induce axonal regeneration. In 1980, a seminal article was published by the Aguayo laboratory showing that a piece of peripheral nerve transplanted into the site of a SCI in rats supported regeneration of transected CNS axons (Richardson et al., 1980). This was an important finding because it was evidence that injured CNS axons could regenerate given the appropriate conditions. Since then, protocols for the purification, characterization, and transplantation of peripheral nerve SCs have been developed (Bunge, 2016; Morrissey et al., 1991). Multiple laboratories have confirmed that nerve-derived SC transplants re-myelinate injured axons (Gilmore & Sims, 1993) and support axonal regeneration (Bunge,

2016; Fouad et al., 2005; Pearse et al., 2004; Vavrek et al., 2007; Xu et al., 1995). The repair ability of grafted SCs can be further improved with adjunctive treatment (Bunge, 2016; Oudega & Xu, 2006; Oudega, 2012). Despite SCs being one of the earliest cell types studied for grafting in SCI (Bunge, 1975; Bunge, 2016; Richardson et al., 1980; Xu et al., 1995), the optimal source of SCs has not been determined and low survival rates of grafted SCs are a continuing challenge. In addition to peripheral nerve, SCs can be differentiated from multipotent dermal stem cells found in skin, called skin derived precursors (SKPs; Biernaskie et al., 2007a). SKP-SCs are, thus, more readily accessible than nerve SCs, which can only be obtained by an invasive nerve biopsy (Biernaskie et al., 2007a). Similar to nerve SCs, SKP-SC grafts have been shown to support axonal growth and re-myelination after SCI (Biernaskie et al., 2007b). The accessibility and repair action of SKP-SCs make them a promising alternative to nerve-derived SCs. However, like nerve SCs, SKP-SCs have poor survival after transplantation in rodent SCI models (Enomoto et al., 2013; Biernaskie et al., 2007b). The purpose of Chapter 1 was, then, to optimize grafted SKP-SC survival and cavity-filling post-SCI in rats. To optimize SKP-SC survival post-transplantation, cells were grafted in hyaluronan/methylcellulose hydrogel (HAMC) or HAMC with added laminin and fibronectin peptide sequences (eHAMC). HAMC reduces inflammation in a rat model of arachnoiditis when injected intrathecally (Austin et al., 2012); hence, HAMC could prevent immune-rejection of grafted cells. eHAMC contains extracellular matrix proteins involved in cell attachment, and, thus, was expected to prevent anoikis, a form of detachment-mediated cell death (Frisch & Francis, 1994).

The success of cell transplantation strategies is largely determined by immunological compatibility between donor and host cells. There are different types of transplantation associated with varying risks of immune rejection (Anderson et al., 2012). Cell grafts with the

greatest risk of rejection are discordant xenografts, where cells are transplanted between distantly related species, such as between a human and a rat. Concordant xenografts have the second highest risk of rejection and involve grafting cells between closely related but separate species; for instance, rat cells into mice. Next are allografts, which are cell transplantations between two non-genetically identical members of the same species, such as between rat strains. Then, there are isografts, which are transplants between genetically identical animals; for example, between littermates from a highly inbred rat strain. Finally, the grafts with the lowest rejection rates are autografts, where the same animal is both cell donor and recipient (Anderson et al., 2012). It is known that pharmacological immune suppression enhances SC survival in the injured rat spinal cord (Hill et al., 2006). In rodent studies, cell donor and recipient are typically matched by rat strain. Albino Fischer rats are highly inbred, ensuring genotypic variance between rats is low (criver.com), and, thus, are preferred over other rat strains in transplantation studies. However, an often overlooked fact is that the Fischer strain can be purchased from different suppliers and the same supplier often sells more than one Fischer sub-strain. Charles River, for example, sells two Fischer sub-strains under the labels SAS^{TM} and CDF^{TM}. Although these sub-strains have the same MHC haplotype RT1^{lv} (criver.com), other unidentified antigens may differ between sub-strains. This raises the possibility that sub-strain mismatching (e.g., SAS^{TM} cells into CDF^{TM}) could mediate immune rejection in studies where sub-strain is not considered or reported. Therefore, one of the questions asked in Chapter 2 was whether mismatched cell donor and graft-recipient rat sub-strains would lead to lower grafted cell-survival.

A different factor possibly mediating grafted cell rejection in SCI is mismatching sex of cell donor and graft recipient rats. Y chromosome proteins (such as H-Y) are expressed only in male cells and may function as minor transplantation antigens (Simpson, 1982). In a nerve

transplantation study with rodents, male to female isografts showed no significant rejection up to 4 weeks following grafting (Midha et al., 2000). However, minor histocompatibility mismatching, as with sex mismatching, may trigger graft rejection in longer term studies (Schaller et al., 1999). In Chapter 2, sex of donor and recipient rats was matched to avoid potential immunocompatibility issues. Future experiments will need to be conducted to evaluate the role, if any, of sex mismatching in post-transplantation grafted cell loss in the injured spinal cord.

Studies specifically on SC survival in the damaged spinal cord suggest a significant role of immune activation in the death of grafted SCs. For instance, SCs transplanted in the acute phase of SCI, when the inflammatory response is strongest (Carlson et al., 1998; Donnelly & Popovich, 2007), die through necrosis and apoptosis (Hill et al., 2006). Delayed transplantation by at least a week greatly increases grafted SC survival rates, albeit there is a second wave of cell death after the SCs have integrated in the spinal cord (Hill et al., 2006). Cyclosporine-mediated immunosuppression also increases SC survival rates and the effect is greatest when combined with delayed transplantation (Hill et al., 2006). Another major factor contributing to post-transplantational SC loss is detachment of SCs as a result of extraction from cell culture plates; detachment from substrata results in a form of apoptotic cell death called anoikis (Frisch & Francis, 1994). SCs are adherent cells and rely on basal lamina proteins, including laminin and fibronectin for cell attachment (Baron-Van Evercooren et al., 1982; Tohyama & Ide, 1984). In fact, when SCs are plated on non-adherent polyhydroxyethyl methacrylate multi-well plates, a material that is not directly toxic to cells, 40% of SCs die within 24 hrs (Koda et al., 2008). A question that has not yet undergone systematic study is whether immune rejection or anoikis is the main contributor to SKP-SC loss after grafting in the injured spinal cord. To answer this

question, the role of the immune system was minimized with cyclosporine immunosuppression in SKP-SC graft-recipient rats with SCI to determine if this manipulation would be sufficient to ensure SKP-SC survival. SKP-SCs were grafted in cyclosporine-treated sub-strain matched rats, and saline-treated sub-strain matched and sub-strain mismatched rats. The sub-strain mismatched group was included to answer the question of whether sub-strain mismatching elicits a stronger immune response than sub-strain matching, lowering grafted cell survival rates.

1.5.2 Chapter 3

As discussed in *1.3 SCI treatment approaches*, injured descending tracts can extend new axon collaterals to contact PrINs that project past a SCI. Instead of descending axons having to regenerate from the severed end of axons back to their original targets over long-distances, descending input can reach its final targets by relaying the information onto PrINs. For example, injured CST axons have the capacity to form relays with PrINs in rodents with SCI (Bareyre et al., 2004; van den Brand et al., 2012; Vavrek et al., 2006), and evidence suggests these connections have a causal effect on locomotor recovery. van den Brand et al. (2012) showed that inactivation of the CST with GABA agonist muscimol, results in a loss of recovered motor function post-SCI, purportedly because CST-PrIN connections are supressed. A number of factors, however, must be taken into consideration when interpreting these data. For instance, inactivation of the CST with muscimol would suppress all CST synaptic connections, not only those between the CST and lumbar-projecting PrINs. Further, van den Brand et al's (2012) findings suggest CST integrity is crucial for locomotion, but this is inconsistent with other findings showing a minor role of the CST. An example is that rats with bilateral damage to the CST are able to locomote effectively over-ground (Kanagal & Muir, 2009). Rather than the CST,

the RtST has been attributed the primary role in driving CPG networks for the initiation of over-ground locomotion (Goulding, 2009; Lawrence & Kuypers, 1968b). We wanted to know if, similar to the CST, the RtST can form relays with lumbar-projecting PrINs to circumvent a SCI and if RtST-PrIN connections are associated with motor recovery. To answer this question, we employed a staggered SCI model, in which rats receive two thoracic lateral hemisection SCIs. The hemisection SCIs are on different thoracic segments and opposite sides of the spinal cord. As a result, all descending axons are transected, leaving an intact tissue bridge between hemisection SCIs (Courtine et al., 2008; Murray et al., 2010; van den Brand et al., 2012). Since all descending axons are transected, the staggered SCI model is similar to a complete injury model, yet greater locomotor recovery is observed following staggered SCIs than spinal cord transections (Basso et al., 1996; Murray et al., 2010). This is likely because of anatomical changes taking place in the intact tissue bridge between SCIs in the staggered lesion model, such as changes in motor neuron properties (Murray et al., 2010) and possibly relay formation with PrINs. For this reason, the staggered SCI model is useful for the study of plasticity. Also, because all descending axons are transected in staggered SCI, plastic changes can be attributed to injured fibers, rather than spared ones, reducing ambiguity in the interpretation of results. Thus, we set out to investigate RtST-PrIN relay formation in the intact tissue bridge between hemisections in rats with staggered SCI.

1.5.3 Chapter 4 and Appendices

Rehabilitation training after traumatic SCI presents many challenges. For instance, individuals who have suffered a traumatic SCI may experience complicating health issues that prevent them from participating in early training. Limited availability and accessibility to core

health care services is also an obstacle for some individuals seeking rehabilitation therapy shortly after SCI (Goodridge et al., 2015). Inability to participate in rehabilitative training shortly after injury limits the potential for recovery. After CNS damage, there is a narrow window of heightened structural plasticity in the spinal cord, as measured by levels of growth-associated protein 43 (GAP-43; Sist et al., 2014). The narrow window of heightened plasticity is associated with accelerated spontaneous recovery (Sist et al., 2014). The window of plasticity opens ~3 days after injury, with maximal levels 7-14 days after injury and a return to baseline levels by 28 days. This is consistent with studies showing that early training (up to 2 weeks post-injury) is more beneficial for motor recovery than late training (>2 weeks post-injury; Sumida et al., 2001). Thus, complicating health issues and availability/accessibility of health care resources may keep patients from maximizing training-induced benefits. Another challenge in implementing rehabilitation training is an absence of treatment standards across SCI patient groups. Variation within and between rehabilitation SCI patient groups is high as assessed by measures of length of stay, intensity of treatment, minutes of treatment per session, and total duration of treatment per week (Whiteneck et al., 2011). This is despite evidence that long-term training (9 months; Hicks et al., 2003) and high-intensity training (as measured by larger maximum heart rate; de Groot et al., 2003) result in more pronounced improvements in physical capacity in individuals with SCI. A third major challenge is in the type of activity that should be used in rehabilitation therapy. An unanswered question is whether task-specific training is superior to general exercise, and whether there are certain kinds of task-specific training that are more helpful than others. The kind of task trained is important, because training in one task results in recovery in the trained task at the expense of performance in a non-trained task (de Leon et al., 1999; Girgis et al., 2007). Interestingly, no detrimental effect on non-trained tasks is found when training is

implemented 2 weeks (Krajacic et al., 2009) compared to 4 days post-SCI (Girgis et al., 2007). A possible explanation for this is that 2 weeks post-SCI, the window for plasticity is still open but the potential for plasticity is lower than 4 days post-SCI. When training occurs too soon after SCI, task-specific training occurs at the peak of heightened plasticity and may result in rigid wiring of neuronal circuits, making it difficult to re-train the system for other tasks. Interference of a motor skill learned previously with the learning of a new similar skill has also been reported in human subjects, such as learning the backhand tennis stroke after learning the forehand stroke (Eason et al., 1989). Together, these data indicate pre-injury task-specific training may increase the challenge of learning new motor strategies post-SCI. Hence, in Chapter 4 we asked what the effect pre-injury task-specific motor pre-training would be on post-SCI motor performance in rats.

The behavioural tests we employed were the single-pellet grasping and swimming tasks. The single-pellet grasping task is a forelimb reaching and grasping task, where a rat has to reach through a slit, grasp a food pellet manually presented by a trainer, and retrieve the pellet to be eaten (Whishaw et al., 1998). Single-pellet grasping is a fine motor task. Single-pellet grasping involves fine forelimb movements, as the reaching movement is composed of multiple specific components, such as accurate positioning of the elbow, whole forelimb extension and retraction, digit control when opening the paw over the pellet and enclosing the pellet in the paw (Whishaw et al., 2003). Further, the reaching movement is under CST descending control (Kanagal & Muir, 2009; Lawrence & Kuypers, 1968a; Whishaw et al., 1998), making the integrity of volitional descending components important. Given the complexity of the reaching movement and importance of volitional control, single-pellet reaching must be trained to improve performance. Indeed, intact rats steadily improve their reaching success with more training sessions (Whishaw

et al., 2003). Conversely, swimming involves placing rats in a pool and videotaping them to record their swimming motion (Magnuson et al., 2009), and unlike single-pellet grasping, swimming is a gross motor task that involves the activation of CPG networks in the spinal cord (Guertin, 2013; Marder & Bucher, 2001). While regulated by descending input, CPG networks can generate rhythmic hindlimb activity when disconnected from brain and brainstem (Brown, 1914; Guertin, 2013; Sherrington, 1910). Since swimming depends on CPG activation, rats' swimming pattern does not change with additional practice (Magnuson et al., 2009). These differences between single-pellet grasping and swimming might differentially influence post-injury recovery. Rats that were not pre-trained in grasping would likely be at a disadvantage, as they are unfamiliar with the task and would take time learning it; thus, non-pre-trained rats would miss the window for heightened plasticity in the first few weeks post-SCI. Early participation of pre-trained rats in the grasping task could counter the effect of pre-training induced interference post-SCI. Since rats do not need to learn how to swim and are forced to do so to avoid drowning in the swimming task, both pre-trained and non-pre-trained groups would be equally active during the period of heightened plasticity after SCI. As a result, the effect of interference might be more apparent in swimming pre-trained rats. These considerations are important, as early participation in rehabilitation therapy could counter the negative effect of motor interference in highly pre-trained individuals with SCI.

In another project described in the appendices, we replaced manual single-pellet grasping training with automated robotic training, as this saves on experimenter time, is easier, more reliable, and results in bigger therapeutic gains. The robot rather than a person presents food pellets and automatically scores the number of reaching attempts and grasping successes and fails. Furthermore, the animals can self-train, saving on researcher time and effort, and can train

at night, which is preferable for rats, as rats are naturally nocturnal (Stephan & Zucker, 1972). Finally, the task can be altered in difficulty by presenting the pellet closer or farther away depending on robot specifications. An inverted U relates task difficulty and performance, with intermediate tasks producing the greatest task-related benefits (Engineer et al., 2012). Therefore, the ability to alter task difficulty is an advantage, because difficulty levels can be tailored to the rats' recovery to produce the greatest functional gains.

Chapter 1: Adult skin-derived precursor Schwann cell grafts form growths in the injured spinal cord of Fischer rats

Zacnicte May[1], Ranjan Kumar[2], Tobias Fuehrmann[3], Roger Tam[3], Katarina Vulic[3], Juan Forero[1], Ana Lucas Osma[1], Keith Fenrich[1], Peggy Assinck[4,5], Michael J. Lee[4], Aaron Moulson[4,6], Molly S. Shoichet[3], Wolfram Tetzlaff[4,6,7], Jeff Biernaskie[2], & Karim Fouad[1]

1. Neuroscience and Mental Health Institute, Faculty of Rehabilitation Medicine, University of Alberta, Edmonton, AB Canada
2. Department of Comparative Biology and Experimental Medicine, Faculty of Veterinary Medicine, Alberta Children's Hospital Research Institute, University of Calgary, Calgary, Alberta, AB Canada
3. Department of Chemical Engineering & Applied Chemistry, Department of Chemistry, Institute of Biomaterials and Biomedical Engineering, University of Toronto, Toronto, ON Canada M5S 3E1
4. International Collaboration on Repair Discoveries and [5]Graduate Program in Neuroscience and [6]Department of Zoology and [7]Department of Surgery, University of British Columbia, Vancouver, British Columbia, Canada V6T 1Z4.

Abstract

Schwann cell (SC) transplantation therapy is one of the oldest cell grafting treatments for spinal cord injury (SCI). Nevertheless, the survival of grafted SCs is still underwhelming. Our goal was to improve cell survival and to fill the cavity at the site of SCI, thereby forming a 3-dimensional bridge for potential axonal regeneration. The source of SCs is commonly a peripheral nerve biopsy; however, harvesting these SCs poses many challenges, including donor site morbidity. Promising alternatives are skin-derived precursor SCs (SKP-SCs). SKP-SCs are differentiated from stem cells found in the dermis and could potentially be used for autologous transplantation. In our study, we grafted GFP^+ SKP-SCs from adult rats into the cavity of a hemisection SCI in immune suppressed rats. Cells were transplanted in either hyaluronan-methylcellulose hydrogel (HAMC) or hyaluronan-methylcellulose modified with laminin- and fibronectin-derived peptide sequences (eHAMC). HAMC forms a gel at physiological temperatures, thus, helping to keep grafted cells inside the SCI cavity. Extracellular matrix (ECM) proteins were added in eHAMC to enhance grafted cell attachment and, thus, prevent cell death due to dissociation from the ECM (i.e., anoikis). Anatomical examination post-mortem revealed large masses of GFP^+ cells in the majority of HAMC (5 out of n = 8) and eHAMC (6 out of n = 8) animals. Cell transplantation in eHAMC caused significantly greater spinal lesions compared to lesion and eHAMC only control groups. A parallel study showed similar masses in the contused spinal cord of rats after transplantation of adult GFP^+ SKP-SCs without a hydrogel matrix or immune suppression. These findings suggest that adult GFP^+ SKP-SCs, cultured/transplanted under the conditions described here, have a capacity for inappropriate or uncontrolled growth.

Keywords: “skin-derived precursor cells”, “Schwann cell”, “cell therapy”, “spinal cord injury”, “hyaluronan-methylcellulose”, “hydrogel”

1. Introduction

Spinal cord injury (SCI) is a devastating event because it results in partial to complete loss of sensory and motor function below the level of injury and secondary complications, such as pain and autonomic dysfunction. In the United States, there are ~282,000 persons living with SCI with 17,000 new cases every year (National SCI Database, 2016), and there is no robust treatment to reliably promote recovery. The complexity of SCI pathophysiology (reviewed in Hagg & Oudega, 2006) explains, in part, the relative absence of effective treatments. Axons are unable to regenerate into and beyond the site of SCI due to lack of growth-promoting molecules (Pearse et al., 2004), various inhibitors to axonal regeneration (Clafferty et al., 2010; Fawcett & Asher, 1999), and the formation of a fluid-filled cavity at the injury epicenter, creating a need for a substrate for growing axons (Oudega et al., 2012). Therefore, grafting cells to create a bridge across the lesion cavity is a frequently attempted avenue. In particular, Schwann cell (SC) grafts have been shown to provide a supportive growth substrate for axons (Bunge, 1975; Oudega & Xu, 2006; Richardson et al., 1980; Tetzlaff et al., 2011; Williams et al., 2015), and release a host of axon growth-promoting factors, including NGF, BDNF, and NT-3 (Funakoshi et al., 1993; Meier et al., 1999; Meyer et al., 1992; Richner et al., 2014; Sahenk et al., 2008). SCs are also involved in myelinating spared and regenerating axons (Biernaskie et al., 2007b; McKenzie et al., 2006; Xu & Onifer, 2009).

Although multiple pre-clinical studies suggested that SC transplantation following SCI

translates into modest functional recovery (Flora et al., 2013; Sharp et al., 2012; Williams et al., 2015), it is generally accepted that in order for SCs to be effective in restoring function combinatory approaches (e.g., pro-regenerative treatments in addition to the cell grafts) are needed (Fouad et al., 2005; Oudega & Xu, 2006; Oudega, 2012). Because of all these potentially beneficial effects there are on-going clinical trials testing the safety of grafting SCs in humans with SCI (http://clinicaltrials.gov/ct2; NCT02354625; NCT01739023).

Despite the multitude of studies on SC grafts, many basic questions about SC therapy remain unanswered, including the best source of SCs (Tetzlaff et al., 2011). Typically, SCs for cell transplantation are obtained from samples of peripheral nerve (Bunge, 1975; Fouad et al., 2005; Murray & Stout, 1942; Pearse et al., 2004; Williams et al., 2005). An alternative source is the skin dermis, which contains multipotent progenitor cells called skin-derived precursors (Joannides et al., 2004; Toma et al., 2005; Toma et al., 2001) that can be successfully differentiated into SCs (Biernaskie et al., 2007a; Biernaskie et al., 2007b; McKenzie et al., 2006). Skin biopsies as compared to nerve are less invasive and do not result in significant morbidity as a consequence of nerve resection (Biernaskie et al. 2007a) making SKP-SCs a highly accessible, autologous source of SCs for cell therapy. In tissue culture, neonatal and adult skin-derived precursor Schwann cells (SKP-SCs) survive well and can be purified to >95% purity (Biernaskie et al., 2007a).

Survival of grafted SCs in the injured spinal cord is a major challenge. Survival rates of peripheral nerve-derived SCs 6-9 weeks post-transplantation range from 1-20% (Enomoto et al., 2013; Golden et al., 2007; Pearse et al., 2007) and survival rates of SKP-SCs 11 weeks post-transplantation are ~18% (Biernaskie et al., 2007b). One of the causes of SC loss post-

transplantation is immune-mediated rejection. In fact, immunosuppression with cyclosporine has been reported to increase SC survival in the injured rat spinal cord (Hill et al., 2006). A second cause of SC loss is anoikis (Koda et al., 2008), a type of apoptosis due to detachment of cells from the extracellular matrix (ECM) and surrounding cells (Frisch & Francis, 1994). These factors need to be addressed in pre-clinical research to ensure maximal survival of grafted cells.

In the present study, we attempted to promote the survival of grafted SKP-SCs in order to create a bridge for regenerating axons in future combinatory treatments. Criteria for successful grafts include: maximal cell survival, filling of the SCI site with SKP-SCs, and possibly axonal growth into the graft (as seen in Biernaskie et al., 2007). To achieve this goal, SKP-SCs were grafted in hydrogel rather than media, since the increased viscosity of hydrogels prevents injected cells from spreading and localizes cells to the injection site (Ballios et al., 2010; Ballios et al., 2015). Tighter clustering of grafted cells due to hydrogels' viscosity was also anticipated to prevent anoikis. Two different hydrogels were used: a blend of hyaluronan (HA) and methylcellulose (MC) called HAMC and a peptide modified HAMC (eHAMC). HAMC was used, because it has recently shown promise in the field of SCI by reducing inflammation (Austin et al., 2012), which could result in enhanced cell survival. Furthermore, HAMC is easily injectable due to the shear thinning properties of HA and the inverse thermal gelling properties of MC (Gupta et al., 2006). For eHAMC, laminin and fibronectin-derived peptide sequences were conjugated to MC (Mothe et al., 2013). Laminin and fibronectin peptides are important molecules in the ECM involved in cell attachment (Baron-Van Evercooren et al., 1982; Tohyama & Ide, 1984). Therefore, this latter formulation was expected to further reduce cell spread and anoikis by providing ECM attachment molecules. As a final measure to ensure grafted cell survival, rats were immunosuppressed with cyclosporine. In sum, our goal was to maximize

SKP-SC survival within the SCI cavity by preventing grafted cell spread and anoikis with HAMC hydrogels and preventing graft rejection with cyclosporine.

2. Materials and Methods

2.1 Animals

Adult female Fischer (CDF®) rats (N = 20; Charles River Laboratories, Wilmington, MA, USA) weighing between 161-182 g were housed in groups of five rats per large (18" x 14") cage under a 12:12h light-dark cycle. Rats were acclimatized for 1 week before starting the experiment. Experimental protocols were approved by the University of Alberta Health Science Animal Care and Use Committee and the University of Calgary Animal Care Committee.

2.2 SKP-SC preparation and freezing

Following an overdose of sodium pentobarbital (27.3mg/kg; IP injection), back skin was shaved, cleaned with 70% EtOH and then removed from 12 week old male Fischer (CDF®) rats (Charles River). Adult SKPs were isolated as previously described (Biernaskie et al., 2007a; Hagner & Biernaskie, 2012; Kumar, Sinha et al. 2016). Briefly, skin was floated on dispase (5 U/ml; Stem Cell Technologies, Vancouver, BC, Canada) for 2 hrs at 37˚C. Epidermis was removed and discarded, while the dermis was digested with collagenase Type IV (1 mg/ml; Worthington, Burlington, ON, Canada) and then subsequently dissociated to single cells by manual trituration. Isolated primary dermal cells were plated at 50,000 cells/ml in SKP proliferation medium consisting of DMEM and F-12 nutrient supplement at a 3:1 ratio (Invitrogen, Carlsbad, CA, USA) with basic fibroblast growth factor (40 ng/ml; BD Biosciences, Mississauga, ON, Canada), 2% B27 supplement (Invitrogen) and 1% penicillin/streptomycin (Invitrogen).

Following two serial passages, floating spherical colonies were pelleted by centrifugation and dissociated in collagenase Type IV for 5 min at 37˚C. SKPs were dissociated via gentle trituration, washed twice with sterile HBSS and then plated on plastic culture dishes coated with poly-d-lysine (20 μg/ml) and laminin (4 μg/ml; both from BD Biosciences) at 50,000 cells/ml in SC proliferation medium, DMEM/F-12 (3:1; Invitrogen) containing 1% N2 supplement (Invitrogen), 1% penicillin/streptomycin (Invitrogen), neuregulin (50 ng/ml; R&D Systems, Minneapolis, MN, USA), and forskolin (5 μM; Sigma-Aldrich Canada Ltd., Oakville, ON, Canada). SC differentiation was verified by their adoption of a bipolar morphology, formation of adherent parallel cellular arrays and their expression of the p75NTR (see below), all well characterized features of rodent SCs (Morrissey et al., 1991; Vroemen & Weidner, 2003).

2.3 Lentiviral transduction and cell sorting

To enable long term tracking, SKP-SCs were labeled using a replication deficient lentiviral vector encoding green fluorescent protein (GFP) as described previously (Rahmani et al., 2014; Kumar et al., 2016). SKP-SCs were allowed to reach 40% confluence and then grown in supernatant containing lentiviral particles in the presence of polybrene (8 μg/ml; Sigma-Aldrich Canada Ltd.) for 18 hrs. Subsequently, SKP-SCs were washed twice with DMEM, the media replaced, and further expanded for 5-10 passages prior to FACS selection of $p75^{+/}GFP^{+}$ cells.

To purify GFP^{+} cells, SKP-SCS were grown to 60% confluence, trypsinized (trypsin-EDTA 0.25%; Thermo Fisher, Waltham, MA, USA) for 3 min, gently triturated and suspended in HBSS containing 10% FBS to quench the trypsin. Cells were resuspended in HBSS containing 1% bovine serum albumin and $p75^{+}/GFP^{+}$ cells were selectively isolated using a FACS Aria III

cell sorting system (BD Biosciences). Gates were determined by comparison to control cultures of GFP^- rat SCs and positive controls consisting of SCs isolated from GFP-expressing transgenic rats (Sparling et al., 2007).

2.4 Mycoplasma Polymerase Chain reaction

Polymerase chain reaction (PCR) was conducted for the presence of mycoplasma, since this has been previously demonstrated to accelerate transformation of other cell types (Feng et al., 1999; Tsai et al., 1995). Frozen stock of GFP^+ SKP-SC lines 1 and 3 from the present study were thawed and cultured for 7 days in the absence of antibiotics. In addition, horizontal spinal cord sections from a recipient rat from the SCs:HAMC group containing GFP^+ cells were scraped off and tested. Supernatant was removed, boiled for 10 min and then diluted in molecular grade water. PCR was performed using iProof HF MasterMix (Bio-Rad Laboratories, Inc., Hercules, CA, USA) amplification in accordance with previously published protocol (Choppa et al., 1998). Primers were as follows: 5' GGG AGC AAA CAG GAT TAG ATA CCC T 3' and 5' TGC ACC ATC TGT CAC TCT GTT AAC CTC 3'. PCR reactions were performed as follows: 98 ˚C, 3 min; followed by 39 cycles of 98˚C for 10 sec; 55˚C, 30 sec (annealing); and then 72˚C for 5 min.

2.4 HAMC and eHAMC preparation

MC (Mw 310 kDa, Shin-Etsu Metolose SM- 4000, Japan) conjugated with the cell adhesive peptides RGD or IKVAV was prepared as previously described (Tam et al., 2012). Briefly, MC was thiolated first, the reactive thiol was then reacted with maleimide-peptide by Michael-type addition. Maleimide-peptides were synthesized using an automated peptide

synthesizer. Since it has been demonstrated that longer peptide sequences have greater biological activity/binding capacity than shorter sequences (Craig et al., 1995), we used the peptide sequences Ac-GRGDS-PASSK-G_4-SR-L_6-R_2KK(Maleimide)G, where RGD is the fibronectin-derived adhesion sequence, and (Maleimide)-GRKQAAS-IKVAV-SG_4SRL_6R_2KK(Alloc)-G, were IKVAV is the laminin-derived adhesion sequence. The peptides were conjugated to different polysaccharide chains. RGD and IKVAV sequences were added, given that these sequences both promote SC adhesion (Kontoveros, 2015; Zheng et al., 2014).

HAMC and eHAMC hydrogels were prepared as previously described (Führmann et al., 2016). Briefly, HA (MW 1500 kDa, Dramen, Norway) and MC or MC-RGD/-IKVAV were sterile filtered, lyophilized and stored at 20°C under sterile conditions. Sterile water was added to HA and MC, MC-RGD/-IKVAV (1% w/v) under aseptic conditions and gently agitated overnight at 4°C. The dissolved hydrogel was mixed in a speedmixer for 20 sec at 3500 rpm, followed by centrifugation at 14,400 RPM for 45 sec and cooled on ice until cell addition. As MC forms a loosely crosslinked network through hydrophobic interactions, no crosslinker was added.

2.5 SKP-SC thawing, plating, and maintenance conditions

Frozen vials of three independent adult lines of GFP^+ SKP-SCs were thawed at 37 ˚C in under 2 min. Thawed suspensions were diluted in DMEM and centrifuged at 1000 rpm for 5 min. The resultant cell pellets were re-suspended at a density of 50,000 cells/ml in SC proliferation medium. 5% heat inactivated fetal bovine serum (FBS; Invitrogen) was added initially to promote cells' adherence. SKP-SCs were plated on polystyrene 25 cm^2 flasks or 10 cm dishes coated with laminin (4 µg/ml) and poly-d-lysine (20 µg/ml; all from Fisher Scientific, Ottawa,

ON, Canada). Cells were cultured in an incubator at 37˚C in an atmosphere containing 5% CO_2 (Thermo Scientific) and fed every 3 days. SKP-SCs on passage 5-10 were transplanted when the cultures were 75% confluent.

2.6 Spinal cord hemisection injury and cell transplantation

All surgical procedures were conducted under isoflurane inhalation anaesthesia (5% for induction; 2.5-3.0% for maintenance) supplied with 50:50 air mixed with pure oxygen. The rats' backs were shaved and the skin was disinfected with chlorhexidine digluconate (Sigma-Aldrich Canada Ltd.). The lubricant Tears Naturale (Alcon Canada, Inc., Mississauga, ON, Canada) was applied to the eyes to protect them from drying. The skin overlaying the thoracic vertebrae was cut, and the muscles were dissected apart to expose the T8 vertebra, which was removed surgically. Following a horizontal incision of the dura mater along the midline, the right side of the spinal cord was cut with spring scissors. To ensure completeness of the hemisection injury, the lesion site was crushed with Dumont #5 forceps. The dura was covered with 1% dry agarose. Muscles were sutured with vicryl 5-0 (Johnson & Johnson Medical Pty Ltd., Sydney, NSW, Australia), and the skin was stapled with 9 mm stainless steel clips (Stoelting Co., Wood Dale, IL, USA). Animals received 0.04 mg/kg buprenorphine SQ (Temgesic, Schering-Plough, Kirkland, QC, Canada) at the start of the operation, followed by a 0.02 mg/kg dose 8 hrs afterwards. Animals were kept hydrated with a 4 ml saline SQ injection immediately post-operatively and a 2 ml dose the day after surgery. Bladders were manually expressed until voiding was re-established. One rat was euthanized with a pentobarbital overdose (Euthanyl; Biomeda-MTC, Cambridge, ON, Canada) at 1000 mg/kg IP due to its lack of recovery.

Two weeks post-SCI, rats received either no treatment (the spinal cord was re-exposed

and a Hamilton needle tip was inserted into the lesion cavity, n = 6) or were given one of three different treatments: 0.5%/0.5% eHAMC injection alone (n = 7), SKP-SCs in 0.5%/0.5% HAMC (n = 8), or SKP-SCs in 0.5%/0.5% eHAMC (n = 8). Immediately before transplantation, SKP-SCs were detached from dishes using Triple E express (Invitrogen) and gently pipetted to create a cell suspension. The suspension was centrifuged at 1000 rpm for 5 min and the pellet re-suspended in DMEM. The cell suspension was mixed with HAMC or eHAMC for a final 0.5%/0.5% dilution (~50,000 cells/µl). A total volume of 4 µl (~200,000 total cells) was injected into the epicenter of the lesion using a 10 µl Hamilton syringe (Figure 1A). The injury site was covered with agarose film. Buprenorphine was administered (0.03 mg/kg) pre-operationally and 2.5 ml of saline was given right after the surgery and the following morning. All of the animals received daily cyclosporine A injections (15 mg/kg, SQ; Novartis, Dorval, QC, Canada) starting 1 day before transplantation and continuing until euthanasia.

2.7 Behavioural Assessment

Hindlimb locomotor recovery was assessed on a weekly basis from 1 week post-SCI to 8 weeks after injury (6 weeks post-grafting) using the Basso, Bresnahan and Beattie (BBB) locomotor rating scale (Basso et al., 1995) by two blinded observers 2 min after voiding the bladder, as spontaneous micturition may elicit reflex hindlimb activity (Tai et al., 2006; Thor et al., 1983).

2.8 Perfusion and Histology

All rats were euthanized 10 weeks post-SCI (8 weeks post-grafting) with a lethal dose of pentobarbital and transcardially perfused with saline containing heparin followed by phosphate-buffered 4% paraformaldehyde with 5% sucrose (PFA; 0.1 M; pH 7.4). Spinal cords were

removed, post-fixed in 4% PFA overnight at 4˚C, and cryoprotected in 30% sucrose for 5 days. Thoracic spinal cord blocks with the lesion in the center were embedded in O.C.T (Sakura Finetek, Torrance, CA, USA), mounted onto filter paper, and frozen in dry ice cooled 2-methylbutane (Fisher Scientific). Sections of the spinal blocks were cut horizontally at a thickness of 25 µm on a NX70 cryostat (Fisher Scientific), staggered across four sets of slides (Fisher Scientific, Ottawa, ON, Canada) and stored in a -20˚C freezer until further processing.

Immunohistochemistry: Spinal cord sections were permeabilized and non-specific IgG binding blocked with 10% normal goat serum (NGS) in 0.5% Triton X-100 (TBS-TX) for 1 hr. Primary antibodies in 1% NGS in TBS were applied to slides overnight at 4˚C. Then, slides were incubated with fluorophore-conjugated secondary antibodies for 2 hrs at room temperature, dehydrated with increasing ethanol concentrations (50%, 75%, and twice with 99% for 2 min each) and mounted with cytoseal or coverslipped without dehydration with Fluoromount G (Southern Biotech, Birmingham, AL, USA). The primary antibodies used were: polyclonal chicken anti-GFP (1:1000; Abcam, Toronto, ON, Canada), monoclonal (clone GA5) mouse anti-glial fibrillary acidic protein (GFAP; 1:700; Chemicon, Temecula, CA, USA), polyclonal rabbit anti-S100 (1:1000; Abcam), monoclonal (clone 192) mouse anti-p75 (1:500; Advanced Targeting Systems, SD, CA, USA), monoclonal (clone 2Q178) mouse anti-nestin (1:1000; Abcam), polyclonal rabbit anti-fibronectin (1:100; Chemicon), and polyclonal rabbit anti-ki-67 (1:100; Abcam).

Secondary antibodies used were: Alexa Fluor 488 goat anti-chicken, Alexa Fluor 555 goat anti-mouse, Alexa Fluor 555 goat anti-rabbit, Alexa Fluor 647 goat anti-mouse, and Alexa Fluor 647 goat anti-rabbit (1:500; all from Invitrogen).

Immunofluorescence imaging was carried out with an automated upright Leica DM6000 B microscope system (Leica Microsystems Inc., Richmond Hill, ON, Canada).

H&E stain: Horizontal sections of spinal cord were stained with hematoxylin and eosin. Slides were hydrated and stained with Ehrlich's hematoxylin for 10 min, followed by differentiation in 1% acid alcohol solution for 10 sec. Sections were "blued-up" with ammonia water solution (0.2% ammonium hydroxide in distilled water) for 1 min, stained with eosin for a few sec, dehydrated, cleared in two 5 min baths of xylene, and mounted with Permount^{R}. Staining was visualized with a Leica DMLB microscope (Leica Microsystems Inc.).

2.9 Quantification of cell survival and spread, cross-sectional lesion size, and lesion length

Cell survival: All analyses were carried out using ImageJ 1.43µ (National Institutes of Health, Bethesda, MD, USA), on five horizontal spinal cord sections 275 µm apart encompassing the lesion epicenter. The perimeter of each horizontal section was drawn and the GFP^+ region within the perimeter was thresholded. The entire horizontal section area in mm^2, area of the GFP^+ region in mm^2, and GFP^+ signal intensity (integrated density: mean grey value of pixels (MGV)*the area analyzed in mm^2) were measured and averaged across the five sections. The area of GFP^+ cells was calculated alone or as a percentage of the area of the horizontal section analyzed.

To estimate the number of surviving SKP-SCs, a z-stack in the center of a graft was captured at 630x with a Leica DMi8 confocal microscope (Leica Microsystems Inc.). Z step size was 0.5 µm. The number of GFP^+ cell bodies in the z-stack was counted using the cell counter plug-in on ImageJ 1.43µ. The "show all" option was selected, so that all cells counted were labeled and cells were not counted twice. Next, the steps of the z-stack were summed and the

resulting image was thresholded to identify the area (mm^2) of GFP^+ cells. The number GFP^+ cells was, then, divided by the GFP^+ area to determine the concentration of GFP^+ cells per unit area. The number of GFP^+ cells per section (Sn_{GFP^+cells}) was calculated by multiplying the GFP^+ area of each section (Sn_a) by the concentration of GFP^+ cells per unit area $[C]$:

$$(Sn_a\ x\ [C]) = Sn_{GFP^+cells}$$

To estimate the number of GFP^+ cells in between sections (Bn_{GFP^+cells}), the average GFP^+ area of two adjacent sections was taken, multiplied by the concentration of GFP^+ cells per unit area, and multiplied by the number of sections in-between adjacent sections on a slide (11 sections):

$$\{[(\frac{Sn_a + S_{n+1_a}}{2})x\ [C]]\}x\ 11 = Bn_{GFP^+\ cells}$$

Lastly, the total number of GFP^+ cells in the spinal cord of each animal (N_{GFP^+cells}) was calculated using the formula:

$$\sum_{n=1}^{5} Sn_{GFP^+cells} + \sum_{n=1}^{4} Bn_{GFP^+cells} = N_{GFP^+cells}$$

Cell spread: The rostral and caudal spread of the GFP^+ cells from the lesion epicenter, which was identified by an inward deformation of the parenchyma, was measured in mm using ImageJ 1.43µ. Results from five tissue sections 275 µm apart imaged at 50x were averaged. We measured the extent of cell spread using two methods. The first method took into consideration GFP^+ cells found within the spinal parenchyma and along the perimeter of the spinal cord. The second method excluded cells located in the perimeter.

Cross-sectional lesion size: Every horizontal spinal cord section comprising the SCI from one set of slides was imaged under phase-contrast microscopy. The lesion was identified by the

disruption of typically linear organization of white matter tracts on the outside of the spinal cord and the loss of darkly appearing cell bodies of the grey matter located centrally. Maximum lesions were re-constructed by hand on a T9 (overlayed by vertebra T8) cross-section schematic obtained from the Atlas of the Rat Spinal Cord (Watson et al., 2009). The area of the lesioned tissue was then calculated as a percentage of the T9 cross-sectional area.

Lesion length: Horizontal spinal cord sections comprising the SCI were stained for GFAP to show the lesion borders. Overview images of the sections at 50x magnification were analyzed on ImageJ 1.43µ. The distance in µm between the rostral and caudal lesion borders (i.e., the length of the lesion) was measured and averaged across five sections 275 µm apart.

2.10 White Matter Compression

Given the finding that grafted GFP^+ SKP-SCs appeared to form growths in the spinal cord, we evaluated if the growths were compressing surrounding spared white matter. One section encompassing the injury epicenter and stained for GFP and GFAP was analyzed. The thickness of the white matter in the hemicord opposite the transplant was measured in µm. The thickness of the white matter was also measured below the transplant. Only rats that were considered to have formed growths were included in this analysis (SCs:HAMC n = 5; SCs:eHAMC n = 6). White matter thickness of lesion only rats (n = 6) ~2000 µm above and below the SCI was measured as a control.

2.11 Transplant Morphological Assessment

Analysis of the transplant for features of Schwannomas was developed based on writings from *Nervous System: Cambridge Illustrated Surgical Pathology* by Hannes Voguel (2009).

Every other horizontal spinal cord section containing the transplant and stained with H&E was assessed under bright-field microscopy at 50x magnification. The presence of dense Antoni A cellular patterns with palisading nuclei surrounding pink regions (Verocay bodies), relatively sparse Antoni B areas (Wippold et al., 2007), and signs of hemorrhage, such as red pigmentation (Hatae et al., 2014), were recorded. The size and shape of the cells were evaluated under 100x magnification.

2.12 Statistical Analysis

All results were analyzed with GraphPad Prism 7 (GraphPad Software Inc., La Jolla, CA, USA). D'Agostino-Pearson omnibus test was used to assess normality. When data were normally distributed, paired and unpaired two-tailed t-tests were used to make between-group comparisons. Non-parametric alternatives used for unpaired and paired t-tests were Mann-Whitney U and Wilcoxon-matched pairs signed rank tests respectively. Kruskal-Wallis followed by Dunn's tests were used for comparing multiple groups. Cross-sectional lesion size and lesion length were first assessed with Kruskal-Wallis and, then, select pairs of data sets were compared with unpaired t-tests or Mann-Whitney U tests. Repeated measures two-way ANOVA followed by Bonferroni's post-test were used to compare weekly locomotor scores. Scores 1 week post-SCI (before transplants) were also analyzed to ensure all groups had similar motor deficits. Data are presented as mean values ± SEM, and the threshold for significance was set at a p-value of <0.05.

2.13 Experiments of SKP-SC grafts following hemi-contusion

We report on a second SKP-SCs transplantation experiment without the use of hydrogels or immune suppression. Experiment 2 was not intended as a direct comparison to experiment 1.

However, experiment 2 shows similar results of grafting SKP-SCs under very different conditions. All procedures were approved by the University of British Columbia Animal Care Committee in accordance with the guidelines of the Canadian Council on Animal Care.

Adult male Fischer rats (NHsd; 250-275 g; N = 31; Harlan, Indianapolis, IN, USA) were used in experiment 1. Rats (n = 26) underwent a unilateral C5 laminectomy followed by a hemi-contusion SCI on the left or right side of the spinal cord. The side of the hemi-contusion was based on paw preference as determined with the single pellet-grasping task developed by Whishaw et al. (1998). Contusions were carried out using the IH impactor with a force of 150 kdynes using a custom clamping system as previously described (Lee et al., 2012) and animal care was similar to that described for experiment 1.

To start a culture of SKPs, a group of rats (n = 5) were euthanized upon arrival to the animal facility. Briefly, the back of the rats was shaved and back skin samples were collected and placed in 50 ml falcon tubes in DMEM with low glucose, placed on ice, and shipped to the University of Calgary, where SKPs were isolated, differentiated into SCs and labeled with GFP. Cell culturing and transduction methods were as described for experiment 1.

Rats received cell (SKP-SC group n = 13) or media injections (injury only control group n = 13) 2 weeks post-SCI. GFP^+ SKP-SCs were re-suspended in DMEM and a Hamilton microsyringe was used to inject 1 µl of cell suspension (~200,000 cells) into the lesion cavity. One week following transplantation, SKP-SC rats demonstrated a health decline and deterioration of forelimb function. Rats were perfused 1-4 weeks post-transplantation when they reached a pre-determined experimental termination point. The termination point was defined as loss of 15% of the original body weight, porphyrin staining around the eyes, and paralysis of the

upper limbs. All injury only rats were perfused 4 weeks post-media injections. Animals received a lethal dose of chloral hydrate (100 mg/kg, IP; BDH VWR Analytical, Radnor, PA, USA) and were transcardially perfused with PBS followed by 4% PFA. The cords were post-fixed in 4% PFA overnight, cryoprotected in graded sucrose solutions and frozen in O.C.T (Fisher Scientific). The injured tissue was sectioned in 20 μm cross-sections.

Tissue from a subset of rats (SKP-SCs n = 5; injury only n = 6) underwent immunohistochemistry to identify the status of the lesion site at 4-5 weeks post-injury (2-3 weeks post-transplantation). For immunohistochemistry, frozen sections were thawed, rehydrated and incubated in 10% normal donkey serum for 30 min and primary antibodies were applied overnight. After washes, secondary antibodies were applied for 2 hrs, and slides were washed and coverslipped. The following primary antibodies were used: mouse anti-neurofilament 200 (NF-200; 1:500; Sigma-Aldrich Canada Ltd.); mouse anti-β-3-tubulin (βIII-tubulin; 1:500; Sigma-Aldrich Canada Ltd.), goat anti-GFP (1:200; Rockland Immunochemicals, Gilbertsville, PA, USA), and rabbit anti-GFAP (1:1000; Dako Canada ULC, Mississauga, ON, Canada). Axons were stained using a combination of NF-200 and βIII-tubulin. The secondary antibodies were generated in donkey and directed to the host of the primary antibody and conjugated with Alexa Fluor fluorochromes 405, 488, and 594 at a concentration of 1:200 (Jackson ImmunoResearch Laboratories, West Grove, PA, USA). Immunofluorescence was captured using a Zeiss AxioObserver Z1 inverted confocal microscope fitted with Yokogawa spinning disk and Zen 2012 software (Zeiss, North York, ON, Canada).

3. Results

3.1 SKP-SCs survive in the injured rat spinal cord 8 weeks post-grafting independent of the

delivery vehicle

To measure survival of grafted cells, the GFP^+ area in the spinal cord was compared between animals that received GFP^+ SKP-SCs in either HAMC or eHAMC. The area covered by SKP-SCs was not significantly different ($p = 0.71$) between the HAMC (0.76 ± 0.35 mm^2) and eHAMC (0.94 ± 0.33 mm^2) groups (Figure 1B). The area populated by GFP^+ cells as a percentage of the horizontal section area also did not differ statistically ($p = 0.72$) between HAMC ($1.8 \pm 0.73\%$) and eHAMC ($2.7 \pm 1.1\%$) groups (Figure 1C). The third measure of cell survival integrated density (see methods) did not show statistical differences ($p = 0.59$; HAMC 34 ± 15 MGV*mm^2; eHAMC 46 ± 16 MGV*mm^2; Figure 1D). Finally, the estimated number of GFP^+ cells was not statistically different ($p = 0.62$; HAMC $1{,}195{,}774 \pm 565{,}604$ GFP^+ cells; eHAMC $1{,}596{,}055 \pm 557{,}613$ GFP^+ cells). This means that ~6x the number of originally grafted cells (~200,000) were found in the spinal cord of HAMC animals and ~8x the number of originally grafted cells were found in the spinal cord of eHAMC animals. These estimates suggest GFP^+ SKP-SCs proliferated post-grafting. It should be noted, two rats from the HAMC group and two rats from the eHAMC group exhibited <10% survival of originally grafted cells. Thus, these rats were excluded from the analysis of cell spread. The majority of cells identified by thresholding were located up to 15 mm beyond the injury/transplantation site.

3.2 SKP-SC transplantation had no effect on the recovery of open-field locomotion

The BBB locomotor rating scale was used to determine the influence of SKP-SC transplantation and hydrogel formulation on functional recovery. Locomotor scores were comparable between groups 1 week after hemisection SCI ($p = 0.64$). As to be expected following a hemisection, open-field scores were significantly improved from week 1 to week 8

post-SCI ($p < 0.0001$****); however, there was no significant difference between the treatment groups in terms of BBB scores at any time point ($p = 0.75$; Figure 2A). Average BBB scores were not significantly different from week 6 to week 8 post-SCI: 13 ± 0.26 to 12.8 ± 0.31; 13.1 ± 0.41 to 12.6 ± 0.39; 12.8 ± 0.19 to 11.4 ± 1.57; and 12.6 ± 0.29 to 11.8 ± 0.74 for the lesion only control, eHAMC, SCs:HAMC, and SCs:eHAMC groups respectively. While the group averages were not significantly different, we noted that between 6 and 8 weeks post-SCI one animal in the SCs:HAMC (score 12 to 0.5) and one in the SCs:eHAMC (score 11.5 to 6.8) groups lost weight-supported hindlimb stepping (Figure 2B). A BBB score of at least 10 represents weight-supported plantar stepping. Weight-supported stepping of rats that did not receive cells was unaffected.

3.3 SKP-SCs spread in spinal parenchyma and along the spinal perimeter

Grafted GFP^+ SKP-SCs spread to undamaged spinal cord tissue near the site of injury in every subject with clear borders between the graft and host tissue. This is shown by the distinct separation between reactive astrocytes and grafted cells, irrespective of where grafted cells where found in the spinal cord (Figure 3). Spread of grafted cells to the perimeter of the spinal cord was seen in all animals. Large masses/growths of GFP^+ cells were found in areas of originally uninjured parenchyma in 5 out of n = 8 HAMC and 6 out of n = 8 eHAMC rats (Figure 4). Masses of GFP^+ cells were considered growths if the masses had more than 2x the original number of grafted cells, morphological features of Schwannomas, and ki-67 positivity.

To further characterize the spread of grafted GFP^+ SKP-SCs, we measured the distance covered by the cells. Distance spread in both parenchyma and along the perimeter did not differ between the SCs:HAMC or SCs:eHAMC groups (Figure 5A; $p = 0.24$). The mean total distance

in mm covered by SCs:HAMC and SCs:eHAMC cells was 12 ± 1.3 mm and 8.8 ± 1.3 mm respectively. The distance GFP^+ SKP-SCs spread exclusively in the parenchyma was comparable between the SCs:HAMC and SCs:eHAMC groups (Figure 5B; $p = 0.39$). The distance covered by the cells within the parenchyma alone was 6.0 ± 1.6 mm and 6.6 ± 0.70 mm for the SCs:HAMC and SCs:eHAMC groups respectively.

Grafted cells spread both rostral and caudal to the SCI. No statistically significant difference was found on the direction of spread. When transplanted in HAMC, cells expanded a total distance of 7.1 ± 1.1 mm rostrally and 4.6 ± 1.1 mm caudally ($p = 0.31$). In eHAMC, cells expanded a total distance of 5.9 ± 1.0 mm rostrally and 3.0 ± 1.1 mm caudally ($p = 0.31$; Figure 5C). Spread in the parenchyma alone was similar with cells expanding both rostrally and caudally in the HAMC (rostral spread: 4.6 ± 1.5 mm; caudal spread: 1.4 ± 0.5 mm; $p = 0.06$) and eHAMC (rostral spread: 5.2 ± 1.1 mm; caudal spread: 1.4 ± 0.5 mm; $p = 0.16$; Figure 5D) groups.

3.4 Graft demonstrated morphological features of a Schwannoma

Comparable to Schwannomas, regions with a high density of cells (Antoni A; Wippold et al., 2007) were found immediately adjacent to regions with few cells (Antoni B; Figure 6A). Overall, GFP^+ SKP-SCs demonstrated a typical SC spindle-like morphology (Figure 6A&B). However, as is seen in Schwannomas, the nuclei were arranged in horizontal rows, termed palisades, and there was a large degree of pleomorphism (Figure 6A&B). Nuclear palisades are normally separated by anuclear zones, forming a Verocay body. Verocay body anuclear zones were not observed, signalling high mitotic activity (Rodriguez et al., 2012). Instead, rows of palisading nuclei in Antoni A regions had a marginal space between them (Figure 6C). There

was evidence of bleeding in and around the graft that may have been caused by the growing mass of GFP^+ cells compressing the spinal cord and damaging local blood vessels (Figure 6C&D).

3.5 Transplanted cells express markers for immature SCs and proliferation antigen ki-67

Transplanted GFP^+ cells expressed p75 and S100, common SC markers (Figure 7A&B). Many of the GFP^+ cells did not stain for either of these markers, raising the possibility that a subset of the SKP-SCs were dedifferentiated, proliferating immature SCs. Staining for immature SC markers nestin and fibronectin showed co-labeling with GFP^+ cells (Figure 7C&D), suggesting the SCs lack a mature phenotype. Ki-67 positive signal confirmed the continued proliferation of GFP^+ cells 8 weeks post-grafting, as ki-67 signal overlapped with GFP^+ cell bodies (Figure 8).

3.6 Cell transplantation in eHAMC resulted in greater cross-sectional lesion size and longer lesions

Grey and white matter lesioned tissue was identified on horizontal sections imaged under phase-contrast microscopy and reconstructed on cross-section schematics. Lesioned tissue at the SCI epicenter as a percent of cross-sectional area was significantly different between groups (Figure 9; $p < 0.05$). However, Dunn's multiple comparisons test did not identify a difference between group pairs. Group pairs were then compared with Mann-Whitney U, and we discovered that the SCs:eHAMC group had significantly greater cross-sectional lesions compared to the lesion only and eHAMC groups (both $p < 0.05$). Cross-sectional lesion size was comparable between lesion only vs eHAMC ($p = 0.63$), SCs:eHAMC vs SCs:HAMC ($p = 0.08$), eHAMC vs SCs:HAMC ($p > 0.99$), and lesion only vs SCs:HAMC ($p = 0.85$). Percent cross-

sectional lesion size averaged 73 ± 5.0% for SCs:HAMC, 82 ± 2.6% for SCs:eHAMC, 71 ± 4.8% for eHAMC, and 71 ± 3.7% for the lesion control groups.

The lesion length was analyzed on horizontal spinal cord sections stained for the astrocyte marker GFAP. Statistical analysis with Kruskal-Wallis test did not detect a group effect on lesion length (Figure 9; $p = 0.15$), although there was marked variation within the animals that received SKP-SCs, particularly when grafted in combination with eHAMC. Therefore, data pairs were then compared with unpaired t-tests and Mann-Whitney U tests. We found that lesion length was significantly greater between the SCs:eHAMC and lesion only control group ($p < 0.05$). No differences were found between lesion only vs eHAMC ($p = 0.37$), SCs:eHAMC vs eHAMC ($p = 0.05$), SCs:eHAMC vs SCs:HAMC ($p = 0.45$), eHAMC vs SCs:HAMC ($p = 0.54$), and lesion only vs SCs:HAMC ($p = 0.95$) groups. The average spinal cord lesion length of the SCs:HAMC, SCs:eHAMC, eHAMC, and lesion only groups were 2.8 ± 1.1, 3.8 ± 0.90, 1.6 ± 0.17, and 1.5 ± 0.30 mm respectively. The finding that the eHAMC cell transplant group had longer lesions is consistent with the observation that GFP^+ signal corresponded perfectly with areas devoid of GFAP labeling.

3.7 SKP-SC growths resulted in compression of spared white matter

Host spinal cord tissue appeared distorted where GFP^+ cells were abundant. Apparent distortion of host tissue prompted analysis of white matter compression. White matter thickness on horizontal sections was similar rostral and caudal to the SCI in lesion only control animals ($p = 0.44$). In these rats, the white matter rostral to the lesion was 677 ± 37 μm thick and the white matter caudal to the lesion was 792 ± 51 μm thick. In SCs:HAMC rats, white matter thickness contralateral to growths and intact tissue was comparable ($p = 0.06$). SCs:HAMC rat white

matter contralateral to growths was 585 ± 107 μm thick and white matter contralateral to intact tissue was 882 ± 82 μm. Contrastingly, SCs:eHAMC rat white matter contralateral to growths was thinner than white matter contralateral to intact tissue ($p < 0.05$; Figure 10). SCs:eHAMC white matter contralateral to transplants was 517 ± 68 μm thick and white matter contralateral to intact tissue was 811 ± 44 μm. In other words, grafted cell growths compressed the white matter of SCs:eHAMC rats only.

3.8 SKP-SCs were mycoplasma positive

In order to investigate possible reasons for excessive cell division, we examined SKP-SC cell lines for the presence of mycoplasma, which has been shown to hasten transformation of cells *in vitro* (Tsai et al., 1995; Feng et al., 1999). Both of the GFP^+ adult SKP-SC lines were found to be positive for mycoplasma, suggesting mycoplasma contamination may have contributed to the uncontrolled proliferation of grafted cells (Namiki et al., 2009).

3.9 SKP-SCs form growths within 4 to 6 weeks post-contusion SCI without HAMC

In an independent experiment, immune competent animals with a contusion SCI had cells transplanted in media or media only injections. The reason for including this study was to show that growth formation can occur with adult SKP-SCs under markedly different conditions.

Many SKP-SC animals demonstrated a behavioural decline 1-4 weeks post-transplantation, reaching pre-determined experiment termination points and as such were euthanized for histological analysis of the injury site. Of the SKP-SC rats: 50% reached the termination point and were perfused before 4 weeks post-transplantation; another 30-40% demonstrated severe health or behavioural deficits compared to control rats when perfused at 4

weeks post-transplantation; and only 10-20% appeared in relatively good health at the time of perfusion. In contrast, not a single rat from the injury only control group showed behavioural deterioration or reached the termination point by 4 weeks post-transplantation.

GFP^+ growths were found in all the spinal cords of the subset of SKP-SC transplanted rats sectioned for histological analysis. Growths were not found in any of the rats without grafts (Figure 11A). The growths filled the injured cord but also spread to the uninjured cord and resulted in a dramatic decrease in the amount of axons at the injury site (Figure 11B&C), likely contributing to the severe behavioural deficits observed.

4. Discussion

In order to create a bridge for regenerating axons, SCs are generally injected into the cavity that forms within the spinal cord after damage (Bunge, 1975; Oudega & Xu, 2006; Tetzlaff et al., 2011; Thuret et al., 2006; Williams et al., 2015). However, the optimal source of SCs and the approach to ensure maximal graft survival have yet to be determined. SCs may be obtained from peripheral nerves (Murray & Stout, 1942) or differentiated from neonatal or adult skin-derived progenitors (Biernaskie et al., 2007a; Kumar, Sinha et al. 2016). Harvesting SKPs is associated with fewer safety concerns and less associated with morbidity than harvesting peripheral nerve SCs (Biernaskie et al., 2007a). Therefore, SKP-SCs were grafted in the present study. Regardless of source, low survival of SCs post-transplantation is a continuing challenge (Biernaskie et al., 2007b; Enomoto et al., 2013; Golden et al., 2007; Pearse et al., 2007). Transplanted SC death results from a combination of factors, including disruption of blood vessels causing ischemic necrosis (Balentine, 1978), the inflammatory environment of the injured spinal cord (Hill et al., 2006), and anoikis (Frisch & Francis, 1994; Koda et al., 2008).

The goal of our study was to maximize SKP-SC survival and, hence, cavity filling in the injured rat spinal cord.

To resolve the contribution of inflammation and anoikis on grafted cell loss, we transplanted SKP-SCs in HAMC containing hydrogels. HAMC hydrogel is injectable through a fine gauge needle, biocompatible and biodegradable (Caicco et al., 2013). HAMC hydrogel intrathecal injection reduces inflammation in a rat model of spinal cord arachnoid inflammation (Austin et al., 2012). As an additional measure to inhibit graft rejection, we pharmacologically suppressed the immune system of rats in our study. Anoikis can be triggered when anchorage-dependent cells are detached from their substrate for transplantation, especially into a cavity formed at the epicenter of a SCI. Transplantation of SKP-SCs in viscous hydrogels served the additional purpose of preventing anoikis by providing a polymer network for cell attachment. Further, SKP-SCs were grafted in a modified version of HAMC called eHAMC, where laminin- and fibronectin-derived peptide sequences were conjugated to MC. Laminin mediates SC attachment to substrata (Tohyama & Ide, 1984) and fibronectin promotes SC attachment and attracts SCs through chemotaxis (Baron-Van Evercooren et al., 1982). Hence, we predicted eHAMC would further reduce anoikis by promoting cell attachment compared to HAMC vehicle, resulting in improved filling of the cavity.

SKP-SCs survived when grafted in HAMC or eHAMC, showing both are supportive hydrogels for transplantation. The polymer network formed by hyaluronan (HA) and methylcellulose (MC) may be sufficient to stop anoikis and sustain cell viability. In fact, HA is a nonsulfated glycosaminoglycan found naturally in the ECM of nervous tissue (Vercruysse & Prestwich, 1998) that exists as a viscous liquid due to molecular entanglements between its long

disaccharide polymers (Balazs, 1991). MC forms hydrophobic junctions thereby forming a gel (Schupper et al., 2008). The SKP-SCs could have interacted with the HA of HAMC via the CD44 transmembrane glycoprotein, which is expressed in high amounts in neonatal SCs and in varying amounts in adult SCs (Sherman et al., 2000). Possibly, this mechanical support provided by MC and molecular interactions with HA could have prevented anoikis, explaining why the addition of fibronectin and laminin peptide sequences to eHAMC had no further impact on cell survival. Alternatively, transformation of SKP-SCs to an oncogenic state might have overridden the effect of eHAMC on cell survival.

The original goal of this study was to inject SKP-SCs into the SCI site with the intention of filling the cavity and forming a bridge for growing axons. However, SKP-SCs formed large growths in the spinal cord of the majority of grafted animals (SCs:HAMC 5 out of n = 8; SCs:eHAMC 6 out of n = 8). Given this alarming finding, the remainder of the discussion will focus on the oncogenic behaviour of SKP-SCs in our study. SKP-SCs were found several mm rostral and caudal to the SCI site. This may have been the result of hyper-proliferation of oncogenic SKP-SCs in the spinal cord, resulting in their expansion outside the injection site. Alternatively, oncogenic SKP-SCs may have migrated to other locations of the spinal cord through the spinal canal. Although rare, migration of spinal Schwannomas has previously been reported in humans (Khan et al., 2013).

The locomotor ability of two rats with SKP-SC growths (one from each cell transplantation group) deteriorated markedly and suddenly. The rats lost the ability for weight supported plantar stepping in the span of 2 weeks. However, we did not see a group difference in locomotor function. This may be explained by the distribution of the growths. The masses

differed in size, and were sometimes located unilaterally and sometimes bilaterally. It is known that even a small percentage of remaining white matter in the ventral funiculus is enough to support rhythmic hindlimb movements (BBB score 8; Schucht et al., 2002). Therefore, it is not surprising that rats with large unilateral masses, such as #2 in Figure 4, scored an average BBB score of 13. In other words, rat #2 could make coordinated weight-supported steps. In contrast, the rats that became paralyzed in a short span of time had bilateral growths, essentially making a complete spinal cord injury (rat from Figure 3 and #1 from Figure 4). Hence, obvious locomotor deterioration in a longer-term study would have depended on the directionality of the expansion of the growths. That is not to say that none of the other transplanted rats had motor deficits at the time of euthanasia. The applied open-field testing was probably not sensitive enough to detect subtle changes.

Lesion size analysis showed SCs:eHAMC rats had larger lesions compared to the lesion only control and HAMC vehicle groups. Further, spared white matter was compressed in SCs:eHAMC rats, which was not seen in SCs:HAMC rats or lesion only controls. These injuries were not due to the original SCIs, as they far exceeded a hemisection. Further evidence for the cell graft induced expansion of the injury comes from the finding that directly after injury (before cells were grafted) BBB scores were comparable between groups. Additionally, the lesion area corresponded to the spread of grafted cells. Thus, SKP-SC transplantation in eHAMC exacerbated the original SCI, deformed and possibly affected the function of initially spared tissue.

While growths were not restricted to the SCs:eHAMC group, the addition of laminin and fibronectin peptide sequences may have further increased SKP-SC mitotic activity. In fact,

laminin is required for SC proliferation during development and provides a PI3-kinase/Akt-mediated survival signal (Yu et al., 2005; Yu et al., 2009), while fibronectin markedly stimulates rat SC proliferation in culture (Baron-Van Evercooren et al., 1982). Hence, the advantages of attachment, survival, and growth-promoting factor inclusion in cell therapy vehicles should be weighed against the possibility of potentiating uncontrolled cell division. Furthermore, the addition of immune suppression interferes with endogenous mechanisms for detection and removal of oncogenic cells (Anderson et al., 2011; Dressel et al., 2008; Itakura et al., 2015). The role of the hydrogels in the formation of growths is clarified by experiment 2, performed without a hydrogel or immune suppressive agent. The results of experiment 2 demonstrate that hyper-proliferation may occur in the absence of both factors. The inclusion of this experiment should not be viewed as a comparison to experiment 1, but as evidence that hyper-proliferation of SKP-SCs post-grafting is not an isolated event and may occur in a variety of conditions.

Further characterization of the phenotype of the transplanted cells revealed that the cell masses resembled Schwannomas morphologically and expressed SC markers. Notably, a subset of GFP^+ cells did not express SC markers and appeared to take on a fibroblastic morphology, indicating that SKP-SCs may have adopted alternate fates within the injured spinal cord. It is also possible that the SKP-SCs acquired mutations in culture that prevented full maturation and allowed them to maintain an undifferentiated proliferative state leading to the exacerbated growths observed. This is supported by the finding that grafted cells expressed immature SC markers nestin and fibronectin and the proliferation antigen ki-67.

Interestingly, neonatal mouse and rat SKP-SCs grown under identical conditions (with neuregulin and forskolin) to those in the present study never exhibited uncontrolled growth even

after long-term transplantation (Biernaskie et al., 2007b; Kumar et al., 2016; McKenzie et al 2006), suggesting that adult SKP-SCs may be more susceptible to chromosomal aberration particularly during excessive cell division. This is consistent with reports that neonatal nerve-derived SCs "aged" through extended expansion (>20 passages) acquire chromosomal abnormalities (Funk et al., 2007). Our data here suggests that unlike neonatal cells, adult SKP-SCs undergo hastened transformation (5-10 passages) following extended culture in the presence of mitogens.

Further, propagation of large numbers of cells from a small starting pool, may inadvertently select for the cells that have acquired these proliferation-promoting mutations. Given that transformation of SKP-SCs is as prevalent with nerve-derived SCs exposed to parallel levels of expansion *in vitro*, there is no additional concern with SKP-derived relative to nerve-derived sources of SCs. Therefore, SKP-derived SCs remain a viable alternative source for SCs to repair the injured nervous system. Another factor that might have contributed to the oncogenic state of grafted cells is exposure to mycoplasma. We found at the conclusion of the experiment, GFP^+ lines 1 and 3 from experiment 1 were both positive for mycoplasma. Mycoplasma has previously been reported to contribute to malignant transformation of mammalian cell types to a hyper-proliferative, oncogenic phenotype (Namiki et al., 2009).

The present article highlights the vulnerability of adult SKP-SCs to transformation and importance of updating current cell culture strategies in pre-clinical research laboratories. We suggest that genetic indicators of transformation and incorporated suicide genes are not only applicable to pluripotent derivatives, but should also be considered for other proliferative progenitors, such as SKP-SCs, being used for cell therapy in order to improve safety for clinical

trials. Ultimately, defining meticulous guidelines for culture expansion that preserve normal SKP-SC function and that of other cell types will be important toward enabling safe and effective clinical translation.

Acknowledgements

The authors acknowledge Romana Vavrek for excellent technical assistance. These studies were supported by CIHR (RES0011338, KF) and CIHR Foundation Grant (MSS) in Canada.

References

Akbik, F., Cafferty, W. B. J., & Strittmatter, S. M. (2012). Myelin associated inhibitors: A link between injury-induced and experience-dependent plasticity. *Experimental Neurology*, *235*(1), 43–52. https://doi.org/10.1016/j.expneurol.2011.06.006

Anderson, A. J., Haus, D. L., Hooshmand, M. J., Perez, H., Sontag, C. J., & Cummings, B. J. (2011). Achieving stable human stem cell engraftment and survival in the CNS: is the future of regenerative medicine immunodeficient? Regenerative Medicine, 6(3), 367–406. http://doi.org/10.2217/rme.11.22

Austin, J. W., Kang, C. E., Baumann, M. D., DiDiodato, L., Satkunendrarajah, K., Wilson, J. R., … Fehlings, M. G. (2012). The effects of intrathecal injection of a hyaluronan-based hydrogel on inflammation, scarring and neurobehavioural outcomes in a rat model of severe spinal cord injury associated with arachnoiditis. *Biomaterials*, *33*(18), 4555–4564. http://doi.org/10.1016/j.biomaterials.2012.03.022

Balazs, E. A. (1991). Medical Applications of Hyaluronan and its Derivatives. In *Cosmetic and*

pharmaceutical applications of polymers (pp. 293–310). New York: Plenum Press.

Balentine, J. D. (1978). Pathology of experimental spinal cord trauma. I. The necrotic lesion as a function of vascular injury. *Laboratory Investigation; a Journal of Technical Methods and Pathology*, *39*(3), 236–253.

Ballios, B. G., Cooke, M. J., Donaldson, L., Coles, B. L. K., Morshead, C. M., van der Kooy, D., & Shoichet, M. S. (2015). A Hyaluronan-Based Injectable Hydrogel Improves the Survival and Integration of Stem Cell Progeny following Transplantation. *Stem Cell Reports*, *4*(6), 1031–1045. http://doi.org/10.1016/j.stemcr.2015.04.008

Ballios, B. G., Cooke, M. J., van der Kooy, D., & Shoichet, M. S. (2010). A hydrogel-based stem cell delivery system to treat retinal degenerative diseases. *Biomaterials*, *31*(9), 2555–2564. http://doi.org/10.1016/j.biomaterials.2009.12.004

Baron-Van Evercooren, A., Kleinman, H. K., Seppä, H. E., Rentier, B., & Dubois-Dalcq, M. (1982). Fibronectin promotes rat Schwann cell growth and motility. *The Journal of Cell Biology*, *93*(1), 211–216.

Basso, D. M., Beattie, M. S., & Bresnahan, J. C. (1995). A sensitive and reliable locomotor rating scale for open field testing in rats. *Journal of Neurotrauma*, *12*(1), 1–21. http://doi.org/10.1089/neu.1995.12.1

Biernaskie, J. A., McKenzie, I. A., Toma, J. G., & Miller, F. D. (2007). Isolation of skin-derived precursors (SKPs) and differentiation and enrichment of their Schwann cell progeny. *Nature Protocols*, *1*(6), 2803–2812. http://doi.org/10.1038/nprot.2006.422

Biernaskie, J., Sparling, J. S., Liu, J., Shannon, C. P., Plemel, J. R., Xie, Y., … Tetzlaff, W. (2007). Skin-Derived Precursors Generate Myelinating Schwann Cells That Promote Remyelination and Functional Recovery after Contusion Spinal Cord Injury. *Journal of Neuroscience*, *27*(36), 9545–9559. http://doi.org/10.1523/JNEUROSCI.1930-07.2007

Bunge, R. P. (1975). Changing uses of nerve tissue culture 1950-1975. In *The Nervous System* (Vol. 1. The Basic Neuroscience). New York: Raven Press.

Cafferty, W. B. J., Duffy, P., Huebner, E., & Strittmatter, S. M. (2010). MAG and OMgp Synergize with Nogo-A to Restrict Axonal Growth and Neurological Recovery after Spinal Cord Trauma. *Journal of Neuroscience*, *30*(20), 6825–6837. https://doi.org/10.1523/JNEUROSCI.6239-09.2010

Caicco, M. J., Zahir, T., Mothe, A. J., Ballios, B. G., Kihm, A. J., Tator, C. H., & Shoichet, M. S. (2013). Characterization of hyaluronan-methylcellulose hydrogels for cell delivery to the injured spinal cord. *Journal of Biomedical Materials Research. Part A*, *101*(5), 1472–1477. http://doi.org/10.1002/jbm.a.34454

Choppa, P. ., Vojdani, A., Tagle, C., Andrin, R., & Magtoto, L. (1998). Multiplex PCR for the detection of Mycoplasma fermentans, M. hominisandM. penetransin cell cultures and blood samples of patients with chronic fatigue syndrome. *Molecular and Cellular Probes*, *12*(5), 301–308. https://doi.org/10.1006/mcpr.1998.0186

Craig, W. S., Cheng, S., Mullen, D. G., Blevitt, J., & Pierschbacher, M. D. (1995). Concept and progress in the development of RGD-containing peptide pharmaceuticals. *Biopolymers*, *37*(2), 157–175. http://doi.org/10.1002/bip.360370209

Dressel, R., Schindehütte, J., Kuhlmann, T., Elsner, L., Novota, P., Baier, P. C., … Mansouri, A. (2008). The Tumorigenicity of Mouse Embryonic Stem Cells and In Vitro Differentiated Neuronal Cells Is Controlled by the Recipients' Immune Response. *PLoS ONE*, *3*(7), e2622. http://doi.org/10.1371/journal.pone.0002622

Enomoto, M., Bunge, M. B., & Tsoulfas, P. (2013). A multifunctional neurotrophin with reduced affinity to p75NTR enhances transplanted Schwann cell survival and axon growth after spinal cord injury. *Experimental Neurology*, *248*, 170–182. https://doi.org/10.1016/j.expneurol.2013.06.013

Fawcett, J. W., & Asher, R. A. (1999). The glial scar and central nervous system repair. *Brain Research Bulletin*, *49*(6), 377–391.

Feng, S. H., Tsai, S., Rodriguez, J., & Lo, S. C. (1999). Mycoplasmal infections prevent apoptosis and induce malignant transformation of interleukin-3-dependent 32D hematopoietic cells. *Molecular and Cellular Biology*, *19*(12), 7995–8002.

Fitch, M. T., Doller, C., Combs, C. K., Landreth, G. E., & Silver, J. (1999). Cellular and molecular mechanisms of glial scarring and progressive cavitation: in vivo and in vitro analysis of inflammation-induced secondary injury after CNS trauma. *The Journal of Neuroscience: The Official Journal of the Society for Neuroscience*, *19*(19), 8182–8198.

Flora, G., Joseph, G., Patel, S., Singh, A., Bleicher, D., Barakat, D. J., … Pearse, D. D. (2013). Combining Neurotrophin-Transduced Schwann Cells and Rolipram to Promote Functional Recovery From Subacute Spinal Cord Injury. *Cell Transplantation*, *22*(12), 2203–2217. http://doi.org/10.3727/096368912X658872

Fouad, K., Schnell, L., Bunge, M. B., Schwab, M. E., Liebscher, T., & Pearse, D. D. (2005). Combining Schwann cell bridges and olfactory-ensheathing glia grafts with chondroitinase promotes locomotor recovery after complete transection of the spinal cord. *The Journal of Neuroscience: The Official Journal of the Society for Neuroscience*, *25*(5), 1169–1178. http://doi.org/10.1523/JNEUROSCI.3562-04.2005

Frisch, S. M., & Francis, H. (1994). Disruption of epithelial cell-matrix interactions induces apoptosis. *The Journal of Cell Biology*, *124*(4), 619–626. http://doi.org/10.1083/jcb.124.4.619

Führmann, T., Tam, R. Y., Ballarin, B., Coles, B., Elliott Donaghue, I., van der Kooy, D., … Shoichet, M. S. (2016). Injectable hydrogel promotes early survival of induced pluripotent stem cell-derived oligodendrocytes and attenuates longterm teratoma formation in a spinal cord injury model. *Biomaterials*, *83*, 23–36. http://doi.org/10.1016/j.biomaterials.2015.12.032

Funakoshi, H., Frisén, J., Barbany, G., Timmusk, T., Zachrisson, O., Verge, V. M., & Persson, H. (1993). Differential expression of mRNAs for neurotrophins and their receptors after axotomy of the sciatic nerve. *The Journal of Cell Biology*, *123*(2), 455–465.

Funk, D., Fricke, C., & Schlosshauer, B. (2007). Aging Schwann cells in vitro. *European Journal of Cell Biology*, *86*(4), 207–219. http://doi.org/10.1016/j.ejcb.2006.12.006

Gilmore, A. P. (2005). Anoikis. *Cell Death and Differentiation*, *12*, 1473–1477. https://doi.org/10.1038/sj.cdd.4401723

Golden, K. L., Pearse, D. D., Blits, B., Garg, M. S., Oudega, M., Wood, P. M., & Bunge, M. B.

(2007). Transduced Schwann cells promote axon growth and myelination after spinal cord injury. *Experimental Neurology*, *207*(2), 203–217. https://doi.org/10.1016/j.expneurol.2007.06.023

Gupta, D., Tator, C. H., & Shoichet, M. S. (2006). Fast-gelling injectable blend of hyaluronan and methylcellulose for intrathecal, localized delivery to the injured spinal cord. *Biomaterials*, *27*(11), 2370–2379. http://doi.org/10.1016/j.biomaterials.2005.11.015

Hagg, T., & Oudega, M. (2006). Degenerative and spontaneous regenerative processes after spinal cord injury. *Journal of Neurotrauma*, *23*(3/4), 264-280. http://doi.org/10.1089/neu.2006.23.263

Hannes, V. (2009). *Nervous System (Cambridge Illustrated Surgical Pathology)*. L. Weiss (Ed.). New York, NY: Cambridge University Press. http://dx.doi.org/10.1017/CBO9780511581076

Hatae, R., Miyazono, M., Kohri, R., Maeda, K., & Naito, S. (2014). Trochlear nerve schwannoma with intratumoral hemorrhage presenting with persistent hiccups: a case report. *Journal of Neurological Surgery Reports*, *75*(1), 183-188. http://doi.org/10.1055/s-0034-1378156

Hill, C. E., Moon, L. D. F., Wood, P. M., & Bunge, M. B. (2006). Labeled Schwann cell transplantation: Cell loss, host Schwann cell replacement, and strategies to enhance survival. *Glia*, *53*(3), 338–343. https://doi.org/10.1002/glia.20287

Horn, K. P., Busch, S. A., Hawthorne, A. L., van Rooijen, N., & Silver, J. (2008). Another barrier to regeneration in the CNS: Activated macrophages induce extensive retraction of

dystrophic axons through direct physical interactions. *Journal of Neuroscience*, *28*(38). 9330-41. http://doi.org/10.1523/JNEUROSCI.2488-08.2008

Itakura, G., Kobayashi, Y., Nishimura, S., Iwai, H., Takano, M., Iwanami, A., … Nakamura, M. (2015). Controlling Immune Rejection Is a Fail-Safe System against Potential Tumorigenicity after Human iPSC-Derived Neural Stem Cell Transplantation. *PLOS ONE*, *10*(2), e0116413. http://doi.org/10.1371/journal.pone.0116413

Joannides, A., Gaughwin, P., Schwiening, C., Majed, H., Sterling, J., Compston, A., & Chandran, S. (2004). Efficient generation of neural precursors from adult human skin: astrocytes promote neurogenesis from skin-derived stem cells. *Lancet (London, England)*, *364*(9429), 172–178. http://doi.org/10.1016/S0140-6736(04)16630-0

Khan, R. A., Rahman, A., Bhandari, P. B., & Khan, S. K. N. (2013). Double migration of a schwannoma of thoracic spine. *Case Reports*, *2013*(jan23 3), bcr2012008182-bcr2012008182. https://doi.org/10.1136/bcr-2012-008182

Koda, M., Someya, Y., Nishio, Y., Kadota, R., Mannoji, C., Miyashita, T., … Yamazaki, M. (2008). Brain-derived neurotrophic factor suppresses anoikis-induced death of Schwann cells. *Neuroscience Letters*, *444*(2), 143–147. https://doi.org/10.1016/j.neulet.2008.07.055

Kontoveros, D. (2015). *Schwann cell proliferation and migration in response to surface bound peptides for nerve regeneration* (Master's dissertation). Retrieved from OhioLINK, Electronic Theses and Dissertations Center. (akron1431035725)

Kumar, R., Sinha, S., Hagner, A., Stykel, M., Raharjo, E., Singh, K. K., … Biernaskie, J. (2016).

Adult skin-derived precursor Schwann cells exhibit superior myelination and regeneration supportive properties compared to chronically denervated nerve-derived Schwann cells. *Experimental Neurology*, *278*, 127–142. http://doi.org/10.1016/j.expneurol.2016.02.006

Lee, J. H., Streijger, F., Tigchelaar, S., Maloon, M., Liu, J., Tetzlaff, W., & Kwon, B. K. (2012). A contusive model of unilateral cervical spinal cord injury using the infinite horizon impactor. *Journal of Visualized Experiments*, *65*, 3313. http://doi.org/10.3791/3313

McKenzie, I. A., Biernaskie, J., Toma, J. G., Midha, R., & Miller, F. D. (2006). Skin-Derived Precursors Generate Myelinating Schwann Cells for the Injured and Dysmyelinated Nervous System. *Journal of Neuroscience*, *26*(24), 6651–6660. http://doi.org/10.1523/JNEUROSCI.1007-06.2006

Meier, C., Parmantier, E., Brennan, A., Mirsky, R., & Jessen, K. R. (1999). Developing Schwann cells acquire the ability to survive without axons by establishing an autocrine circuit involving insulin-like growth factor, neurotrophin-3, and platelet-derived growth factor-BB. *The Journal of Neuroscience: The Official Journal of the Society for Neuroscience*, *19*(10), 3847–3859.

Meyer, M., Matsuoka, I., Wetmore, C., Olson, L., & Thoenen, H. (1992). Enhanced synthesis of brain-derived neurotrophic factor in the lesioned peripheral nerve: different mechanisms are responsible for the regulation of BDNF and NGF mRNA. *The Journal of Cell Biology*, *119*(1), 45–54.

Morrissey, T. K., Kleitman, N., & Bunge, R. P. (1991). Isolation and functional characterization

of Schwann cells derived from adult peripheral nerve. *The Journal of Neuroscience: The Official Journal of the Society for Neuroscience*, *11*(8), 2433–2442.

Mothe, A. J., Tam, R. Y., Zahir, T., Tator, C. H., & Shoichet, M. S. (2013). Repair of the injured spinal cord by transplantation of neural stem cells in a hyaluronan-based hydrogel. *Biomaterials*, *34*(15), 3775–3783. http://doi.org/10.1016/j.biomaterials.2013.02.002

Murray, M. R., & Stout, A. P. (1942). Characteristics of human Schwann cells in vitro. *The Anatomical Record*, *84*(3), 275–293. http://doi.org/10.1002/ar.1090840305

Namiki, K., Goodison, S., Porvasnik, S., Allan, R. W., Iczkowski, K. A., Urbanek, C., … Rosser, C. J. (2009). Persistent Exposure to Mycoplasma Induces Malignant Transformation of Human Prostate Cells. *PLoS ONE*, *4*(9), e6872. https://doi.org/10.1371/journal.pone.0006872

National Spinal Cord Injury Statistical Center. (2016). Spinal Cord Injury (SCI) Facts and Figures at a Glance. Birmingham, AL: University of Alabama at Birmingham.

Oudega, M., Bradbury, E. J., & Ramer, M. S. (2012). Combination therapies. *Handbook of Clinical Neurology*, *109*, 617–636. http://doi.org/10.1016/B978-0-444-52137-8.00038-3

Oudega, M., & Xu, X.-M. (2006). Schwann cell transplantation for repair of the adult spinal cord. *Journal of Neurotrauma*, *23*(3–4), 453–467. https://doi.org/10.1089/neu.2006.23.453

Pakulska, M. M., Ballios, B. G., & Shoichet, M. S. (2012). Injectable hydrogels for central nervous system therapy. *Biomedical Materials*, *7*(2), 24101. http://doi.org/10.1088/1748-

6041/7/2/024101

Pearse, D. D., Pereira, F. C., Marcillo, A. E., Bates, M. L., Berrocal, Y. A., Filbin, M. T., & Bunge, M. B. (2004). cAMP and Schwann cells promote axonal growth and functional recovery after spinal cord injury. *Nature Medicine*, *10*(6), 610–616. http://doi.org/10.1038/nm1056

Pearse, D. D., Sanchez, A. R., Pereira, F. C., Andrade, C. M., Puzis, R., Pressman, Y., … Bunge, M. B. (2007). Transplantation of Schwann cells and/or olfactory ensheathing glia into the contused spinal cord: Survival, migration, axon association, and functional recovery. *Glia*, *55*(9), 976–1000. https://doi.org/10.1002/glia.20490

Rahmani, W., Abbasi, S., Hagner, A., Raharjo, E., Kumar, R., Hotta, A., … Biernaskie, J. (2014). Hair follicle dermal stem cells regenerate the dermal sheath, repopulate the dermal papilla, and modulate hair type. *Developmental Cell*, *31*(5), 543–558. http://doi.org/10.1016/j.devcel.2014.10.022

Richardson, P. M., McGuinness, U. M., & Aguayo, A. J. (1980). Axons from CNS neurons regenerate into PNS grafts. *Nature*, *284*(5753), 264–265.

Richner, M., Ulrichsen, M., Elmegaard, S. L., Dieu, R., Pallesen, L. T., & Vaegter, C. B. (2014). Peripheral nerve injury modulates neurotrophin signaling in the peripheral and central nervous system. *Molecular Neurobiology*, *50*(3), 945–970. http://doi.org/10.1007/s12035-014-8706-9

Rodriguez, F. J., Folpe, A. L., Giannini, C., & Perry, A. (2012). Pathology of peripheral nerve sheath tumors: diagnostic overview and update on selected diagnostic problems. *Acta*

Neuropathologica, *123*(3), 295–319. https://doi.org/10.1007/s00401-012-0954-z

Safety of Autologous Human Schwann Cells (ahSC) in Subjects With Subacute SCI (Identification No. NCT01739023). (2012). Retrieved from https://clinicaltrials.gov/ct2/show/NCT01739023?term=NCT01739023&rank=1

Sahenk, Z., Oblinger, J., & Edwards, C. (2008). Neurotrophin-3 deficient Schwann cells impair nerve regeneration. *Experimental Neurology*, *212*(2), 552–556. http://doi.org/10.1016/j.expneurol.2008.04.015

Schucht, P., Raineteau, O., Schwab, M. E., & Fouad, K. (2002). Anatomical correlates of locomotor recovery following dorsal and ventral lesions of the rat spinal cord. *Experimental Neurology*, *176*(1), 143–153.

Schupper, N., Rabin, Y., & Rosenbluh, M. (2008). Multiple Stages in the Aging of a Physical Polymer Gel. *Macromolecules*, *41*(11), 3983–3994. http://doi.org/10.1021/ma702613j

Sharp, K. G., Flanagan, L. A., Yee, K. M., & Steward, O. (2012). A re-assessment of a combinatorial treatment involving Schwann cell transplants and elevation of cyclic AMP on recovery of motor function following thoracic spinal cord injury in rats. *Experimental Neurology*, *233*(2), 625–644. http://doi.org/10.1016/j.expneurol.2010.12.020

Sherman, L. S., Rizvi, T. A., Karyala, S., & Ratner, N. (2000). CD44 enhances neuregulin signaling by Schwann cells. *The Journal of Cell Biology*, *150*(5), 1071–1084.

Sparling, J. S., Bretzner, F., Biernaskie, J., Assinck, P., Jiang, Y., Arisato, H., … Tetzlaff, W. (2015). Schwann Cells Generated from Neonatal Skin-Derived Precursors or Neonatal

Peripheral Nerve Improve Functional Recovery after Acute Transplantation into the Partially Injured Cervical Spinal Cord of the Rat. *Journal of Neuroscience*, *35*(17), 6714–6730. http://doi.org/10.1523/JNEUROSCI.1070-14.2015

Tai, C., Miscik, C. L., Ungerer, T. D., Roppolo, J. R., & de Groat, W. C. (2006). Suppression of bladder reflex activity in chronic spinal cord injured cats by activation of serotonin 5-HT1A receptors. *Experimental Neurology*, *199*(2), 427–437. http://doi.org/10.1016/j.expneurol.2006.01.007

Tam, R. Y., Cooke, M. J., & Shoichet, M. S. (2012). A covalently modified hydrogel blend of hyaluronan–methyl cellulose with peptides and growth factors influences neural stem/progenitor cell fate. *Journal of Materials Chemistry*, *22*(37), 19402. http://doi.org/10.1039/c2jm33680d

Tetzlaff, W., Okon, E. B., Karimi-Abdolrezaee, S., Hill, C. E., Sparling, J. S., Plemel, J. R., … Kwon, B. K. (2011). A systematic review of cellular transplantation therapies for spinal cord injury. *Journal of Neurotrauma*, *28*(8), 1611–1682. https://doi.org/10.1089/neu.2009.1177

The Safety of ahSC in Chronic SCI With Rehabilitation (Identification No. NCT02354625. (2015). Retrieved from https://clinicaltrials.gov/ct2/show/NCT02354625?term=NCT02354625&rank=1

Thor, K. B., Roppolo, J. R., & deGroat, W. C. (1983). Naloxone induced micturition in unanesthetized paraplegic cats. *The Journal of Urology*, *129*(1), 202–205.

Thuret, S., Moon, L. D. F., & Gage, F. H. (2006). Therapeutic interventions after spinal cord

injury. *Nature Reviews Neuroscience*, *7*(8), 628–643. http://doi.org/10.1038/nrn1955

Tohyama, K., & Ide, C. (1984). The localization of laminin and fibronectin on the Schwann cell basal lamina. *Archivum Histologicum Japonicum = Nihon Soshikigaku Kiroku*, *47*(5), 519–532.

Toma, J. G., Akhavan, M., Fernandes, K. J., Barnabé-Heider, F., Sadikot, A., Kaplan, D. R., & Miller, F. D. (2001). Isolation of multipotent adult stem cells from the dermis of mammalian skin. *Nature Cell Biology*, *3*(9), 778–784. http://doi.org/10.1038/ncb0901-778

Toma, J. G., McKenzie, I. A., Bagli, D., & Miller, F. D. (2005). Isolation and characterization of multipotent skin-derived precursors from human skin. *Stem Cells (Dayton, Ohio)*, *23*(6), 727–737. http://doi.org/10.1634/stemcells.2004-0134

Tsai, S., Wear, D. J., Shih, J. W., & Lo, S. C. (1995). Mycoplasmas and oncogenesis: persistent infection and multistage malignant transformation. *Proceedings of the National Academy of Sciences of the United States of America*, *92*(22), 10197–10201.

Vercruysse, K. P., & Prestwich, G. D. (1998). Hyaluronate derivatives in drug delivery. *Critical Reviews in Therapeutic Drug Carrier Systems*, *15*(5), 513–555.

Vroemen, M., & Weidner, N. (2003). Purification of Schwann cells by selection of p75 low affinity nerve growth factor receptor expressing cells from adult peripheral nerve. *Journal of Neuroscience Methods*, *124*(2), 135–143.

Watson, C., Paxinos, G., Kayalioglu, G., & Heise, C. (2009). Atlas of the Rat Spinal Cord. In

The Spinal Cord (pp. 238–306). Elsevier. https://doi.org/10.1016/B978-0-12-374247-6.50019-5

Whishaw, I. Q., Gorny, B., & Sarna, J. (1998). Paw and limb use in skilled and spontaneous reaching after pyramidal tract, red nucleus and combined lesions in the rat: behavioral and anatomical dissociations. *Behavioural Brain Research*, *93*(1-2), 167-183.

Williams, R. R., Henao, M., Pearse, D. D., & Bunge, M. B. (2015). Permissive Schwann cell graft/spinal cord interfaces for axon regeneration. *Cell Transplantation*, *24*(1), 115–131. http://doi.org/10.3727/096368913X674657

Williams, R. R., Pearse, D. D., Tresco, P. A., & Bunge, M. B. (2012). The assessment of adeno-associated vectors as potential intrinsic treatments for brainstem axon regeneration: Assessing AAV vectors for axonal growth. *The Journal of Gene Medicine*, *14*(1), 20–34. http://doi.org/10.1002/jgm.1628

Wippold, F. J., Lubner, M., Perrin, R. J., Lämmle, M., & Perry, A. (2007). Neuropathology for the neuroradiologist: Antoni A and Antoni B tissue patterns. American Journal of Neuroradiology, 28, 1633-1638. http://doi.org/10.3174/ajnr.A0682

Xu, X.-M., & Onifer, S. M. (2009). Transplantation-mediated strategies to promote axonal regeneration following spinal cord injury. *Respiratory Physiology & Neurobiology*, *169*(2), 171–182. http://doi.org/10.1016/j.resp.2009.07.016

Yu, W.-M. (2005). Schwann Cell-Specific Ablation of Laminin 1 Causes Apoptosis and Prevents Proliferation. *Journal of Neuroscience*, *25*(18), 4463–4472. http://doi.org/10.1523/JNEUROSCI.5032-04.2005

Yu, W.-M., Chen, Z.-L., North, A. J., & Strickland, S. (2009). Laminin is required for Schwann cell morphogenesis. *Journal of Cell Science*, *122*(7), 929–936. http://doi.org/10.1242/jcs.033928

Zheng, J., Kontoveros, D., Lin, F., Hua, G., Reneker, D. H., Becker, M. L., & Willits, R. K. (2015). Enhanced Schwann cell attachment and alignment using one-pot "dual click" GRGDS and YIGSR derivatized nanofibers. *Biomacromolecules*, *16*(1), 357–363. https://doi.org/10.1021/bm501552t

Chapter 2: Immune rejection is not the main factor involved in post-transplantational loss of skin-derived precursor Schwann cells in the injured rat spinal cord

Zacnicte May[1], Abel Torres Espín[1], Ana Lucas Osma[1], Nicholas J. Batty[1], Pamela Raposo[1], Keith F. Fenrich[1], Morgan Stykel[2], Tobias Führmann[3], Molly Shoichet[3], Jeff Biernaskie[2], & Karim Fouad[1]

1. Neuroscience and Mental Health Institute, Faculty of Rehabilitation Medicine, University of Alberta, Edmonton, AB Canada
2. Department of Comparative Biology and Experimental Medicine, Faculty of Veterinary Medicine, Alberta Children's Hospital Research Institute, University of Calgary, Calgary, AB Canada
3. Department of Chemical Engineering & Applied Chemistry, Department of Chemistry, Institute of Biomaterials and Biomedical Engineering, University of Toronto, Toronto, ON Canada

Abstract

A major goal of Schwann cell (SC) therapy for spinal cord injury (SCI) is to fill the cavity forming at the injury site with SCs to create a bridge for regenerating axons. However, transplantation of peripheral nerve SCs requires an invasive biopsy, which results in nerve damage. SCs derived from multipotent stem cells found in the skin dermis (SKP-SCs) are a promising alternative. Regardless of source, SC loss post-grafting in the SCI cavity is an issue, with survival rates ranging from ~1-20% after ≥6 weeks. Immune rejection has been implicated in SC loss post-grafting in the injured rat spinal cord. Therefore, the aim of this study was to minimize the immune response and assess how this impacts SKP-SC survival in rats with SCI. We compared three different groups: cyclosporine-immunosuppressed rats (n=8), immunocompetent rats (n=9), and rats of a different sub-strain from SKP-SC donor rats (n=7). Dying SKP-SCs underwent immune-mediated clearance. However, SKP-SC survival was unaffected by treatment, suggesting that immune rejection is not the main factor involved in SKP-SC loss in rats with SCI. SKP-SCs were consistently found on laminin, indicating detachment-mediated apoptosis (i.e. anoikis) plays the major role in grafted cell loss.

Keywords: “Skin-derived precursor”, “Schwann cell”, “spinal cord injury”, “immune rejection”, “anoikis”

1. Introduction

Inducing regeneration of damaged axons has been proposed as a treatment for spinal cord injury (SCI; Tuszynski & Steward, 2012). However, a fluid-filled cavity forms at the epicenter of SCIs, presenting an obstacle for axonal growth. One strategy to create a bridge for regeneration is grafting cells into the cavity. Schwann cells (SCs) are one of the most investigated cell types for grafting (Tetzlaff et al., 2011). The pre-clinical literature on SCI shows that SC grafts form permissive bridges for regeneration (Williams et al., 2015), re-myelinate axons (Sparling et al., 2016), and release growth-promoting factors (Meier et al., 1999). SCs are typically harvested from peripheral nerve biopsies (Bunge, 1975; Fouad et al., 2005), but this method causes patient discomfort and possible sensory deficits (Hilton et al., 2007). An alternative source of SCs are multipotent dermal stem cells, which can be obtained from skin samples and differentiated into SCs in culture to >95% purity (Biernaskie et al., 2007a). Skin-derived precursor SCs (SKP-SCs) have shown promise by promoting axonal growth and re-myelination in a rat model of SCI (Biernaskie et al., 2007b).

A major challenge in SC transplantation into the SCI is poor grafted cell survival, with SC survival rates 6-9 weeks post-transplantation ranging from ~1-20% (Enomoto et al., 2013; Golden et al., 2007; Pearse et al., 2007) and SKP-SC survival rates 11 weeks post-transplantation reported as ~18% (Biernaskie et al., 2007b). One cause of SC loss post-grafting is immune-mediated rejection (Hill et al., 2006). Hence, the highly inbred Fischer rat strain is preferred over other strains for transplantation studies. However, different suppliers sell Fischer rats and the same supplier may carry more than one Fischer rat sub-strain. For example, Charles River carries two Fischer sub-strains SAS^{TM} and CDF^{TM}. The SAS^{TM} sub-strain originated in 1992 from NIH

stock and was acquired by Charles River in 1996, while the CDF^{TM} sub-strain originated in 1920 and was acquired by Charles River in 1960. SAS^{TM} and CDF^{TM} rats share the same MHC haplotype RT1^{lv} (criver.com); however, there may be unidentified antigens that differ between the two sub-strains. Sub-strain is seldom reported in scientific articles, raising the possibility that sub-strain mismatching of donor and recipient may explain transplant rejection in some studies. This and other questions relating to immune-mediated grafted cell death need resolving.

Anoikis, apoptosis due to detachment from extracellular matrix (ECM) molecules and neighbouring cells (Frisch, 1994), may also contribute to post-transplantational SC loss. This is supported by reports that SCs plated on non-adherent multi-well plates undergo anoikis (Koda et al., 2008). The relative contributions and interactions of immune rejection, anoikis, and other factors (e.g., vascularization) to transplanted SC loss are yet to be determined. Although death of cells post-transplantation is often discussed, systematic exploration of the factors leading to grafted cell loss is lacking. Thus, the goal of our study was to explore the involvement of the immune system in SKP-SC loss post-transplantation in rats with SCI. We compared SKP-SC survival at the SCI site in sub-strain matched immunosuppressed rats, sub-strain matched rats, and sub-strain mismatched rats. We predicted that if the immune response was the main factor in SKP-SC survival, the greatest survival would be found in sub-strain matched immunosuppressed rats. Our experimental set-up also addressed the question of whether sub-strain mismatching lowers grafted cell survival.

2. Materials and Methods

2.1 Animals

Adult female Fischer rats of the sub-strains CDF^{TM} (N=18) and SAS^{TM} (N=7) from

Charles River Laboratories were used in this study. The CDF™ and SAS™ rats weighed between 154-189g and 153-161g respectively. Sub-strains were housed separately in groups of 6-7 rats in large (18"x14") cages under a 12:12h light-dark cycle. There were three experimental groups: the first group were CDF™ rats (CDF; n=10), the second group were CDF™ rats immunosuppressed with cyclosporine (CDF-C; n=8), and the third group were SAS™ rats (SAS; n=7). All rats were acclimatized to the housing conditions for 1 week before the experiment. All protocols were approved by the University of Alberta Health Science Animal Care and Use Committee, and the University of Calgary Animal Care Committee.

2.2 SKP-SC preparation and GFP transduction

SKPs were isolated from adult female Fischer (CDF™) rats and differentiated into SCs as described in Biernaskie et al. (2007a). The single change from the protocol was the regular treatment of cultures with the antibiotic Plasmocin™ (InvivoGen). SKP-SCs were transduced with a lentivirus encoding green fluorescent protein (GFP) as described in Rahmani et al. (2014). After transduction, SKP-SCs were FACS sorted for $p75^+$ and GFP^+ cells.

2.3 HAMC hydrogel preparation

The hyaluronan-methylcellulose (HAMC) hydrogel used as a vehicle for the transplantation of SKP-SCs was prepared as described in Führmann et al. (2016).

2.4 SKP-SC thawing, plating, and maintenance conditions

Frozen GFP^+ SKP-SCs on passage five were thawed in 2 min at 37˚C and diluted in DMEM (Invitrogen). SKP-SCs were pelleted at 1000rpm for 5 min and re-suspended in SC proliferation medium (Biernaskie et al., 2007a) at a density of 100,000 cells/ml. SKP-SCs were

plated on laminin (4µg/ml) and poly-d-lysine (20µg/ml) coated polystyrene 10cm dishes and fed every 3 days. Cultures were kept at 37˚C with 5% CO_2 until 75% confluence.

2.5 Spinal cord hemisection injury and SKP-SC transplantation

Rats were anesthetised with isoflurane gas (5% for induction; 2-3% for maintenance). Rats' back skin was shaved in a room separate from the surgical area and disinfected with chlorhexidine digluconate (Sigma-Aldrich Canada Ltd.). Tears Naturale lubricant (Alcon Canada, Inc.) was applied to the rats' eyes for protection. Shaved skin was cut longitudinally and the muscles below were dissected to expose vertebra T8, which was removed by laminectomy. A lateral hemisection of the right half of the spinal cord was made with spring scissors through an opening in the dura mater. To ensure lesion completeness, the injury site was compressed with dumont #5 forceps with one forcep arm inserted inside the dura and the other outside the dura. 1% dry agarose was used to cover the opening in the dura mater. Lastly, muscles were sutured with vicryl 5-0 (Johnson & Johnson Medical Pty Ltd.), and the skin incision was closed with 9mm stainless steel staples (Stoelting Co.). Rats were treated for pain with SQ buprenorphine injections (0.03mg/kg; Temgesic, Schering-Plough) and kept hydrated with SQ saline injections (2.5ml).

SKP-SCs were transplanted 2 weeks post-SCI. SKP-SCs were detached from culture plates with Triple E express (Invitrogen). SKP-SC suspensions were pelleted at 1200rpm for 6 min, re-suspended in DMEM, and pelleted again at 1000rpm for 5 min. SKP-SCs were then mixed with 0.5%/0.5% HAMC at a concentration of 50,000 cells/µl. ~200,000 total cells (4µl) were injected into the SCI site with a 10µl Hamilton syringe. The SCI/transplant site was covered with dry agarose. Surgical procedures and post-operative care were identical for the SCI

and transplantation surgeries. One CDF™ rat stopped breathing under anaesthesia and could not be resuscitated. No data was analyzed from this animal. The CDF-C group received daily cyclosporine injections (15mg/kg, SQ; Novartis) starting the day before transplantation until euthanasia. The CDF and SAS groups were given daily control saline injections over the same time period as the CDF-C group.

2.6 Behavioural Assessment

Locomotor ability was assessed using the Basso, Bresnahan and Beattie (BBB) rating scale (Basso et al., 1995) and BBB sub-scale (Popovich et al., 2012) by two blinded observers. While the BBB score is out of 21 points, the BBB sub-score is out of 13 points and only takes into consideration toe clearance, paw rotation, trunk stability, and tail position. Testing was performed weekly post-SCI for 8 weeks, excepting week 2 for transplant surgeries.

2.7 Perfusion and Histology

Rats were euthanized 8 weeks post-SCI with pentobarbital (1000mg/kg; Euthanyl; Biomeda-MTC) and perfused with saline containing heparin and phosphate-buffered 4% paraformaldehyde with 5% sucrose (PFA; 0.1 M; pH 7.4). The spinal cord was removed surgically, post-fixed in PFA overnight at 4˚C, and immersed in 30% sucrose for 5 days. Spinal tissue was coated with O.C.T cryoprotectant (Sakura Finetek) before freezing in 2-methylbutane (Fisher Scientific) over dry ice. 1.8cm long segments of spinal cord with the SCI in the middle were cut horizontally at 25µm on a NX70 cryostat (Fisher Scientific) and staggered across four sets of slides (Fisher Scientific). Slides were stored at -20°C until histological processing.

Immunohistochemistry: Spinal sections were warmed at 37°C for 1 hr and washed 3x in

tris-buffered saline (TBS). Washes were always 10 min long. Sections were blocked for 1 hr at room temperature with 10% normal goat serum (NGS) in TBS with 0.5% Triton X-100 (TBS-TX). Primary antibodies were diluted in 1% NGS in TBS and applied to slides overnight at 4˚C, and then washed 3x with TBS. Fluorescent secondary antibodies were diluted in 1% NGS in TBS and applied to slides for 2 hrs at room temperature. Slides were washed 2x in TBS-TX and 2x in TBS before coverslipping with Fluoromount G (Southern Biotech) and imaged with an upright Leica DM6000 B microscope and a Leica DMi8 confocal microscope (Leica Microsystems Inc.).

Primary antibodies: polyclonal chicken (ck) anti-GFP (1:1000; Abcam), monoclonal clone GA5 mouse (ms) anti-glial fibrillary acidic protein (GFAP; 1:700), polyclonal rabbit (rb) anti-ionized calcium-binding adapter molecule 1 (Iba-1; 1:1000; Wako), and polyclonal rabbit (rb) anti-laminin (1:500; Abcam).

Secondary antibodies: AF555 goat (gt) anti-ms, AF555 gt anti-rb, and AF647 gt anti-ck (1:500; all from Invitrogen).

DAB stain: Spinal sections were warmed at 37˚C and washed 2x in TBS. Sections were blocked with 0.3% hydrogen peroxide in phosphate-buffered saline (PBS). Slides were washed 1x in TBS and 1x in TBS-TX, and blocked with 10% NGS in TBS-TX for 1hr at room temperature. The primary antibody rb anti-GFP (1:500; Invitrogen) was diluted in 1% NGS in TBS and applied to slides overnight at 4˚C. The next morning, slides were washed 3x in TBS and incubated with biotinylated goat anti-rb IgG from the Vectastain Elite ABC HRP kit (Vector Laboratories) in 1% NGS in TBS for 2 hrs at room temperature. Slides were washed 3x in TBS and incubated with avidin/biotinylated horseradish peroxidase solution from the same kit for 2

hrs at room temperature. Then, sections were washed 3x in TBS and reacted with 3,3'-diaminobenzidine (DAB) stain solution (DAB peroxidase HRP reaction kit; Vector Laboratories Inc.) for 30sec. Sections were washed a final 3x in TBS, immersed in 0.5% cresyl violet for 2min, and rinsed in distilled water. Tissue was serially dehydrated in increasing ethanol concentrations (50%, 75%, twice in 99% for 3min each), cleared in two 3min baths of xylene, and coverslipped with Permount^{R}. Slides were imaged with a Leica DMLB light microscope (Leica Microsystems Inc.).

2.8 SCI cross-sectional size and length and SKP-SC survival

Lesion cross-sectional size: One set of slides with sections 75µm apart extending from the dorsal to ventral surfaces of the spinal cord was analyzed under phase-contrast microscopy. The SCI was identified by the disruption of linear organization of white matter tracts and loss of darkly appearing soma in the grey matter. Maximum lesions were re-constructed by hand on T9 (overlayed by vertebra T8) cross-section schematics obtained from the Atlas of the Rat Spinal Cord (Watson et al., 2009). The SCI area was calculated as a percentage of the total cross-sectional area.

Lesion length: Spinal sections were stained with GFAP to show the borders of the SCI. Overview images of five sections ~275µm apart were taken at 50x magnification and the distance in µm between the rostral and caudal SCI borders was measured on ImageJ 1.43µ (National Institutes of Health). The SCI length of the five sections was averaged.

SKP-SC survival: The area of GFP^{+} cells stained with DAB at the SCI and rostral and caudal to the SCI (up to a 2.5mm distance from the injury) was measured. Overview images of five sections ~275µm apart were taken at 50x magnification. Images were analyzed on ImageJ

1.43µ. The division of interest (SCI, rostral or caudal) was selected with the polygon selection tool, and the color threshold was adjusted until the DAB signal was highlighted. The DAB labeled areas at the SCI, rostral, and caudal divisions were averaged across sections and calculated as a percentage of the total area of each division.

2.9 SKP-SC morphology and immune clearance

SKP-SCs were labeled with ck anti-GFP/gt anti-ck AF647 and microglia/macrophages were labeled with rb anti-Iba-1/gt anti-rb AF555. Every section 75µm apart on one set of slides was inspected at 100x magnification to locate SKP-SCs. To assess the shape of the SKP-SCs and their proximity to microglia/macrophages, sections containing SKP-SCs were imaged at 200x magnification. The location of the SKP-SCs in relation to the SCI site was also noted. All imaging was performed with an epifluorescence microscope.

2.10 SKP-SC association with laminin

SKP-SCs were labeled with ck anti-GFP/gt anti-ck AF647 and laminin was labeled with rb anti-Iba-1/gt anti-rb AF555. Every section 75µm apart on one set of slides was inspected at 100x magnification to locate SKP-SCs. Sections containing SKP-SCs were then imaged at 200x magnification. Imaging at 100x and 200x was carried out with an epifluorescence microscope. Association of SKP-SCs with laminin was assessed with an oil-immersion lens at 630x magnification on a confocal microscope. The association was confirmed by scrolling up and down z-stacks and finding SKP-SCs in contact with laminin in the same focal plane. Z-step size was 0.76µm.

2.11 Statistical Analysis

All results were analyzed with GraphPad Prism 7 (GraphPad Software Inc.). Data were assessed for normality using the Shapiro-Wilk test. Between-group comparisons were made with one-way ANOVA or Kruskal-Wallis for non-parametric data. Between-group comparisons of weekly BBB scores and sub-scores were made with repeated measures two-way ANOVA. Within-group comparisons were conducted with repeated measures one-way ANOVA followed by Tukey's multiple comparison test or with the non-parametric equivalent Friedman's test with Dunn's multiple comparisons. Data are shown as mean values±SEM with a significance threshold of $p<0.05$.

3. Results

3.1 Locomotor recovery, SCI cross-sectional size and length, and SKP-SC survival were unaffected by immune suppression or sub-strain mismatching

Locomotor recovery: The BBB locomotor rating scale and BBB sub-scale were used to assess locomotor recovery of rats after SCI and SKP-SC transplantation. Two-way repeated measures ANOVA did not find a significant group effect on BBB score over the course of 8 weeks post-SCI; 6 weeks post-transplantation ($p=0.14$; Fig. 1A). The three experimental groups were: Fischer rats of the CDF™ sub-strain (CDF; n=10 total, n=9 for the results), CDF™ rats immunosuppressed with cyclosporine (CDF-C; n=8), and Fischer rats of the SAS™ sub-strain (SAS; n=7). CDF group BBB scores were 10.17±0.19 at week 1 post-SCI and 10.5±0.26 at week 8 post-SCI. CDF-C group scores at weeks 1 and 8 post-SCI were 10.94±0.36 and 11.25±0.16 respectively. SAS group scores at weeks 1 and 8 post-SCI were 10.43±0.30 and 11.36±0.45 respectively. Similarly, no group effect on BBB sub-score was found ($p=0.74$; Fig. 1A). Mean sub-scores at weeks 1 and 8 post-SCI were 0.22±0.22 and 1±0.24 for the CDF group, 0.5±0.27

and 1±0.19 for the CDF-C group, and 0.14±0.14 and 1.3±0.18 for the SAS group. These results show that the effect of cyclosporine-mediated immunosuppression and sub-strain mismatching in combination with cell grafts did not impact the locomotor recovery of the animals.

SCI cross-sectional size and length: The SCI cross-sectional size and length were analyzed to assess the impact of cyclosporine mediated immunosuppression and sub-strain mismatching on SCI severity.

No significant differences in SCI cross-sectional size ($p=0.27$) or length ($p=0.58$; Fig. 1B) were found between groups as assessed by one-way ANOVA. Mean lesion sizes were 73.18±4.28% for the CDF group, 64.6±3.7% for the CDF-C group, and 67.3±3.03% for the SAS group. Mean lesion lengths were 1.47±0.17mm for the CDF group, 1.69±0.19mm for the CDF-C group, and 1.49±0.09mm for the SAS group. To summarize, neither immune suppression nor sub-strain mismatching in combination with cell grafts influenced SCI severity.

SKP-SC survival was assessed at the SCI site, and rostral and caudal to the SCI. The GFP^+ area as a percentage of each division was used to measure SKP-SC survival. No significant differences between groups were found on GFP^+ area at the injury site ($p=0.64$), rostral to the injury ($p=0.72$), or caudal to it ($p=0.77$; Fig. 1C). However, within-group comparisons showed a significant difference in GFP^+ area between the lesion, rostral, and caudal divisions (CDF group $p<0.001$; CDF-C group $p<0.01$; SAS group $p<0.01$). GFP^+ area was greatest at the SCI compared to rostral and caudal to the injury irrespective of treatment group (CDF group $p<0.01$ compared to rostral and caudal divisions; CDF-C group $p<0.05$ compared to rostral and caudal divisions; SAS group $p<0.01$ compared to rostral division and $p<0.05$ compared to caudal division; Fig. 1C). Mean GFP^+ areas at the injury, rostral and caudal

divisions were 2.65±0.95, 0.43±0.11, and 0.38±0.11% for the CDF group, 1.23±0.28, 0.29±0.08, and 0.29±0.06% for the CDF-C group, and 1.22±0.24, 0.26±0.04, and 0.34±0.07% for the SAS group. Two conclusions can be drawn from these data. First, SKP-SCs do not migrate from the site of SCI, which shows SKP-SCs are useful for cavity filling and possibly bridging the injury for growing axons. Second, survival is unaffected by immunosuppression or sub-strain mismatching, indicating immune rejection is not the major factor in SKP-SC post-transplantational loss.

3.2 SKP-SCs showed characteristic morphologies of dying cells under immune clearance and appositions with laminin

Morphology: The morphological characteristics of SKP-SCs were recorded for all animals and compared between groups. Three characteristic SKP-SC morphologies were identified: first was a bipolar-shape characteristic of SCs with one central cell body and an extension on either end (Fig. 2Aa), the second were unipolar or small round cells (Fig. 2Ab), and the last were large hyper-fluorescing spheres (Fig. 2Ac). Bipolar and unipolar SKP-SCs often appeared to contact microglia/macrophages (Fig. 2Aa & 2Ab) and hyper-fluorescing spheres were surrounded by immune cells (Fig. 2Ac). Qualitative differences were not observed between groups. In conclusion, SKP-SC morphology was varied and some grafted cells appeared to be under phagocytic immune clearance.

Laminin: SKP-SCs were consistently found to sit on a laminin substrate in the injured rat spinal cord. The soma or processes of SKP-SCs, without exception, contacted laminin in the same z-plane of confocal z-stacks (Fig. 2B). In other words, no distance was found between SKP-SCs and laminin. This result suggests that attachment to substrata is important for SKP-SC

survival post-transplantation, since laminin is a SC basal lamina protein mediating attachment (Tohyama & Ide, 1984).

4. Discussion

An important goal in cell therapy research for SCI is to fill the cavity that forms at the SCI site with grafted cells, thereby bridging the injury for regenerating axons (Tetzlaff et al., 2011). SCs are one of the most investigated cell types to achieve this goal (Tetzlaff et al., 2011). However, low grafted SC survival numbers in the injured spinal cord present a continuing problem (Biernaskie et al., 2007b; Enomoto et al., 2013; Golden et al., 2007; Pearse et al., 2007). It is assumed that immune rejection is the main cause of grafted cell loss (Hill et al., 2006), which is why inbred rat strains are used in transplantation studies. Despite this, many questions regarding immune rejection remain unanswered, such as the impact of donor and host sub-strain mismatching and the contribution of different factors to grafted cell loss. Addressing these questions is important for the development of approaches to increase survival rates. In our study, we investigated the effect of minimizing the immune response and sub-strain mismatching on grafted SC survival. We grafted SKP-SCs into the injured rat spinal cord, since this cell type has been proposed as a more accessible alternative to nerve-derived SCs (Biernaskie et al., 2007a). SKP-SCs are differentiated from stem cells found in skin (Biernaskie et al., 2007a), compared to SCs obtained from peripheral nerve biopsies that will result in nerve damage (Hilton et al., 2007).

Locomotor function post-transplantation of SKP-SCS into the SCI cavity was comparable between immunosuppressed, immunocompetent, and host rats of a different sub-strain from SKP-SC donor rats. This was expected, as SC transplantation post-SCI typically requires adjunct

therapy to promote locomotor recovery (Pearse et al., 2004). Similarity of locomotor function between groups in the first week post-SCI (before SKP-SC transplantation) showed SCI severity was consistent across groups. Lesion cross-sectional size and length were equivalent between groups 8 weeks post-SCI, confirming group differences in SCI severity did not confound our results. Cyclosporine was given after secondary damage had occurred, so no effect of immunosuppression was expected on SCI severity or locomotor ability.

SKP-SCs were mainly found at the SCI site, where cells were grafted, with few cells migrating rostral and caudal to the injury. The limited migration of SKP-SCs makes them useful for bridging the injury and possibly supporting axonal growth. Immune suppression did not increase SKP-SC survival relative to immunocompetent and sub-strain mismatched rats. This finding does not imply that immune rejection is uninvolved in SKP-SC loss. SKP-SCs were found in close proximity to Iba-1^{+} immune cells and adopted a round morphology associated with dying SCs (Nakao et al., 1997; Syroid et al., 1996). Large spherical SKP-SCs appeared to be undergoing necrotic swelling (Elmore, 2007). Also, cyclosporine does not suppress all aspects of the immune system. Cyclosporine inhibits T and B lymphocytes, some antigen-presenting cells, mast cells, eosinophils, and natural killer cells (Thomson, 1992). However, macrophage activity, including phagocytosis, reactive oxygen species production, and MHC gene expression, is largely unaffected by cyclosporine (Thomson, 1992). Therefore, macrophage activity could have precipitated SKP-SC death and clearance. Sub-strain mismatching did not decrease SKP-SC survival compared to sub-strain matching. Sub-strain mismatched rats might be too similar genetically to SKP-SC donor rats, and not elicit a strong enough immune response to lower survival below that seen with sub-strain matching. Nevertheless, our results suggest that the immune response is not the only or most important factor in grafted cell loss. To pursue this, we

assessed the association between SKP-SCs and laminin, since laminin is an important ECM molecule involved in cell attachment (Tohyama & Ide, 1984). Surviving SKP-SCs were consistently found in close proximity to laminin. Association between SKP-SCs and laminin was confirmed with confocal imaging showing no distance between grafted cells and laminin. This agrees with the idea that anoikis, apoptosis resulting from substrate detachment (Frisch, 1994), is possibly a key factor in grafted cell survival. In fact, Yu et al., (2005) found that inhibition of the laminin y1 gene in SCs results in depletion of all laminin isoforms expressed by SCs and increased rates of SC apoptosis/caspase signaling. Further, plating SCs on non-adherent substrates leads to SC death (Koda et al., 2008). Future experiments manipulating the amount of substrate in SCI models will be necessary to establish a causal relation between detachment and SC post-transplantational loss. Another factor likely contributing to grafted SC death is vascular disruption in SCI, leading to ischemic necrosis (Balentine, 1978). Vascularization is, therefore, another factor that should be systematically explored in SC transplantation studies.

Grafted cell survival in pre-clinical models is frequently discussed but not systematically explored. Here we show that the immune system is not the main factor involved in SKP-SC survival in SCI. Understanding the factors regulating grafted cell survival will permit us to maximize survival and SCI cavity filling, bridging the injury for regenerating axons in pre-clinical models and human patients.

Acknowledgements

This study was supported by a CIHR Foundation Grant (RES0011338, KF).

References

Balentine, J. D. (1978). Pathology of experimental spinal cord trauma. I. The necrotic lesion as a function of vascular injury. *Laboratory Investigation; a Journal of Technical Methods and Pathology*, *39*(3), 236–253.

Basso, D. M., Beattie, M. S., & Bresnahan, J. C. (1996). Graded Histological and Locomotor Outcomes after Spinal Cord Contusion Using the NYU Weight-Drop Device versus Transection. *Experimental Neurology*, *139*(2), 244–256. https://doi.org/10.1006/exnr.1996.0098

Biernaskie, J. A., McKenzie, I. A., Toma, J. G., & Miller, F. D. (2007). Isolation of skin-derived precursors (SKPs) and differentiation and enrichment of their Schwann cell progeny. *Nature Protocols*, *1*(6), 2803–2812. https://doi.org/10.1038/nprot.2006.422

Biernaskie, J., Sparling, J. S., Liu, J., Shannon, C. P., Plemel, J. R., Xie, Y., … Tetzlaff, W. (2007). Skin-derived precursors generate myelinating Schwann cells that promote remyelination and functional recovery after contusion spinal cord injury. *The Journal of Neuroscience: The Official Journal of the Society for Neuroscience*, *27*(36), 9545–9559. https://doi.org/10.1523/JNEUROSCI.1930-07.2007

Bunge, R. P. (1975). Changing uses of nerve tissue culture 1950-1975. In *The Nervous System* (Vol. Volume 1. The Basic Neuroscience). New York: Raven Press.

Charles River Laboratories. (2015). Inbred Rats Datasheet. Retrieved from http://www.criver.com/files/pdfs/rms/inbred-rats.aspx

Elmore, S. (2007). Apoptosis: A Review of Programmed Cell Death. *Toxicologic Pathology*, *35*(4), 495–516. https://doi.org/10.1080/01926230701320337

Enomoto, M., Bunge, M. B., & Tsoulfas, P. (2013). A multifunctional neurotrophin with reduced affinity to p75NTR enhances transplanted Schwann cell survival and axon growth after spinal cord injury. *Experimental Neurology*, *248*, 170–182. https://doi.org/10.1016/j.expneurol.2013.06.013

Fouad, K., Schnell, L., Bunge, M. B., Schwab, M. E., Liebscher, T., & Pearse, D. D. (2005). Combining Schwann cell bridges and olfactory-ensheathing glia grafts with chondroitinase promotes locomotor recovery after complete transection of the spinal cord. *The Journal of Neuroscience: The Official Journal of the Society for Neuroscience*, *25*(5), 1169–1178. https://doi.org/10.1523/JNEUROSCI.3562-04.2005

Frisch, S. M. (1994). Disruption of epithelial cell-matrix interactions induces apoptosis. *The Journal of Cell Biology*, *124*(4), 619–626. https://doi.org/10.1083/jcb.124.4.619

Führmann, T., Tam, R. Y., Ballarin, B., Coles, B., Elliott Donaghue, I., van der Kooy, D., … Shoichet, M. S. (2016). Injectable hydrogel promotes early survival of induced pluripotent stem cell-derived oligodendrocytes and attenuates longterm teratoma formation in a spinal cord injury model. *Biomaterials*, *83*, 23–36. https://doi.org/10.1016/j.biomaterials.2015.12.032

Golden, K. L., Pearse, D. D., Blits, B., Garg, M. S., Oudega, M., Wood, P. M., & Bunge, M. B. (2007). Transduced Schwann cells promote axon growth and myelination after spinal cord injury. *Experimental Neurology*, *207*(2), 203–217. https://doi.org/10.1016/j.expneurol.2007.06.023

Hill, C. E., Moon, L. D. F., Wood, P. M., & Bunge, M. B. (2006). Labeled Schwann cell

transplantation: Cell loss, host Schwann cell replacement, and strategies to enhance survival. *Glia*, *53*(3), 338–343. https://doi.org/10.1002/glia.20287

Hilton, D. A., Jacob, J., Househam, L., & Tengah, C. (2007). Complications following sural and peroneal nerve biopsies. *Journal of Neurology, Neurosurgery & Psychiatry*, *78*(11), 1271–1272. https://doi.org/10.1136/jnnp.2007.116368

Koda, M., Someya, Y., Nishio, Y., Kadota, R., Mannoji, C., Miyashita, T., … Yamazaki, M. (2008). Brain-derived neurotrophic factor suppresses anoikis-induced death of Schwann cells. *Neuroscience Letters*, *444*(2), 143–147. https://doi.org/10.1016/j.neulet.2008.07.055

Meier, C., Parmantier, E., Brennan, A., Mirsky, R., & Jessen, K. R. (1999). Developing Schwann cells acquire the ability to survive without axons by establishing an autocrine circuit involving insulin-like growth factor, neurotrophin-3, and platelet-derived growth factor-BB. *The Journal of Neuroscience: The Official Journal of the Society for Neuroscience*, *19*(10), 3847–3859.

Nakao, J., Shinoda, J., Nakai, Y., Murase, S., & Uyemura, K. (1997). Apoptosis regulates the number of Schwann cells at the premyelinating stage. *Journal of Neurochemistry*, *68*(5), 1853–1862.

Pearse, D. D., Pereira, F. C., Marcillo, A. E., Bates, M. L., Berrocal, Y. A., Filbin, M. T., & Bunge, M. B. (2004). cAMP and Schwann cells promote axonal growth and functional recovery after spinal cord injury. *Nature Medicine*, *10*(6), 610–616. https://doi.org/10.1038/nm1056

Pearse, D. D., Sanchez, A. R., Pereira, F. C., Andrade, C. M., Puzis, R., Pressman, Y., … Bunge, M. B. (2007). Transplantation of Schwann cells and/or olfactory ensheathing glia into the contused spinal cord: Survival, migration, axon association, and functional recovery. *Glia*, *55*(9), 976–1000. https://doi.org/10.1002/glia.20490

Popovich, P. G., Tovar, C. A., Wei, P., Fisher, L., Jakeman, L. B., & Basso, D. M. (2012). A reassessment of a classic neuroprotective combination therapy for spinal cord injured rats: LPS/pregnenolone/indomethacin. *Experimental Neurology*, *233*(2), 677–685. https://doi.org/10.1016/j.expneurol.2011.11.045

Rahmani, W., Abbasi, S., Hagner, A., Raharjo, E., Kumar, R., Hotta, A., … Biernaskie, J. (2014). Hair follicle dermal stem cells regenerate the dermal sheath, repopulate the dermal papilla, and modulate hair type. *Developmental Cell*, *31*(5), 543–558. https://doi.org/10.1016/j.devcel.2014.10.022

Sparling, J. S., Bretzner, F., Biernaskie, J., Assinck, P., Jiang, Y., Arisato, H., … Tetzlaff, W. (2015). Schwann cells generated from neonatal skin-derived precursors or neonatal peripheral nerve improve functional recovery after acute transplantation into the partially injured cervical spinal cord of the rat. *The Journal of Neuroscience: The Official Journal of the Society for Neuroscience*, *35*(17), 6714–6730. https://doi.org/10.1523/JNEUROSCI.1070-14.2015

Syroid, D. E., Maycox, P. R., Burrola, P. G., Liu, N., Wen, D., Lee, K. F., … Kilpatrick, T. J. (1996). Cell death in the Schwann cell lineage and its regulation by neuregulin. *Proceedings of the National Academy of Sciences of the United States of America*, *93*(17), 9229–9234.

Tetzlaff, W., Okon, E. B., Karimi-Abdolrezaee, S., Hill, C. E., Sparling, J. S., Plemel, J. R., … Kwon, B. K. (2011). A systematic review of cellular transplantation therapies for spinal cord injury. *Journal of Neurotrauma*, *28*(8), 1611–1682. https://doi.org/10.1089/neu.2009.1177

Thomson, A. W. (1992). The effects of cyclosporin A on non-T cell components of the immune system. *Journal of Autoimmunity*, *5 Suppl A*, 167–176.

Tohyama, K., & Ide, C. (1984). The Localization of Laminin and Fibronectin on the Schwann Cell Basal Lamina. *Archives of Histology and Cytology*, *47*(5), 519–532. https://doi.org/10.1679/aohc.47.519

Tuszynski, M. H., & Steward, O. (2012). Concepts and methods for the study of axonal regeneration in the CNS. *Neuron*, *74*(5), 777–791. https://doi.org/10.1016/j.neuron.2012.05.006

Watson, C., Paxinos, G., Kayalioglu, G., & Heise, C. (2009). Atlas of the Rat Spinal Cord. In *The Spinal Cord* (pp. 238–306). Elsevier. https://doi.org/10.1016/B978-0-12-374247-6.50019-5

Williams, R. R., Henao, M., Pearse, D. D., & Bunge, M. B. (2015). Permissive Schwann cell graft/spinal cord interfaces for axon regeneration. *Cell Transplantation*, *24*(1), 115–131. https://doi.org/10.3727/096368913X674657

Yu, W.-M., Feltri, M. L., Wrabetz, L., Strickland, S., & Chen, Z.-L. (2005). Schwann Cell-Specific Ablation of Laminin 1 Causes Apoptosis and Prevents Proliferation. *Journal of Neuroscience*, *25*(18), 4463–4472. https://doi.org/10.1523/JNEUROSCI.5032-04.2005

Chapter 3: Following complete disruption of the reticulospinal tract, new collaterals to interneurons parallel locomotor recovery

Zacnicte May[1,2*], Keith K. Fenrich[1,2*], Julia Dahlby[2], Nicholas J. Batty[1,2], Abel Torres-Espín[1,2] & Karim Fouad[1,2]

1. Neuroscience and Mental Health Institute, University of Alberta, Edmonton, AB Canada T6G 2E1
2. Department of Physical Therapy, Faculty of Rehabilitation Medicine, University of Alberta, Edmonton, AB Canada T6G 2G4

∗ These authors contributed equally to this work

Abstract

The reticulospinal tract (RtST) descends from the reticular formation and terminates in the spinal cord. The RtST drives the initiation of locomotion and postural control. RtST axons form new contacts with propriospinal interneurons (PrINs) after incomplete spinal cord injury (SCI); however, it is unclear if injured or uninjured axons make these connections. We completely transected all RtST axons in rats using a staggered model, where a hemisection SCI at vertebra T10 is followed by a contralateral hemisection at vertebra T7. In one group of animals the T7 SCI was performed 2 weeks after the T10 SCI (delayed; dSTAG) and in another group the T10 and T7 SCIs were concomitant (cSTAG). dSTAG animals had significantly more RtST-PrIN contacts in the grey matter compared to cSTAG animals ($p < 0.05$*). These results were accompanied by enhanced locomotor recovery with dSTAG animals significantly outperforming cSTAG animals (BBB test; $p < 0.05$*). This difference suggests that activity in neuronal networks below the first SCI is necessary for enhanced recovery, because dSTAG rats recovered locomotor ability before the second hemisection. In conclusion, our findings support the hypothesis that the injured RtST forms new connections and is a key player in the recovery of locomotion post-SCI.

Keywords: spinal cord injury, reticulospinal, rat, staggered model, propriospinal interneurons

1. Introduction

Regrowth of adult central nervous system (CNS) axons after spinal cord injury (SCI) is limited due to intrinsic factors [1] as well as by a growth inhibitory environment including myelin associated inhibitors [2] and chondroitin sulfate proteoglycans (CSPGs) in the scar and perineuronal net [3,4]. Still, adaptive changes in the brain and spinal cord (i.e., plasticity) do occur and are important mechanisms and treatment targets for functional recovery after CNS injuries in humans and animal models. Plasticity in the spinal cord includes changes such as axon collateral sprouting (i.e., axon growth from new or existing collaterals) [5,6,7], synaptic rearrangements [8,9,10], and changes in cellular properties [11,12,13].

The corticospinal tract (CST) is a descending system that has received special attention in regards to neuroplasticity after SCI [6,8, 14,15]. Possible reasons for this attention includes the ease of neuroanatomical tracing of cortical neurons, the simplicity of transecting the dorsally located tract in rodents, and the importance of the CST in voluntary motor control in primates [16] and humans [17]. Injured CST axons can sprout rostral to a SCI, contributing to recovery of motor function [6,8]. Collateral sprouting rostral to a lesion may support recovery by allowing descending CST axons to form new synaptic connections with propriospinal interneurons (PrINs). Many PrINs are commissural interneurons (i.e., crossing the midline) with many of them projecting to the lumbar enlargement; thus, providing a detour connection for the CST [7,8]. The significance of CST axon relays via PrINs has been demonstrated in rodents with staggered SCIs [10]. In this SCI model, the animal receives two lateral hemisections at different thoracic segments on opposite sides of the spinal cord. This model completely transects all axons connecting locomotor circuits in the lumbar spinal cord with the brain and brainstem, but leaves

an intervening bridge of tissue containing PrINs. Due to rewiring within this bridge and changes in motoneuon properties animals can recover substantial locomotor function compared to spinalized animals [12,18].

The reticulospinal tract (RtST) is important for initiating walking in cats and rodents [19,20]. It has also been noted that RtST axons have a remarkable ability for neurite outgrowth/regeneration compared to CST axons [21,22,23], making it a promising target for plasticity-promoting treatments. Despite this knowledge, research on collateral sprouting/plasticity of the RtST lags behind that of the CST [24].

First demonstrations that, like the CST, the RtST can form new connections to circumvent SCI were made by Filli et al. (2014) [9]. They reported increased reticulo-propriospinal contacts after unilateral cervical hemisection in adult rats. This plasticity was accompanied by substantial locomotor improvements, implicating interactions between the lesioned RtST and PrINs as important structural relays post-SCI. Given that in the study by Filli and colleagues the RtST tract was lesioned unilaterally, it is likely that plasticity in spared RtST axons also contributed to the improvements in hindlimb function [5]. Thus, it is not possible to make a clear conclusion on the contribution of the sprouting of lesioned versus spared axons on recovery. Therefore, the aim of the current study was to clarify the role of injured RtST axons and their connection to PrINs in locomotor recovery following staggered SCIs, where no spared RtST axons are present.

2. Materials and Methods

2.1 Subjects

Experiments were conducted using adult female Lewis rats (N = 17; Charles River Laboratories, Wilmington, MA, USA), weighing 230-270 g. The dSTAG group was made up of n = 9 rats and the cSTAG group of n = 8 rats. One of the dSTAG animals was found to have axonal sparing (see section 2.5.4 for details) and one animal from the cSTAG group died during neuronal tracing surgery. Hence, these animals were removed from the study for a final dSTAG n = 8 and cSTAG n = 7. Rats were housed in pairs in standard home-cages and kept on a 12:12 light-dark cycle. Water and food were provided ad libitum. Experiments were approved by the Health Sciences Animal Care and Use Committee of the University of Alberta.

2.2 Surgical Procedures

All surgeries were performed under isoflurane anesthesia; 5% for induction and 2-2.5% for maintenance. To prevent anesthesia induced hypothermia, surgical procedures were conducted on a heating blanket set to 37°C. At the start of surgeries, rats were shaved and their skin was disinfected with 2% chlorhexidine digluconate (Sigma-Aldrich Canada Ltd., Oakville, ON, Canada) and ETOH. Eyes were lubricated with Tears Naturale (Alcon Canada, Inc., Mississauga, ON, Canada).

The dSTAG group underwent a lateral hemisection at vertebral level T10 (right spinal cord), followed 2 weeks later by a lateral over-hemisection at vertebral level T7 (left spinal cord; Fig. 1A). For the hemisection SCIs, one half of the spinal cord was cut, while for the over-hemisections the dorsal funiculus was bilaterally transected in addition to one half of the spinal cord [10]. In contrast to the dSTAG group, the cSTAG animals received both hemisections concomitantly (received the T7 and T10 lesions in the same surgery). For all SCI surgeries, a dorsal midline skin incision was made from vertebral level T6 to T11, and the underlying

muscles were dissected from the T10 and/or T7 vertebrae. A dorsal laminectomy was performed on vertebra T10 and/or T7, the dura mater was lifted with fine forceps and cut open with spring scissors, and the spinal cord was transected using a custom-blade. After the hemisection(s), muscles were sutured with Vicryl 5-0 (Johnson & Johnson Medical Pty Ltd., Sydney, NSW, Australia), and the skin incision was closed with stainless steel clips (Stoelting Co., Wood Dale, IL, USA). Following each operation, the animals received 4 ml of saline (s.c.) and placed in a heated cage until fully awake. Buprenorphine (0.05 mg/kg, s.c.; Temgesic, Schering-Plough, Kirkland, QC, Canada) was given at the end of surgery and every 8 hours for 2 days to maintain post-operative analgesia. Bladder fullness was checked two to three times daily post-SCI and manually expressed as needed until the experimental end-point.

Seven weeks post-SCI, all rats underwent surgery to inject neuronal tracers. Small cranial windows (~1 mm x 1 mm) located 0.8 mm lateral to the midline and 2.8 mm caudal of the interaural line were made using a dental drill. RtST axons were stained using the anterograde tracer biotinylated dextran amine **(**BDA 10 000 MW; Invitrogen, Carlsbad, CA, USA). BDA (1 µl of 10% BDA dissolved in 0.01 M PB) was pressure injected manually into the right gigantocellular (Gi) nucleus of the reticular formation in the brainstem using a stereotaxic frame (coordinates: 0.8 mm lateral to the midline, 2.8 mm caudal to the interaural line, and 7.6 mm deep) with a 10 µl Hamilton syringe (26s with an outer diameter of 0.47 mm and an inner diameter of 0.13 mm; Fig. 1B-C). Next, a laminectomy of vertebra T13 was performed to expose the L3 spinal cord. PrINs located in the inter-hemisection tissue bridge and projecting to the lumbar enlargement were stained using the retrograde tracer dextran tetramethylrhodamine (TMR 10 000 MW; Invitrogen). TMR (0.5 µl of 10% TMR dissolved in 0.01 M PB) was pressure injected manually into the bilateral intermediate lamina of L3 (coordinates: ~200-300

um lateral to the midline, 400 um deep) using a pulled glass microelectrode mounted onto a Hamilton syringe connected to a micromanipulator (Fig. 1B-C). Tracer injections were carried out over the span of 2 min/injection, with a 2 min waiting period before withdrawal of the syringe/microelectrode tip. Spinal tracing of PrINs with TMR was performed immediately following BDA-brainstem tracing. One animal from the cSTAG group died during neuronal tracing while under surgical plane anesthesia and was, thus, removed from the study.

2.3 Behavioural testing

The BBB locomotor rating scale was used to assess functional recovery post-SCI. In short, each rat was individually assessed for 4 min by two independent observers in an open field (30 x 90 x 120 cm) and scored according to the scale developed by Basso et al. (1995) [25]. Testing was performed 1 day after bilateral SCI and continued weekly for 7 weeks. Mean group scores for the left and right hindlimb, as well as the average score of the two hindlimbs, were assessed.

2.4 Perfusion and Tissue processing

Two weeks after tracing, the animals were euthanized with an overdose of pentobarbital (1000 mg/kg i.p.; Euthanyl; Biomeda-MTC, Cambridge, ON, Canada) and perfused with saline containing heparin followed by 4% paraformaldehyde with 5% sucrose (PFA; 0.1 M PB; pH 7.4). Spinal cords were removed, post-fixed in 4% PFA overnight, and cryoprotected in 30% sucrose for 3 days. The perfused CNS was divided into blocks for cutting, including the cervical spinal cord (C1), T7 SCI, T10 SCI, the inter-lesion thoracic cord (T8-9), and the lumbar spinal cord (L3). Individual tissue blocks were coated in O.C.T cryoprotectant (Sakura Finetek,

Torrance, CA, USA) and frozen at -60°C in 2-methylbutane (Fisher Scientific, Ottawa, ON, Canada). Blocks of spinal cord (each ~ 4 mm long) containing the T10 and T7 SCIs, C1, and L3 and brainstems were cut in cross-section, while the inter-lesion spinal cord was cut horizontally. All tissue sections were 25 μm thick and cut with a cryostat (Cryostar NX70; Fisher Scientific). Sections were mounted onto slides (Fisher Scientific) and stored at -20°C.

2.5 Histology and Analysis

All tissue sections were dehydrated at 37°C and rehydrated by rinsing 2 or 3 x 10 min in tris buffered saline (TBS). Tissue from each of the blocks was processed as follows:

2.5.1 Lesion size: Slides containing cross-sections from the T7 and T10 SCI sites were immersed in 0.5% cresyl violet for 4 min. Slides were rinsed in distilled water for 2 min then serially dehydrated in increasing ethanol concentrations: 50%, 75%, and 99% for 2 min each. This was followed by clearing 2 x 2 min in xylene. Finally, samples were coverslipped with Permount (Fisher Scientific).

Cresyl violet stained sections were imaged under bright-field microscopy using a Leica DMLB microscope equipped with a 5x (0.15 NA) objective lens (Leica Microsystems Inc., Richmond Hill, ON, Canada). The maximal lesion extent was drawn on schematics of the cross-sections and the lesioned area was calculated as a percent of the total area of the cross-section. Spinal tissue was considered injured if the structural integrity of the tissue was compromised, such as when cavitation occurred, the grey matter was deformed, and/or the parenchyma was infiltrated by inflammatory cells stained darkly with cresyl violet. To ensure lesion completeness, the T10 and T7 lesion schematics were overlaid and the percent of spared

ventrolateral funiculus white matter was quantified as a percentage using the formula: 100 x (area of spared tissue / total cross-sectional area).

2.5.2 Evaluation of BDA injection: Brainstems of randomly selected rats (n = 4 dSTAG; n = 2 cSTAG) were processed to confirm the location of injection sites. Cross-sections were incubated with streptavidin-conjugated Alexa Fluor 488 (AF488; 1:100; Cedarlane, Burlington, ON, Canada) in 1% normal goat serum (NGS) and TBS with triton-X (0.5%; TBS-TX). Sections were then rinsed 2 x 10 min in TBS-TX (0.5%) and 2 x 10 min in TBS. After washing, samples were coverslipped with Fluoromount G (Cedarlane), and the slide edges were sealed with nail polish. Sections were imaged using a Leica DM6000 B epifluorescence microscope equipped with a 5x (0.15 NA) objective lens (Leica Microsystems Inc.). Images were compared to representations of the Gi reticular nucleus in Paxinos and Watson (1998) [26] to confirm tracing accuracy.

2.5.3 Traced RtST axon counts: C1 cross-sections were stained in all animals as described in 2.5.2. Tile scan images of the C1 sections were captured using a Leica epifluorescence microscope with the 5x objective lens. The tile scan images were analyzed with ImageJ (v.1.43µ; National Institutes of Health, Bethesda, MD, USA), and the number of BDA-traced RtST axons was counted using the cell counter plugin.

2.5.4 RtST axonal sparing: To investigate whether traced RtST axons were spared in animals with some structurally intact tissue (n = 4 dSTAG; n = 1 cSTAG), 3,3'-diaminobenzidine (DAB) was used to stain cross-sections caudal to the T10 SCI epicenter. Sections were permeabilized using 2 x 45 min in TBS-TX (0.5%) detergent. While slides were being permeabilized, an avidin/biotin complex (ABC) solution was made using the Vectastain Elite

ABC HRP kit (peroxidase, rabbit IgG; Vector Laboratories Inc., Burlington, ON, Canada). Slides were placed in a humidifying chamber; ABC solution was applied over the tissue and allowed to incubate overnight at 4°C. The following day, slides were washed 3 x 10 min in TBS then incubated in DAB stain solution (DAB peroxidase HRP reaction kit; Vector Laboratories Inc.) until the appearance of the dark brown precipitate from the DAB reaction. This was followed by washing with TBS for 10 min, dehydration through increasing concentrations of alcohol (50%, 75%, and twice in 99% for 2 min each), and clearing twice in xylene (2 min). Slides were coverslipped with Permount (Fisher Scientific) and left to dry.

To search for any putatively spared RtST axons, approximately 20 sections 25 µm apart were inspected per animal for a total distance assessed of 975 µm. Slides were visualized under bright-field microscopy using a Leica DMLB microscope equipped with a 40x (0.75 NA) objective lens (Leica Microsystems Inc.) and, using an attached camera, images were taken of one section below the injuries and axons counted using the cell counter plugin on ImageJ (v.1.43µ; National Institutes of Health). Only one animal (from the dSTAG group) had spared RtST axons below the injuries. Therefore, this animal was removed from the study. To determine the ratio of spared axons to those originally traced with BDA, cross-sections of the brainstem of the animal were stained, imaged, and analyzed using the same protocols as with the spinal sections. Brainstem rather than C1 sections were stained with DAB and used to determine the ratio, because all C1 sections had already been processed for other analyses.

2.5.5 Evaluation of TMR injection: L3 cross-sections were coverslipped with Fluoromount G, and the coverslip was fixed in place with nail polish. Sections were analyzed to confirm that all of the TMR injections were located in the intermediate grey matter of the lumbar

spinal cord using a Leica DM6000 B epifluorescence microscope equipped with a 10x (0.3 NA) objective lens (Leica Microsystems Inc.).

2.5.6 Counting of RtST collaterals, PrINs, and contacts between collaterals and PrINs, and quantifying collateral growth: Slides containing horizontal sections of inter-lesion spinal cord were incubated in 10% NGS in TBS-TX for 1 hr. Next, the samples were incubated with AF488-strepdavidin (1:100) and rabbit anti-synaptophysin antibody (1:200; Sigma-Aldrich Canada Ltd.) in 1% NGS in TBS-TX overnight at 4°C. Slides were rinsed 3 x 10 min in TBS then incubated with AF647 conjugated secondary antibodies (goat anti-mouse; 1:500; Invitrogen) in 1% NGS in TBS. To prevent over-staining, samples were bathed 2 x 10 min in TBS-TX (0.5%) and 2 x 10 min TBS. Lastly, slides were coverslipped with Permount (Fisher Scientific). For each animal, three sections encompassing the intermediate grey matter were analyzed.

The number of TMR labeled cell bodies between the two spinal injuries was quantified. Tile scans of tissue sections were captured under epifluorescence using a 10x (0.3 NA) objective lens, and the number of TMR positive cell bodies in the left and right grey matter were counted using the ImageJ cell counter plugin. To be considered a TMR stained PrIN each cell body had to meet three criteria: (1) contained TMR in the cytoplasm, (2) the nucleus was clearly visible based on its round shape and lack of TMR staining, (3) and at least one TMR stained proximal process was clearly visible. Cell body counts were normalized to the rostro-caudal length (in μm) of the section analyzed. To determine the ratio of soma between sides, we divided the average number of cell bodies/μm on the left by the number of cell bodies/μm on the right.

Tile scans were also used to count RtST collaterals and measure collateral growth. The

number of collaterals branching from the right RtST and crossed into the grey matter were counted with epifluorescence using a 10x (0.3 NA) objective lens. Collateral numbers are reported as the average number of collaterals normalized to the average length (in μm) of the analyzed sections and the total number of traced RtST axons. To assess collateral growth, RtST collaterals were manually traced on ImageJ. One section per animal was traced and a macro was created for ImageJ to automatically count the number of collateral intersections at 0-1000 μm from the grey/white matter interface on the right side. The right side was used as the starting point, as only the right RtST was labeled with BDA and the majority of RtST axons descend ipsilaterally [27]. Collateral intersections were counted every 25 μm and normalized to the length (μm) of the section analyzed and the number of traced axons.

For analysis of reticulo-propriospinal contacts, Z-stack image sets containing brightly stained TMR stained PrINs were acquired using a Leica DM4000 B confocal microscope equipped with a 40x (1.15 NA) objective lens. Identification of PrINs for analysis was based on the same criteria used to count PrIN cell bodies. Similar to previous studies [28,29,30,31,32], contacts were identified based on three criteria: (1) the RtST bouton must be a round or elliptical swelling with a diameter twice that of the parent collateral; (2) there was no discernible gap between the RtST bouton and TMR labeled dendrite/soma; and (3) both the RtST bouton and TMR labeled dendrite/soma were in the same focal plane at the site of the putative contact. Appositions meeting these criteria have been shown to correspond to synaptic contacts (~90% correlation) at the electron microscopic level [33,34,35,36,37, 38]. Additionally, to further validate these inclusion criteria for bouton identification, contacts from three animals in the dSTAG group were examined for the presence of the synaptic marker synaptophysin.

Identification of contacts was performed by scrolling up and down the z-stacks and finding appositions in the same plane of focus or ± 1-step (0.76 μm each; Fig. 2). The average number of contacts in the right and left grey matter, and average total number of contacts were analyzed.

2.6 Statistical Analysis

Statistical analysis was carried out using SigmaPlot 13 (Systat Software Inc., San Jose, CA, USA) and GraphPad Prism 7 (GraphPad Software Inc., La Jolla, CA, USA). Normality was assessed using D'Agostino-Pearson omnibus test. Given a small n, the cSTAG group did not meet the conditions for normality. So, all between-group comparisons were made with Mann-Whitney U tests. The number of collateral intersections was assessed with two-way repeated measures analysis of variance (two-way RM ANOVA) and Tukey's multiple comparisons test. Weekly BBB open-field locomotion scores were tested with two-way RM ANOVA and Holm-Šídák method for post-hoc analysis. Data are presented as mean values ± SEM, and the threshold for significance was set at a p-value of ≤ 0.05.

3. Results

3.1 Behavioural Testing

Overground open-field locomotion was evaluated using the BBB scale once every week for 7 weeks, beginning 1 day after T7 over-hemisection SCI. Left and right hind leg scores improved steadily for both dSTAG and cSTAG animals until the fourth week post-injury and reached a plateau thereafter (Fig. 3A & 3B). However, it is notable that there was a significant main effect between the left and right hindlimbs for the cSTAG group ($p < 0.05$*). The right

hindlimb of cSTAG animals had significantly lower BBB scores than the left hindlimb at weeks 3 ($p < 0.01$**), 4 ($p < .001$***), 5 ($p < 0.01$**), 6 ($p < 0.01$**), and 7 ($p < 0.05$*; Fig. 3B). Over the course of testing, the average right hindlimb score of cSTAG animals was 0.27 ± 0.47 and the average left hindlimb score was 2.27 ± 0.47. This means that the right hindlimb of cSTAG animals was paralyzed, while the left hindlimb showed movement of at least one joint, hip, knee, or ankle [18]. Although right hind leg performance also trailed behind that of the left leg in dSTAG animals, this difference was not statistically significant (Fig. 3A; $p = 0.13$). The average hind leg scores of dSTAG animals over the 7 weeks of testing were 3.25 ± 0.6 and 4.68 ± 0.6 for the right and left legs respectively. In other words, the right leg of dSTAG animals showed movement of at least two joints and the left leg showed movement of three joints. In addition, separating the T10 and T7 SCIs by 2 weeks resulted in significantly better average (both left and right) hindlimb motor performance ($p < 0.05$*; Fig. 3C). Motor ability of dSTAG rats was superior compared to that of cSTAG rats at all time points except Day 1 and week 4 ($p < 0.05$*; Fig. 3C). Average BBB scores of the two hindlimbs throughout the duration of the experiment were 3.97 ± 0.86 for the dSTAG group and 1.27 ± 0.88 for the cSTAG group. This means that the dSTAG group had movement in all three joints and the cSTAG group had, at best, movement of two joints. In summary, dSTAG rats recovered better than those with cSTAG.

3.2 Histology

3.2.1 Lesion size was assessed to evaluate the completeness of the staggered SCI. No significant differences in the cross-sectional areas of the T10 SCIs were found between the dSTAG (average $64.4\% \pm 4.5$) and cSTAG (average $63.3\% \pm 4.7$) groups ($p = 0.87$; Fig. 4A). Similarly, no significant differences in the cross-sectional areas of the T7 SCIs were found

between the dSTAG (average 55.6% ± 1.4) and cSTAG (average 59.8 ± 2.2; p = 0.07; Fig. 4B). Analysis of cresyl violet stained sections revealed a small percentage (<8%) of spared tissue near the RtST tracts in the ventrolateral funiculi at the T7 lesion of some animals. To ensure that tissue that appeared intact with cresyl violet staining did not also contain spared RtST axons, cross-sections caudal to the two SCIs were inspected under the microscope for the presence of BDA-traced RtST axons. No axons were present caudal to the lesions in n = 3 of the dSTAG animals and the cSTAG animal, indicating completeness of the SCIs. One dSTAG animal had 4.1% tissue sparing and 9.5% of traced RtST axons spared and was taken out of the study.

3.2.2 Counting of traced RtST axons and PrINs and evaluation of neuronal tracer injections: The accuracy of the tracer injections into the right Gi reticular nucleus and bilateral intermediate lamina of the lumbar spinal cord were verified (Fig. 1B). No significant differences in the number of traced RtST axons were found between dSTAG and cSTAG animals (p = 0.87). The dSTAG group averaged 304 ± 60 traced axons, while the cSTAG group averaged 372 ± 142 traced axons (Fig. 5A & 5B). PrIN cell bodies that were retrogradely stained with TMR and located in the intermediate grey matter between the T7 and T10 SCIs were counted and normalized to the length of the section analyzed. No significant difference between groups was found for the sum of cell bodies/µm on each side of the grey matter (p = 0.54; Fig. 5C & 5D). dSTAG animals averaged $29.8 \times 10^{-4} \pm 4.40 \times 10^{-4}$ cell bodies/µm and cSTAG animals averaged $40.8 \times 10^{-4} \pm 8.69 \times 10^{-4}$ cell bodies/µm. There was a trend for higher numbers of soma in the left side compared to the right. However, the left/right ratios did not statistically differ between groups (p = 0.07). Collectively, these data show that RtST and PrIN tracing was comparable between dSTAG and cSTAG.

3.2.3 Counting of RtST collaterals, quantifying collateral growth, and counting contacts between collaterals and PrINs: The average number of traced RtST collaterals that entered the grey matter (normalized to traced RtST axon count and the length of section analyzed) was similar between dSTAG ($2.96 \times 10^{-6} \pm 6.5 \times 10^{-7}$ collaterals/traced axon/μm) and cSTAG ($1.43 \times 10^{-6} \pm 3.48 \times 10^{-7}$ collaterals/traced axon/μm) animals ($p = 0.12$; Fig. 6A & 6B).

A significant main group effect was found on the number of collateral intersections 0-1000 μm from the grey/white matter interface (normalized to traced axon count and length of section; $p < 0.05$*; Fig. 6C). Multiple comparisons showed the dSTAG group had significantly more collateral intersections 425 μm from the grey/white matter interface ($P < 0.05$*). At this distance, dSTAG animals had $5.63 \times 10^{-6} \pm 2.02 \times 10^{-6}$ collaterals/traced axon/μm and cSTAG animals had $1.17 \times 10^{-6} \pm 6.1 \times 10^{-7}$ collaterals/traced axon/μm. Taken together, these analyses show that dSTAG animals had more extensive collateralization in the grey matter between injury sites than cSTAG animals. Contacts between RtST collaterals and PrINs were found in both the left and right grey matter between the spinal injuries. An average of 18.0 ± 2.0 (dSTAG) and 14.7 ± 0.3 (cSTAG) TMR stained PrINs per animal were analyzed on the left side of the grey matter and an average of 16.6 ± 1.63 (dSTAG) and 15.0 (cSTAG) cell bodies/animal were analyzed on the right side. Contacts are reported as number of contacts/traced RtST axon. In dSTAG animals the number of reticulo-propriospinal contacts was higher in the left side of the grey matter ($p < 0.05$*; Fig. 7A), the right side ($p < 0.05$*; Fig. 7B), and the total of both sides ($p < 0.05$*; Fig. 7C) compared to cSTAG animals. The differences in connections was most pronounced in the left spinal cord where the dSTAG animals had ~5.9 times more contacts than cSTAG animals (dSTAG: $29.3 \times 10^{-4} \pm 9.5 \times 10^{-4}$; cSTAG: $5.0 \times 10^{-4} \pm 2.1 \times 10^{-4}$), compared to the right spinal cord where dSTAG animals had ~3.4 times more contacts than cSTAG (dSTAG:

$24.1 \times 10^{-4} \pm 5.9 \times 10^{-4}$; cSTAG: $7.0 \times 10^{-4} \pm 4.5 \times 10^{-4}$). The dSTAG group also had ~4.4 times more total contacts than the cSTAG group (dSTAG: $26.6 \times 10^{-4} \pm 7.1 \times 10^{-4}$; cSTAG: $6.0 \times 10^{-4} \pm 2.5 \times 10^{-4}$). RtST boutons that formed a contact with a PrIN were further evaluated for synaptophysin immunoreactivity. Twelve randomly selected contacts were all synaptophysin-positive, suggesting that contacts between the RtST tract and intermediate lamina PrINs were functional synapses (Fig. 8). To conclude, more contacts were found between RtST boutons and PrINs in dSTAG rats as compared to cSTAG rats.

4. Discussion

In this study, we show that transection of all RtST axons using a staggered spinal lesion model allows for rewiring of RtST axons onto PrINs that project to the lumbar spinal cord. Notably, this RtST plasticity occurs in parallel to improved locomotor performance. Considering the role of RtST axons in triggering locomotor activity [19, 39], these data suggest that rewiring of lesioned RtST axons might be a mechanism in locomotor recovery in our staggered hemisection SCI model. Interestingly, more synaptic connections with PrINs were found when the second hemisection was delayed by 2 weeks (dSTAG) compared to animals that received both hemisections at the same time (cSTAG), which could explain the superior recovery of these animals.

Recent studies indicate that injured RtST axons can sprout and connect onto PrINs rostral to cervical lateral hemisections [9]. It was proposed that these connections were involved in promoting recovery, without taking into account that spared axons also increase their input into lumbar CPGs [5]. Here, we confirm that injured RtST axons can form contacts with PrINs after thoracic SCI with a staggered lesion model, where no RtST axons are spared. Further, the group

of animals with the most RtST-PrIN connectivity showed the greatest improvements in locomotor function. Our data, however, do not consider the number of naturally occurring RtST collaterals projecting towards PrINs in intact animals, as this relation has already been established by Filli et al. (2014) [9].

The effect of temporally spacing out the two SCIs on RtST-PrIN contact formation cannot be accounted for by differences in lesion size or the number of traced PrIN soma and RtST axons, given that these measures were comparable between groups. The number of RtST axons entering the grey matter also did not differ between groups. However, dSTAG collaterals exhibited enhanced growth compared to cSTAG collaterals. Therefore, the rise in contacts in the dSTAG group compared to the cSTAG group might reflect an increase in total collateral length, rather than an increase in synapses per unit length of collateral. Alternatively, the group effect on contact formation might be due to a lack of excitability of PrINs in cSTAG rats. Following the more severe lesion scenario of the cSTAG group, spinal shock would have involved a greater spinal area and likely a longer time frame to resolve [40]; thus, making PrINs poor targets for the formation of new synapses in the first days following the lesion.

Superior recovery of dSTAG animals could be because rats with a single hemisection recover locomotor movements quickly and are very active in their cages (also because the leg opposite the SCI is largely functional) [5]. It is known that activity in the cage after SCI acts as rehabilitative training [41] and promotes plasticity like the formation and consolidation of new contacts. Activity drives plasticity by inducing increases in growth factors BDNF and NT-3 in the spinal cord [42]. Furthermore, training after an incomplete SCI results in adaptations of spinal CPG networks, contributing to recovery. These adaptations remain functionally relevant

even after subsequent complete spinal transections in cats [43] and rats [44]. In fact, cat [45] and rat [46] spinal CPGs can be trained to a point that animals can recover walking on a treadmill. However, perineal stimulation is required with training in rats [46]. Consequently, by the time dSTAG animals receive the second injury (2 weeks following the first hemisection), the spinal cord has already adapted and, thus, these animals have a greater capacity for locomotion. Since cSTAG animals can hardly generate movements, self-rehabilitation and the resulting plasticity are hindered. That is to say, activity below the lesion is likely a key for rewiring.

Our results on the difference in recovery between dSTAG and cSTAG groups are consistent with reports by Courtine et al. (2008) [47] where mice that underwent delayed, but not simultaneous contralateral hemisections, recovered locomotion. Courtine and colleagues speculated that supraspinal-propriospinal relay connections were responsible for the observed recovery in rats with a delay between the hemisection injuries, but did not provide evidence of these connections. In our experiment, we provide evidence of increased numbers of RtST-PrIN connections in animals with temporally separated lesions compared to simultaneous lesions. Furthermore, RtST-PrIN connections occurred in parallel to functional recovery. However, a causal relation between the connections and functional changes remains to be established. A possible approach to establish causality would be to reversibly shut down PrINs in the tissue bridge connecting staggered SCIs and assess function. For example, PrINs could be double infected with a retrograde gene-transfer lentiviral vector in the lumbar spinal cord and an adeno-associated vector at the soma [48]. The lentiviral vector would transfer a tetanus neurotoxin gene downstream of the tetracycline-responsive element, while the adeno-associated vector would carry a Tet-ON sequence (a type of reverse tetracycline transactivator). Double infected PrINs could, then, be selectively and temporarily shut down via doxycycline-dependent transcriptional

activation of the tetanus neurotoxin gene [48]. Alternatively, PrINs could be reversibly silenced with designer receptors exclusively activated by designer drugs (DREADDs) technology [49]. A limitation of reversibly silencing PrINs is that resulting functional drops could be due to the shutting down of connections between descending axons and PrINs or shutting down of PrINs alone. Indeed, plasticity in CPG networks can support some degree of motor recovery post-SCI by itself. For example, Martinez et al. (2012) [43] showed adaptations of motor function occur in cats with incomplete SCI, and some of these adaptations are retained after subsequent complete spinal cord transection. Further, Cowley et al. (2008) [50] induced locomotor-like activity by stimulating the brainstem electrically soon after cSTAG SCI in an *in vitro* preparation. In other words, plasticity of descending systems over-time post-injury was unnecessary for transmission of locomotor command signals to the spinal cord. To determine whether RtST descending input is needed for the support of motor recovery in the staggered SCI model *in vivo*, neurons of the RtST projecting to the tissue bridge between hemisection injuries could be reversibly silenced using double infection techniques [48] or DREADDs technology [49]. Also, silencing data could be complemented with electrical stimulation of brainstem nuclei giving rise to the RtST and electromyographic recordings of hindlimb muscles [51].

It is noteworthy that in the cSTAG group the right hindlimbs were nearly paralyzed as compared to the left hindlimbs. Left hindlimb function of the dSTAG and cSTAG groups was similar. However, unlike cSTAG, the right hindlimb of dSTAG animals recovered to the point where there was no difference between sides (Fig. 3A & 3B). In other words, locomotor benefits of temporally separating the two spinal lesions are attributable to improvements of the right hindlimb. The differences in function between the left and right hindlimb are consistent with the location of the SCIs (Fig. 1C; the left lesion was at vertebral level T7 above the right lesion at

level T10). Following the two injuries, RtST axons would have descended on the right side and innervated lumbar projecting PrINs there. Most PrINs are single-crossing (crossing the midline once only) [7,52). Therefore, most of the innervated PrINs would have projected to the left side, helping restore left axis function (Fig. 1C). It is also possible that descending RtST axons innervated double-crossing PrINs to restore the right axis, but these double-crossings are relatively rare [9]. Although the RtST descended on the right, it sprouted to the left side, contacting PrINs there. These PrINs could have improved the left axis via ipsilateral projections or the right axis via single-crossings (Fig. 1C). On the whole, fewer routes of communication were possible for the right leg. Increased RtST-PrIN contact formation in dSTAG animals could have provided the missing input to the right leg to support recovery.

The finding of PrIN-RtST connections does not eliminate the possibility that other pathways are involved in the observed recovery. Pontine reticular, vestibulospinal, and rubrospinal pathways have all been implicated in the modulation of locomotion [53,54]. In addition to these pathways, the CST can form relays with PrINs in rodents with staggered hemisection SCIs [10]. The CST, moreover, has a causal effect on the locomotor function of staggered rats, as shown by the loss of locomotion following cortical inactivation with the GABA agonist muscimol [10]. Although convincing, these results are surprising as rodents without any CST input are able to walk effectively over open ground [55]. Taking into consideration the multiplicity of descending control of locomotor networks, our earlier work with the staggered SCI model on adaptations in motor neuron properties [12] and the current study's results, it becomes increasingly clear that even in experimental SCI, the contribution of plasticity at different levels to recovery is complex and not yet fully understood.

Neuroplasticity is a key mechanism in functional recovery after SCI in both animal models and humans. As reviewed by Raineteau and Schwab (2001) [56], several studies have indicated that the main functional adaptation following SCI is synaptic plasticity in pre-existing pathways and the formation of new circuits through collateral sprouting of injured and uninjured axons [6,7,8,9,10]. Therefore, continued investigation of the exact spinal tracts and systems involved and nature of the circuit rewiring is of the utmost importance to understand the full complexity of the mechanisms of recovery. Complete knowledge of the mechanisms of recovery can then be harnessed to discover and inform new treatments for individuals living with SCI.

5. Conclusions

Our work shows that injured RtST axons form synaptic contacts with lumbar-projecting PrINs after SCI in rats. Further, RtST-PrIN contact formation is paralleled by locomotor recovery, suggesting RtST rewiring is key for locomotor recovery post-SCI. Finally, enhanced contact formation in rats with a delay between SCIs compared to rats with simultaneous injuries shows neuronal activity might be key for rewiring to occur.

Acknowledgements

We would like to acknowledge our funding agency CIHR (RES0011338) (KF) in Canada and Romana Vavrek for excellent technical assistance. The authors declare that there is no conflict of interest regarding the publication of this paper.

References

1. Park, K. K., Liu, K., Hu, Y., Smith, P. D., Wang, C., Cai, B., … He, Z. (2008). Promoting Axon Regeneration in the Adult CNS by Modulation of the PTEN/mTOR Pathway.

Science, *322*(5903), 963–966. http://doi.org/10.1126/science.1161566

2. Caroni, P., & Schwab, M. E. (1988). Antibody against myelin associated inhibitor of neurite growth neutralizes nonpermissive substrate properties of CNS white matter. *Neuron*, *1*(1), 85–96. http://doi.org/10.1016/0896-6273(88)90212-7

3. Jones, L. L., Margolis, R. U., & Tuszynski, M. H. (2003). The chondroitin sulfate proteoglycans neurocan, brevican, phosphacan, and versican are differentially regulated following spinal cord injury. *Experimental Neurology*, *182*(2), 399–411. http://doi.org/10.1016/S0014-4886(03)00087-6

4. Massey, J. M., Hubscher, C. H., Wagoner, M. R., Decker, J. A., Amps, J., Silver, J., & Onifer, S. M. (2006). Chondroitinase ABC digestion of the perineuronal net promotes functional collateral sprouting in the cuneate nucleus after cervical spinal cord injury. *Journal of Neuroscience*, *26*(16), 4406–4414. http://doi.org/10.1523/JNEUROSCI.5467-05.2006

5. Ballermann, M., & Fouad, K. (2006). Spontaneous locomotor recovery in spinal cord injured rats is accompanied by anatomical plasticity of reticulospinal fibers. *The European Journal of Neuroscience*, *23*(8), 1988–1996. http://doi.org/10.1111/j.1460-9568.2006.04726.x

6. Fouad, K., Pedersen, V., Schwab, M. E., & Brösamle, C. (2001). Cervical sprouting of corticospinal fibers after thoracic spinal cord injury accompanies shifts in evoked motor responses. *Current Biology*, *11*(22), 1766–1770. http://doi.org/10.1016/S0960-9822(01)00535-8

7. Vavrek, R., Girgis, J., Tetzlaff, W., Hiebert, G. W., & Fouad, K. (2006). BDNF promotes

connections of corticospinal neurons onto spared descending interneurons in spinal cord injured rats. *Brain*, *129*(6), 1534–1545. http://doi.org/10.1093/brain/awl087

8. Bareyre, F. M., Kerschensteiner, M., Raineteau, O., Mettenleiter, T. C., Weinmann, O., & Schwab, M. E. (2004). The injured spinal cord spontaneously forms a new intraspinal circuit in adult rats. *Nature Neuroscience*, *7*(3), 269–277. http://doi.org/10.1038/nn1195

9. Filli, L., Engmann, A. K., Zorner, B., Weinmann, O., Moraitis, T., Gullo, M., … Schwab, M. E. (2014). Bridging the Gap: A Reticulo-Propriospinal Detour Bypassing an Incomplete Spinal Cord Injury. *Journal of Neuroscience*, *34*(40), 13399–13410. http://doi.org/10.1523/JNEUROSCI.0701-14.2014

10. van den Brand, R., Heutschi, J., Barraud, Q., DiGiovanna, J., Bartholdi, K., Huerlimann, M., … Courtine, G. (2012). Restoring Voluntary Control of Locomotion after Paralyzing Spinal Cord Injury. *Science*, *336*(6085), 1182–1185. http://doi.org/10.1126/science.1217416

11. Hayashi, M., Ueyama, T., Nemoto, K., Tamaki, T., & Senba, E. (2000). Sequential mRNA expression for immediate early genes, cytokines, and neurotrophins in spinal cord injury. *Journal of Neurotrauma*, *17*(3), 203–218. http://doi.org/10.1089/neu.2000.17.203

12. Murray, K. C., Nakae, A., Stephens, M. J., Rank, M., D'Amico, J., Harvey, P. J., … Fouad, K. (2010). Recovery of motoneuron and locomotor function after spinal cord injury depends on constitutive activity in 5-HT2C receptors. *Nature Medicine*, *16*(6), 694–700. http://doi.org/10.1038/nm.2160

13. Tillakaratne, N. J., Mouria, M., Ziv, N. B., Roy, R. R., Edgerton, V. R., & Tobin, A. J.

(2000). Increased expression of glutamate decarboxylase (GAD(67)) in feline lumbar spinal cord after complete thoracic spinal cord transection. *Journal of Neuroscience Research*, *60*(2), 219–230. http://doi.org/10.1002/(SICI)1097-4547(20000415)60:2<219::AID-JNR11>3.0.CO;2-F

14. García-Alías, G., Barkhuysen, S., Buckle, M., & Fawcett, J. W. (2009). Chondroitinase ABC treatment opens a window of opportunity for task-specific rehabilitation. *Nature Neuroscience*, *12*(9), 1145–1151. http://doi.org/10.1038/nn.2377.

15. Martin, J. H. (2005). The Corticospinal System: From Development to Motor Control. *The Neuroscientist*, *11*(2), 161–173. http://doi.org/10.1177/1073858404270843

16. Lemon, R. N., Johansson, R. S., & Westling, G. (1995). Corticospinal control during reach, grasp, and precision lift in man. *Journal of Neuroscience*, *15*(9), 6145–6156.

17. Lang, C. E. (2004). Reduced Muscle Selectivity During Individuated Finger Movements in Humans After Damage to the Motor Cortex or Corticospinal Tract. *Journal of Neurophysiology*, *91*(4), 1722–1733. https://doi.org/10.1152/jn.00805.2003

18. Basso, D. M., Beattie, M. S., & Bresnahan, J. C. (1996). Graded Histological and Locomotor Outcomes after Spinal Cord Contusion Using the NYU Weight-Drop Device versus Transection. *Experimental Neurology*, *139*(2), 244–256. https://doi.org/10.1006/exnr.1996.0098

19. Schucht, P., Raineteau, O., Schwab, M. E., & Fouad, K. (2002). Anatomical correlates of locomotor recovery following dorsal and ventral lesions of the rat spinal cord. *Experimental Neurology*, *176*(1), 143–153.

20. Steeves, J. D., & Jordan, L. M. (1980). Localization of a descending pathway in the spinal cord which is necessary for controlled treadmill locomotion. *Neuroscience Letters*, *20*(3), 283–288.

21. Tuszynski, M. H., & Steward, O. (2012). Concepts and Methods for the Study of Axonal Regeneration in the CNS. *Neuron*, *74*(5), 777–791. http://doi.org/10.1016/j.neuron.2012.05.006

22. Vavrek, R., Pearse, D. D., & Fouad, K. (2007). Neuronal Populations Capable of Regeneration following a Combined Treatment in Rats with Spinal Cord Transection. *Journal of Neurotrauma*, *24*(10), 1667–1673. http://doi.org/10.1089/neu.2007.0290

23. Xu, X. M., Guénard, V., Kleitman, N., Aebischer, P., & Bunge, M. B. (1995). A combination of BDNF and NT-3 promotes supraspinal axonal regeneration into Schwann cell grafts in adult rat thoracic spinal cord. *Experimental Neurology*, *134*(2), 261–272. http://doi.org/10.1006/exnr.1995.1056

24. Filli, L., & Schwab, M. (2015). Structural and functional reorganization of propriospinal connections promotes functional recovery after spinal cord injury. *Neural Regeneration Research*, *10*(4), 509. http://doi.org/10.4103/1673-5374.155425

25. Basso, D. M., Beattie, M. S., & Bresnahan, J. C. (1995). A Sensitive and Reliable Locomotor Rating Scale for Open Field Testing in Rats. *Journal of Neurotrauma*, *12*(1), 1–21. https://doi.org/10.1089/neu.1995.12.1

26. Paxinos, G. & Watson, C. (1998) *The Rat Brain in Stereotaxic Coordinates*. San Diego, CA: Academic Press.

27. Reed, W. R., Shum-Siu, A., & Magnuson, D. S. K. (2008). Reticulospinal pathways in the ventrolateral funiculus with terminations in the cervical and lumbar enlargements of the adult rat spinal cord. *Neuroscience*, *151*(2), 505-517. doi:10.1016/j.neuroscience.2007.10.025

28. Fenrich, K. K., Skelton, N., MacDermid, V. E., Meehan, C. F., Armstrong, S., Neuber-Hess, M. S., & Rose, P. K. (2007). Axonal regeneration and development of de novo axons from distal dendrites of adult feline commissural interneurons after a proximal axotomy. *The Journal of Comparative Neurology*, *502*(6), 1079–1097. http://doi.org/10.1002/cne.21362

29. Grande, G., Armstrong, S., Neuber-Hess, M., & Rose, P. K. (2005). Distribution of contacts from vestibulospinal axons on the dendrites of splenius motoneurons. *The Journal of Comparative Neurology*, *491*(4), 339–351. http://doi.org/10.1002/cne.20699

30. Grande, G., Bui, T. V., & Rose, P. K. (2010). Distribution of vestibulospinal contacts on the dendrites of ipsilateral splenius motoneurons: An anatomical substrate for push-pull interactions during vestibulocollic reflexes. *Brain Research*, *1333*, 9–27. http://doi.org/10.1016/j.brainres.2010.03.065

31. Maratta, R., Fenrich, K. K., Zhao, E., Neuber-Hess, M. S., & Rose, P. K. (2015). Distribution and density of contacts from noradrenergic and serotonergic boutons on the dendrites of neck flexor motoneurons in the adult cat: NA and 5-HT contacts on flexor motoneurons. *Journal of Comparative Neurology*, *523*(11), 1701–1716. http://doi.org/10.1002/cne.23765

32. Montague, S. J., Fenrich, K. K., Mayer-Macaulay, C., Maratta, R., Neuber-Hess, M. S., & Rose, P. K. (2013). Nonuniform distribution of contacts from noradrenergic and serotonergic boutons on the dendrites of cat splenius motoneurons. *Journal of Comparative Neurology*, *521*(3), 638–656. http://doi.org/10.1002/cne.23196

33. Alvarez, F. J., Pearson, J. C., Harrington, D., Dewey, D., Torbeck, L., & Fyffe, R. E. W. (1998). Distribution of 5-hydroxytryptamine-immunoreactive boutons on ?-motoneurons in the lumbar spinal cord of adult cats. *The Journal of Comparative Neurology*, *393*(1), 69–83. http://doi.org/10.1002/(SICI)1096-9861(19980330)393:1<69::AID-CNE7>3.0.CO;2-O

34. Fyffe, R. E. (1991). Spatial distribution of recurrent inhibitory synapses on spinal motoneurons in the cat. *Journal of Neurophysiology*, *65*(5), 1134–1149.

35. Lübke, J., Egger, V., Sakmann, B., & Feldmeyer, D. (2000). Columnar organization of dendrites and axons of single and synaptically coupled excitatory spiny neurons in layer 4 of the rat barrel cortex. *Journal of Neuroscience*, *20*(14), 5300–5311.

36. Markram, H., Lübke, J., Frotscher, M., Roth, A., & Sakmann, B. (1997). Physiology and anatomy of synaptic connections between thick tufted pyramidal neurones in the developing rat neocortex. *The Journal of Physiology*, *500*(2), 409–440. http://doi.org/10.1113/jphysiol.1997.sp022031

37. Rose, P. K., Ely, S., Norkum, V., & Neuber-Hess, M. (1999). Projections from the lateral vestibular nucleus to the upper cervical spinal cord of the cat: A correlative light and electron microscopic study of axon terminals stained with PHA-L. *The Journal of*

Comparative Neurology, *410*(4), 571–585.

38. Silver, R. A. (2003). High-Probability Uniquantal Transmission at Excitatory Synapses in Barrel Cortex. *Science*, *302*(5652), 1981–1984. http://doi.org/10.1126/science.1087160

39. Loy, D. N., Magnuson, D. S., Zhang, Y. P., Onifer, S. M., Mills, M. D., Cao, Q., Darnall, J. B., Fajardo, L. C., Burke, D. A., & Whittmore, S. R. (2002). Functional redundancy of ventral spinal locomotor pathways. *Journal of Neuroscience*, *22*(1), 315-323.

40. Kiss, Z. H., & Tator, C. H. (1993). Neurogenic Shock. In E. R. Geller (Ed.), *Shock and Resuscitation* (421-440). New York, NY: McGraw Hill.

41. Caudle, K. L., Brown, E. H., Shum-Siu, A., Burke, D. A., Magnuson, T. S. G., Voor, M. J., & Magnuson, D. S. K. (2011). Hindlimb Immobilization in a Wheelchair Alters Functional Recovery Following Contusive Spinal Cord Injury in the Adult Rat. *Neurorehabilitation and Neural Repair*, *25*(8), 729–739. https://doi.org/10.1177/1545968311407519

42. Ying, Zhe, Roy, R. R., Edgerton, V. R., & Gómez-Pinilla, F. (2005). Exercise restores levels of neurotrophins and synaptic plasticity following spinal cord injury. *Experimental Neurology*, *193*(2), 411–419. https://doi.org/10.1016/j.expneurol.2005.01.015

43. Martinez, M., Delivet-Mongrain, H., Leblond, H., & Rossignol, S. (2012). Incomplete spinal cord injury promotes durable functional changes within the spinal locomotor circuitry. *Journal of Neurophysiology*, *108*(1), 124–134. https://doi.org/10.1152/jn.00073.2012

44. Singh, A., Balasubramanian, S., Murray, M., Lemay, M., & Houle, J. (2011). Role of spared

pathways in locomotor recovery after body-weight-supported treadmill training in contused rats. Journal of Neurotrauma, 28(12), 2405-2416. doi: 10.1089/neu.2010.1660

45. Rossignol, S., Drew, T., Brustein, E., & Jiang, W. (1999). Locomotor performance and adaptation after partial or complete spinal cord lesions in the cat. *Progress in Brain Research*, *123*, 349–365.

46. Alluin, O., Delivet-Mongrain, H., & Rossignol, S. (2015). Inducing hindlimb motor recovery in adult rat after complete thoracic spinal cord section using repeated treadmill training with perineal stimulation only. *Journal of Neurophysiology*, *114*(3), 1931-1946. doi:10.1152/jn.00416.2015

47. Courtine, G., Song, B., Roy, R. R., Zhong, H., Herrmann, J. E., Ao, Y., … Sofroniew, M. V. (2008). Recovery of supraspinal control of stepping via indirect propriospinal relay connections after spinal cord injury. *Nature Medicine*, *14*(1), 69–74. http://doi.org/10.1038/nm1682

48. Kinoshita, M., Matsui, R., Kato, S., Hasegawa, T., Kasahara, H., Isa, K., Watakabe, A., Yamamori, T., Nishimura, Y., Alstermark, B., Watanabe, D., Kobayashi, K., & Isa, T. (2012). Genetic dissection of the circuit for hand dexterity in primates. *Nature*, *487*(7406), 235-238. http://doi.org/10.1038/nature11206

49. Hilton, B. J., Anenberg, E., Harrison, T. C., Boyd, J. D., Murphy, T. H., & Tetzlaff, W. (2016). Re-Establishment of Cortical Motor Output Maps and Spontaneous Functional Recovery via Spared Dorsolaterally Projecting Corticospinal Neurons after Dorsal Column Spinal Cord Injury in Adult Mice. *Journal of Neuroscience*, *36*(14), 4080–4092.

https://doi.org/10.1523/JNEUROSCI.3386-15.2016

50. Cowley, K., Zaporozhets, E., & Schmidt, B. (2008). Propriospinal neurons are sufficient for bulbospinal transmission of the locomotor command signal in the neonatal rat spinal cord. *Journal of Physiology*, *586*(6), 1623-1635. http://doi.org/10.1113/jphysiol.2007.148361

51. Drew, T., & Rossignol, S. (1990). Functional organization within the medullary reticular formation of intact unanesthetized cat. II. Electromyographic activity evoked by microstimulation. *Journal of Neurophysiology*, *64*(3), 782–795.

52. Fenrich, K. K., & Rose, P. K. (2009). Spinal interneuron axons spontaneously regenerate after spinal cord injury in the adult feline. *Journal of Neuroscience*, *29*(39), 12145–12158. https://doi.org/10.1523/JNEUROSCI.0897-09.2009

53. Goulding. (2009). Circuits controlling vertebrate locomotion: moving in a new direction. *Nature Reviews Neuroscience*, *10*, 507-518. http://doi.org/10.1038/nrn2608

54. Siegel. (1979). Behavioral functions of the reticular formation. *Brain Research Reviews*, *1*, 69-105. http://dx.doi.org/10.1016/0165-0173(79)90017-1

55. Kanagal, S. G., & Muir, G. D. (2009). Task-dependent compensation after pyramidal tract and dorsolateral spinal lesions in rats. *Experimental Neurology*, *216*(1), 193–206. https://doi.org/10.1016/j.expneurol.2008.11.028

56. Raineteau, O., & Schwab, M. E. (2001). Plasticity of motor systems after incomplete spinal cord injury. *Nature Reviews. Neuroscience*, *2*(4), 263–273. http://doi.org/10.1038/35067570

Chapter 4: Challenges of animal models in SCI research: Effects of pre-injury task-specific training in adult rats before lesion

Zacnicte May[1], Karim Fouad [1], Alice Shum-Siu[2], David S. K. Magnuson[2]

1. Faculty of Rehabilitation Research, University of Alberta, Edmonton, AB Canada
2. Department of Neurological Surgery, Kentucky Spinal Cord Injury Research Center, University of Louisville, Louisville, KY USA

Corresponding Author:

David S. K. Magnuson, PhD

Department of Neurological Surgery,

511 S. Floyd St, MDR 616

University of Louisville, Louisville, KY 40292

dsmagn01@louisville.edu, (502)852-6551

Abstract

A rarely explored subject in animal research is the effect of pre-injury variables on behavioural outcome post-SCI. Low reporting of such variables may underlie some discrepancies in findings between laboratories. Particularly, intensive task-specific training before a SCI might be important, considering that sports injuries are one of the leading causes of SCI. Thus, individuals with SCI often underwent rigorous training before their injuries. In the present study, we asked whether training before SCI on a grasping task or a swimming task would influence motor recovery in rats. Swim pre-training impaired recovery of swimming 2 and 4 weeks post-injury. This result fits with the idea of motor learning interference, which posits that previous learning may disrupt learning of a new task; in this case, learning strategies to compensate for functional loss after SCI. In contrast to swimming, grasp pre-training did not influence grasping ability after SCI at any time point. However, grasp pre-trained rats attempted to grasp more times than untrained rats in the first 4 weeks post-injury. Also, lesion volume of grasp pre-trained rats was greater than that of untrained rats, a finding which may be related to stress or activity. The increased participation in rehabilitative training of the pre-trained rats in the early weeks post-injury may have potentiated spontaneous plasticity in the spinal cord and counteracted the deleterious effect of interference and bigger lesions. Thus, our findings suggest that pre-training plays a significant role in recovery after CNS damage and needs to be carefully controlled for.

1. Introduction

Spinal cord injury (SCI) results in deficits of sensory, motor and autonomic function below the level of the injury. Thus, depending on its severity, SCI may lead to significant disability and to a steep drop in the quality of life. Unfortunately, no truly successful treatments exist for SCI including the most common intervention, rehabilitative training (Fouad & Tetzlaff, 2012). One of the reasons for a lack of effective treatments is the challenge in reproducing results with animal models, let alone human subjects (Filli & Schwab, 2012). The complexity of animal models is frequently underestimated in part due to missing details in published research, a challenge that could be rectified by applying reporting standards as proposed by Lemmon and colleagues (Lemmon et al., 2014). For example, the presence/absence of outliers, treatment side effects and negative outcomes are rarely revealed. Another factor that is frequently ignored and not described sufficiently is the training of the animals prior to experimental injury. This is important information, given that treadmill exercise in rats was reported to increase levels of brain-derived neurotrophic factor (BDNF; Gomez-Pinilla et al., 2001) and other factors associated with plasticity, such as neurotrophin-3 (NT-3; Ying et al., 2003). Elevation of BDNF levels as a result of training/exercise counteracts a SCI induced decline in BDNF (Gomez-Pinilla et al., 2012). BDNF is a neurotrophin associated with cell survival, neurite outgrowth, re-myelination, and neuroprotection (Weishaupt et al., 2012). Hence, animals trained before SCI might display a better recovery following injury than animals left alone in their cages.

In addition, recovery following nervous system injuries frequently involves compensation, or the implementation of a new movement strategy to make up for the loss of function (Hurd et al., 2013). Consequently, one could hypothesize that pre-training a task will

make it more challenging to learn a compensatory strategy following injury. This is based on findings that rehabilitative training in one task may interfere with performance in another task in animal models (Girgis et al., 2007; de Leon et al., 1999). In human subjects, a related phenomenon, termed proactive interference, occurs when learning a new motor skill is adversely affected by a previously learned skill. This phenomenon has, for example, been reported in subjects who first learned the forehand tennis stroke and then had difficulty learning the backhand stroke (Eason & Smith, 1989). Thus, the role of pre-injury training of specific tasks could translate easily to the clinical setting. It may be that the highly variable pre-injury activities and types of exercise humans engage in could influence treatment and rehabilitation decisions and ultimately functional outcomes after injury. Therefore, for the present studies, we explored the effect of task-specific training applied pre-SCI on functional recovery using two different rat models of SCI and two different motor tasks; grasping in animals with a cervical dorsal quadrant lesion and swimming in animals with a thoracic contusion lesion. We chose these models to examine a unilateral fine-motor task with the former (Whishaw et al., 1998) and a bilateral locomotor task with the latter (Smith et al., 2006). The two paradigms involve the use of compensatory movement strategies, which might be susceptible to motor learning interference. Specifically, rats often scoop or drag food pellets rather than actually grasp pellets following cervical SCI (Hurd et al., 2013), and after thoracic SCI, rats switch from relying on their hindlimbs to their forelimbs to swim (Smith et al., 2006).

2. Materials and Methods

2.1. Subjects

For the grasping study, adult female Lewis rats (N = 20; Charles River Laboratories,

Wilmington, MA, USA) were housed in groups of 5 rats per large (18" x 14") cage. For the swimming study, adult female Sprague-Dawley rats (N =14; Harlan, Indianapolis, IN, USA) were housed 2 per cage in smaller (10" x 18") cages under a 12:12h light-dark cycle. All the animals were acclimatized to their respective facility for a minimum of 1 week prior to the start of the experiments. For each study, rats were divided into two groups, the pre-trained group (n = 10 & 7, respectively) and the non-pre-trained group (n = 10 & 7 respectively). For the grasping study, all the animals were food restricted to 9 g per animal on the day before training sessions and were otherwise fed *ad libitum*. Pre-trained rats received daily grasping (SPG) training for 4 weeks before the injury, while the non-pre-trained rats did not.

For the swimming study, pre-trained animals were swim trained daily, receiving 6 x 4 minute swim sessions 5 days a week for 4 weeks as described previously (Magnuson et al., 2009). During this same period of time, untrained animals were moved to/from the exercise room and were handled daily. In both studies, subject weights ranged between 210-240 g at the time of the lesion. Experimental procedures were approved by the University of Alberta Health Science Animal Care and Use Committee (Grasping) or by the University of Louisville Institutional Animal Care and Use Committee (Swimming).

2.2 Surgery

Grasping Study: Rats received a dorsolateral quadrant (DLQ) spinal cord lesion at the cervical level on the same side of their preferred paw, ablating the ipsilateral corticospinal (CST) and rubrospinal (RST) tracts. Surgical procedures were carried out under isoflurane anaesthesia (5% for induction; 2.7-3% for maintenance) supplied with oxygen. Once anaesthetized, the rats were shaved and mounted into a stereotaxic frame (Kopf Instruments, Tujunga, CA, USA). The

surgical site was disinfected with chlorhexidine digluconate (Sigma-Aldrich Canada Ltd., Oakville, ON, Canada) and the eyes were protected with the lubricant Tears Naturale (Alcon Canada, Inc., Mississauga, ON, Canada). A skin incision was made over the cervical region of the spinal cord and the muscles were dissected apart. This was followed by a laminectomy of the C4 vertebra. The lesion was performed at the C4 level with a custom-made surgical microblade. Muscles were sutured with vicryl 5-0 (Johnson & Johnson Medical Pty Ltd., Sydney, NSW, Australia) and the skin was stapled with 9 mm stainless steel clips (Stoelting Co., Wood Dale, IL, USA). After the surgery, the rats were given 0.03 mg/kg of buprenorphine (Temgesic, Schering-Plough, Kirkland, QC, Canada) and 4.0 ml of saline. This was followed up by a 0.02 mg/kg dose of buprenorphine 8 hrs later and 2.0 ml of saline if the animals showed signs of dehydration.

Swimming Study: Rats received a moderate (12.5 g-cm) thoracic (T10) spinal cord contusion delivered by the New York University Impactor as described previously (Magnuson et al., 2009). Briefly, surgical procedures were carried out under Pentobarbital (IP, 50 mg/Kg) anesthesia and all animals received prophylactic antibiotics (Gentamicin, 15mg/Kg sc). Once anaesthetized, the surgical site was shaved and disinfected with chlorhexidine digluconate (Sigma-Aldrich, St. Louis, MO). The eyes were protected with Lacri-lube (Allergan, Irvine, CA). A midline dorsal skin incision was made exposing the thoracic and upper lumbar spinal column and the muscles were dissected to expose the vertebral laminae from T8 to T11. This was followed by a laminectomy of the T9 vertebra and, following securing the vertebral column with clamps at T8 and T10, delivery of the contusion to the T10 spinal cord leaving the dura intact. Muscles were sutured with vicryl 5-0 (Ethicon Endo-Surgery, Blue Ash, OH) and the skin was closed with stainless steel staples. After the surgery, the rats were given 0.05 mg/kg of

buprenorphine (Henry Schein, Indianapolis, IN, USA) and 5.0 ml of saline. This was followed up by a 0.03 mg/kg dose of buprenorphine 8 hrs later and additional saline if the animals showed signs of dehydration.

2.3 Pre-training and Rehabilitation

Grasping Study: Pre-training and rehabilitation were undertaken based on Whishaw et al. (1998). The testing apparatus was a clear plexiglass chamber (38.5 cm l x 12.4 cm w x 45 cm h), with a slit at the front through which the rats could grasp a sucrose pellet (45 mg/each) from a shelf. The pre-trained group received daily 10 min training sessions on the SPG task for 4 weeks 5 days a week before the surgery. During this time, the untrained group was habituated to the task conditions. Untrained animals were placed in the SPG chamber with the reaching slit blocked off for 10 min. In order to determine the paw preference of the untrained animals, the rats in this group were allowed to reach through the slit for 1-3 sessions before the lesion. Untrained rats were allowed to reach for more than one session if they failed to reach during the first session or if they reached with both paws, making their paw preference ambiguous. Rats from both groups received rehabilitative training on the SPG task for 6 weeks/3-5 days/week for a total of 25 rehabilitation days starting 1 week post-spinal cord injury. Grasping success rate was calculated by dividing the number of pellets grasped by the number of reaching attempts. The highest success rate achieved by each rat during rehabilitation was used to calculate the final average success rate. Weekly average success rates post-injury were also calculated. Some rats compensate after injury by dragging pellets across the shelf and shoveling the pellets into their mouths (termed “scooping”), rather than grasping the pellets “properly”. To quantify this type of compensation, the number of pellets scooped was divided by the number of attempts, and the

averages/week were compared between groups.

Swimming Study: Swim pre-training and post-injury assessments were undertaken based on Smith et al., (2006) and Magnuson et al., (2009). Swimming was performed in a clear plexiglass tank (150 cm l x 20cm w x 30 cm deep) with a black neoprene covered ramp at one end onto which the rats could easily climb. The pre-trained group received 6 x 4 min swimming sessions daily, 5 days each week for 4 weeks, with the final session 3 days before the spinal cord injury surgery. Throughout the pre-training period, animals in the untrained group were handled daily and were transported to and from the training room with the trained animals. Rats from both groups received rehabilitative swim training, 4 days/week for 6 weeks post-spinal cord injury, as described previously (Smith et al., 2006; Magnuson et al., 2009). Swim training started 2 weeks post-injury with 2 x 4 min sessions each day and ramped up to the maximum of 6 x 4 min sessions over the first 2 weeks (8 days) of training. The initiation of swim training was delayed until 2 weeks post-injury in order to avoid stressing the cardiovascular system during the period of vascular permeability that is thought to make the injury epicenter and penumbra susceptible to increased inflammation (Smith et al., 2009). Swimming was assessed weekly (on Fridays) using the Louisville Swim Scale (LSS; Smith et al., 2006b) and hindlimb kinematics (Magnuson et al., 2009). Normal animals swim bipedally, with their hindlimbs only and use their forelimbs only for steering and obstacle avoidance. After a moderate thoracic SCI animals initially rely on their forelimbs for propulsion, but quickly re-learn to use their hindlimbs. The LSS is a visual scale (0-17) based on forelimb dependence, hindlimb movement and alternation in addition to body position during a 4 min swimming session. Animals that score 0-5 rely heavily on their forelimbs for propulsion and show very little hindlimb movement, poor body angle (tail-down) and rotation (on their side). Animals scoring 6-11 utilize both forelimbs and

hindlimbs for propulsion, but retain a poor body position and may not kick consistently with their hindlimbs. Animals scoring 12-17 display consistent hindlimb movement with alternation rely little on their forelimbs for propulsion and have a good body position in the water (parallel to the water surface and correct dorso-ventral orientation).

2.4 Other Behavioural Measures:

2.4.1 Grasping Study

Movement Rating Scale: Video recordings were made at the end of the rehabilitation period with a high-speed video camera (IPX-VGA, 210 fields/s). Three reaches for the lesioned limb of each rat were qualitatively analyzed. A reach was broken down into 10 components and each component was rated on a 3-point scale. If the movement was normal, a score of (2) was given. If the movement was performed abnormally, a score of (1) was given. If the movement failed to occur, a score of (0) was given. In cases where there was uncertainty as to the presence of a movement, a score of (0.5) was given. The component movements analyzed were based on the description from Whishaw et al. (2003).

Horizontal Ladder Task: Rats were trained on the horizontal ladder task 5 weeks post-SCI for two sessions on 2 consecutive days with five runs a session. Testing was conducted 2 days after the last training session. The animals had to cross a ladder with unevenly spaced rungs from a neutral cage to reach their home cage. The home cage with cage mates served as the positive reinforcement. During testing, a camera (JVC, 60 fields/s) was mounted on a tripod in front of the ladder. Six runs were recorded for each rat, three in the left to right direction and three in the opposite direction. However, only three runs were assessed for each animal, those with the lesioned forelimb at the front in the recording. Frame by frame analysis of forelimb

placements within a 60 cm stretch of the ladder was performed. Placements at the start or end of the ladder were excluded. Placements of the lesioned forelimb were rated on the foot fault 7-point scale (Metz & Whishaw, 2009), with higher scores indicating better paw placement.

2.4.2 Swimming Study

Hindlimb function during overground stepping was assessed pre-injury and every second week post-injury using the Basso, Bresnahan and Beattie (BBB) Locomotor Scale as described previously (Basso et al., 1995; Magnuson et al., 2005). Briefly, animals were observed moving about in an open field (empty children's wading pool, 39" in diameter) for 4 min. Hindlimb movements were scored by two experienced raters that were blind to the experimental groups. In addition to the LSS (described earlier) and the BBB scales, hindlimb function during swimming was objectively assessed using 2D kinematics, as described previously (Magnuson et al., 2009). Black sharpie marks were placed on the iliac crest (IC), the ischial tuberosity of the hip (H), the lateral malleolus of the ankle (A) and the metatarsophalangeal joint of the 4^{th} toe (T). These markers were tracked in high-speed (60Hz) video (Basler 602f, Basler Inc., Exton, PA) taken during 3 pool laps where the animal swam continuously and smoothly through the cameras field of view. A minimum of 6 complete stroke cycles were digitized using MaxTraq (Innovision Systems, Columbiaville, MI) and angle-angle plots were created for the IC-H-A and H-A-T angles using a three-segment, two-angle hindlimb model that avoids the inaccuracies of the rodent knee (Magnuson et al., 2009; Kuerzi et al., 2010). The angle-angle plot areas were then calculated, representing the in-phase excursions of the two angles, a measure that is exquisitely sensitive to changes in swimming stroke kinematics (Magnuson et al., 2009).

2.5 Perfusion, Tissue Collection and Histology

Grasping Study: Rats were euthanized with a pentobarbital overdose (Euthanyl; Biomeda-MTC, Cambridge, ON, Canada), and perfused with 4% paraformaldehyde. The brain and spinal cord were then dissected and post-fixed overnight in 4% paraformaldehyde, after which the tissue was cryoprotected in 30% sucrose for 2-4 days. Spinal tissue was cut into blocks, covered in O.C.T (Sakura Finetek, Torrance, CA, USA), mounted onto filter paper and frozen at -60°C in 2-methylbutane (Fisher Scientific, Ottawa, ON, Canada). Tissue cross-sections containing the lesion were cut at 25 µm in a Cryostar NX70 (Fisher Scientific, Ottawa, ON, Canada) and staggered on four slides (Fischer Scientific, Ottawa, ON, Canada). The slides were stored at -20°C until further processing.

Spinal cord cross-sections were counterstained with cresyl violet. Sections were warmed at 37°C for 1 hr and rehydrated in TBS for 3 x 10 min. Slides were then immersed in fresh 0.5% cresyl violet for 4 min in a fume hood. To remove excess cresyl violet dye, the slides were quickly dipped in distilled water before the tissue was serially dehydrated in increasing ethanol concentrations (50%, 75%, 99%, and 99%) for 2 min each. This was followed by 2 x 2 min clearing steps in xylene. After clearing, the slides were coverslipped with permount.

Fifteen sections 200 µm apart including the lesion epicenter were analyzed. Images of the tissue were captured under bright-field microscopy and the image processing program ImageJ 1.43µ (National Institutes of Health, Bethesda, MD, USA) was used to measure the area of necrotic tissue. Tissue was considered necrotic if cresyl violet stained inflammatory cells invading the tissue. The lesion volume (V_l) was obtained with the Cavalieri method (Hains, Saab, Lo, &Waxman, 2004) using the formula $V_l = \sum(a \times d)$ with (a) as the lesion area of each section and (d) as the inter-section distance. The total volume of the spinal cord block analyzed

was extrapolated from the total area of a representative section rostral to the lesion epicenter. Percent lesion volume was calculated by dividing the lesion volume by the volume of the total spinal cord block. For two-dimensional qualitative analysis, lesions were reconstructed on schematics at the C4 level and the lesioned area was calculated as a percent of the total cross-sectional area. Additionally, spared white matter area was calculated as a percent of the cross-sectional area.

Swimming Study: Rats were euthanized with a pentobarbital overdose (250mg/Kg. i.p.) and perfused with 4% paraformaldehyde. Spinal cords were dissected out and post-fixed overnight, also in 4% paraformaldehyde. Spinal cords were then cryoprotected in 30% sucrose for 2-4 days, blocked to isolate the injury epicenter ±3mm, mounted in OCT cutting media and 30 μm sections were prepared on a Zeiss Microm cryostat and mounted on charged microscope slides (Fisher Scientific, Pittsburgh, PA, USA) in five sets. One set of sections were stained using Eriochrome Cyanine, as described previously. A minimum of 6 sections were photographed, opened in iDraw (Apple Computer, Cupertino, CA) and densely stained "spared" white matter was traced using a Wacom Intuous drawing tablet (Wacom, Vancouver, WA). Percent spared white matter was determined using cross sectional areas in ImageJ as compared with age, gender and weight matched controls. The section with the minimum percent spared white matter was identified as the injury epicenter.

2.6 Statistical Analysis

Data were analyzed with GraphPad Prism 4 for the grasping study and with IBM SPSS v21 for the swimming study (GraphPad Software Inc., La Jolla, CA, USA; IBM SPSS v21, IBM, Armonk, NY, USA). For the grasping study, unpaired two-tailed t-tests were used to make

between-group comparisons when the data followed a normal distribution. Normality was tested with the D'Agostino-Pearson omnibus test. Mann-Whitney U tests were employed otherwise. Repeated measures two-way ANOVA with Bonferroni post-test was used to compare weekly scooping and grasping performance during rehabilitation. Pearson's correlation coefficient was used to determine whether there was a relationship between two variables. The data presented are mean values ± SEM. The threshold for significance was set at a P-value of < 0.05. For the swimming study, LSS, BBB and angle-angle plot area data were analyzed with repeated measures ANOVA. Following a significant main effect, comparisons between groups were performed using Tukey HSD post-hoc t-tests. Data are presented as mean ± SD, and results are considered significant for P-values ≤ 0.05.

3. Results

3.1 Grasping Study

3.1.1 Single pellet Grasping

Reaching scores post-SCI were compared between rats that were trained to grasp for 4 weeks before the injury and rats that were not. Average weekly grasping scores were compared. Two-way factor analysis of variance revealed a significant main effect of time ($F (5, 90) = 6.31$, $P < 0.001$). Average weekly success rate improved over time. No significant main effect of treatment ($F (1, 90) = 1.74$, $P = 0.204$) was found. No differences in grasping performance between pre-trained and non-pre-trained rats were found (Fig. 1B). There was no significant interaction between time and treatment ($F (5, 90 = 0.427$, $P = 0.829$). Furthermore, the highest scores obtained by each animal during the 6 weeks of rehabilitation were compared between groups. In line with the weekly data, there was a non-significant trend for pre-trained rats (36.6 ±

10.4%) to successfully retrieve more pellets through the reaching slit than non-pre-trained rats (24.1 ± 11.5%; Fig. 1C). Use of compensatory movement strategies did not differ between the groups. There was no significant main effect of time ($F(5, 90) = 0.94$, $P = 0.461$), treatment ($F(1, 90) = 0.70$, $P = 0.413$) or a significant interaction between time and treatment ($F(5, 90) = 1.13$, $P = 0.350$). That is, pre-trained and non-pre-trained rats scooped pellets to a similar extent after injury (data not shown). Reaching frequency in the first 4 weeks of rehabilitation was also analyzed to determine if rats differed in their motivation to perform the task shortly after their injury. Rats trained before the injury reached significantly (37.9 ± 3.95; $P < 0.05$) more times than untrained rats (27.9 ± 2.14; Fig. 1D). However, by the last 8 days of rehabilitation training, there was no longer a statistical difference in the number of attempts (37.4 ± 3.79% versus 33.2 ± 3.95% for the trained and untrained groups respectively; Fig. 1E).

3.1.2 Movement Rating Scale

To provide a qualitative outcome measure, a movement rating analysis was conducted. No significant differences between the untrained and trained group were found on any of the 10 components of the grasping motion, although a trend was found for trained rats to perform better at the elbow in, advance, arpeggio, grasp, supination I, supination II, and release components of the grasping movement, while untrained rats tended to perform better at digit extension (Fig. 1F).

3.1.3 Horizontal Ladder

To assess the effect of pre-training on an untrained task, the rats were tested on the horizontal ladder task. The number of errors per step made by rats from the pre-trained (17.5 ± 5.00%) and untrained (15.3 ± 3.45%) groups were not significantly different (Fig. 2B). Foot fault scores were also compared. Again, no group differences were found, with rats from the pre-

trained group obtaining mean scores of 4.51 ± 0.305 and rats from the untrained group obtaining scores of 4.69 ± 0.139 (Fig. 2C). There was a trend for pre-trained rats to take more time crossing the ladder (7.47 ± 1.42 s) than untrained rats (5.07 ± 0.523 s), but the trend did not reach statistical significance (Fig. 2D).

3.1.4 Lesion Size

Histological analysis revealed that rats trained before the injury had significantly greater lesion volumes than rats that were not pre-trained ($P < 0.05$; Fig. 3A). The average spinal cord lesion volume of pre-trained rats was 16.2 ± 1.98% and that of untrained rats was 11.3 ± 0.573%. However, when the cross sectional area of damaged tissue was compared between groups, there was not a significant difference, although a similar trend existed with pre-trained rats having lesion areas of 32.9 ±3.91% and untrained rats 26.4 ± 2.04% (Fig. 3B). Cross-sectional spared white matter was also not significantly different between groups. Pre-trained rats had 41.27 ± 2.491% and untrained rats had 46.31 ± 1.134% spared white matter (Fig. 3C). No correlation was found between the lesion volume and grasping success rate of animals from both groups ($r = -0.435$, $P = 0.209$ for pre-trained rats and $r = -0.257$, $P = 0.474$ for non-trained rats; Fig. 3D). There was also no relationship between lesion area and success rate ($r = -0.557$, $P = 0.095$ and $r = -0.274$, $P = 0.444$ for pre-trained and non-pre-trained rats respectively; Fig. 3E). Lastly, no correlation between spared white matter area and success rate was found ($r = 0.488$, $P = 0.153$ for pre-trained rats and $r = 0.288$, $P = 0.420$ for non-trained rats; Fig. 3F). These results indicate that with the lesion size variability in this experiment, lesion size was not predictive of success scores.

3.2 Swimming Study

3.2.1 Swimming and Stepping

Swimming and stepping scores for the two experimental groups, pre-trained and non-trained, were obtained every second week starting at week 2. BBB scores were not different at any time point, and these are shown for week 2 only in Figure 4. These animals achieved frequent weight-supported stepping with their hindlimbs with no forelimb-hindlimb coordination, a level of recovery often reported for animals with 12.5g-cm NYU injuries at T9 or 10 (Basso et al. 1995; Smith et al., 2006, Magnuson et al., 2005, 2009). Despite the very similar BBB scores, the animals that received swim training pre-injury had significantly lower LSS scores at weeks 2 and 4 post-injury (Fig. 4). These animals scored less than 5 on the LSS at week 2 post-injury, indicating that they had very little hindlimb movement, were almost totally dependent on their forelimbs for forward motion and in addition had severe trunk instability. In contrast, the animals that received no swim training pre-injury scored 7-8 at week two post-injury indicating that they exhibited, at a minimum, occasional hindlimb movement, occasional hindlimb alternation and only moderate trunk instability, while retaining a high degree of dependence on forelimbs for forward motion. In addition to the LSS, we also assessed the hindlimb movements during swimming using a 2D kinematic approach where the limb is assessed as a three segment, two-angle model and the knee is ignored, as can be seen in Figure 5A. When the two angles measured (iliac crest-hip-ankle and hip-ankle-toe) are plotted against each other, the resultant ellipsoid describes the movement and position of the limbs by its size, shape and position on the graph. Fig. 5B shows a single swimming stroke for one representative pre-trained animal at 1 week post-injury indicating very little movement of the extended proximal limb segment (iliac crest-hip-ankle) and somewhat larger excursion of the distal limb segment (hip-ankle-toe), while the mean angle-angle excursion (plot area) is significantly lower

than for the untrained animals (Fig. 5C). As we have observed previously (Smith et al., 2006; Magnuson et al., 2009) post-injury swim training resulted in significant improvements in both LSS scores and hindlimb kinematics over the first 4-6 weeks post-injury, however, even after 2 weeks of daily swim training, the animals that received swim training pre-injury had lower LSS scores (4 weeks post-injury). Since angle-angle plot area was not different at 4 weeks, it can be concluded that aspects of the LSS other than hindlimb movement, such as trunk instability or hindlimb alternation, were lagging.

3.2.2 Lesion Size

The percent spared white matter at the injury epicenter was not different for the two groups (Fig. 5D), averaging approximately 8% in cross sectional area of only densely stained, normal appearing white matter using our standard Eriochrome Cyanine technique (Kuerzi et al., 2010). This shows that while the pre-training negatively influenced post-injury swimming, it did not significantly alter white matter sparing.

4. Discussion

Experimental SCI research is faced with numerous challenges, such as the reproducibility of functional outcomes (Filli & Schwab, 2012). Although animal experiments are designed to control all known variables, inter-laboratory and even intra-laboratory variability is high. Such variability could be partly attributed to poor reporting of methods (Lemmon et al., 2014). One example is that the detailed description of handling/training protocols prior to the start of experimentation is often missing. This is significant, because training pre-injury is known to influence outcomes after CNS damage, which is problematic when comparing experimental outcomes between laboratories. For instance, pre-injury treadmill training was reported to reduce

infarct size and edema after cerebral ischemia in rats (Wang et al., 2001). Also, voluntary wheel running before SCI in rats reduces weight loss after the injury (Erschbamer et al., 2006). The present study addressed the question of how training in two different tasks before SCI might influence motor recovery.

Contrary to earlier results, training in the SPG task increased lesion severity after cervical SCI (Fig. 3A). This is unexpected, because exercise prior to SCI was reported to prevent an injury induced drop in levels of BDNF (Gomez-Pinilla et al., 2012), a neuroprotective neurotrophin (Kobayashi et al., 1997). In our study, it may be that pre-training did not increase BDNF levels sufficiently to confer neuroprotection. The lesion may have been aggravated in pre-trained rats due to stress. It is widely accepted that delaying the onset of rehabilitative training is beneficial in rats with incomplete SCI (Krajacic et al., 2009; Smith et al., 2009). One of the possible explanations for this is that handling/training is stressful for animals. It has long been known that mere movement of rat cages is sufficient to induce a circulatory shock reaction (i.e., increased heart rate) and alter plasma concentration profiles of molecules linked with stress, including glucose, pyruvate and lactate (Gartner et al., 1980). Thus, it may be argued that since untrained and pre-trained rats were exposed to the experimenter and testing apparatus before the injury, both groups should have experienced similar amounts of stress. However, pre-trained rats went through the experience of repeated unrewarded reaching attempts for longer than untrained rats. Average of the best reaching success scores achieved by the pre-trained group before SCI was only 56%; failed attempts were due to knocking pellets away or dropping the pellets after grasping them. Unexpected omission of a reward is known to produce an aversive emotional reaction, accompanied by increased corticosteroid levels and emission of odours and vocalizations in rodents (Papini & Dudley, 1997). Chronic stress can result in systemic

inflammation, exacerbated inflammatory processes and increased levels of apoptosis post-SCI (Maldonado Bouchard & Hooke, 2014). If pre-trained rats indeed experienced higher levels of stress, this could have led to worsening of the lesion.

Although we did not measure activity levels, pre-trained rats may have also engaged in more activity within their home cages immediately after the injury compared to non-trained rats. Exercise initiated acutely after SCI was reported to be detrimental to recovery (Kyoung-Hee et al., 2013). Physical activity increases blood pressure and flow at a time when the blood-brain barrier is compromised, leading to greater infiltration of inflammatory cells and necrosis (Silva et al., 2014). Post-contusion angiogenesis peaks at 7-10 days (Popovich et al., 1997; Benton et al., 2008) and these new vessels may be responsible, in part, for the blood-brain barrier weakness and exacerbation of damage during the post-injury stressor of exercise (Smith et al., 2009). However, exacerbation of the injury did not influence the rats' ability to adopt a compensatory reaching strategy post-injury. Pre-trained rats achieved similar reaching scores to untrained rats (Fig. 1B, C & F) and use of "scooping" to compensate for functional loss was analogous between the two groups. Pre-training in the reaching task also did not affect walking across a ladder (Fig. 2B, C, & D). This could be partly explained by our earlier finding that a small variability in lesion size does not necessarily translate into differences in successful use of the forelimb (Hurd et al., 2013). Although pre-trained rats had a larger volumetric lesion size than non-trained rats, all rats had lesion volumes lower than 30% of the 3 mm spinal cord block analyzed regardless of which group they belonged to (Fig. 3A). In addition, lesion volume as measured with a cresyl violet stain does not assess the health of the tissue and the number of surviving neurons.

In contrast to the grasping study, no differences were found in lesion severity in the

swimming study, which might be attributed to the fact that only spared white matter at the epicenter was assessed. Similarly, when spared white matter was compared between groups in the grasping study, there was no effect of pre-training on this measure. The findings may also be discrepant because the SCI was at the cervical level in the grasping study and at the thoracic level in the swimming study. Grey matter is more susceptible than white matter to secondary damage spread after SCI (Ek et al., 2010), and cervical spinal cord has a greater percentage of grey matter than thoracic levels (Turnbull, 1971).

Previously, we found that the recovery of swimming and stepping in untrained animals, as assessed by the LSS and BBB scales, were correlated, but that the correlation was stronger when animals received daily swim training (Smith et al., 2006). Locomotor training after a spinal cord injury has been assumed for many years to be largely dependent on re-engaging the pattern generating circuitry using an appropriately applied repetition of limb movements. This approach is successful in the fully transected cat model where outcomes are hindlimb kinematics and EMG during treadmill stepping (Barriere et al., 2008). This approach has proven to be much less successful when applied to incompletely injured rodents when overground performance is a primary outcome (Fouad et al., 2000; Kuerzi et al., 2010) or when applied to incompletely injured patients with either treadmill or overground performance as the outcome (Dobkin et al., 2007; Harkema et al., 2012). Why these apparent disparities exist is unknown, but certainly few laboratories consider the possibility that pre-injury training might influence post-injury plasticity or performance of a locomotor task. In addition to demonstrating that post-injury swim training successfully improves swimming performance without altering overground performance (Smith et al., 2006a, b), we also showed that adult female SD rats do not learn to swim when first exposed to the activity. We found that their hindlimb performance when first exposed to the

activity is kinematically similar to that following 4 weeks of daily swim training (Magnuson et al., 2009). This observation suggests that there is no overt plasticity with the initiation or practice of the activity of swimming, yet our current results suggest strongly that some change has occurred and that this change is revealed as a lower level of performance in the amount and quality of hindlimb movement during swimming, over the first few weeks post-injury (Fig. 4 & Fig. 5C). Thus, the current results provide a potent example of how pre-injury task-specific training, in the form of daily swimming sessions for a month, can dramatically influence post-injury outcomes. The data also suggests that this only applies when the task assessed is similar to the pre-injury exercise, as swimming pre-training did not impact overground locomotion as assessed by the BBB locomotor rating scale (Fig. 4).

Interestingly, while rats that were trained in grasping recovered well post-SCI (Fig. 1B, C& F), rats trained in swimming performed worse after the injury (Fig. 4 & Fig. 5C). It is known that training in a specific task may lead to a decline in the performance in another task, possibly because training "uses up" limited neuronal circuitry (Girgis et al., 2007; de Leon et al., 1999; Eason & Smith, 1989). The results support the postulate that rats trained to swim before an SCI could not re-train after their injuries as easily as non-pre-trained rats. This may not have applied to rats trained in grasping due to the role of motivation in the SPG task. Spinal cord plasticity post-CNS trauma is most pronounced in the first 2 weeks after injury (Sist et al., 2014). Pre-trained rats were more motivated to grasp 1 week after the injury, as they were familiar with the task. Additionally, rats were only allowed use of their injured forelimb to grasp; something that would have been quite difficult for rats that had never trained to grasp. Indeed, rats trained in grasping before the injury grasped significantly more times than non-trained rats in the first few weeks after the SCI (Fig. 1D). The number of grasping attempts of untrained rats did not match

that of trained ones (Fig. 1E) until after the window of opportunity for plasticity had already closed (Sist et al., 2014). In contrast, swimming is a forced task involving spinal pattern generating circuitry. When first introduced to the water, rats swim in place for a second or two, and then rapidly adopt a horizontal swimming position and make hindlimb kicking movements that do not change with additional practice, suggesting that swimming is a pattern that is not learned but is "hardwired" (Magnuson et al., 2009). Post- thoracic contusion SCI, the use of hindlimbs was compromised but not use of the forelimbs. So, rats had access to an intact pair of limbs to propel them forward. Thus, acute swimming forced both pre-trained and untrained rats to activate neuronal networks when plasticity was still high. Despite this, pre-trained rats were not able to engage their hindlimbs significantly at 2 weeks post-injury showing very limited joint excursions, in particular of the proximal (hip-knee) limb segment, relying almost entirely on their forelimbs for forward motion (Fig. 5C). Hindlimb joint angular excursions improved with 2 weeks of daily training (4 weeks post-injury); however, the overall quality of swimming remained significantly different from controls that swam only post-SCI. Swimming ability of pre-trained rats did not recover to the same extent as that of untrained rats until 6 weeks post-injury. Hence, these results suggest that using the "wired" pattern of swimming pre-injury reduced the capacity to engage novel circuits shortly after injury and that both the necessity to retrain a well-established/utilized motor pattern and the motivation to train can have an impact on functional recovery post-SCI.

In conclusion, our results stress the importance of detailed reporting of the training and handling regimes before experimental procedures (i.e., injuries) are performed in order to enhance transparency and reproducibility of animal studies. They also suggest a disparity between cortically dominated fine motor tasks, like grasping, and spinally mediated tasks, like

swimming, as regards how acclimatization to the task might influence outcomes.

Acknowledgements

We acknowledge CIHR (RES0011338; KF) in Canada for granting the funding for our research and declare there is no conflict of interest concerning the publication of this manuscript.

References

Barrière, G., Leblond, H., Provencher, J., Rossignol, S. (2008) Prominent role of the spinal central pattern generator in the recovery of locomotion after partial spinal cord injuries. Journal of Neuroscience 28(15): 3976-87. doi: 10.1523/JNEUROSCI.5692-07.

Basso, D. M., Beattie, M. S., & Bresnahan, J. C. (1995). A sensitive and reliable locomotor rating scale for open field testing in rats. *Journal of Neurotrauma*, *12*(1), 1–21.

Benton, R. L., Maddie, M.A., Minillo, D.R., Hagg, T., & Whittemore, S.R. (2008) *Griffonia simplicifolia* Isolectin B4 identifies a specific subpopulation of angiogenic blood vessels following contusive spinal cord injury in the adult mouse. *Journal of Comparative Neurology* 507: 1031-1052. Doi: 10.1002/cne.21570

de Leon, R. D., Tamaki, H., Hodgson, J. A., Roy, R. R., & Edgerton, V. R. (1999). Hindlimb locomotor and postural training modulates glycinergic inhibition in the spinal cord of the adult spinal cat. *Journal of Neurophysiology*, *82*(1), 359–369.

Dobkin, B., Barbeau, H., Deforge, D., Ditunno, J., Elashoff, R., Apple, D., Basso, M., Behrman, A., Harkema., S, Saulino, M., Scott, M. (2007) Spinal Cord Injury Locomotor Trial Group. The evolution of walking-related outcomes over the first 12 weeks of

rehabilitation for incomplete traumatic spinal cord injury: the multicenter randomized Spinal Cord Injury Locomotor Trial. Neurorehabiltation and Neural Repair 21(1):25-35. doi:10.1177/1545968306295556.

Eason, R. L., Smith, T. L., & Plaisance, E. (1989). Effects of proactive interference on learning the tennis backhand stroke. *Perceptual and Motor Skills*, *68*(3), 923–930. doi:10.2466/pms.1989.68.3.923

Erschbamer, M. K., Pham, T. M., Zwart, M. C., Baumans, V., & Olson, L. (2006). Neither environmental enrichment nor voluntary wheel running enhances recovery from incomplete spinal cord injury in rats. *Experimental Neurology*, *201*(1), 154–164. doi:10.1016/j.expneurol.2006.04.003

Ek, C. J., Habgood, M. D., Callaway, J. K., Dennis, R., Dziegielewska, K. M., Johansson, P. A., … Saunders, N. R. (2010). Spatio-Temporal Progression of Grey and White Matter Damage Following Contusion Injury in Rat Spinal Cord. *PLoS ONE*, *5*(8), e12021. doi:10.1371/journal.pone.0012021

Filli, L., & Schwab, M. E. (2012). The rocky road to translation in spinal cord repair. *Annals of Neurology*, *72*(4), 491–501. doi:10.1002/ana.23630

Fouad, K., & Tetzlaff, W. (2012). Rehabilitative training and plasticity following spinal cord injury. *Experimental Neurology*, *235*(1), 91–99. doi:10.1016/j.expneurol.2011.02.009

García-Alías, G., Barkhuysen, S., Buckle, M., & Fawcett, J. W. (2009). Chondroitinase ABC treatment opens a window of opportunity for task-specific rehabilitation. *Nature Neuroscience*, *12*(9), 1145–1151. https://doi.org/10.1038/nn.2377Gartner, K., Buttner,

D., Dohler, K., Friedel, R., Lindena, J., & Trautschold, I. (1980). Stress response of rats to handling and experimental procedures. Laboratory Animals, 14(3), 267–274. http://doi.org/10.1258/002367780780937454

Girgis, J., Merrett, D., Kirkland, S., Metz, G. A. S., Verge, V., & Fouad, K. (2007). Reaching training in rats with spinal cord injury promotes plasticity and task specific recovery. *Brain*, *130*(11), 2993–3003. doi:10.1093/brain/awm245

Gómez-Pinilla, F., Ying, Z., Opazo, P., Roy, R. R., & Edgerton, V. R. (2001). Differential regulation by exercise of BDNF and NT-3 in rat spinal cord and skeletal muscle. *The European Journal of Neuroscience*, *13*(6), 1078–1084.

Gomez-Pinilla, F., Ying, Z., & Zhuang, Y. (2012). Brain and Spinal Cord Interaction: Protective Effects of Exercise Prior to Spinal Cord Injury. *PLoS ONE*, *7*(2), e32298. doi:10.1371/journal.pone.0032298

Harkema, S.J., Schmidt-Read, M., Lorenz, D.J., Edgerton, V.R., Behrman, A.L. (2012) Balance and ambulation improvements in individuals with chronic incomplete spinal cord injury using locomotor training-based rehabilitation. Arch Phys Med Rehabil. 93(9):1508-17. doi: 10.1016/j.apmr.2011.01.024.

Hurd, C., Weishaupt, N., & Fouad, K. (2013). Anatomical correlates of recovery in single pellet reaching in spinal cord injured rats. *Experimental Neurology*, *247*, 605–614. doi:10.1016/j.expneurol.2013.02.013

Kobayashi, N. R., Fan, D. P., Giehl, K. M., Bedard, A. M., Wiegand, S. J., & Tetzlaff, W. (1997). BDNF and NT-4/5 prevent atrophy of rat rubrospinal neurons after cervical

axotomy, stimulate GAP-43 and Talpha1-tubulin mRNA expression, and promote axonal regeneration. *The Journal of Neuroscience: The Official Journal of the Society for Neuroscience*, *17*(24), 9583–9595.

Krajacic, A., Ghosh, M., Puentes, R., Pearse, D. D., & Fouad, K. (2009). Advantages of delaying the onset of rehabilitative reaching training in rats with incomplete spinal cord injury. *European Journal of Neuroscience*, *29*(3), 641–651. doi:10.1111/j.1460-9568.2008.06600.x

Kuerzi, J., Brown, E. H., Shum-Siu, A., Siu, A., Burke, D., Morehouse, J., … Magnuson, D. S. K. (2010). Task-specificity vs. ceiling effect: Step-training in shallow water after spinal cord injury. *Experimental Neurology*, *224*(1), 178–187. doi:10.1016/j.expneurol.2010.03.008

Kyoung-Hee, L., Ji-Hye, K., Dong-Hee, C., & Jongmin, L. (2013). Effect of task-specific training on functional recovery and corticospinal tract plasticity after stroke. *Restorative Neurology and Neuroscience*, (6), 773–785. doi:10.3233/RNN-130336

Lemmon, V. P., Ferguson, A. R., Popovich, P. G., Xu, X.-M., Snow, D. M., Igarashi, M., … the MIASCI Consortium. (2014). Minimum Information about a Spinal Cord Injury Experiment: A Proposed Reporting Standard for Spinal Cord Injury Experiments. *Journal of Neurotrauma*, *31*(15), 1354–1361. doi:10.1089/neu.2014.3400

Magnuson, D. S. K., Lovett, R., Coffee, C., Gray, R., Han, Y., Zhang, Y. P., & Burke, D. A. (2005). Functional Consequences of Lumbar Spinal Cord Contusion Injuries in the Adult Rat. *Journal of Neurotrauma*, *22*(5), 529–543. https://doi.org/10.1089/neu.2005.22.529

Magnuson, D. S. K., Smith, R. R., Brown, E. H., Enzmann, G., Angeli, C., Quesada, P. M., & Burke, D. (2009). Swimming as a Model of Task-Specific Locomotor Retraining After Spinal Cord Injury in the Rat. *Neurorehabilitation and Neural Repair*, *23*(6), 535–545. https://doi.org/10.1177/1545968308331147

Maldonado Bouchard, S., & Hook, M. A. (2014). Psychological Stress as a Modulator of Functional Recovery Following Spinal Cord Injury. *Frontiers in Neurology*, *5*. https://doi.org/10.3389/fneur.2014.00044

Papini, M. R., & Dudley, R. T. (1997). Consequences of surprising reward omissions. *Review of General Psychology*, *1*(2), 175–197. http://doi.org/10.1037/1089-2680.1.2.175

Popovich, P.G., Wei, P., Stokes, B.T. (1997) Cellular inflammatory response after spinal cord injury in Sprague-Dawley and Lewis rats. *Journal of Comparative Neurology 377*:443–464. doi: 10.1002/(SICI)1096-9861(19970120)377:3<443::AID-CNE10>3.0.CO;2-S

Silva, N. A., Sousa, N., Reis, R. L., & Salgado, A. J. (2014). From basics to clinical: A comprehensive review on spinal cord injury. *Progress in Neurobiology*, *114*, 25–57. doi:10.1016/j.pneurobio.2013.11.002

Sist, B., Fouad, K., & Winship, I. R. (2014). Plasticity beyond peri-infarct cortex: Spinal up regulation of structural plasticity, neurotrophins, and inflammatory cytokines during recovery from cortical stroke. *Experimental Neurology*, *252*, 47–56. doi:10.1016/j.expneurol.2013.11.019

Smith, R. R., Brown, E. H., Shum-Siu, A., Whelan, A., Burke, D. A., Benton, R. L., & Magnuson, D. S. K. (2009). Swim training initiated acutely after spinal cord injury is

ineffective and induces extravasation in and around the epicenter. *Journal of Neurotrauma*, *26*(7), 1017–1027. doi:10.1089/neu.2008-0829

Smith, R. R., Burke, D. A., Baldini, A. D., Shum-Siu, A., Baltzley, R., Bunger, M., & Magnuson, D. S. K. (2006). The Louisville Swim Scale: A Novel Assessment of Hindlimb Function following Spinal Cord Injury in Adult Rats. *Journal of Neurotrauma*, *23*(11), 1654–1670. doi:10.1089/neu.2006.23.1654

Smith, R. R., Shum-Siu, A., Baltzley, R., Bunger, M., Baldini, A., Burke, D. A., & Magnuson, D. S. K. (2006). Effects of Swimming on Functional Recovery after Incomplete Spinal Cord Injury in Rats. *Journal of Neurotrauma*, *23*(6), 908–919. https://doi.org/10.1089/neu.2006.23.908

Turnbull, I. M. (1971). Microvasculature of the human spinal cord. *Journal of Neurosurgery*, *35*(2), 141–147. doi:10.3171/jns.1971.35.2.0141

Wang, R. Y., Yang, Y. R., & Yu, S. M. (2001). Protective effects of treadmill training on infarction in rats. *Brain Research*, *922*(1), 140–143.

Weishaupt, N., Blesch, A., & Fouad, K. (2012). BDNF: The career of a multifaceted neurotrophin in spinal cord injury. *Experimental Neurology*, *238*(2), 254–264. doi:10.1016/j.expneurol.2012.09.001

Whishaw, I. Q., Gorny, B., Foroud, A., & Kleim, J. A. (2003). Long-Evans and Sprague-Dawley rats have similar skilled reaching success and limb representations in motor cortex but different movements: some cautionary insights into the selection of rat strains for neurobiological motor research. *Behavioural Brain Research*, *145*(1-2), 221–232.

Whishaw, I. Q., Gorny, B., & Sarna, J. (1998). Paw and limb use in skilled and spontaneous reaching after pyramidal tract, red nucleus and combined lesions in the rat: behavioral and anatomical dissociations. *Behavioural Brain Research*, *93*(1-2), 167–183.

Ying, Z., Roy, R. R., Edgerton, V. R., & Gómez-Pinilla, F. (2003). Voluntary exercise increases neurotrophin-3 and its receptor TrkC in the spinal cord. *Brain Research*, *987*(1), 93–99.

2. Conclusions, limitations, and future research

2.1 Chapters 1 and 2

The results of Chapters 1 and 2 on the surface conflict one another and must be reconciled. Chapter 1 showed hyper-proliferation of SKP-SCs and growth-formation in the spinal cords of grafted animals. This deleterious effect of grafting SKP-SCs was not seen in graft-recipients in Chapter 2. The SCI model, transplantation technique, vehicle for transplantation (HAMC), and cyclosporine immunosuppression regimen were the same between experiments, ruling out all of these factors as the cause of growth-formation in Chapter 1. A key difference between experiments were SKP-SC culture conditions. SKP-SCs were expanded in culture by different researchers for each experiment. SKP-SC cell lines from Chapter 1 were found to be infected with mycoplasma at the end of the experiment. To prevent infection in Chapter 2, SKP-SCs were treated with the anti-mycoplasma reagent Plasmocin™ and were periodically tested for infection. Hence, it is possible that mycoplasma infection caused the transformation of SKP-SCs to an oncogenic phenotype in Chapter 1 (Namiki et al., 2009). However, this is only a possibility, as we did not systematically manipulate culture conditions to find the causal variable in transformation of SKP-SCs. SKP-SC culture parameters should be systematically manipulated, including: experimenter culturing the cells, antibiotic treatment, number of passages before transplantation, and details of mitogen exposure. Aberrant cellular proliferation should be tested for with immunocytochemistry for proliferation markers (e.g., ki-67), and stem cell markers (e.g., nestin), as well as PCR for chromosomal abnormalities.

SKP-SCs are not the only cell type that has the potential for malignant transformation. Tumourigenesis in pre-clinical research has been documented post-transplantation of numerous

cells types, including: human induced pluripotent stem cell-derived neural stem cells (Itakura et al., 2015), embryonic stem cells and embryonic stem cell-derived neurons (Brederlau et al., 2006; Dressel et al., 2008), bone marrow derived mesenchymal stem cells (Jeong et al., 2011), and rat nerve-derived SCs following mitogen exposure *in vitro* for > 11 passages (Funk et al., 2007; Langford et al., 1988; Morrissey et al., 1991). It should be noted that human nerve-derived SCs expanded with mitogens for up to 6 passages do not form tumours when transplanted *in vivo* (Emery et al., 1999). Tumour formation in humans following stem cell treatment from clinics abroad has been previously reported. Tumour formation also occurred after autologous transplantation of OEGs into the spinal cord of an 18-year-old woman with paraplegia. The tumour primarily consisted of nasal tissue and contained large amounts of mucus-like material (Dlouhy et al., 2014). In another case, a 13-year-old male with a hereditary neurodegenerative disease was treated with intracerebellar and intrathecal injections of human fetal neural stem cells in a Russian clinic. Four years later the boy was diagnosed with tumours in his brain and spinal cord of non-host origin, suggesting the tumour was derived from the transplanted neural stem cells (Amariglio et al., 2009; Baker, 2009). More recently, a 66-year-old man developed a spinal tumour composed of non-host cells after receiving intrathecal injections of mesenchymal, embryonic, and fetal neural stem cells in China, Mexico, and Argentina over the course of 4 years. Before the transplants, the man could not use his left arm and had a weak left leg, but could still walk with the assistance of a cane. As a result of the spinal tumour, the man became paralyzed from the neck down, incontinent, and started experiencing severe back pain (Berkowitz et al., 2016). Patients were not immunosuppressed in any of these clinical cases. These cases of "stem-cell" tourism suggest tumourigenesis is a risk only when receiving treatment in countries where medical regulations are lax. However, hundreds of businesses in the

U.S engage in direct-to-consumer marketing of unsubstantiated stem cell interventions (e.g., stem cell infusions for autism), raising concern about non-compliance with federal regulations (Turner & Knoepfler, 2016).

Given the inherent potential of stem cells and stem-cell derived cells for malignant transformation, I suggest quality controls such as limited expansion and mycoplasma screens should be incorporated into all pre-clinical animal studies in order to obtain the most accurate data regarding cell survival, differentiation capacity, and safety. Moreover, experiments should incorporate sufficiently long enough survival times to detect cellular abnormality within donor cells. Further work defining precise parameters for *in vitro* expansion of proliferative cells that maintain normal function for safe and effective use of cell therapy for SCI in humans is urgently needed.

Until we understand the factors responsible for transformation, stem cell and stem cell-derived clinical trials should not move forward. Furthermore, if the balance of these factors is easily tipped to tumourigenesis, we might consider alternatives to stem cell/stem cell-derived cell grafting, such as activating a patient's own mesenchymal stem cells and attracting them to injured tissue to promote repair (Kang et al., 2012; Karp & Leng Teo, 2009) or injecting a gel matrix with slow-release of neurotrophic factors into the site of damage (Pakulska et al., 2016). Activation of a patients' own mesenchymal stem cells has the advantage of reducing the risk of malignant transformation of cells. *In vitro* culturing of cells, even the patient's own, is a risk factor, possibly contributing to malignant transformation (Herberts et al., 2011). Further, if the patients' own mesenchymal stem cells are activated, there is no need to wait for the expansion of cells *in vitro* to sufficiently high numbers for transplantation.

Chapter 2 brought up a different issue, that of cell survival after transplantation into the injured spinal cord. In our study, immunosuppression did not result in increased cell survival, bringing into question immunosuppressive regimens as the sole method of improving grafted cell survival. Since our results suggest that anoikis might be a more critical factor in cell survival, the grafting vehicle in clinical studies needs to be considered carefully and should, ideally, be a vehicle that promotes cell-adhesion. It might also be necessary to graft cells in growth factor cocktails (Lu et al., 2012), as maximal survival might only be achieved with survival factors to counter anoikis. Indeed, BDNF treatment stops SCs from undergoing anoikis *in vitro* (Koda et al., 2008). Further, patients with a large amount of cavitation might benefit from higher numbers of transplanted cells, assuming a large number of cells die post-grafting. Some studies indicate that grafted cell number is positively correlated with motor recovery (Torres-Espín et al., 2015). Lastly, it is important that clinical studies begin carefully assessing transplanted cell survival. Magnetic resonance imaging is sometimes used as a tool to visualize the transplant site. Out of 39 clinical trials of cell transplantation for SCI (one was excluded as it did not list any outcome measures), 17 (~44%) trials listed magnetic resonance imaging as a primary or secondary outcome measure (clinical trials.gov, last access April 2nd, 2017). None of the clinical trials included an alternate way of evaluating transplanted cell survival *in vivo*. However, magnetic resonance imaging cannot distinguish transplanted from host cells, and is not a true measure of cell survival. For transplanted cells to be visualized with MRI, cells must be tagged with contrast agents, such as paramagnetic gadolinium agents, paramagnetic manganese agents, superparamagnetic iron-oxide nanoparticles, or fluorinated agents (Srivastava et al., 2015). Owing to the metal toxicity of gadolinium and manganese once de-chelated, these contrast agents are unlikely to see clinical use (Srivastava et al., 2015). Monitoring transplanted cells in

patients with superparamagnetic iron-oxide nanoparticles and fluorinated agents, has been performed safely (Ahrens et al., 2014; Bulte, 2009). Nevertheless, there are limitations with these techniques; the clinical application of iron-oxide nanoparticles is restricted to short-term use and fluorinated agents require special coils for image acquisition that are unavailable at many MRI research centers (Srivastava et al., 2015). Techniques to track transplanted cells and monitor their survival need to be further developed and made more available, so that they can start being used in cell transplantation clinical trials for SCI.

2.2 Chapter 3

The main conclusion of Chapter 3 is that injured RtST axons form contacts with PrINs after staggered SCI, with associated improvements in locomotor recovery. Further, greater locomotor recovery was found in rats with a time delay between hemisection SCIs compared to rats that received both SCIs in the same surgery, suggesting a role of activity-driven plasticity below the injury in the observed recovery. A major limitation of Chapter 3 is that a causal link between RtST-PrIN contact formation and motor recovery post-SCI was not confirmed. A strategy to establish causality would be to reversibly silence PrINs in the tissue bridge between hemisection SCIs and assess how this influences motor function. For example, PrINs within the bridge could be inactivated by forcing the PrINs to express tetanus neurotoxin (Kinoshita et al., 2012). Tetanus neurotoxin blocks the release of neurotransmitter from presynaptic terminals, thereby inactivating neurons (Link et al., 1992). PrINs can be double infected with viral vectors, so that the tetanus neurotoxin is expressed only when doxycycline is administered, (Kinoshita et al., 2012). PrINs could also be silenced with designer receptors exclusively activated by designer drugs (DREADD; Hilton et al., 2016). The advantage of these methods compared to simply

transecting the tissue bridge is that PrINs could be turned back on to restore motor function, providing more convincing evidence of causality. A drawback, however, with silencing PrINs is that connections with other tracts would be removed too, and functional losses could be attributed to these other connections. Thus, silencing approaches should be complemented with electrophysiological data, where brainstem nuclei giving rise to the RtST are stimulated and electromyographic assessment of the hindlimbs is done (Drew & Rossignol, 1990). Only through multiple approaches will we establish the functionality of connections between PrINs and the RtST.

As evidenced in Chapter 3, RtST axons and PrINs have great synaptic potential, so it would be interesting to run an experiment where mesenchymal stem cells are drawn to the site of a SCI, the RtST is stimulated electrically, and neurotrophic factor expression is forced at the soma of PrINs below the injury. As a result, the SCI cavity could be filled with the mesenchymal stem cells and RtST axons could be induced to grow and form connections with lumbar-projecting PrINs to re-establish supraspinal control of CPG networks below the injury.

The conclusions from Chapter 3 raise questions relating to pre-training. While undergoing changes, synapses compete for limited neural resources, such as available energy (Peters et al., 2004), plasticity-related factors (Fonseca et al., 2004; Frey & Morris, 1997), and neurotrophic support (Elliot & Shadbolt, 2002). If so, it is possible these neural resources could be exhausted through pre-training, resulting in a reduction in the ability of the injured spinal cord to reorganize and rewire. To answer these questions, future studies should look at plasticity before and after training in intact animals, and after SCI in pre-trained animals. For example, a measure of plasticity could be the number of PrIN-RtST contacts. In intact animals, this could be

studied by tracing the RtST and thoracic PrINs and counting the number of contacts. To determine the projection patterns of connections (e.g., ipsilateral RtST collaterals contacting ipsilateral or contralateral PrINs) different methods could be used, such as 3-dimensional reconstruction of the spinal cord from serial tissue sections (Duerstock, 2004) or 3-dimensional imaging of unsectioned spinal cord rendered transparent with tetrahydrofuran clearing procedures (Ertürk et al., 2011). Assessment of contacts before training, after training, and after SCI (with and without pre-training), can give us an idea of the plastic potential of the healthy spinal cord and how this influences plastic mechanisms and recovery post-SCI.

The finding of PrIN-RtST connections does not in any way imply other mechanisms are unimportant in the observed recovery in our study. Numerous tracts are involved in the regulation of locomotion, including the pontine reticular, vestibulospinal, rubrospinal, raphespinal, and corticospinal pathways (Goulding, 2009; Li et al., 2007; Siegel, 1979; van den Brand et al., 2012). Additionally, CST relay formation with PrINs has been linked to recovery of locomotion (van den Brand et al., 2012). Plasticity in descending pathways, however, is not the only mechanism for functional recovery after spinal injury. Adaptations in intraspinal circuits can support locomotor recovery. Treadmill training promotes durable locomotor recovery in cats (Martinez et al., 2012) and rats (Singh et al., 2011), even after complete transection of the spinal cord. This indicates that training induces lumbar plasticity that can, on its own, support locomotion. Although it should be noted that continued training may be required to maintain recovery (Singh et al., 2011). Further, recovery may not depend on reorganization of neural circuits. Locomotor recovery has also been associated with changes in motor neuron properties, such as upregulation of spontaneously active 5-HT_{2C} receptor isoforms (Murray et al., 2010). Given the multitude of factors underlying improvements post-SCI, a reductionist approach to

understand plasticity does not appear promising. In fact, a complete understanding of the mechanisms of recovery in humans might not be possible. This does not mean that we cannot encourage the process of rewiring. Laboratories have shown that BNDF delivery at the soma of injured CST axons increases CST-PrIN contact formation (Vavrek et al., 2006). In a separate study, a combination of epidural electrical stimulation, monoamine agonist administration, and robotic enabled bipedal training promoted CST-PrIN contact formation (van den Brand et al., 2012). Increased CST-PrIN contact numbers were associated with functional recovery in both studies (Vavrek et al., 2006; van den Brand et al., 2012). These and other studies have shown that we can encourage rewiring, as well as functional recovery. Even if full comprehension of the mechanisms of recovery is not possible, continued research on plasticity after spinal injury will suggest new ways of promoting recovery and refining techniques currently available.

2.3 Chapter 4 and Appendices

At the end of Chapter 4, I concluded that task-specific training before a SCI matters, potentially causing neural resources to be devoted to a particular movement strategy that cannot be re-produced after damage to the spinal cord. Further, the effects of pre-training depend on the task trained, with swimming pre-training having a stronger effect than single-pellet grasping pre-training. This is probably because rats pre-trained in grasping made more grasping attempts in the first few weeks after SCI than non-pre-trained rats. In other words, pre-trained rats showed higher rates of participation in rehabilitation training, taking full advantage of the window of heightened plasticity after injury (Sist et al., 2014). The effect of early rehabilitation training could have, thus, countered the negative impact of motor interference on recovery. In contrast, swimming pre-trained rats and non-pre-trained were forced to swim in equal amounts after

injury. Thus, no group showed higher participation rates than the other. In this case, motor interference was demonstrated. Swimming ability of pre-trained rats was inferior to that of non-pre-trained rats until ~6 weeks post-SCI. These results suggest that motor pre-training can adversely affect motor recovery after spinal injury (i.e., interference). The results also suggest that interference can possibly be countered with active participation in rehabilitation. However, it is unclear what neuronal changes underlie the interference caused by pre-training. Future experiments should assess spinal plasticity before and after pre-training and after SCI. Measures of plasticity could include descending tract collateral sprouting (Fouad et al., 2001; Vavrek et al., 2006; Girgis et al., 2007), descending fiber contact formation with spinal PrINs (Vavrek et al., 2006), and cortical map reorganization (Girgis et al., 2007; Krajacic et al., 2009). Numerous studies have reported plastic changes in healthy brains; for example, cortical responses can be induced following short-term musical training (Lappe et al., 2008). In line with this, we would expect the healthy spinal cord to also have a plastic potential. Assessing the plastic potential of the healthy spinal cord and how maximizing it influences plastic mechanisms and recovery post-SCI will be important towards tailoring treatments to specific patients. In clinical trials, tailoring of treatments to individuals is gaining more and more recognition. For instance, genetic polymorphisms are widely recognized to influence treatment responsiveness in cancer patients (Tecza et al., 2016). It is likely that people will not all respond in the same way to SCI therapies, and therapies may need to be customized to individuals. Pre-injury variables, such as task-specific pre-training can help us determine the best treatment for a particular patient. Since high levels of pre-training might cause patients to stick with a particular movement strategy that is disadvantageous, rehabilitation treatment for highly pre-trained patients might benefit from axon collateral sprouting increasing treatments (e.g., neurotrophic factor delivery; Schnell et al., 1994;

Vavrek et al., 2006) and focus on compensatory movement strategies. Further, we showed that participation in training may counter the deleterious effects of interference, since task-specific pre-trained rats made many more reaching attempts than non-pre-trained rats. This means that maintaining patient motivation to ensure high participation rates in therapy is important to counter the deleterious effect of interference. Indeed, recent evidence shows that activity in the nucleus accumbens, a major structure in motivation-driven effort, is associated with motor recovery after SCI in primates (Sawada et al., 2015). To increase motivation, a patient-centered approach is recommended, where rehabilitation professionals educate patients about their condition and engage in discourse with patients to help guide treatment (Jordan et al., 1991). Another important finding from Chapter 4 was that task specific training resulted in bigger lesions post-SCI. One possible explanation for this is that injured rats made a high number of failed attempts; repeated failure is known to produce chronic stress, which is associated with adverse physiological changes (Maldonado Bouchard & Hook, 2014). To prevent this from happening with humans, rehabilitation training difficulty should be gradually increased, so that patients are not discouraged by seemingly impossible challenges. Finally, the fact that we found clear evidence that pre-injury variables influence motor recovery post-SCI advises caution in future studies. For instance, the practice of using subjects in multiple experiments perceived not to interfere with each other is common (Silverman, 2008). This is especially the case if the first study used behavioural methods, as non-invasive procedures are not expected to influence ability and physiology of the animals in the next study. Some have gone as far as proposing "recycling" of animal subjects should be the fourth R in ethical guidelines for the use of animals in research (Balani et al., 2008). Here, we show that behavioural pre-training can very much alter the ability and physiology of animals following spinal injury, and thus, recycling, while well-intended, must

be carefully considered. Since profile of patients with SCI varies widely (Feng et al., 2011), behavioural pre-training (e.g., athletes) should also be carefully considered in human clinical trials. At the very least, pre-treatment of subjects in basic research and patient history in clinical trials should be meticulously described in methods. Chapter 4 also tells us that results of some studies might be questionable if pre-injury variables have not been controlled for. Lastly, more investigations are needed to confirm the importance of pre-injury variables, broaden the category of pre-injury variables that influence post-SCI outcomes (e.g., sex, housing conditions, type of pre-trained task), and assess if pre-training effects occur with other activities (e.g., wheel running, treadmill training). Study of these factors will give us a better idea of the pre-injury variables that should be considered when designing customized treatments for individuals.

The main conclusion of the Appendix articles was that automated robotic training in single pellet grasping yields reduced variability in performance before and after cervical SCI and created larger therapeutic windows than manual training. Therapeutic windows refer to the difference in grasping performance before and after SCI. Robot-trained rats had a larger drop in performance post-injury compared to manually-trained rats. A larger drop in performance means that beneficial effects of therapies can be more easily detected. Moreover, robot-assisted training required less researcher time, increasing laboratory throughput. Therefore, automated training of single-pellet grasping is a highly useful research tool that will allow us to run a greater number of more controlled and better designed experiments of forelimb rehabilitation in rodent models of SCI.

3. Overall conclusions

Single treatments for SCI are untenable considering the intricacies of primary and secondary injury processes. Despite a general scientific consensus that single treatments are very moderate in their effects (Oudega et al., 2012), combinatory therapies (with at least two non-rehabilitation components) for SCI have not been attempted in the clinical stage. An important reason for this is that translation of even the most promising basic research findings is slow and rare (Contopoulos-Ioannidis et al., 2003). When repeating even single treatment studies is a challenge (Sharp et al., 2014; Steward et al., 2008), how can we expect to repeat combined treatments, let alone translate them successfully? For example, Lu et al. (2012) reported neural stem cells (NSI-566) transplanted into the injured rat spinal cord with a growth factor cocktail formed synapses with host cells, resulting in functional recovery. Nevertheless, independent replication of these findings failed, even with the same surgeon performing the transplants and harvesting and preparation of the cells in Dr. Lu's laboratory (Sharp et al., 2014). Clinical translation is also difficult, because positive research data is exaggerated in scientific publications and negative research data is minimized or discarded. Positive research findings are, in fact, published at a higher rate and in less time than negative research outcomes (Suñé et al., 2013). Chapter 1 of this thesis is a good example. It was not until growth-formation after transplantation of SKP-SCs was found that it was discovered ours was not an isolated event, and had also occurred in an experiment previously run by the Tetzlaff laboratory in Vancouver. After the discovery of SKP-SC growths in the separate experiments, we decided to publish the results jointly. There was opposition from various parties, however, to the publication of these data, which had to be thoroughly discussed over multiple audio/video conferences before all parties involved were in conditional agreement to publish. In the replication study of Lu et al. (2012),

transplant-derived cells formed masses long distances from the transplant site, causing expansion of the central canal (Steward et al., 2014). Despite these worrying findings, Sharp et al. (2014) and Steward et al. (2014) have only been cited 29 and 24 times respectively since publication, while Lu et al. (2012) was cited 212 times in the first 3 years after publication and has now been cited 308 times. Also in spite of the negative findings, FDA-approved NSI-566 Phase I clinical trial with transient immune suppression for patients with chronic SCI completed surgeries in 2015 (clinical trials.gov; NCT01772810). NSI-566 Phase I/II clinical trial for patients with acute SCI is presently awaiting IND approval (Neuralstem.com). These examples raise the question of how many studies where stem cell or stem cell-derived cell transplantation resulted in tumour formation have been overlooked, minimized or altogether unreported before proceeding to clinical trials. Biomedical research data is commonly unreported due to a lack of statistical significance or perceived novelty and, more concerningly, because the data contradicts current scientific thinking (Matosin et al., 2014). Recently, Chapter 3 on RtST-PrIN connections was submitted for publication. Reviewer feedback suggested modifying statistical analysis, including new anatomical measures, and changing the tone of the paper. After addressing this feedback, the submission was rejected on the grounds of being incremental work. That is, the study built upon the work of others and, thus, was not perceived as novel. The difficulty of publishing non-significant data or data that is not completely novel, is counterproductive as non-significant data is informative and reproducibility of research is necessary to establish scientific validity (Casadevall & Fang, 2010). The bias in publishing also exists in cell transplantation therapy, and, so, it should not come as a surprise then when ill-informed individuals with SCI (and other conditions) desperate for a cure resort to “stem cell tourism” and risk worsening their deficits (Berkowitz et al., 2016). Is there anything that can be done to increase the reproducibility and

accuracy of research findings? Research outcomes, whether positive or negative, should no longer influence the dissemination of research findings. Full data disclosure at conferences and negative data journals with linked DOIs must be encouraged. Global standards for data reporting should be implemented, as well as centralized databases linking research articles based on common data elements to streamline the generation of new hypotheses (Lemmon et al., 2014). One of the standards that should be implemented is description of pre-injury variables, as we have shown that pre-injury variables affect post-SCI recovery (May et al., 2015). Lastly, to improve success in the clinic, complex clinical trials must be designed that test combinations of treatments rather than individual ones. However, before this is done, combination treatments should show success in pre-clinical animal studies and independent replications. Pushing ahead with human studies of treatments that have not been reproduced successfully in the pre-clinical literature will retard rather than advance scientific knowledge. To do this, we must recognize our bias against non-significant results and results that do not fit with current scientific thought. As Tolstoy (1894) once put it, "the simplest thing cannot be made clear to the most intelligent man if he is firmly persuaded that he knows already…what is laid before him."

4. Acknowledgements

I would like to acknowledge the University of Alberta for accepting me into the Neuroscience graduate program and for being an institution with the highest standards for their professors, research, and infrastructure. I am grateful to the Neuroscience and Mental Health Institute for being my family, source of my identity, and for supporting me throughout my degree. I hope the NMHI will continue to grow its presence within the University of Alberta and the broader community. I am grateful to the granting agency that supported me throughout my degree CIHR (RES0011338, KF). There are many individuals I am grateful to for the completion of my PhD. First and foremost is my PhD supervisor, Dr. Karim Fouad. He is tough and has high expectations, which push us to always be better. He spends a tremendous amount of time helping us hone our scientific, writing and presenting skills. His door is always open. Although he does not have to do any of this, he does it regardless, because more than anything he wants us to be proud of our work and to succeed in our careers. He is an amazing scientist. I feel immensely privileged to have been part of his laboratory. I would like to thank my supervisory committee, which includes my supervisor, Dr. Bradley Kerr, and Dr. David Bennett. My committee was always supportive, always came up with great ideas and suggestions, and was fair. I am thankful to my internal examiners Dr. Simon Gogsnach and Dr. Christine Webber who together with my committee assessed me during my candidacy exam. Dr. Christine Webber is also acting as an internal examiner for my thesis defense, and I am thankful for that as well. I am also grateful to Dr. Martin Oudega, who will be coming all the way from Miami to act as external examiner. I am honoured to be meeting such an illustrious scientist. I am grateful to all my laboratory mates, both old and new: Dr. Nina Weishaupt and Caitlin Hurd for showing me the ropes, Dr. Mashary Binnahil and Dr. Andrew Jack for voicing their clinical perspective, Nicholas Justin Batty and

Emma Schmidt for supporting me in the last months of my degree, technician Pamela Raposo for her superlative management of the laboratory, postdoctoral research fellow Dr. Juan Forero for sharing his engineering and technical expertise, postdoctoral research fellow Dr. Abel Torres-Espín for sharing his brilliant mind and offering invaluable help trouble-shooting, postdoctoral research fellow Dr. Keith Fenrich, whose scientific curiousity and intellect have always impressed me, postdoctoral research fellow Dr. Ana Lucas Osma, whose rigorous scientific approach is unparalleled. Special thanks to Romana Vavrek, without whose technical assistance the research presented in this thesis would not have been at all possible.

5. Complete Bibliography

Abbott, N. J., Patabendige, A. A. K., Dolman, D. E. M., Yusof, S. R., & Begley, D. J. (2010). Structure and function of the blood–brain barrier. *Neurobiology of Disease*, *37*(1), 13–25. https://doi.org/10.1016/j.nbd.2009.07.030

Abraham, K. E., McGinty, J. F., & Brewer, K. L. (2001). The role of kainic acid/AMPA and metabotropic glutamate receptors in the regulation of opioid mRNA expression and the onset of pain-related behavior following excitotoxic spinal cord injury. *Neuroscience*, *104*(3), 863–874.

Ahrens, E. T., Helfer, B. M., O'Hanlon, C. F., & Schirda, C. (2014). Clinical cell therapy imaging using a perfluorocarbon tracer and fluorine-19 MRI: Clinical Cell Therapy. *Magnetic Resonance in Medicine*, *72*(6), 1696–1701. https://doi.org/10.1002/mrm.25454

Akbik, F., Cafferty, W. B. J., & Strittmatter, S. M. (2012). Myelin associated inhibitors: A link between injury-induced and experience-dependent plasticity. *Experimental Neurology*, *235*(1), 43–52. https://doi.org/10.1016/j.expneurol.2011.06.006

Alluin, O., Delivet-Mongrain, H., & Rossignol, S. (2015). Inducing hindlimb motor recovery in adult rat after complete thoracic spinal cord section using repeated treadmill training with perineal stimulation only. *Journal of Neurophysiology*, *114*(3), 1931-1946. doi:10.1152/jn.00416.2015

Alvarez, F. J., Pearson, J. C., Harrington, D., Dewey, D., Torbeck, L., & Fyffe, R. E. W. (1998). Distribution of 5-hydroxytryptamine-immunoreactive boutons on ?-motoneurons in the lumbar spinal cord of adult cats. *The Journal of Comparative Neurology*, *393*(1), 69–83.

http://doi.org/10.1002/(SICI)1096-9861(19980330)393:1<69::AID-CNE7>3.0.CO;2-O

Amariglio, N., Hirshberg, A., Scheithauer, B. W., Cohen, Y., Loewenthal, R., Trakhtenbrot, L., … Rechavi, G. (2009). Donor-Derived Brain Tumor Following Neural Stem Cell Transplantation in an Ataxia Telangiectasia Patient. *PLoS Medicine*, *6*(2), e1000029. https://doi.org/10.1371/journal.pmed.1000029

Anderson, A. J., Haus, D. L., Hooshmand, M. J., Perez, H., Sontag, C. J., & Cummings, B. J. (2011). Achieving stable human stem cell engraftment and survival in the CNS: is the future of regenerative medicine immunodeficient? *Regenerative Medicine*, *6*(3), 367–406. https://doi.org/10.2217/rme.11.22

Ankeny, D. P., Lucin, K. M., Sanders, V. M., McGaughy, V. M., & Popovich, P. G. (2006). Spinal cord injury triggers systemic autoimmunity: evidence for chronic B lymphocyte activation and lupus-like autoantibody synthesis. *Journal of Neurochemistry*, *99*(4), 1073–1087. https://doi.org/10.1111/j.1471-4159.2006.04147.x

Austin, J. W., Kang, C. E., Baumann, M. D., DiDiodato, L., Satkunendrarajah, K., Wilson, J. R., … Fehlings, M. G. (2012). The effects of intrathecal injection of a hyaluronan-based hydrogel on inflammation, scarring and neurobehavioural outcomes in a rat model of severe spinal cord injury associated with arachnoiditis. *Biomaterials*, *33*(18), 4555–4564. https://doi.org/10.1016/j.biomaterials.2012.03.022

Baker, M. (2009). Unregulated stem cell transplant causes tumours. *Nature Reports Stem Cells*. https://doi.org/10.1038/stemcells.2009.32

Balani, S. K., Lu, C., Cardoza, K., Berg, C., Zhang, J., & Lee, F. W. (2008). Proposed new

addition to 3Rs for ethical and humane use of rats in pharmacokinetic studies--'Recycle'. *Drug Metabolism Letters*, *2*(3), 193–197.

Balentine, J. D. (1978). Pathology of experimental spinal cord trauma. I. The necrotic lesion as a function of vascular injury. *Laboratory Investigation; a Journal of Technical Methods and Pathology*, *39*(3), 236–253.

Balazs, E. A. (1991). Medical Applications of Hyaluronan and its Derivatives. In *Cosmetic and pharmaceutical applications of polymers* (pp. 293–310). New York: Plenum Press.

Ballermann, M., & Fouad, K. (2006). Spontaneous locomotor recovery in spinal cord injured rats is accompanied by anatomical plasticity of reticulospinal fibers. *The European Journal of Neuroscience*, *23*(8), 1988–1996. http://doi.org/10.1111/j.1460-9568.2006.04726.x

Ballios, B. G., Cooke, M. J., Donaldson, L., Coles, B. L. K., Morshead, C. M., van der Kooy, D., & Shoichet, M. S. (2015). A Hyaluronan-Based Injectable Hydrogel Improves the Survival and Integration of Stem Cell Progeny following Transplantation. *Stem Cell Reports*, *4*(6), 1031–1045. http://doi.org/10.1016/j.stemcr.2015.04.008

Ballios, B. G., Cooke, M. J., van der Kooy, D., & Shoichet, M. S. (2010). A hydrogel-based stem cell delivery system to treat retinal degenerative diseases. *Biomaterials*, *31*(9), 2555–2564. http://doi.org/10.1016/j.biomaterials.2009.12.004

Bandtlow, C., Zachleder, T., & Schwab, M. E. (1990). Oligodendrocytes arrest neurite growth by contact inhibition. *The Journal of Neuroscience: The Official Journal of the Society for Neuroscience*, *10*(12), 3837–3848.

Barbeau, H., & Rossignol, S. (1987). Recovery of locomotion after chronic spinalization in the adult cat. *Brain Research*, *412*(1), 84–95.

Bareyre, F. M., Kerschensteiner, M., Raineteau, O., Mettenleiter, T. C., Weinmann, O., & Schwab, M. E. (2004). The injured spinal cord spontaneously forms a new intraspinal circuit in adult rats. *Nature Neuroscience*, *7*(3), 269–277. https://doi.org/10.1038/nn1195

Baron-Van Evercooren, A., Kleinman, H. K., Seppä, H. E., Rentier, B., & Dubois-Dalcq, M. (1982). Fibronectin promotes rat Schwann cell growth and motility. *The Journal of Cell Biology*, *93*(1), 211–216.

Barrière, G., Leblond, H., Provencher, J., Rossignol, S. (2008) Prominent role of the spinal central pattern generator in the recovery of locomotion after partial spinal cord injuries. *Journal of Neuroscience* 28(15): 3976-87. doi: 10.1523/JNEUROSCI.5692-07.

Basso, D. M., Beattie, M. S., & Bresnahan, J. C. (1995). A sensitive and reliable locomotor rating scale for open field testing in rats. *Journal of Neurotrauma*, *12*(1), 1–21. http://doi.org/10.1089/neu.1995.12.1

Basso, D. M., Beattie, M. S., & Bresnahan, J. C. (1996). Graded Histological and Locomotor Outcomes after Spinal Cord Contusion Using the NYU Weight-Drop Device versus Transection. *Experimental Neurology*, *139*(2), 244–256. https://doi.org/10.1006/exnr.1996.0098

Behrman, A. L., & Harkema, S. J. (2000). Locomotor training after human spinal cord injury: a series of case studies. *Physical Therapy*, *80*(7), 688–700.

Benton, R. L., Maddie, M.A., Minillo, D.R., Hagg, T., & Whittemore, S.R. (2008) *Griffonia simplicifolia* Isolectin B4 identifies a specific subpopulation of angiogenic blood vessels following contusive spinal cord injury in the adult mouse. *Journal of Comparative Neurology* 507: 1031-1052. Doi: 10.1002/cne.21570

Berkowitz, A. L., Miller, M. B., Mir, S. A., Cagney, D., Chavakula, V., Guleria, I., … Chi, J. H. (2016). Glioproliferative Lesion of the Spinal Cord as a Complication of "Stem-Cell Tourism." *New England Journal of Medicine*, *375*(2), 196–198. https://doi.org/10.1056/NEJMc1600188

Betker, A. L., Desai, A., Nett, C., Kapadia, N., & Szturm, T. (2007). Game-based Exercises for Dynamic Short-Sitting Balance Rehabilitation of People With Chronic Spinal Cord and Traumatic Brain Injuries. *Physical Therapy*, *87*(10), 1389–1398. https://doi.org/10.2522/ptj.20060229

Biernaskie, J. A., McKenzie, I. A., Toma, J. G., & Miller, F. D. (2007). Isolation of skin-derived precursors (SKPs) and differentiation and enrichment of their Schwann cell progeny. *Nature Protocols*, *1*(6), 2803–2812. https://doi.org/10.1038/nprot.2006.422

Biernaskie, J., Sparling, J. S., Liu, J., Shannon, C. P., Plemel, J. R., Xie, Y., … Tetzlaff, W. (2007). Skin-Derived Precursors Generate Myelinating Schwann Cells That Promote Remyelination and Functional Recovery after Contusion Spinal Cord Injury. *Journal of Neuroscience*, *27*(36), 9545–9559. https://doi.org/10.1523/JNEUROSCI.1930-07.2007

Blesch, A., Lu, P., & Tuszynski, M. H. (2002). Neurotrophic factors, gene therapy, and neural stem cells for spinal cord repair. *Brain Research Bulletin*, *57*(6), 833–838.

Blesch, A., & Tuszynski, M. H. (2009). Spinal cord injury: plasticity, regeneration and the challenge of translational drug development. *Trends in Neurosciences*, *32*(1), 41–47. https://doi.org/10.1016/j.tins.2008.09.008

Böhme, H. (1976). Photoreactions of cytochrome b6 and cytochrome f in chloroplast photosystem I fragments. *Zeitschrift Fur Naturforschung. Section C, Biosciences*, *31*(1–2), 68–77.

Bracken, M. B., Shepard, M. J., Collins, W. F., Holford, T. R., Baskin, D. S., Eisenberg, H. M., … Young, W. (1992). Methylprednisolone or naloxone treatment after acute spinal cord injury: 1-year follow-up data: Results of the second National Acute Spinal Cord Injury Study. *Journal of Neurosurgery*, *76*(1), 23–31. https://doi.org/10.3171/jns.1992.76.1.0023

Brederlau, A., Correia, A. S., Anisimov, S. V., Elmi, M., Paul, G., Roybon, L., … Li, J.-Y. (2006). Transplantation of Human Embryonic Stem Cell-Derived Cells to a Rat Model of Parkinson's Disease: Effect of In Vitro Differentiation on Graft Survival and Teratoma Formation. *STEM CELLS*, *24*(6), 1433–1440. https://doi.org/10.1634/stemcells.2005-0393

Bregman, B. S., Kunkel-Bagden, E., Schnell, L., Dai, H. N., Gao, D., & Schwab, M. E. (1995). Recovery from spinal cord injury mediated by antibodies to neurite growth inhibitors. *Nature*, *378*(6556), 498–501. https://doi.org/10.1038/378498a0

Brown, T. G. (1914). On the nature of the fundamental activity of the nervous centres; together with an analysis of the conditioning of rhythmic activity in progression, and a theory of

the evolution of function in the nervous system. *The Journal of Physiology*, *48*(1), 18–46.

Bulte, J. W. M. (2009). In Vivo MRI Cell Tracking: Clinical Studies. *American Journal of Roentgenology*, *193*(2), 314–325. https://doi.org/10.2214/AJR.09.3107

Bunge, M. B. (2016). Efficacy of Schwann cell transplantation for spinal cord repair is improved with combinatorial strategies: Improving Schwann cell transplantation. *The Journal of Physiology*, *594*(13), 3533–3538. https://doi.org/10.1113/JP271531

Bunge, R. P. (1968). Glial cells and the central myelin sheath. *Physiological Reviews*, *48*(1), 197–251.

Bunge, R. P. (1975). Changing uses of nerve tissue culture 1950-1975. In *The Nervous System* (Vol. Volume 1. The Basic Neuroscience). New York: Raven Press.

Cafferty, W. B. J., Duffy, P., Huebner, E., & Strittmatter, S. M. (2010). MAG and OMgp Synergize with Nogo-A to Restrict Axonal Growth and Neurological Recovery after Spinal Cord Trauma. *Journal of Neuroscience*, *30*(20), 6825–6837. https://doi.org/10.1523/JNEUROSCI.6239-09.2010

Cafferty, William B.J., McGee, A. W., & Strittmatter, S. M. (2008). Axonal growth therapeutics: regeneration or sprouting or plasticity? *Trends in Neurosciences*, *31*(5), 215–220. https://doi.org/10.1016/j.tins.2008.02.004

Cai, D., Qiu, J., Cao, Z., McAtee, M., Bregman, B. S., & Filbin, M. T. (2001). Neuronal cyclic AMP controls the developmental loss in ability of axons to regenerate. *The Journal of Neuroscience: The Official Journal of the Society for Neuroscience*, *21*(13), 4731–4739.

Caicco, M. J., Zahir, T., Mothe, A. J., Ballios, B. G., Kihm, A. J., Tator, C. H., & Shoichet, M. S. (2013). Characterization of hyaluronan-methylcellulose hydrogels for cell delivery to the injured spinal cord. *Journal of Biomedical Materials Research. Part A*, *101*(5), 1472–1477. http://doi.org/10.1002/jbm.a.34454

Cajal, S. R. y. (1914). *Estudios sobre la degeneración y regeneración del Sistema nervioso*. Madrid: Hijos de Nicolás Moya.

Carlson, S. L., Parrish, M. E., Springer, J. E., Doty, K., & Dossett, L. (1998). Acute Inflammatory Response in Spinal Cord Following Impact Injury. *Experimental Neurology*, *151*(1), 77–88. https://doi.org/10.1006/exnr.1998.6785

Carmel, J. B., Berrol, L. J., Brus-Ramer, M., & Martin, J. H. (2010). Chronic Electrical Stimulation of the Intact Corticospinal System after Unilateral Injury Restores Skilled Locomotor Control and Promotes Spinal Axon Outgrowth. *Journal of Neuroscience*, *30*(32), 10918–10926. https://doi.org/10.1523/JNEUROSCI.1435-10.2010

Caroni, P., & Schwab, M. E. (1988). Antibody against myelin associated inhibitor of neurite growth neutralizes nonpermissive substrate properties of CNS white matter. *Neuron*, *1*(1), 85–96. https://doi.org/10.1016/0896-6273(88)90212-7

Caudle, K. L., Brown, E. H., Shum-Siu, A., Burke, D. A., Magnuson, T. S. G., Voor, M. J., & Magnuson, D. S. K. (2011). Hindlimb Immobilization in a Wheelchair Alters Functional Recovery Following Contusive Spinal Cord Injury in the Adult Rat. *Neurorehabilitation and Neural Repair*, *25*(8), 729–739. https://doi.org/10.1177/1545968311407519

Casadevall, A., & Fang, F. C. (2010). Reproducible Science. *Infection and Immunity*, *78*(12),

4972–4975. https://doi.org/10.1128/IAI.00908-10

Charles River Laboratories. (2015). Inbred Rats Datasheet. Retrieved from http://www.criver.com/files/pdfs/rms/inbred-rats.aspx

Chen, M. S., Huber, A. B., van der Haar, M. E., Frank, M., Schnell, L., Spillmann, A. A., … Schwab, M. E. (2000). Nogo-A is a myelin-associated neurite outgrowth inhibitor and an antigen for monoclonal antibody IN-1. *Nature*, *403*(6768), 434–439. https://doi.org/10.1038/35000219

Chen, Q., Smith, G. M., & Shine, H. D. (2008). Immune activation is required for NT-3-induced axonal plasticity in chronic spinal cord injury. *Experimental Neurology*, *209*(2), 497–509. https://doi.org/10.1016/j.expneurol.2007.11.025

Choppa, P. ., Vojdani, A., Tagle, C., Andrin, R., & Magtoto, L. (1998). Multiplex PCR for the detection of Mycoplasma fermentans, M. hominisandM. penetransin cell cultures and blood samples of patients with chronic fatigue syndrome. *Molecular and Cellular Probes*, *12*(5), 301–308. https://doi.org/10.1006/mcpr.1998.0186

Contopoulos-Ioannidis, D. G., Ntzani, E., & Ioannidis, J. P. A. (2003). Translation of highly promising basic science research into clinical applications. *The American Journal of Medicine*, *114*(6), 477–484.

Courtine, G., Song, B., Roy, R. R., Zhong, H., Herrmann, J. E., Ao, Y., … Sofroniew, M. V. (2008). Recovery of supraspinal control of stepping via indirect propriospinal relay connections after spinal cord injury. *Nature Medicine*, *14*(1), 69–74. https://doi.org/10.1038/nm1682

Cowley, K., Zaporozhets, E., & Schmidt, B. (2008). Propriospinal neurons are sufficient for bulbospinal transmission of the locomotor command signal in the neonatal rat spinal cord. *Journal of Physiology*, *586*(6), 1623-1635. http://doi.org/10.1113/jphysiol.2007.148361

Craig, W. S., Cheng, S., Mullen, D. G., Blevitt, J., & Pierschbacher, M. D. (1995). Concept and progress in the development of RGD-containing peptide pharmaceuticals. *Biopolymers*, *37*(2), 157–175. http://doi.org/10.1002/bip.360370209

Crowe, M. J., Bresnahan, J. C., Shuman, S. L., Masters, J. N., & Crowe, M. S. (1997). Apoptosis and delayed degeneration after spinal cord injury in rats and monkeys. *Nature Medicine*, *3*(1), 73–76. https://doi.org/10.1038/nm0197-73

Cusimano, M., Biziato, D., Brambilla, E., Donega, M., Alfaro-Cervello, C., Snider, S., … Pluchino, S. (2012). Transplanted neural stem/precursor cells instruct phagocytes and reduce secondary tissue damage in the injured spinal cord. *Brain*, *135*(2), 447–460. https://doi.org/10.1093/brain/awr339

de Groot, P. C. E., Hjeltnes, N., Heijboer, A. C., Stal, W., & Birkeland, K. (2003). Effect of training intensity on physical capacity, lipid profile and insulin sensitivity in early rehabilitation of spinal cord injured individuals. *Spinal Cord*, *41*(12), 673–679. https://doi.org/10.1038/sj.sc.3101534

de Leon, R. D., Tamaki, H., Hodgson, J. A., Roy, R. R., & Edgerton, V. R. (1999). Hindlimb locomotor and postural training modulates glycinergic inhibition in the spinal cord of the adult spinal cat. *Journal of Neurophysiology*, *82*(1), 359–369.

De Winter, F., Oudega, M., Lankhorst, A. J., Hamers, F. P., Blits, B., Ruitenberg, M. J., … Verhaagen, J. (2002). Injury-Induced Class 3 Semaphorin Expression in the Rat Spinal Cord. *Experimental Neurology*, *175*(1), 61–75. https://doi.org/10.1006/exnr.2002.7884

Deepa, S. S., Carulli, D., Galtrey, C., Rhodes, K., Fukuda, J., Mikami, T., … Fawcett, J. W. (2006). Composition of Perineuronal Net Extracellular Matrix in Rat Brain: A DIFFERENT DISACCHARIDE COMPOSITION FOR THE NET-ASSOCIATED PROTEOGLYCANS. *Journal of Biological Chemistry*, *281*(26), 17789–17800. https://doi.org/10.1074/jbc.M600544200

Delghandi, M. P., Johannessen, M., & Moens, U. (2005). The cAMP signalling pathway activates CREB through PKA, p38 and MSK1 in NIH 3T3 cells. *Cellular Signalling*, *17*(11), 1343–1351. https://doi.org/10.1016/j.cellsig.2005.02.003

Demopoulos, H. B., Flamm, E. S., Pietronigro, D. D., & Seligman, M. L. (1980). The free radical pathology and the microcirculation in the major central nervous system disorders. *Acta Physiologica Scandinavica. Supplementum*, *492*, 91–119.

Dergham, P., Ellezam, B., Essagian, C., Avedissian, H., Lubell, W. D., & McKerracher, L. (2002). Rho signaling pathway targeted to promote spinal cord repair. *The Journal of Neuroscience: The Official Journal of the Society for Neuroscience*, *22*(15), 6570–6577. https://doi.org/20026637

Ding, A. H., Nathan, C. F., & Stuehr, D. J. (1988). Release of reactive nitrogen intermediates and reactive oxygen intermediates from mouse peritoneal macrophages. Comparison of activating cytokines and evidence for independent production. *Journal of Immunology*

(Baltimore, Md.: 1950), *141*(7), 2407–2412.

Ditunno, J. F., Little, J. W., Tessler, A., & Burns, A. S. (2004). Spinal shock revisited: a four-phase model. *Spinal Cord*, *42*(7), 383–395. https://doi.org/10.1038/sj.sc.3101603

Dlouhy, B. J., Awe, O., Rao, R. C., Kirby, P. A., & Hitchon, P. W. (2014). Autograft-derived spinal cord mass following olfactory mucosal cell transplantation in a spinal cord injury patient: Case report. *Journal of Neurosurgery: Spine*, *21*(4), 618–622. https://doi.org/10.3171/2014.5.SPINE13992

Dobkin, B., Barbeau, H., Deforge, D., Ditunno, J., Elashoff, R., Apple, D., Basso, M., Behrman, A., Harkema., S, Saulino, M., Scott, M. (2007) Spinal Cord Injury Locomotor Trial Group. The evolution of walking-related outcomes over the first 12 weeks of rehabilitation for incomplete traumatic spinal cord injury: the multicenter randomized Spinal Cord Injury Locomotor Trial. *Neurorehabiltation and Neural Repair* 21(1):25-35. doi:10.1177/1545968306295556.

Domeniconi, M., Cao, Z., Spencer, T., Sivasankaran, R., Wang, K., Nikulina, E., … Filbin, M. (2002). Myelin-associated glycoprotein interacts with the Nogo66 receptor to inhibit neurite outgrowth. *Neuron*, *35*(2), 283–290.

Donnelly, D. J., & Popovich, P. G. (2008). Inflammation and its role in neuroprotection, axonal regeneration and functional recovery after spinal cord injury. *Experimental Neurology*, *209*(2), 378–388. https://doi.org/10.1016/j.expneurol.2007.06.009

Dressel, R., Schindehütte, J., Kuhlmann, T., Elsner, L., Novota, P., Baier, P. C., … Mansouri, A. (2008). The Tumorigenicity of Mouse Embryonic Stem Cells and In Vitro Differentiated

Neuronal Cells Is Controlled by the Recipients' Immune Response. *PLoS ONE*, *3*(7), e2622. https://doi.org/10.1371/journal.pone.0002622

Drew, T., & Rossignol, S. (1990). Functional organization within the medullary reticular formation of intact unanesthetized cat. II. Electromyographic activity evoked by microstimulation. *Journal of Neurophysiology*, *64*(3), 782–795.

D'Souza, S., Alinauskas, K., McCrea, E., Goodyer, C., & Antel, J. P. (1995). Differential susceptibility of human CNS-derived cell populations to TNF-dependent and independent immune-mediated injury. *The Journal of Neuroscience: The Official Journal of the Society for Neuroscience*, *15*(11), 7293–7300.

Duerstock, B. S. (2004). Double labeling serial sections to enhance three-dimensional imaging of injured spinal cord. *Journal of Neuroscience Methods*, *134*(1), 101–107. https://doi.org/10.1016/j.jneumeth.2003.11.012

Eason, R., Smith, T., & Plaisance, E. (1989). Effects of Proactive Interference on Learning the Tennis Backhand Stroke. *Perceptual and Motor Skills*, *68*(3), 923–930.

Ek, C. J., Habgood, M. D., Callaway, J. K., Dennis, R., Dziegielewska, K. M., Johansson, P. A., … Saunders, N. R. (2010). Spatio-Temporal Progression of Grey and White Matter Damage Following Contusion Injury in Rat Spinal Cord. *PLoS ONE*, *5*(8), e12021. https://doi.org/10.1371/journal.pone.0012021

Elliott, T., & Shadbolt, N. R. (2002). Multiplicative Synaptic Normalization and a Nonlinear Hebb Rule Underlie a Neurotrophic Model of Competitive Synaptic Plasticity. *Neural Computation*, *14*(6), 1311–1322. https://doi.org/10.1162/089976602753712954

Elmore, S. (2007). Apoptosis: A Review of Programmed Cell Death. *Toxicologic Pathology*, *35*(4), 495–516. https://doi.org/10.1080/01926230701320337

Emery, E., Li, X., Brunschwig, J. P., Olson, L., & Levi, A. D. (1999). Assessment of the malignant potential of mitogen stimulated human Schwann cells. *Journal of the Peripheral Nervous System: JPNS*, *4*(2), 107–116.

Engineer, N. D., Engineer, C. T., Reed, A. C., Pandya, P. K., Jakkamsetti, V., Moucha, R., & Kilgard, M. P. (2012). Inverted-U function relating cortical plasticity and task difficulty. *Neuroscience*, *205*, 81–90. https://doi.org/10.1016/j.neuroscience.2011.12.056

Enomoto, M., Bunge, M. B., & Tsoulfas, P. (2013). A multifunctional neurotrophin with reduced affinity to p75NTR enhances transplanted Schwann cell survival and axon growth after spinal cord injury. *Experimental Neurology*, *248*, 170–182. https://doi.org/10.1016/j.expneurol.2013.06.013

Erschbamer, M. K., Pham, T. M., Zwart, M. C., Baumans, V., & Olson, L. (2006). Neither environmental enrichment nor voluntary wheel running enhances recovery from incomplete spinal cord injury in rats. *Experimental Neurology*, *201*(1), 154–164. doi:10.1016/j.expneurol.2006.04.003

Ertürk, A., Mauch, C. P., Hellal, F., Förstner, F., Keck, T., Becker, K., … Bradke, F. (2011). Three-dimensional imaging of the unsectioned adult spinal cord to assess axon regeneration and glial responses after injury. *Nature Medicine*, *18*(1), 166–171. https://doi.org/10.1038/nm.2600

Farry, Angela, & Baxter, David. (n.d.). The Incidence and Prevalence of Spinal Cord Injury in

Canada Overview and esti mates based on current evidence. *Rick Hansen Institute and Urban Futures*, 1–57.

Fawcett, J. W., & Asher, R. A. (1999). The glial scar and central nervous system repair. *Brain Research Bulletin*, *49*(6), 377–391.

Feng, H.-Y., Ning, G.-Z., Feng, S.-Q., Yu, T.-Q., & Zhou, H.-X. (2011). Epidemiological profile of 239 traumatic spinal cord injury cases over a period of 12 years in Tianjin, China. *The Journal of Spinal Cord Medicine*, *34*(4), 388–394. https://doi.org/10.1179/2045772311Y.0000000017

Fenrich, K. K., May, Z., Hurd, C., Boychuk, C. E., Kowalczewski, J., Bennett, D. J., … Fouad, K. (2015). Improved single pellet grasping using automated *ad libitum* full-time training robot. *Behavioural Brain Research*, *281*, 137–148. https://doi.org/10.1016/j.bbr.2014.11.048

Fenrich, K. K., May, Z., Torres-Espín, A., Forero, J., Bennett, D. J., & Fouad, K. (2016). Single pellet grasping following cervical spinal cord injury in adult rat using an automated full-time training robot. *Behavioural Brain Research*, *299*, 59–71. https://doi.org/10.1016/j.bbr.2015.11.020

Fenrich, K. K., & Rose, P. K. (2009). Spinal interneuron axons spontaneously regenerate after spinal cord injury in the adult feline. *Journal of Neuroscience*, *29*(39), 12145–12158. https://doi.org/10.1523/JNEUROSCI.0897-09.2009

Fenrich, K. K., Skelton, N., MacDermid, V. E., Meehan, C. F., Armstrong, S., Neuber-Hess, M. S., & Rose, P. K. (2007). Axonal regeneration and development of de novo axons from

distal dendrites of adult feline commissural interneurons after a proximal axotomy. *The Journal of Comparative Neurology*, *502*(6), 1079–1097. http://doi.org/10.1002/cne.21362

Filbin, M. T. (2003). Myelin-associated inhibitors of axonal regeneration in the adult mammalian CNS. *Nature Reviews Neuroscience*, *4*(9), 703–713. https://doi.org/10.1038/nrn1195

Filli, L., Engmann, A. K., Zorner, B., Weinmann, O., Moraitis, T., Gullo, M., … Schwab, M. E. (2014). Bridging the Gap: A Reticulo-Propriospinal Detour Bypassing an Incomplete Spinal Cord Injury. *Journal of Neuroscience*, *34*(40), 13399–13410. https://doi.org/10.1523/JNEUROSCI.0701-14.2014

Filli, L., & Schwab, M. E. (2012). The rocky road to translation in spinal cord repair. *Annals of Neurology*, *72*(4), 491–501. doi:10.1002/ana.23630

Filli, L., & Schwab, M. (2015). Structural and functional reorganization of propriospinal connections promotes functional recovery after spinal cord injury. *Neural Regeneration Research*, *10*(4), 509. http://doi.org/10.4103/1673-5374.155425

Fitch, M. T., Doller, C., Combs, C. K., Landreth, G. E., & Silver, J. (1999). Cellular and molecular mechanisms of glial scarring and progressive cavitation: in vivo and in vitro analysis of inflammation-induced secondary injury after CNS trauma. *The Journal of Neuroscience: The Official Journal of the Society for Neuroscience*, *19*(19), 8182–8198.

Fleming, J. C., Norenberg, M. D., Ramsay, D. A., Dekaban, G. A., Marcillo, A. E., Saenz, A. D., … Weaver, L. C. (2006). The cellular inflammatory response in human spinal cords after injury. *Brain: A Journal of Neurology*, *129*(Pt 12), 3249–3269.

Fonseca, R., Nägerl, U. V., Morris, R. G. M., & Bonhoeffer, T. (2004). Competing for Memory. *Neuron*, *44*(6), 1011–1020. https://doi.org/10.1016/j.neuron.2004.10.033

Forgione, N., & Fehlings, M. G. (2014). Rho-ROCK Inhibition in the Treatment of Spinal Cord Injury. *World Neurosurgery*, *82*(3–4), e535–e539. https://doi.org/10.1016/j.wneu.2013.01.009

Fouad, K., Bennett, D. J., Vavrek, R., & Blesch, A. (2013). Long-Term Viral Brain-Derived Neurotrophic Factor Delivery Promotes Spasticity in Rats with a Cervical Spinal Cord Hemisection. *Frontiers in Neurology*, *4*. https://doi.org/10.3389/fneur.2013.00187

Fouad, K., Pedersen, V., Schwab, M. E., & Brösamle, C. (2001). Cervical sprouting of corticospinal fibers after thoracic spinal cord injury accompanies shifts in evoked motor responses. *Current Biology: CB*, *11*(22), 1766–1770.

Fouad, K., Schnell, L., Bunge, M. B., Schwab, M. E., Liebscher, T., & Pearse, D. D. (2005). Combining Schwann cell bridges and olfactory-ensheathing glia grafts with chondroitinase promotes locomotor recovery after complete transection of the spinal cord. *The Journal of Neuroscience: The Official Journal of the Society for Neuroscience*, *25*(5), 1169–1178. http://doi.org/10.1523/JNEUROSCI.3562-04.2005

Fouad, K., & Tetzlaff, W. (2012). Rehabilitative training and plasticity following spinal cord injury. *Experimental Neurology*, *235*(1), 91–99. https://doi.org/10.1016/j.expneurol.2011.02.009

Fournier, A. E., GrandPre, T., & Strittmatter, S. M. (2001). Identification of a receptor mediating Nogo-66 inhibition of axonal regeneration. *Nature*, *409*(6818), 341–346.

https://doi.org/10.1038/35053072

Frey, U., & Morris, R. G. M. (1997). Synaptic tagging and long-term potentiation. *Nature*, *385*(6616), 533–536. https://doi.org/10.1038/385533a0

Frisch, S. M., & Francis, H. (1994). Disruption of epithelial cell-matrix interactions induces apoptosis. *The Journal of Cell Biology*, *124*(4), 619–626. https://doi.org/10.1083/jcb.124.4.619

Führmann, T., Tam, R. Y., Ballarin, B., Coles, B., Elliott Donaghue, I., van der Kooy, D., … Shoichet, M. S. (2016). Injectable hydrogel promotes early survival of induced pluripotent stem cell-derived oligodendrocytes and attenuates longterm teratoma formation in a spinal cord injury model. *Biomaterials*, *83*, 23–36. http://doi.org/10.1016/j.biomaterials.2015.12.032

Funakoshi, H., Frisén, J., Barbany, G., Timmusk, T., Zachrisson, O., Verge, V. M., & Persson, H. (1993). Differential expression of mRNAs for neurotrophins and their receptors after axotomy of the sciatic nerve. *The Journal of Cell Biology*, *123*(2), 455–465.

Funk, D., Fricke, C., & Schlosshauer, B. (2007). Aging Schwann cells in vitro. *European Journal of Cell Biology*, *86*(4), 207–219. https://doi.org/10.1016/j.ejcb.2006.12.006

Fyffe, R. E. (1991). Spatial distribution of recurrent inhibitory synapses on spinal motoneurons in the cat. *Journal of Neurophysiology*, *65*(5), 1134–1149.

García-Alías, G., Barkhuysen, S., Buckle, M., & Fawcett, J. W. (2009). Chondroitinase ABC treatment opens a window of opportunity for task-specific rehabilitation. *Nature*

Neuroscience, *12*(9), 1145–1151. http://doi.org/10.1038/nn.2377.

Garner, C. W., & Behal, F. J. (1975). Effect of pH on substrate and inhibitor kinetic constants of human liver alanine aminopeptidase. Evidence for two ionizable active center groups. *Biochemistry*, *14*(23), 5084–5088.

Garraway, S. M., & Huie, J. R. (2016). Spinal Plasticity and Behavior: BDNF-Induced Neuromodulation in Uninjured and Injured Spinal Cord. *Neural Plasticity*, *2016*, 1–19. https://doi.org/10.1155/2016/9857201

Garraway, S. M., Petruska, J. C., & Mendell, L. M. (2003). BDNF sensitizes the response of lamina II neurons to high threshold primary afferent inputs. *The European Journal of Neuroscience*, *18*(9), 2467–2476.

Gartner, K., Buttner, D., Dohler, K., Friedel, R., Lindena, J., & Trautschold, I. (1980). Stress response of rats to handling and experimental procedures. Laboratory Animals, 14(3), 267–274. http://doi.org/10.1258/002367780780937454

Gilmore, A. P. (2005). Anoikis. *Cell Death and Differentiation*, *12*, 1473–1477. https://doi.org/10.1038/sj.cdd.4401723

Gilmore, S. A., & Sims, T. J. (1993). Patterns of Schwann cell myelination of axons within the spinal cord. *Journal of Chemical Neuroanatomy*, *6*(4), 191–199.

Girgis, J., Merrett, D., Kirkland, S., Metz, G. a. S., Verge, V., & Fouad, K. (2007). Reaching training in rats with spinal cord injury promotes plasticity and task specific recovery. *Brain: A Journal of Neurology*, *130*(Pt 11), 2993–3003.

https://doi.org/10.1093/brain/awm245

Golden, K. L., Pearse, D. D., Blits, B., Garg, M. S., Oudega, M., Wood, P. M., & Bunge, M. B. (2007). Transduced Schwann cells promote axon growth and myelination after spinal cord injury. *Experimental Neurology*, *207*(2), 203–217. https://doi.org/10.1016/j.expneurol.2007.06.023

Gómez-Pinilla, F., Ying, Z., Opazo, P., Roy, R. R., & Edgerton, V. R. (2001). Differential regulation by exercise of BDNF and NT-3 in rat spinal cord and skeletal muscle. *The European Journal of Neuroscience*, *13*(6), 1078–1084.

Gomez-Pinilla, F., Ying, Z., & Zhuang, Y. (2012). Brain and Spinal Cord Interaction: Protective Effects of Exercise Prior to Spinal Cord Injury. *PLoS ONE*, *7*(2), e32298. https://doi.org/10.1371/journal.pone.0032298

Goodridge, D., Rogers, M., Klassen, L., Jeffery, B., Knox, K., Rohatinsky, N., & Linassi, G. (2015). Access to health and support services: perspectives of people living with a long-term traumatic spinal cord injury in rural and urban areas. *Disability and Rehabilitation*, *37*(16), 1401–1410. https://doi.org/10.3109/09638288.2014.972593

Goulding, M. (2009a). Circuits controlling vertebrate locomotion: moving in a new direction. *Nature Reviews Neuroscience*, *10*(7), 507–518. https://doi.org/10.1038/nrn2608

Goulding, M. (2009b). Circuits controlling vertebrate locomotion: moving in a new direction. *Nature Reviews Neuroscience*, *10*(7), 507–518. https://doi.org/10.1038/nrn2608

Grande, G., Armstrong, S., Neuber-Hess, M., & Rose, P. K. (2005). Distribution of contacts

from vestibulospinal axons on the dendrites of splenius motoneurons. *The Journal of Comparative Neurology*, *491*(4), 339–351. http://doi.org/10.1002/cne.20699

Grande, G., Bui, T. V., & Rose, P. K. (2010). Distribution of vestibulospinal contacts on the dendrites of ipsilateral splenius motoneurons: An anatomical substrate for push-pull interactions during vestibulocollic reflexes. *Brain Research*, *1333*, 9–27. http://doi.org/10.1016/j.brainres.2010.03.065

GrandPré, T., Nakamura, F., Vartanian, T., & Strittmatter, S. M. (2000). Identification of the Nogo inhibitor of axon regeneration as a Reticulon protein. *Nature*, *403*(6768), 439–444. https://doi.org/10.1038/35000226

GrandPré, Tadzia, Li, S., & Strittmatter, S. M. (2002). Nogo-66 receptor antagonist peptide promotes axonal regeneration. *Nature*, *417*(6888), 547–551. https://doi.org/10.1038/417547a

Granger, N., Blamires, H., Franklin, R. J. M., & Jeffery, N. D. (2012). Autologous olfactory mucosal cell transplants in clinical spinal cord injury: a randomized double-blinded trial in a canine translational model. *Brain*, *135*(11), 3227–3237. https://doi.org/10.1093/brain/aws268

Guertin, P. A. (2013). Central Pattern Generator for Locomotion: Anatomical, Physiological, and Pathophysiological Considerations. *Frontiers in Neurology*, *3*. https://doi.org/10.3389/fneur.2012.00183

Guest, J. D., Hiester, E. D., & Bunge, R. P. (2005). Demyelination and Schwann cell responses adjacent to injury epicenter cavities following chronic human spinal cord injury.

Experimental Neurology, *192*(2), 384–393. https://doi.org/10.1016/j.expneurol.2004.11.033

Gupta, D., Tator, C. H., & Shoichet, M. S. (2006). Fast-gelling injectable blend of hyaluronan and methylcellulose for intrathecal, localized delivery to the injured spinal cord. *Biomaterials*, *27*(11), 2370–2379. http://doi.org/10.1016/j.biomaterials.2005.11.015

Horn, K. P., Busch, S. A., Hawthorne, A. L., van Rooijen, N., & Silver, J. (2008). Another barrier to regeneration in the CNS: Activated macrophages induce extensive retraction of dystrophic axons through direct physical interactions. *Journal of Neuroscience*, *28*(38). 9330-41. http://doi.org/10.1523/JNEUROSCI.2488-08.2008

Hagg, T., & Oudega, M. (2006). Degenerative and Spontaneous Regenerative Processes after Spinal Cord Injury. *Journal of Neurotrauma*, *23*(3–4), 263–280. https://doi.org/10.1089/neu.2006.23.263

Hannes, V. (2009). *Nervous System (Cambridge Illustrated Surgical Pathology)*. L. Weiss (Ed.). New York, NY: Cambridge University Press. http://dx.doi.org/10.1017/CBO9780511581076

Hannila, S. S., & Filbin, M. T. (2008). The role of cyclic AMP signaling in promoting axonal regeneration after spinal cord injury. *Experimental Neurology*, *209*(2), 321–332. https://doi.org/10.1016/j.expneurol.2007.06.020

Harkema, S. J. (2001). Neural Plasticity after Human Spinal Cord Injury: Application of Locomotor Training to the Rehabilitation of Walking. *The Neuroscientist*, *7*(5), 455–468. https://doi.org/10.1177/107385840100700514

Harkema, S.J., Schmidt-Read, M., Lorenz, D.J., Edgerton, V.R., Behrman, A.L. (2012) Balance and ambulation improvements in individuals with chronic incomplete spinal cord injury using locomotor training-based rehabilitation. Arch Phys Med Rehabil. 93(9):1508-17. doi: 10.1016/j.apmr.2011.01.024.

Hashimoto, M., Ino, H., Koda, M., Murakami, M., Yoshinaga, K., Yamazaki, M., & Moriya, H. (2004). Regulation of semaphorin 3A expression in neurons of the rat spinal cord and cerebral cortex after transection injury. *Acta Neuropathologica*, *107*(3), 250–256. https://doi.org/10.1007/s00401-003-0805-z

Hatae, R., Miyazono, M., Kohri, R., Maeda, K., & Naito, S. (2014). Trochlear nerve schwannoma with intratumoral hemorrhage presenting with persistent hiccups: a case report. *Journal of Neurological Surgery Reports*, *75*(1), 183-188. http://doi.org/10.1055/s-0034-1378156

Hayashi, M., Ueyama, T., Nemoto, K., Tamaki, T., & Senba, E. (2000). Sequential mRNA expression for immediate early genes, cytokines, and neurotrophins in spinal cord injury. *Journal of Neurotrauma*, *17*(3), 203–218. http://doi.org/10.1089/neu.2000.17.203

Herberts, C. A., Kwa, M. S., & Hermsen, H. P. (2011). Risk factors in the development of stem cell therapy. *Journal of Translational Medicine*, *9*(1), 29. https://doi.org/10.1186/1479-5876-9-29

Herrera, J. J., Nesic, O., & Narayana, P. A. (2009). Reduced vascular endothelial growth factor expression in contusive spinal cord injury. *Journal of Neurotrauma*, *26*(7), 995–1003. https://doi.org/10.1089/neu.2008.0779

Hicks, A. L., Martin, K. A., Ditor, D. S., Latimer, A. E., Craven, C., Bugaresti, J., & McCartney, N. (2003). Long-term exercise training in persons with spinal cord injury: effects on strength, arm ergometry performance and psychological well-being. *Spinal Cord*, *41*(1), 34–43. https://doi.org/10.1038/sj.sc.3101389

Hill, C. E., Beattie, M. S., & Bresnahan, J. C. (2001). Degeneration and Sprouting of Identified Descending Supraspinal Axons after Contusive Spinal Cord Injury in the Rat. *Experimental Neurology*, *171*(1), 153–169. https://doi.org/10.1006/exnr.2001.7734

Hill, C. E., Moon, L. D. F., Wood, P. M., & Bunge, M. B. (2006). Labeled Schwann cell transplantation: Cell loss, host Schwann cell replacement, and strategies to enhance survival. *Glia*, *53*(3), 338–343. https://doi.org/10.1002/glia.20287

Hilton, B. J., Anenberg, E., Harrison, T. C., Boyd, J. D., Murphy, T. H., & Tetzlaff, W. (2016). Re-Establishment of Cortical Motor Output Maps and Spontaneous Functional Recovery via Spared Dorsolaterally Projecting Corticospinal Neurons after Dorsal Column Spinal Cord Injury in Adult Mice. *Journal of Neuroscience*, *36*(14), 4080–4092. https://doi.org/10.1523/JNEUROSCI.3386-15.2016

Hilton, D. A., Jacob, J., Househam, L., & Tengah, C. (2007). Complications following sural and peroneal nerve biopsies. *Journal of Neurology, Neurosurgery & Psychiatry*, *78*(11), 1271–1272. https://doi.org/10.1136/jnnp.2007.116368

Horn, K. P., Busch, S. A., Hawthorne, A. L., van Rooijen, N., & Silver, J. (2008). Another barrier to regeneration in the CNS: Activated macrophages induce extensive retraction of dystrophic axons through direct physical interactions. *Journal of Neuroscience*, *28*(38).

9330-41. http://doi.org/10.1523/JNEUROSCI.2488-08.2008

Huebner, E. A., & Strittmatter, S. M. (2009). Axon Regeneration in the Peripheral and Central Nervous Systems. In E. Koenig (Ed.), *Cell Biology of the Axon* (Vol. 48, pp. 305–360). Berlin, Heidelberg: Springer Berlin Heidelberg. https://doi.org/10.1007/400_2009_19

Hunt, R. S., Meltzer, G. E., & Landau, W. M. (1963). FUSIMOTOR FUNCTION. I. SPINAL SHOCK OF THE CAT AND THE MONKEY. *Archives of Neurology*, *9*, 120–126.

Hurd, C., Weishaupt, N., & Fouad, K. (2013). Anatomical correlates of recovery in single pellet reaching in spinal cord injured rats. *Experimental Neurology*, *247*, 605–614. doi:10.1016/j.expneurol.2013.02.013

Itakura, G., Kobayashi, Y., Nishimura, S., Iwai, H., Takano, M., Iwanami, A., … Nakamura, M. (2015). Controlling Immune Rejection Is a Fail-Safe System against Potential Tumorigenicity after Human iPSC-Derived Neural Stem Cell Transplantation. *PLOS ONE*, *10*(2), e0116413. https://doi.org/10.1371/journal.pone.0116413

James, N. D., Bartus, K., Grist, J., Bennett, D. L. H., McMahon, S. B., & Bradbury, E. J. (2011). Conduction Failure following Spinal Cord Injury: Functional and Anatomical Changes from Acute to Chronic Stages. *Journal of Neuroscience*, *31*(50), 18543–18555. https://doi.org/10.1523/JNEUROSCI.4306-11.2011

Janzer, R. C., & Raff, M. C. (1987). Astrocytes induce blood–brain barrier properties in endothelial cells. *Nature*, *325*(6101), 253–257. https://doi.org/10.1038/325253a0

Jeong, J.-O., Han, J. W., Kim, J.-M., Cho, H.-J., Park, C., Lee, N., … Yoon, Y.-S. (2011).

Malignant Tumor Formation After Transplantation of Short-Term Cultured Bone Marrow Mesenchymal Stem Cells in Experimental Myocardial Infarction and Diabetic Neuropathy. *Circulation Research*, *108*(11), 1340–1347. https://doi.org/10.1161/CIRCRESAHA.110.239848

Joannides, A., Gaughwin, P., Schwiening, C., Majed, H., Sterling, J., Compston, A., & Chandran, S. (2004). Efficient generation of neural precursors from adult human skin: astrocytes promote neurogenesis from skin-derived stem cells. *Lancet (London, England)*, *364*(9429), 172–178. http://doi.org/10.1016/S0140-6736(04)16630-0

Jones, L. L., Margolis, R. U., & Tuszynski, M. H. (2003). The chondroitin sulfate proteoglycans neurocan, brevican, phosphacan, and versican are differentially regulated following spinal cord injury. *Experimental Neurology*, *182*(2), 399–411. http://doi.org/10.1016/S0014-4886(03)00087-6

Jordan, S. A., Wellborn, W. R., Kovnick, J., & Saltzstein, R. (1991). Understanding and treating motivation difficulties in ventilator-dependent SCI patients. *Paraplegia*, *29*(7), 431–442. https://doi.org/10.1038/sc.1991.59

Kakulas, B. A. (1984). Pathology of spinal injuries. *Central Nervous System Trauma: Journal of the American Paralysis Association*, *1*(2), 117–129.

Kakulas, B. A. (1999). A review of the neuropathology of human spinal cord injury with emphasis on special features. *The Journal of Spinal Cord Medicine*, *22*(2), 119–124.

Kanagal, S. G., & Muir, G. D. (2009). Task-dependent compensation after pyramidal tract and dorsolateral spinal lesions in rats. *Experimental Neurology*, *216*(1), 193–206.

https://doi.org/10.1016/j.expneurol.2008.11.028

Kaneko, S., Iwanami, A., Nakamura, M., Kishino, A., Kikuchi, K., Shibata, S., … Okano, H. (2007). A selective Sema3A inhibitor enhances regenerative responses and functional recovery of the injured spinal cord. *Nature Medicine*, *12*(12), 1380–1389. https://doi.org/10.1038/nm1505

Kang, S. K., Shin, I. S., Ko, M. S., Jo, J. Y., & Ra, J. C. (2012). Journey of Mesenchymal Stem Cells for Homing: Strategies to Enhance Efficacy and Safety of Stem Cell Therapy. *Stem Cells International*, *2012*, 1–11. https://doi.org/10.1155/2012/342968

Karimi-Abdolrezaee, S., Eftekharpour, E., Wang, J., Schut, D., & Fehlings, M. G. (2010). Synergistic Effects of Transplanted Adult Neural Stem/Progenitor Cells, Chondroitinase, and Growth Factors Promote Functional Repair and Plasticity of the Chronically Injured Spinal Cord. *Journal of Neuroscience*, *30*(5), 1657–1676. https://doi.org/10.1523/JNEUROSCI.3111-09.2010

Karp, J. M., & Leng Teo, G. S. (2009). Mesenchymal stem cell homing: the devil is in the details. *Cell Stem Cell*, *4*(3), 206–216. https://doi.org/10.1016/j.stem.2009.02.001

Keipert, S., Schultze, H. H., & Voigt, R. (1977). [Interactions between macromolecular adjuvants and drugs. 9. Association-trends between dextran and phenothiazine derivatives]. *Die Pharmazie*, *32*(6), 339–340.

Kennedy, P., & Rogers, B. A. (2000). Anxiety and depression after spinal cord injury: A longitudinal analysis. *Archives of Physical Medicine and Rehabilitation*, *81*(7), 932–937. https://doi.org/10.1053/apmr.2000.5580

Kerr, B. J., Bradbury, E. J., Bennett, D. L., Trivedi, P. M., Dassan, P., French, J., … Thompson, S. W. (1999). Brain-derived neurotrophic factor modulates nociceptive sensory inputs and NMDA-evoked responses in the rat spinal cord. *The Journal of Neuroscience: The Official Journal of the Society for Neuroscience*, *19*(12), 5138–5148.

Kerschensteiner, M., Gallmeier, E., Behrens, L., Leal, V. V., Misgeld, T., Klinkert, W. E., … Hohlfeld, R. (1999). Activated human T cells, B cells, and monocytes produce brain-derived neurotrophic factor in vitro and in inflammatory brain lesions: a neuroprotective role of inflammation? *The Journal of Experimental Medicine*, *189*(5), 865–870.

Khan, R. A., Rahman, A., Bhandari, P. B., & Khan, S. K. N. (2013). Double migration of a schwannoma of thoracic spine. *Case Reports*, *2013*(jan23 3), bcr2012008182-bcr2012008182. https://doi.org/10.1136/bcr-2012-008182

Kigerl, K. A., Gensel, J. C., Ankeny, D. P., Alexander, J. K., Donnelly, D. J., & Popovich, P. G. (2009). Identification of Two Distinct Macrophage Subsets with Divergent Effects Causing either Neurotoxicity or Regeneration in the Injured Mouse Spinal Cord. *Journal of Neuroscience*, *29*(43), 13435–13444. https://doi.org/10.1523/JNEUROSCI.3257-09.2009

Kinoshita, M., Matsui, R., Kato, S., Hasegawa, T., Kasahara, H., Isa, K., … Isa, T. (2012). Genetic dissection of the circuit for hand dexterity in primates. *Nature*, *487*(7406), 235–238. https://doi.org/10.1038/nature11206

Kirshblum, S. C., Burns, S. P., Biering-Sorensen, F., Donovan, W., Graves, D. E., Jha, A., … Waring, W. (2011). International standards for neurological classification of spinal cord

injury (Revised 2011). *The Journal of Spinal Cord Medicine*, *34*(6), 535–546. https://doi.org/10.1179/204577211X13207446293695

Kiss, Z. H., & Tator, C. H. (1993). Neurogenic Shock. In E. R. Geller (Ed.), *Shock and Resuscitation* (421-440). New York, NY: McGraw Hill.

Kobayashi, N. R., Fan, D. P., Giehl, K. M., Bedard, A. M., Wiegand, S. J., & Tetzlaff, W. (1997). BDNF and NT-4/5 prevent atrophy of rat rubrospinal neurons after cervical axotomy, stimulate GAP-43 and Talpha1-tubulin mRNA expression, and promote axonal regeneration. *The Journal of Neuroscience: The Official Journal of the Society for Neuroscience*, *17*(24), 9583–9595.

Koda, M., Someya, Y., Nishio, Y., Kadota, R., Mannoji, C., Miyashita, T., … Yamazaki, M. (2008). Brain-derived neurotrophic factor suppresses anoikis-induced death of Schwann cells. *Neuroscience Letters*, *444*(2), 143–147. https://doi.org/10.1016/j.neulet.2008.07.055

Kontoveros, D. (2015). *Schwann cell proliferation and migration in response to surface bound peptides for nerve regeneration* (Master's dissertation). Retrieved from OhioLINK, Electronic Theses and Dissertations Center. (akron1431035725)

Krajacic, A., Ghosh, M., Puentes, R., Pearse, D. D., & Fouad, K. (2009). Advantages of delaying the onset of rehabilitative reaching training in rats with incomplete spinal cord injury. *European Journal of Neuroscience*, *29*(3), 641–651. https://doi.org/10.1111/j.1460-9568.2008.06600.x

Kuerzi, J., Brown, E. H., Shum-Siu, A., Siu, A., Burke, D., Morehouse, J., … Magnuson, D. S.

K. (2010). Task-specificity vs. ceiling effect: Step-training in shallow water after spinal cord injury. *Experimental Neurology*, *224*(1), 178–187. doi:10.1016/j.expneurol.2010.03.008

Kumar, R., Sinha, S., Hagner, A., Stykel, M., Raharjo, E., Singh, K. K., … Biernaskie, J. (2016). Adult skin-derived precursor Schwann cells exhibit superior myelination and regeneration supportive properties compared to chronically denervated nerve-derived Schwann cells. *Experimental Neurology*, *278*, 127–142. http://doi.org/10.1016/j.expneurol.2016.02.006

Kyoung-Hee, L., Ji-Hye, K., Dong-Hee, C., & Jongmin, L. (2013). Effect of task-specific training on functional recovery and corticospinal tract plasticity after stroke. *Restorative Neurology and Neuroscience*, (6), 773–785. doi:10.3233/RNN-130336

Lang, C. E. (2004). Reduced Muscle Selectivity During Individuated Finger Movements in Humans After Damage to the Motor Cortex or Corticospinal Tract. *Journal of Neurophysiology*, *91*(4), 1722–1733. https://doi.org/10.1152/jn.00805.2003

Langford, L. A., Porter, S., & Bunge, R. P. (1988). Immortalized rat Schwann cells produce tumours in vivo. *Journal of Neurocytology*, *17*(4), 521–529.

Lappe, C., Herholz, S. C., Trainor, L. J., & Pantev, C. (2008). Cortical Plasticity Induced by Short-Term Unimodal and Multimodal Musical Training. *Journal of Neuroscience*, *28*(39), 9632–9639. https://doi.org/10.1523/JNEUROSCI.2254-08.2008

Lawrence, D. G., & Kuypers, H. G. (1968a). The functional organization of the motor system in the monkey. I. The effects of bilateral pyramidal lesions. *Brain: A Journal of Neurology*,

91(1), 1–14.

Lawrence, D. G., & Kuypers, H. G. (1968b). The functional organization of the motor system in the monkey. II. The effects of lesions of the descending brain-stem pathways. *Brain: A Journal of Neurology*, *91*(1), 15–36.

Lee, J. H., Streijger, F., Tigchelaar, S., Maloon, M., Liu, J., Tetzlaff, W., & Kwon, B. K. (2012). A contusive model of unilateral cervical spinal cord injury using the infinite horizon impactor. *Journal of Visualized Experiments*, *65*, 3313. http://doi.org/10.3791/3313

Lee, R. H., & Heckman, C. J. (2000). Adjustable amplification of synaptic input in the dendrites of spinal motoneurons in vivo. *The Journal of Neuroscience: The Official Journal of the Society for Neuroscience*, *20*(17), 6734–6740.

Lemmon, V. P., Ferguson, A. R., Popovich, P. G., Xu, X.-M., Snow, D. M., Igarashi, M., … the MIASCI Consortium. (2014). Minimum Information about a Spinal Cord Injury Experiment: A Proposed Reporting Standard for Spinal Cord Injury Experiments. *Journal of Neurotrauma*, *31*(15), 1354–1361. https://doi.org/10.1089/neu.2014.3400

Lemon, R. N., Johansson, R. S., & Westling, G. (1995). Corticospinal control during reach, grasp, and precision lift in man. *Journal of Neuroscience*, *15*(9), 6145–6156.

Li, S., & Stys, P. K. (2000). Mechanisms of ionotropic glutamate receptor-mediated excitotoxicity in isolated spinal cord white matter. *The Journal of Neuroscience: The Official Journal of the Society for Neuroscience*, *20*(3), 1190–1198.

Li, X., Murray, K., Harvey, P. J., Ballou, E. W., & Bennett, D. J. (2006). Serotonin Facilitates a

Persistent Calcium Current in Motoneurons of Rats With and Without Chronic Spinal Cord Injury. *Journal of Neurophysiology*, *97*(2), 1236–1246. https://doi.org/10.1152/jn.00995.2006

Li, Y., Gorassini, M. A., & Bennett, D. J. (2003). Role of Persistent Sodium and Calcium Currents in Motoneuron Firing and Spasticity in Chronic Spinal Rats. *Journal of Neurophysiology*, *91*(2), 767–783. https://doi.org/10.1152/jn.00788.2003

Lingor, P., Tonges, L., Pieper, N., Bermel, C., Barski, E., Planchamp, V., & Bahr, M. (2007). ROCK inhibition and CNTF interact on intrinsic signalling pathways and differentially regulate survival and regeneration in retinal ganglion cells. *Brain*. https://doi.org/10.1093/brain/awm284

Link, E., Edelmann, L., Chou, J. H., Binz, T., Yamasaki, S., Eisel, U., … Jahn, R. (1992). Tetanus toxin action: inhibition of neurotransmitter release linked to synaptobrevin proteolysis. *Biochemical and Biophysical Research Communications*, *189*(2), 1017–1023.

Liu, K., Lu, Y., Lee, J. K., Samara, R., Willenberg, R., Sears-Kraxberger, I., … He, Z. (2010). PTEN deletion enhances the regenerative ability of adult corticospinal neurons. *Nature Neuroscience*, *13*(9), 1075–1081. https://doi.org/10.1038/nn.2603

Liu, X. Z., Xu, X. M., Hu, R., Du, C., Zhang, S. X., McDonald, J. W., … Choi, D. W. (1997). Neuronal and glial apoptosis after traumatic spinal cord injury. *The Journal of Neuroscience: The Official Journal of the Society for Neuroscience*, *17*(14), 5395–5406.

Loy, D. N., Magnuson, D. S., Zhang, Y. P., Onifer, S. M., Mills, M. D., Cao, Q., Darnall, J. B.,

Fajardo, L. C., Burke, D. A., & Whittmore, S. R. (2002). Functional redundancy of ventral spinal locomotor pathways. *Journal of Neuroscience*, *22*(1), 315-323.

Lu, P., Wang, Y., Graham, L., McHale, K., Gao, M., Wu, D., … Tuszynski, M. H. (2012). Long-Distance Growth and Connectivity of Neural Stem Cells after Severe Spinal Cord Injury. *Cell*, *150*(6), 1264–1273. https://doi.org/10.1016/j.cell.2012.08.020

Lübke, J., Egger, V., Sakmann, B., & Feldmeyer, D. (2000). Columnar organization of dendrites and axons of single and synaptically coupled excitatory spiny neurons in layer 4 of the rat barrel cortex. *Journal of Neuroscience*, *20*(14), 5300–5311.

Magnuson, D. S. K., Lovett, R., Coffee, C., Gray, R., Han, Y., Zhang, Y. P., & Burke, D. A. (2005). Functional Consequences of Lumbar Spinal Cord Contusion Injuries in the Adult Rat. *Journal of Neurotrauma*, *22*(5), 529–543. https://doi.org/10.1089/neu.2005.22.529

Magnuson, D. S. K., Smith, R. R., Brown, E. H., Enzmann, G., Angeli, C., Quesada, P. M., & Burke, D. (2009). Swimming as a Model of Task-Specific Locomotor Retraining After Spinal Cord Injury in the Rat. *Neurorehabilitation and Neural Repair*, *23*(6), 535–545. https://doi.org/10.1177/1545968308331147

Maldonado Bouchard, S., & Hook, M. A. (2014). Psychological Stress as a Modulator of Functional Recovery Following Spinal Cord Injury. *Frontiers in Neurology*, *5*. https://doi.org/10.3389/fneur.2014.00044

Maratta, R., Fenrich, K. K., Zhao, E., Neuber-Hess, M. S., & Rose, P. K. (2015). Distribution and density of contacts from noradrenergic and serotonergic boutons on the dendrites of neck flexor motoneurons in the adult cat: NA and 5-HT contacts on flexor motoneurons.

Journal of Comparative Neurology, *523*(11), 1701–1716. http://doi.org/10.1002/cne.23765

Markram, H., Lübke, J., Frotscher, M., Roth, A., & Sakmann, B. (1997). Physiology and anatomy of synaptic connections between thick tufted pyramidal neurones in the developing rat neocortex. *The Journal of Physiology*, *500*(2), 409–440. http://doi.org/10.1113/jphysiol.1997.sp022031

Marder, E., & Bucher, D. (2001). Central pattern generators and the control of rhythmic movements. *Current Biology*, *11*(23), R986–R996. https://doi.org/10.1016/S0960-9822(01)00581-4

Martin, J. H. (2005). The Corticospinal System: From Development to Motor Control. *The Neuroscientist*, *11*(2), 161–173. http://doi.org/10.1177/1073858404270843

Martinez, M., Delivet-Mongrain, H., Leblond, H., & Rossignol, S. (2012). Incomplete spinal cord injury promotes durable functional changes within the spinal locomotor circuitry. *Journal of Neurophysiology*, *108*(1), 124–134. https://doi.org/10.1152/jn.00073.2012

Massey, J. M., Hubscher, C. H., Wagoner, M. R., Decker, J. A., Amps, J., Silver, J., & Onifer, S. M. (2006). Chondroitinase ABC digestion of the perineuronal net promotes functional collateral sprouting in the cuneate nucleus after cervical spinal cord injury. *Journal of Neuroscience*, *26*(16), 4406–4414. http://doi.org/10.1523/JNEUROSCI.5467-05.2006

Massey, James M., Amps, J., Viapiano, M. S., Matthews, R. T., Wagoner, M. R., Whitaker, C. M., … Onifer, S. M. (2008). Increased chondroitin sulfate proteoglycan expression in denervated brainstem targets following spinal cord injury creates a barrier to axonal

regeneration overcome by chondroitinase ABC and neurotrophin-3. *Experimental Neurology*, *209*(2), 426–445. https://doi.org/10.1016/j.expneurol.2007.03.029

Matosin, N., Frank, E., Engel, M., Lum, J. S., & Newell, K. A. (2014). Negativity towards negative results: a discussion of the disconnect between scientific worth and scientific culture. *Disease Models & Mechanisms*, *7*(2), 171–173. https://doi.org/10.1242/dmm.015123

May, Z., Fouad, K., Shum-Siu, A., & Magnuson, D. S. K. (2015). Challenges of animal models in SCI research: Effects of pre-injury task-specific training in adult rats before lesion. *Behavioural Brain Research*, *291*, 26–35. https://doi.org/10.1016/j.bbr.2015.04.058

Maynard, F. M., Bracken, M. B., Creasey, G., Ditunno, J. F., Donovan, W. H., Ducker, T. B., … Young, W. (1997). International Standards for Neurological and Functional Classification of Spinal Cord Injury. American Spinal Injury Association. *Spinal Cord*, *35*(5), 266–274.

Maynard, F. M., Karunas, R. S., & Waring, W. P. (1990). Epidemiology of spasticity following traumatic spinal cord injury. *Archives of Physical Medicine and Rehabilitation*, *71*(8), 566–569.

McKenzie, I. A., Biernaskie, J., Toma, J. G., Midha, R., & Miller, F. D. (2006). Skin-Derived Precursors Generate Myelinating Schwann Cells for the Injured and Dysmyelinated Nervous System. *Journal of Neuroscience*, *26*(24), 6651–6660. http://doi.org/10.1523/JNEUROSCI.1007-06.2006

McKerracher, L., David, S., Jackson, D. L., Kottis, V., Dunn, R. J., & Braun, P. E. (1994). Identification of myelin-associated glycoprotein as a major myelin-derived inhibitor of

neurite growth. *Neuron*, *13*(4), 805–811.

Meier, C., Parmantier, E., Brennan, A., Mirsky, R., & Jessen, K. R. (1999). Developing Schwann cells acquire the ability to survive without axons by establishing an autocrine circuit involving insulin-like growth factor, neurotrophin-3, and platelet-derived growth factor-BB. *The Journal of Neuroscience: The Official Journal of the Society for Neuroscience*, *19*(10), 3847–3859.

Mekler, L. B. (1975). On the problem of oncogene of tumour viruses. *Acta Virologica*, *19*(6), 501–508.

Meyer, M., Matsuoka, I., Wetmore, C., Olson, L., & Thoenen, H. (1992). Enhanced synthesis of brain-derived neurotrophic factor in the lesioned peripheral nerve: different mechanisms are responsible for the regulation of BDNF and NGF mRNA. *The Journal of Cell Biology*, *119*(1), 45–54.

Midha, R., Ramakrishna, V., Munro, C. A., Matsuyama, T., & Gorczynski, R. M. (2000). Detection of host and donor cells in sex-mismatched rat nerve allografts using RT-PCR for a Y chromosome (H-Y) marker. *Journal of the Peripheral Nervous System*, *5*(3), 140–146. https://doi.org/10.1046/j.1529-8027.2000.00017.x

Montague, S. J., Fenrich, K. K., Mayer-Macaulay, C., Maratta, R., Neuber-Hess, M. S., & Rose, P. K. (2013). Nonuniform distribution of contacts from noradrenergic and serotonergic boutons on the dendrites of cat splenius motoneurons. *Journal of Comparative Neurology*, *521*(3), 638–656. http://doi.org/10.1002/cne.23196

Morrissey, T. K., Kleitman, N., & Bunge, R. P. (1991). Isolation and functional characterization

of Schwann cells derived from adult peripheral nerve. *The Journal of Neuroscience: The Official Journal of the Society for Neuroscience*, *11*(8), 2433–2442.

Mothe, A. J., Tam, R. Y., Zahir, T., Tator, C. H., & Shoichet, M. S. (2013). Repair of the injured spinal cord by transplantation of neural stem cells in a hyaluronan-based hydrogel. *Biomaterials*, *34*(15), 3775–3783. http://doi.org/10.1016/j.biomaterials.2013.02.002

Murray, K. C., Nakae, A., Stephens, M. J., Rank, M., D'Amico, J., Harvey, P. J., … Fouad, K. (2010). Recovery of motoneuron and locomotor function after spinal cord injury depends on constitutive activity in 5-HT2C receptors. *Nature Medicine*, *16*(6), 694–700. https://doi.org/10.1038/nm.2160

Murray, M. R., & Stout, A. P. (1942). Characteristics of human Schwann cells in vitro. *The Anatomical Record*, *84*(3), 275–293. http://doi.org/10.1002/ar.1090840305

Nakao, J., Shinoda, J., Nakai, Y., Murase, S., & Uyemura, K. (1997). Apoptosis regulates the number of Schwann cells at the premyelinating stage. *Journal of Neurochemistry*, *68*(5), 1853–1862.

Namiki, K., Goodison, S., Porvasnik, S., Allan, R. W., Iczkowski, K. A., Urbanek, C., … Rosser, C. J. (2009). Persistent Exposure to Mycoplasma Induces Malignant Transformation of Human Prostate Cells. *PLoS ONE*, *4*(9), e6872. https://doi.org/10.1371/journal.pone.0006872

National Spinal Cord Injury Statistical Center. (2016). Spinal Cord Injury (SCI) Facts and Figures at a Glance. Birmingham, AL: University of Alabama at Birmingham.

Neuralstem Inc. (2013, 2017). Safety Study of Human Spinal Cord-derived Neural Stem Cell Transplantation for the Treatment of Chronic SCI (SCI). Retrieved from In: Clinicaltrials.gov. Bethesda (MD): National Library of Medicine (US). Available from: https://clinicaltrials.gov/ct2/show/NCT01772810?term=NEURALSTEM+INC&rank=5. NLM identifier: NCT01772810.

Neuralstem Inc. (2016). Neuralstem Cell Therapy for Spinal Cord Injury. Retrieved from http://www.neuralstem.com/cell-therapy-for-sci

Nielsen, J. B., Crone, C., & Hultborn, H. (2007). The spinal pathophysiology of spasticity ? from a basic science point of view. *Acta Physiologica*, *189*(2), 171–180. https://doi.org/10.1111/j.1748-1716.2006.01652.x

Oudega, M., Bradbury, E. J., & Ramer, M. S. (2012). Combination therapies. In *Handbook of Clinical Neurology* (Vol. 109, pp. 617–636). Elsevier. https://doi.org/10.1016/B978-0-444-52137-8.00038-3

Oudega, Martin, & Xu, X.-M. (2006). Schwann cell transplantation for repair of the adult spinal cord. *Journal of Neurotrauma*, *23*(3–4), 453–467. https://doi.org/10.1089/neu.2006.23.453

Oyinbo, C. A. (2011). Secondary injury mechanisms in traumatic spinal cord injury: a nugget of this multiply cascade. *Acta Neurobiologiae Experimentalis*, *71*(2), 281–299.

Pakulska, M. M., Elliott Donaghue, I., Obermeyer, J. M., Tuladhar, A., McLaughlin, C. K., Shendruk, T. N., & Shoichet, M. S. (2016). Encapsulation-free controlled release: Electrostatic adsorption eliminates the need for protein encapsulation in PLGA

nanoparticles. *Science Advances*, *2*(5), e1600519–e1600519. https://doi.org/10.1126/sciadv.1600519

Papini, M. R., & Dudley, R. T. (1997). Consequences of surprising reward omissions. *Review of General Psychology*, *1*(2), 175–197. http://doi.org/10.1037/1089-2680.1.2.175

Park, E., Velumian, A. A., & Fehlings, M. G. (2004). The Role of Excitotoxicity in Secondary Mechanisms of Spinal Cord Injury: A Review with an Emphasis on the Implications for White Matter Degeneration. *Journal of Neurotrauma*, *21*(6), 754–774. https://doi.org/10.1089/0897715041269641

Park, K. K., Liu, K., Hu, Y., Smith, P. D., Wang, C., Cai, B., … He, Z. (2008). Promoting Axon Regeneration in the Adult CNS by Modulation of the PTEN/mTOR Pathway. *Science*, *322*(5903), 963–966. http://doi.org/10.1126/science.1161566

Pasterkamp, R. J., Giger, R. J., Ruitenberg, M.-J., Holtmaat, A. J. G. D., De Wit, J., De Winter, F., & Verhaagen, J. (1999). Expression of the Gene Encoding the Chemorepellent Semaphorin III Is Induced in the Fibroblast Component of Neural Scar Tissue Formed Following Injuries of Adult But Not Neonatal CNS. *Molecular and Cellular Neuroscience*, *13*(2), 143–166. https://doi.org/10.1006/mcne.1999.0738

Pastor, D., Viso-León, M. C., Jones, J., Jaramillo-Merchán, J., Toledo-Aral, J. J., Moraleda, J. M., & Martínez, S. (2012). Comparative Effects between Bone Marrow and Mesenchymal Stem Cell Transplantation in GDNF Expression and Motor Function Recovery in a Motorneuron Degenerative Mouse Model. *Stem Cell Reviews and Reports*, *8*(2), 445–458. https://doi.org/10.1007/s12015-011-9295-x

Paxinos, G. & Watson, C. (1998) *The Rat Brain in Stereotaxic Coordinates*. San Diego, CA: Academic Press.

Pearse, D. D., Pereira, F. C., Marcillo, A. E., Bates, M. L., Berrocal, Y. A., Filbin, M. T., & Bunge, M. B. (2004). cAMP and Schwann cells promote axonal growth and functional recovery after spinal cord injury. *Nature Medicine*, *10*(6), 610–616. https://doi.org/10.1038/nm1056

Pearse, D. D., Sanchez, A. R., Pereira, F. C., Andrade, C. M., Puzis, R., Pressman, Y., … Bunge, M. B. (2007). Transplantation of Schwann cells and/or olfactory ensheathing glia into the contused spinal cord: Survival, migration, axon association, and functional recovery. *Glia*, *55*(9), 976–1000. https://doi.org/10.1002/glia.20490

Peters, A., Schweiger, U., Pellerin, L., Hubold, C., Oltmanns, K. M., Conrad, M., … Fehm, H. L. (2004). The selfish brain: competition for energy resources. *Neuroscience & Biobehavioral Reviews*, *28*(2), 143–180. https://doi.org/10.1016/j.neubiorev.2004.03.002

Pointner, H., & Flegel, U. (1975). [Treatment of exocrine pancreatic insufficiency with fungal lipase (author's transl)]. *Arzneimittel-Forschung*, *25*(11), 1833–1835.

Popovich, P. G., Tovar, C. A., Wei, P., Fisher, L., Jakeman, L. B., & Basso, D. M. (2012). A reassessment of a classic neuroprotective combination therapy for spinal cord injured rats: LPS/pregnenolone/indomethacin. *Experimental Neurology*, *233*(2), 677–685. https://doi.org/10.1016/j.expneurol.2011.11.045

Popovich, P.G., Wei, P., Stokes, B.T. (1997) Cellular inflammatory response after spinal cord injury in Sprague-Dawley and Lewis rats. *Journal of Comparative Neurology 377*:443–

464. doi: 10.1002/(SICI)1096-9861(19970120)377:3<443::AID-CNE10>3.0.CO;2-S

Quevedo, J., Eguibar, J. R., Jiménez, I., Schmidt, R. F., & Rudomin, P. (1993). Primary afferent depolarization of muscle afferents elicited by stimulation of joint afferents in cats with intact neuraxis and during reversible spinalization. *Journal of Neurophysiology*, *70*(5), 1899–1910.

Rahmani, W., Abbasi, S., Hagner, A., Raharjo, E., Kumar, R., Hotta, A., … Biernaskie, J. (2014). Hair follicle dermal stem cells regenerate the dermal sheath, repopulate the dermal papilla, and modulate hair type. *Developmental Cell*, *31*(5), 543–558. http://doi.org/10.1016/j.devcel.2014.10.022

Raineteau, O., & Schwab, M. E. (2001). Plasticity of motor systems after incomplete spinal cord injury. *Nature Reviews. Neuroscience*, *2*(4), 263–273. http://doi.org/10.1038/35067570

Reed, W. R., Shum-Siu, A., & Magnuson, D. S. K. (2008). Reticulospinal pathways in the ventrolateral funiculus with terminations in the cervical and lumbar enlargements of the adult rat spinal cord. *Neuroscience*, *151*(2), 505-517. doi:10.1016/j.neuroscience.2007.10.025

Richardson, P. M., McGuinness, U. M., & Aguayo, A. J. (1980). Axons from CNS neurones regenerate into PNS grafts. *Nature*, *284*(5753), 264–265. https://doi.org/10.1038/284264a0

Richner, M., Ulrichsen, M., Elmegaard, S. L., Dieu, R., Pallesen, L. T., & Vaegter, C. B. (2014). Peripheral nerve injury modulates neurotrophin signaling in the peripheral and central nervous system. *Molecular Neurobiology*, *50*(3), 945–970.

http://doi.org/10.1007/s12035-014-8706-9

Ritfeld, G., & Oudega, M. (2014). Bone Marrow-derived Mesenchymal Stem Cell Transplant Survival in the Injured Rodent Spinal Cord. *Journal of Bone Marrow Research*, *02*(02). https://doi.org/10.4172/2329-8820.1000146

Rodriguez, F. J., Folpe, A. L., Giannini, C., & Perry, A. (2012). Pathology of peripheral nerve sheath tumors: diagnostic overview and update on selected diagnostic problems. *Acta Neuropathologica*, *123*(3), 295–319. https://doi.org/10.1007/s00401-012-0954-z

Rolls, A., Shechter, R., London, A., Segev, Y., Jacob-Hirsch, J., Amariglio, N., … Schwartz, M. (2008). Two Faces of Chondroitin Sulfate Proteoglycan in Spinal Cord Repair: A Role in Microglia/Macrophage Activation. *PLoS Medicine*, *5*(8), e171. https://doi.org/10.1371/journal.pmed.0050171

Romero, M. I., Rangappa, N., Li, L., Lightfoot, E., Garry, M. G., & Smith, G. M. (2000). Extensive sprouting of sensory afferents and hyperalgesia induced by conditional expression of nerve growth factor in the adult spinal cord. *The Journal of Neuroscience: The Official Journal of the Society for Neuroscience*, *20*(12), 4435–4445.

Rose, P. K., Ely, S., Norkum, V., & Neuber-Hess, M. (1999). Projections from the lateral vestibular nucleus to the upper cervical spinal cord of the cat: A correlative light and electron microscopic study of axon terminals stained with PHA-L. *The Journal of Comparative Neurology*, *410*(4), 571–585.

Rossignol, S., Drew, T., Brustein, E., & Jiang, W. (1999). Locomotor performance and adaptation after partial or complete spinal cord lesions in the cat. *Progress in Brain*

Research, *123*, 349–365.

Safety of Autologous Human Schwann Cells (ahSC) in Subjects With Subacute SCI (Identification No. NCT01739023). (2012). Retrieved from https://clinicaltrials.gov/ct2/show/NCT01739023?term=NCT01739023&rank=1

Sahenk, Z., Oblinger, J., & Edwards, C. (2008). Neurotrophin-3 deficient Schwann cells impair nerve regeneration. *Experimental Neurology*, *212*(2), 552–556. http://doi.org/10.1016/j.expneurol.2008.04.015

Sawada, M., Kato, K., Kunieda, T., Mikuni, N., Miyamoto, S., Onoe, H., … Nishimura, Y. (2015). Function of the nucleus accumbens in motor control during recovery after spinal cord injury. *Science*, *350*(6256), 98–101. https://doi.org/10.1126/science.aab3825

Schaller, E., Lassner, F., Becker, M., Walter, G., & Berger, A. (1991). Regeneration of Autologous and Allogenic Nerve Grafts in a Rat Genetic Model: Preliminary Report. *Journal of Reconstructive Microsurgery*, *7*(01), 9–12. https://doi.org/10.1055/s-2007-1006757

Schnell, L., Schneider, R., Kolbeck, R., Barde, Y. A., & Schwab, M. E. (1994). Neurotrophin-3 enhances sprouting of corticospinal tract during development and after adult spinal cord lesion. *Nature*, *367*(6459), 170–173. https://doi.org/10.1038/367170a0

Schnell, L., & Schwab, M. E. (1993). Sprouting and regeneration of lesioned corticospinal tract fibres in the adult rat spinal cord. *The European Journal of Neuroscience*, *5*(9), 1156–1171.

Schnell, Lisa, & Schwab, M. E. (1990). Axonal regeneration in the rat spinal cord produced by an antibody against myelin-associated neurite growth inhibitors. *Nature*, *343*(6255), 269–272. https://doi.org/10.1038/343269a0

Schucht, P., Raineteau, O., Schwab, M. E., & Fouad, K. (2002). Anatomical correlates of locomotor recovery following dorsal and ventral lesions of the rat spinal cord. *Experimental Neurology*, *176*(1), 143–153.

Schupper, N., Rabin, Y., & Rosenbluh, M. (2008). Multiple Stages in the Aging of a Physical Polymer Gel. *Macromolecules*, *41*(11), 3983–3994. http://doi.org/10.1021/ma702613j

Seif, G. I., Nomura, H., & Tator, C. H. (2007). Retrograde axonal degeneration "dieback" in the corticospinal tract after transection injury of the rat spinal cord: a confocal microscopy study. *Journal of Neurotrauma*, *24*(9), 1513–1528. https://doi.org/10.1089/neu.2007.0323

Sharp, K. G., Flanagan, L. A., Yee, K. M., & Steward, O. (2012). A re-assessment of a combinatorial treatment involving Schwann cell transplants and elevation of cyclic AMP on recovery of motor function following thoracic spinal cord injury in rats. *Experimental Neurology*, *233*(2), 625–644. http://doi.org/10.1016/j.expneurol.2010.12.020

Sharp, K. G., Yee, K. M., & Steward, O. (2014). A re-assessment of long distance growth and connectivity of neural stem cells after severe spinal cord injury. *Experimental Neurology*, *257*, 186–204. https://doi.org/10.1016/j.expneurol.2014.04.008

Shechter, R., Raposo, C., London, A., Sagi, I., & Schwartz, M. (2011). The Glial Scar-Monocyte Interplay: A Pivotal Resolution Phase in Spinal Cord Repair. *PLoS ONE*, *6*(12), e27969. https://doi.org/10.1371/journal.pone.0027969

Sherrington, C. S. (1910). Flexion-reflex of the limb, crossed extension-reflex, and reflex stepping and standing. *The Journal of Physiology*, *40*(1–2), 28–121.

Sherman, L. S., Rizvi, T. A., Karyala, S., & Ratner, N. (2000). CD44 enhances neuregulin signaling by Schwann cells. *The Journal of Cell Biology*, *150*(5), 1071–1084.

Shuman, S. L., Bresnahan, J. C., & Beattie, M. S. (1997). Apoptosis of microglia and oligodendrocytes after spinal cord contusion in rats. *Journal of Neuroscience Research*, *50*(5), 798–808. https://doi.org/10.1002/(SICI)1097-4547(19971201)50:5<798::AID-JNR16>3.0.CO;2-Y

Siddall, P. J., & Loeser, J. D. (2001). Pain following spinal cord injury. *Spinal Cord*, *39*(2), 63–73.

Siebert, J. R., Conta Steencken, A., & Osterhout, D. J. (2014). Chondroitin Sulfate Proteoglycans in the Nervous System: Inhibitors to Repair. *BioMed Research International*, *2014*, 1–15. https://doi.org/10.1155/2014/845323

Siegel, J. (1979). Behavioral functions of the reticular formation. *Brain Research Reviews*, *1*(1), 69–105. https://doi.org/10.1016/0165-0173(79)90017-1

Silva, N. A., Sousa, N., Reis, R. L., & Salgado, A. J. (2014). From basics to clinical: A comprehensive review on spinal cord injury. *Progress in Neurobiology*, *114*, 25–57. doi:10.1016/j.pneurobio.2013.11.002

Silver, R. A. (2003). High-Probability Uniquantal Transmission at Excitatory Synapses in Barrel Cortex. *Science*, *302*(5652), 1981–1984. http://doi.org/10.1126/science.1087160

Silverman, J. (2008). Protocol review: collaborative studies and animal reuse. *Lab Animal*, *37*(2), 61–63.

Simpson, E. (1982). The role of H-Y as a minor transplantation antigen. *Immunology Today*, *3*(4), 97–106. https://doi.org/10.1016/S0167-5699(82)80025-X

Singh, A., Balasubramanian, S., Murray, M., Lemay, M., & Houle, J. (2011). Role of Spared Pathways in Locomotor Recovery after Body-Weight-Supported Treadmill Training in Contused Rats. *Journal of Neurotrauma*, *28*(12), 2405–2416. https://doi.org/10.1089/neu.2010.1660

Sist, B., Fouad, K., & Winship, I. R. (2014). Plasticity beyond peri-infarct cortex: Spinal up regulation of structural plasticity, neurotrophins, and inflammatory cytokines during recovery from cortical stroke. *Experimental Neurology*, *252*, 47–56. https://doi.org/10.1016/j.expneurol.2013.11.019

Smith, R. R., Brown, E. H., Shum-Siu, A., Whelan, A., Burke, D. A., Benton, R. L., & Magnuson, D. S. K. (2009). Swim training initiated acutely after spinal cord injury is ineffective and induces extravasation in and around the epicenter. *Journal of Neurotrauma*, *26*(7), 1017–1027. doi:10.1089/neu.2008-0829

Smith, R. R., Burke, D. A., Baldini, A. D., Shum-Siu, A., Baltzley, R., Bunger, M., & Magnuson, D. S. K. (2006). The Louisville Swim Scale: A Novel Assessment of Hindlimb Function following Spinal Cord Injury in Adult Rats. *Journal of Neurotrauma*, *23*(11), 1654–1670. doi:10.1089/neu.2006.23.1654

Smith, R. R., Shum-Siu, A., Baltzley, R., Bunger, M., Baldini, A., Burke, D. A., & Magnuson,

D. S. K. (2006). Effects of Swimming on Functional Recovery after Incomplete Spinal Cord Injury in Rats. *Journal of Neurotrauma*, *23*(6), 908–919. https://doi.org/10.1089/neu.2006.23.908

Sparling, J. S., Bretzner, F., Biernaskie, J., Assinck, P., Jiang, Y., Arisato, H., … Tetzlaff, W. (2015). Schwann Cells Generated from Neonatal Skin-Derived Precursors or Neonatal Peripheral Nerve Improve Functional Recovery after Acute Transplantation into the Partially Injured Cervical Spinal Cord of the Rat. *Journal of Neuroscience*, *35*(17), 6714–6730. http://doi.org/10.1523/JNEUROSCI.1070-14.2015

Spencer, T., & Filbin, M. T. (2004). A role for cAMP in regeneration of the adult mammalian CNS. *Journal of Anatomy*, *204*(1), 49–55. https://doi.org/10.1111/j.1469-7580.2004.00259.x

Srivastava, A. K., Kadayakkara, D. K., Bar-Shir, A., Gilad, A. A., McMahon, M. T., & Bulte, J. W. M. (2015). Advances in using MRI probes and sensors for in vivo cell tracking as applied to regenerative medicine. *Disease Models & Mechanisms*, *8*(4), 323–336. https://doi.org/10.1242/dmm.018499

Stanley, T. H. (1988). Species differences. *British Journal of Anaesthesia*, *60*(8 Suppl 1), 116S–118S.

Steeves, J. D., & Jordan, L. M. (1980). Localization of a descending pathway in the spinal cord which is necessary for controlled treadmill locomotion. *Neuroscience Letters*, *20*(3), 283–288.

Stephan, F. K., & Zucker, I. (1972). Circadian rhythms in drinking behavior and locomotor

activity of rats are eliminated by hypothalamic lesions. *Proceedings of the National Academy of Sciences of the United States of America*, *69*(6), 1583–1586.

Steward, O., Sharp, K. G., & Matsudaira Yee, K. (2014). Long-Distance Migration and Colonization of Transplanted Neural Stem Cells. *Cell*, *156*(3), 385–387. https://doi.org/10.1016/j.cell.2014.01.017

Steward, O., Sharp, K., Yee, K. M., & Hofstadter, M. (2008). A re-assessment of the effects of a Nogo-66 receptor antagonist on regenerative growth of axons and locomotor recovery after spinal cord injury in mice. *Experimental Neurology*, *209*(2), 446–468. https://doi.org/10.1016/j.expneurol.2007.12.010

Suñé, P., Suñé, J. M., & Montoro, J. B. (2013). Positive Outcomes Influence the Rate and Time to Publication, but Not the Impact Factor of Publications of Clinical Trial Results. *PLoS ONE*, *8*(1), e54583. https://doi.org/10.1371/journal.pone.0054583

Swiech, L., Perycz, M., Malik, A., & Jaworski, J. (2008). Role of mTOR in physiology and pathology of the nervous system. *Biochimica et Biophysica Acta (BBA) - Proteins and Proteomics*, *1784*(1), 116–132. https://doi.org/10.1016/j.bbapap.2007.08.015

Syroid, D. E., Maycox, P. R., Burrola, P. G., Liu, N., Wen, D., Lee, K. F., … Kilpatrick, T. J. (1996). Cell death in the Schwann cell lineage and its regulation by neuregulin. *Proceedings of the National Academy of Sciences of the United States of America*, *93*(17), 9229–9234.

Tai, C., Miscik, C. L., Ungerer, T. D., Roppolo, J. R., & de Groat, W. C. (2006). Suppression of bladder reflex activity in chronic spinal cord injured cats by activation of serotonin 5-

HT1A receptors. *Experimental Neurology*, *199*(2), 427–437. http://doi.org/10.1016/j.expneurol.2006.01.007

Takei, N., & Nawa, H. (2014). mTOR signaling and its roles in normal and abnormal brain development. *Frontiers in Molecular Neuroscience*, *7*. https://doi.org/10.3389/fnmol.2014.00028

Tam, R. Y., Cooke, M. J., & Shoichet, M. S. (2012). A covalently modified hydrogel blend of hyaluronan–methyl cellulose with peptides and growth factors influences neural stem/progenitor cell fate. *Journal of Materials Chemistry*, *22*(37), 19402. http://doi.org/10.1039/c2jm33680d

Tator, C. H., & Fehlings, M. G. (1991). Review of the secondary injury theory of acute spinal cord trauma with emphasis on vascular mechanisms. *Journal of Neurosurgery*, *75*(1), 15–26. https://doi.org/10.3171/jns.1991.75.1.0015

Tecza, K., Pamula-Pilat, J., Lanuszewska, J., & Grzybowska, E. (2016). Genetic polymorphisms and response to 5-fluorouracil, doxorubicin and cyclophosphamide chemotherapy in breast cancer patients. *Oncotarget*. https://doi.org/10.18632/oncotarget.11053

Tetzlaff, W., Okon, E. B., Karimi-Abdolrezaee, S., Hill, C. E., Sparling, J. S., Plemel, J. R., … Kwon, B. K. (2011). A systematic review of cellular transplantation therapies for spinal cord injury. *Journal of Neurotrauma*, *28*(8), 1611–1682. https://doi.org/10.1089/neu.2009.1177

The Safety of ahSC in Chronic SCI With Rehabilitation (Identification No. NCT02354625. (2015). Retrieved from

https://clinicaltrials.gov/ct2/show/NCT02354625?term=NCT02354625&rank=1

Thirabanjasak, D., Tantiwongse, K., & Thorner, P. S. (2010). Angiomyeloproliferative Lesions Following Autologous Stem Cell Therapy. *Journal of the American Society of Nephrology*, *21*(7), 1218–1222. https://doi.org/10.1681/ASN.2009111156

Thomson, A. W. (1992). The effects of cyclosporin A on non-T cell components of the immune system. *Journal of Autoimmunity*, *5 Suppl A*, 167–176.

Thor, K. B., Roppolo, J. R., & deGroat, W. C. (1983). Naloxone induced micturition in unanesthetized paraplegic cats. *The Journal of Urology*, *129*(1), 202–205.

Thuret, S., Moon, L. D. F., & Gage, F. H. (2006). Therapeutic interventions after spinal cord injury. *Nature Reviews Neuroscience*, *7*(8), 628–643. https://doi.org/10.1038/nrn1955

Tillakaratne, N. J., Mouria, M., Ziv, N. B., Roy, R. R., Edgerton, V. R., & Tobin, A. J. (2000). Increased expression of glutamate decarboxylase (GAD(67)) in feline lumbar spinal cord after complete thoracic spinal cord transection. *Journal of Neuroscience Research*, *60*(2), 219–230. http://doi.org/10.1002/(SICI)1097-4547(20000415)60:2<219::AID-JNR11>3.0.CO;2-F

Tohyama, K., & Ide, C. (1984). The Localization of Laminin and Fibronectin on the Schwann Cell Basal Lamina. *Archives of Histology and Cytology*, *47*(5), 519–532. https://doi.org/10.1679/aohc.47.519

Tolstoy, L. (1894). *The Kingdom of God Is Within You*. Germany.

Toma, J. G., Akhavan, M., Fernandes, K. J., Barnabé-Heider, F., Sadikot, A., Kaplan, D. R., &

Miller, F. D. (2001). Isolation of multipotent adult stem cells from the dermis of mammalian skin. *Nature Cell Biology*, *3*(9), 778–784. http://doi.org/10.1038/ncb0901-778

Toma, J. G., McKenzie, I. A., Bagli, D., & Miller, F. D. (2005). Isolation and characterization of multipotent skin-derived precursors from human skin. *Stem Cells (Dayton, Ohio)*, *23*(6), 727–737. http://doi.org/10.1634/stemcells.2004-0134

Torres-Espín, A., Redondo-Castro, E., Hernandez, J., & Navarro, X. (2015). Immunosuppression of Allogenic Mesenchymal Stem Cells Transplantation after Spinal Cord Injury Improves Graft Survival and Beneficial Outcomes. *Journal of Neurotrauma*, *32*(6), 367–380. https://doi.org/10.1089/neu.2014.3562

Totoiu, M. O., & Keirstead, H. S. (2005). Spinal cord injury is accompanied by chronic progressive demyelination. *The Journal of Comparative Neurology*, *486*(4), 373–383. https://doi.org/10.1002/cne.20517

Tsai, E. C., & Tator, C. H. (2005). Neuroprotection and regeneration strategies for spinal cord repair. *Current Pharmaceutical Design*, *11*(10), 1211–1222.

Tsai, S., Wear, D. J., Shih, J. W., & Lo, S. C. (1995). Mycoplasmas and oncogenesis: persistent infection and multistage malignant transformation. *Proceedings of the National Academy of Sciences of the United States of America*, *92*(22), 10197–10201.

Turnbull, I. M. (1971). Microvasculature of the human spinal cord. *Journal of Neurosurgery*, *35*(2), 141–147. https://doi.org/10.3171/jns.1971.35.2.0141

Turner, L., & Knoepfler, P. (2016). Selling Stem Cells in the USA: Assessing the Direct-to-Consumer Industry. *Cell Stem Cell*, *19*(2), 154–157. https://doi.org/10.1016/j.stem.2016.06.007

Tuszynski, M. H., & Steward, O. (2012). Concepts and Methods for the Study of Axonal Regeneration in the CNS. *Neuron*, *74*(5), 777–791. https://doi.org/10.1016/j.neuron.2012.05.006

U.S. National Library of Medicine, 8600 Rockville Pike, Bethesda, MD 20894. (2017, April 2). Clinical trials.gov: A service of the U.S. National Institutes of Health. Retrieved from https://clinicaltrials.gov/ct2/home

van den Berg, M. E. L., Castellote, J. M., Mahillo-Fernandez, I., & de Pedro-Cuesta, J. (2010). Incidence of Spinal Cord Injury Worldwide: A Systematic Review. *Neuroepidemiology*, *34*(3), 184–192. https://doi.org/10.1159/000279335

van den Brand, R., Heutschi, J., Barraud, Q., DiGiovanna, J., Bartholdi, K., Huerlimann, M., … Courtine, G. (2012). Restoring voluntary control of locomotion after paralyzing spinal cord injury. *Science (New York, N.Y.)*, *336*(6085), 1182–1185. https://doi.org/10.1126/science.1217416

Vargas, M. E., & Barres, B. A. (2007). Why is Wallerian degeneration in the CNS so slow? *Annual Review of Neuroscience*, *30*, 153–179. https://doi.org/10.1146/annurev.neuro.30.051606.094354

Varró, J., Radovits, B., & Révész, I. (1977). [Pathological sagittal shifting of vertebral bodies]. *Magyar Traumatologia, Orthopaedia Es Helyreallito Sebeszet*, *20*(2), 94–99.

Vavrek, R., Girgis, J., Tetzlaff, W., Hiebert, G. W., & Fouad, K. (2006). BDNF promotes connections of corticospinal neurons onto spared descending interneurons in spinal cord injured rats. *Brain: A Journal of Neurology*, *129*(Pt 6), 1534–1545. https://doi.org/10.1093/brain/awl087

Vavrek, Romana, Pearse, D. D., & Fouad, K. (2007). Neuronal populations capable of regeneration following a combined treatment in rats with spinal cord transection. *Journal of Neurotrauma*, *24*(10), 1667–1673. https://doi.org/10.1089/neu.2007.0290

Vercruysse, K. P., & Prestwich, G. D. (1998). Hyaluronate derivatives in drug delivery. *Critical Reviews in Therapeutic Drug Carrier Systems*, *15*(5), 513–555.

Vroemen, M., & Weidner, N. (2003). Purification of Schwann cells by selection of p75 low affinity nerve growth factor receptor expressing cells from adult peripheral nerve. *Journal of Neuroscience Methods*, *124*(2), 135–143.

Wahl, S., Barth, H., Ciossek, T., Aktories, K., & Mueller, B. K. (2000). Ephrin-A5 Induces Collapse of Growth Cones by Activating Rho and Rho Kinase, *149*(2), 263–270.

Wang, K. C., Koprivica, V., Kim, J. A., Sivasankaran, R., Guo, Y., Neve, R. L., & He, Z. (2002). Oligodendrocyte-myelin glycoprotein is a Nogo receptor ligand that inhibits neurite outgrowth. *Nature*, *417*(6892), 941–944. https://doi.org/10.1038/nature00867

Wang, Z., Reynolds, A., Kirry, A., Nienhaus, C., & Blackmore, M. G. (2015). Overexpression of Sox11 Promotes Corticospinal Tract Regeneration after Spinal Injury While Interfering with Functional Recovery. *Journal of Neuroscience*, *35*(7), 3139–3145. https://doi.org/10.1523/JNEUROSCI.2832-14.2015

Wang, R. Y., Yang, Y. R., & Yu, S. M. (2001). Protective effects of treadmill training on infarction in rats. *Brain Research*, *922*(1), 140–143.

Watson, C., Paxinos, G., Kayalioglu, G., & Heise, C. (2009). Atlas of the Rat Spinal Cord. In *The Spinal Cord* (pp. 238–306). Elsevier. https://doi.org/10.1016/B978-0-12-374247-6.50019-5

Weidner, N., Ner, A., Salimi, N., & Tuszynski, M. H. (2001). Spontaneous corticospinal axonal plasticity and functional recovery after adult central nervous system injury. *Proceedings of the National Academy of Sciences*, *98*(6), 3513–3518. https://doi.org/10.1073/pnas.051626798

Weishaupt, N., Blesch, A., & Fouad, K. (2012). BDNF: The career of a multifaceted neurotrophin in spinal cord injury. *Experimental Neurology*, *238*(2), 254–264. https://doi.org/10.1016/j.expneurol.2012.09.001

Weishaupt, N., Li, S., Di Pardo, A., Sipione, S., & Fouad, K. (2013). Synergistic effects of BDNF and rehabilitative training on recovery after cervical spinal cord injury. *Behavioural Brain Research*, *239*, 31–42. https://doi.org/10.1016/j.bbr.2012.10.047

Wenjin, W., Wenchao, L., Hao, Z., Feng, L., Yan, W., Wodong, S., … Wenlong, D. (2011). Electrical Stimulation Promotes BDNF Expression in Spinal Cord Neurons Through Ca2+- and Erk-Dependent Signaling Pathways. *Cellular and Molecular Neurobiology*, *31*(3), 459–467. https://doi.org/10.1007/s10571-010-9639-0

Westgren, N., & Levi, R. (1998). Quality of life and traumatic spinal cord injury. *Archives of Physical Medicine and Rehabilitation*, *79*(11), 1433–1439.

https://doi.org/10.1016/S0003-9993(98)90240-4

Whishaw, Ian Q., Gorny, B., Foroud, A., & Kleim, J. A. (2003). Long-Evans and Sprague-Dawley rats have similar skilled reaching success and limb representations in motor cortex but different movements: some cautionary insights into the selection of rat strains for neurobiological motor research. *Behavioural Brain Research*, *145*(1–2), 221–232.

Whishaw, I. Q., Gorny, B., & Sarna, J. (1998). Paw and limb use in skilled and spontaneous reaching after pyramidal tract, red nucleus and combined lesions in the rat: behavioral and anatomical dissociations. *Behavioural Brain Research*, *93*(1–2), 167–183.

Whiteneck, G., Gassaway, J., Dijkers, M., Backus, D., Charlifue, S., Chen, D., … Smout, R. J. (2011). Inpatient treatment time across disciplines in spinal cord injury rehabilitation. *The Journal of Spinal Cord Medicine*, *34*(2), 133–148. https://doi.org/10.1179/107902611X12971826988011

Williams, R. R., Henao, M., Pearse, D. D., & Bunge, M. B. (2015). Permissive Schwann cell graft/spinal cord interfaces for axon regeneration. *Cell Transplantation*, *24*(1), 115–131. http://doi.org/10.3727/096368913X674657

Williams, R. R., Pearse, D. D., Tresco, P. A., & Bunge, M. B. (2012). The assessment of adeno-associated vectors as potential intrinsic treatments for brainstem axon regeneration: Assessing AAV vectors for axonal growth. *The Journal of Gene Medicine*, *14*(1), 20–34. http://doi.org/10.1002/jgm.1628

Wippold, F. J., Lubner, M., Perrin, R. J., Lämmle, M., & Perry, A. (2007). Neuropathology for the neuroradiologist: Antoni A and Antoni B tissue patterns. American Journal of

Neuroradiology, 28, 1633-1638. http://doi.org/10.3174/ajnr.A0682

Xu, X. M., Guénard, V., Kleitman, N., Aebischer, P., & Bunge, M. B. (1995). A Combination of BDNF and NT-3 Promotes Supraspinal Axonal Regeneration into Schwann Cell Grafts in Adult Rat Thoracic Spinal Cord. *Experimental Neurology*, *134*(2), 261–272. https://doi.org/10.1006/exnr.1995.1056

Xu, X.-M., & Onifer, S. M. (2009). Transplantation-mediated strategies to promote axonal regeneration following spinal cord injury. *Respiratory Physiology & Neurobiology*, *169*(2), 171–182. http://doi.org/10.1016/j.resp.2009.07.016

Yajima, Y., Narita, M., Usui, A., Kaneko, C., Miyatake, M., Narita, M., … Suzuki, T. (2005). Direct evidence for the involvement of brain-derived neurotrophic factor in the development of a neuropathic pain-like state in mice. *Journal of Neurochemistry*, *93*(3), 584–594. https://doi.org/10.1111/j.1471-4159.2005.03045.x

Yick, L. W., Wu, W., So, K. F., Yip, H. K., & Shum, D. K. (2000). Chondroitinase ABC promotes axonal regeneration of Clarke's neurons after spinal cord injury. *Neuroreport*, *11*(5), 1063–1067.

Ying, Zhe, Roy, R. R., Edgerton, V. R., & Gómez-Pinilla, F. (2003). Voluntary exercise increases neurotrophin-3 and its receptor TrkC in the spinal cord. *Brain Research*, *987*(1), 93–99.

Ying, Zhe, Roy, R. R., Edgerton, V. R., & Gómez-Pinilla, F. (2005). Exercise restores levels of neurotrophins and synaptic plasticity following spinal cord injury. *Experimental Neurology*, *193*(2), 411–419. https://doi.org/10.1016/j.expneurol.2005.01.015

Ying, Z., Roy, R. R., Zhong, H., Zdunowski, S., Edgerton, V. R., & Gomez-Pinilla, F. (2008). BDNF–exercise interactions in the recovery of symmetrical stepping after a cervical hemisection in rats. *Neuroscience*, *155*(4), 1070–1078. https://doi.org/10.1016/j.neuroscience.2008.06.057

Yu, W.-M. (2005). Schwann Cell-Specific Ablation of Laminin 1 Causes Apoptosis and Prevents Proliferation. *Journal of Neuroscience*, *25*(18), 4463–4472. http://doi.org/10.1523/JNEUROSCI.5032-04.2005

Yu, W.-M., Chen, Z.-L., North, A. J., & Strickland, S. (2009). Laminin is required for Schwann cell morphogenesis. *Journal of Cell Science*, *122*(7), 929–936. http://doi.org/10.1242/jcs.033928

Zhang, L., Kaneko, S., Kikuchi, K., Sano, A., Maeda, M., Kishino, A., … Nakamura, M. (2014). Rewiring of regenerated axons by combining treadmill training with semaphorin3A inhibition. *Molecular Brain*, *7*(1), 14. https://doi.org/10.1186/1756-6606-7-14

Zhang, Y., Granholm, A.-C., Huh, K., Shan, L., Diaz-Ruiz, O., Malik, N., … Backman, C. M. (2012). PTEN deletion enhances survival, neurite outgrowth and function of dopamine neuron grafts to MitoPark mice. *Brain*, *135*(9), 2736–2749. https://doi.org/10.1093/brain/aws196

Zheng, J., Kontoveros, D., Lin, F., Hua, G., Reneker, D. H., Becker, M. L., & Willits, R. K. (2015). Enhanced Schwann cell attachment and alignment using one-pot “dual click” GRGDS and YIGSR derivatized nanofibers. *Biomacromolecules*, *16*(1), 357–363. https://doi.org/10.1021/bm501552t

Zuo, J., Neubauer, D., Dyess, K., Ferguson, T. A., & Muir, D. (1998). Degradation of Chondroitin Sulfate Proteoglycan Enhances the Neurite-Promoting Potential of Spinal Cord Tissue. *Experimental Neurology*, *154*(2), 654–662. https://doi.org/10.1006/exnr.1998.6951

6. Chapter Figures

6.1 Chapter 1

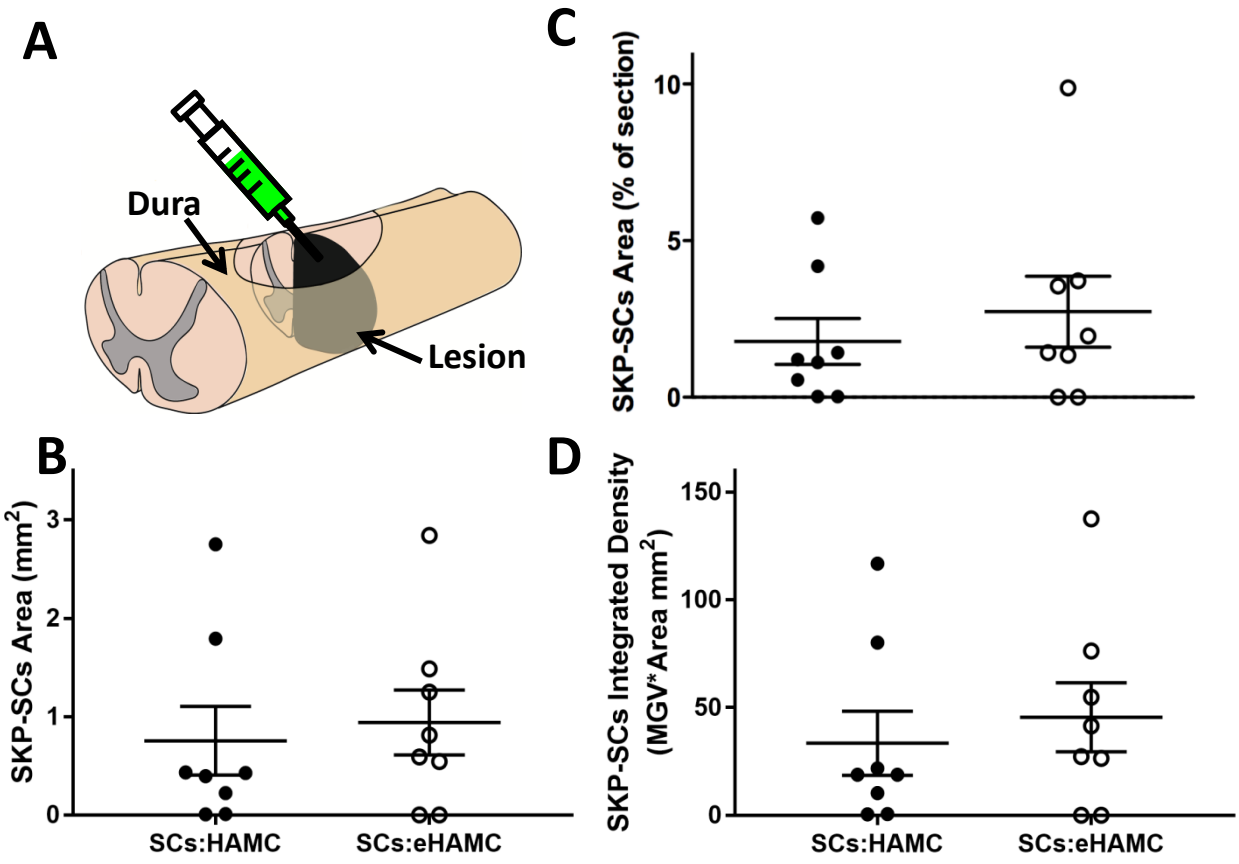

Figure 1. Adult skin-derived precursor Schwann cells (SKP-SCs) survive in the injured rat spinal cord 8 weeks post-grafting. (A) SKP-SCs expressing green fluorescent protein (GFP^+) were injected into the cavity of a thoracic SCI through an opening in the meninges. (B) Points on the graph represent the area occupied by SKP-SCs in individual rats transplanted with hyaluronan/methylcellulose (HAMC) or hyaluronan methylcellulose modified with laminin and fibronectin peptide sequences (eHAMC). (C) In this graph, the area occupied by SKP-SCs in every rat is shown as a percentage of the total area analyzed. (D) Shown here is the signal intensity representing the density of SKP-SCs in every transplanted rat. Error bars represent the SEM.

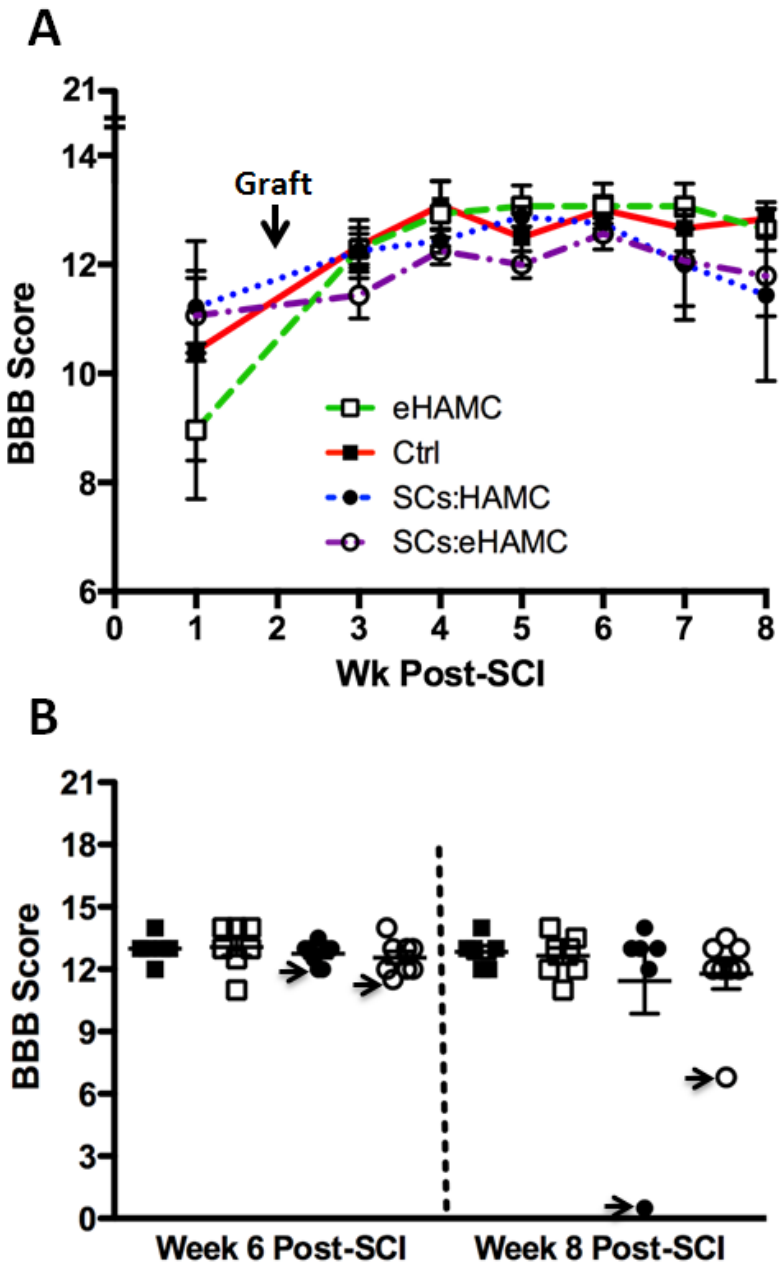

Figure 2. Locomotor ability of two graft recipient rats dropped suddenly between weeks 6 to 8 post-SCI without recovering. (A) There was no overall treatment effect on locomotor function as assessed by two-way ANOVA. (B) Notably, graft recipients capable of weight-supported plantar steps lost walking ability from week 6 to week 8 post-SCI (pointed to by the arrows), which did not occur in the no cell conditions. Error bars represent the SEM.

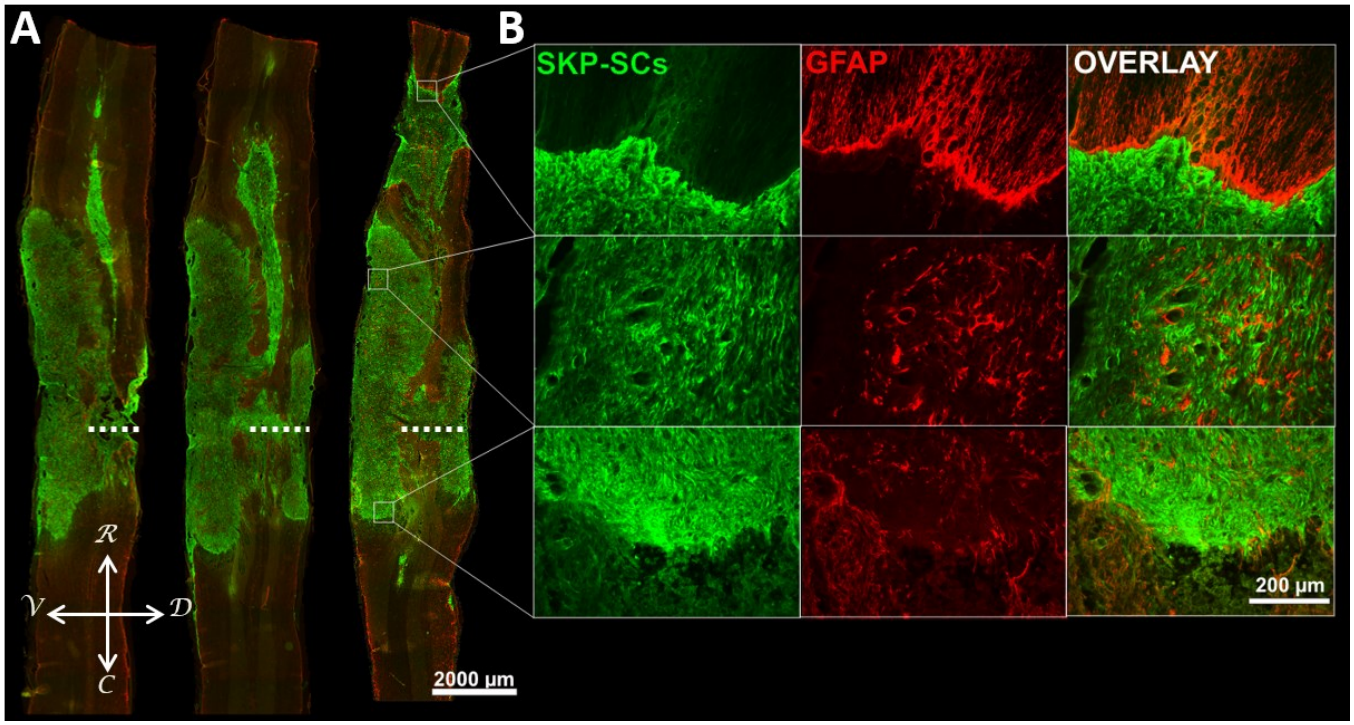

Figure 3. Adult SKP-SCs spread extensively in the spinal cord and are sharply bordered by reactive astrocytes. (A) Horizontal sections of spinal cord immunolabeled for GFP, expressed by transplanted SKP-SCs (green). Sections were also stained for the reactive astrocyte marker GFAP (red). Although SKP-SCs were injected into the lesion cavity, the cells were found throughout most of the dorso-ventral and rostro-caudal axes of the spinal block analyzed. *R* = rostral. *C* = caudal. *V* = ventral. *D* = Dorsal. (B) Magnification images of insets reveal intense GFAP signal along the graft borders. Data shown belongs to the SCs:HAMC subject whose walking deteriorated. The dotted white line denotes the hemisection level.

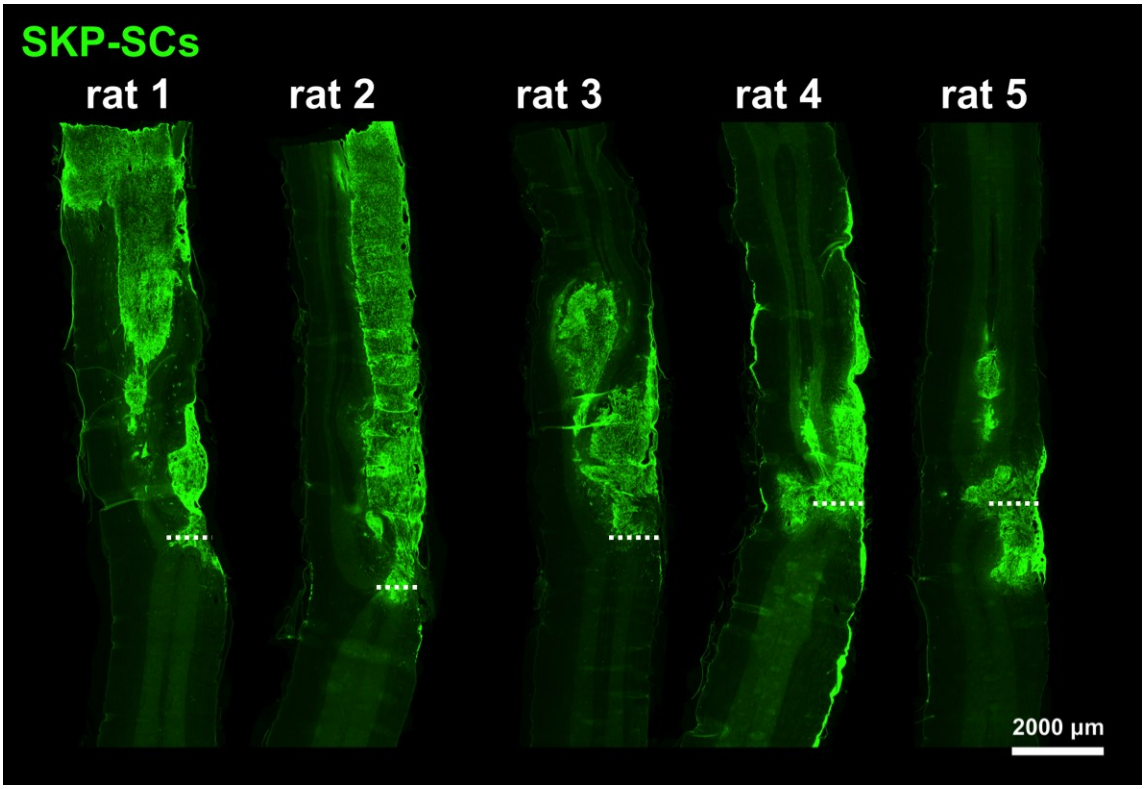

Figure 4. Extent of adult SKP-SC spread varies between graft recipient rats. Shown here are horizontal spinal cord sections near the central canal of five different animals. The SKP-SCs spread in all cases but cell distribution and magnitude of spread were dissimilar. Rat 1 is the SCs:eHAMC subject whose function worsened. Rats 2-5 did not exhibit a functional decline. The dotted white line denotes the hemisection level.

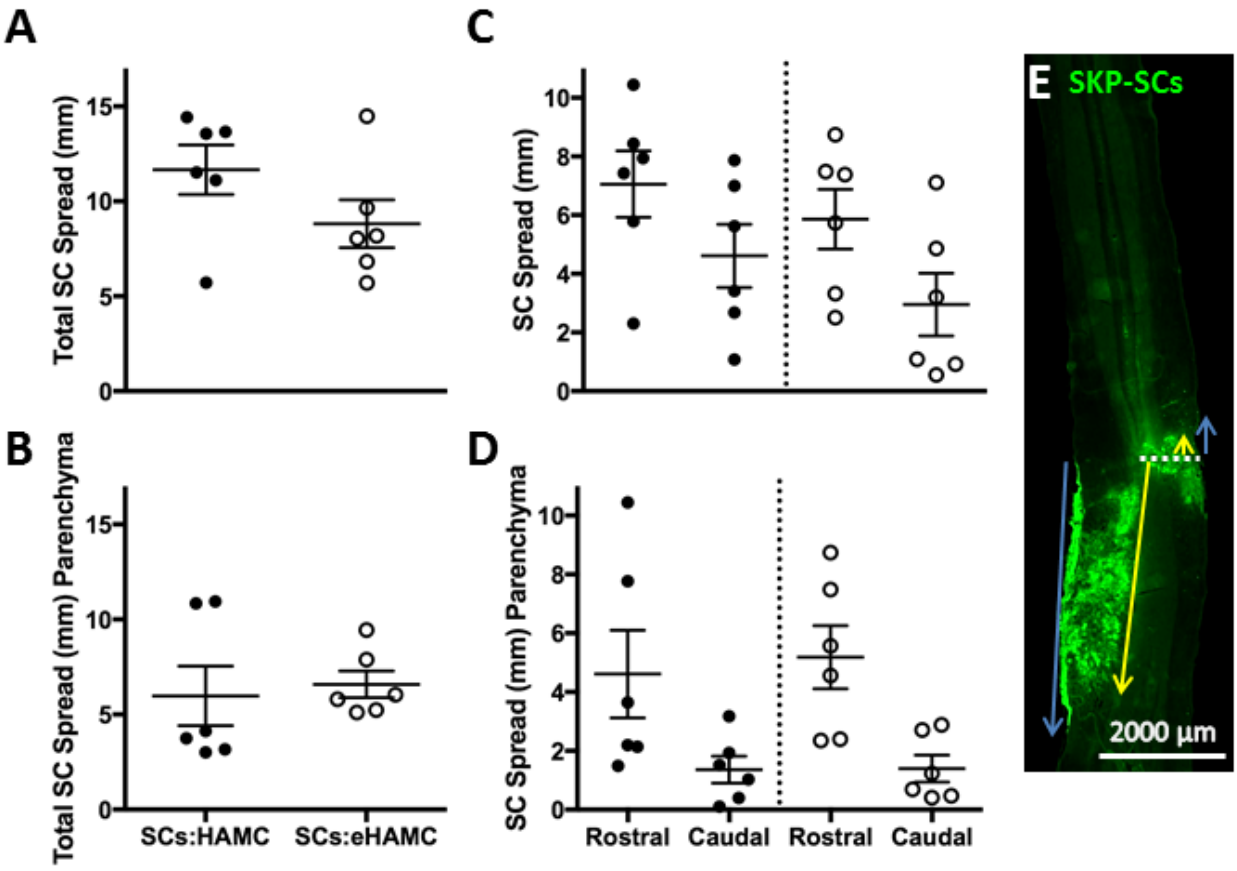

Figure 5. Extent of spread of adult SKP-SCs is independent of hydrogel matrix used. (A) The points represent the total distance SKP-SCs spread in the rostro-caudal axis when the medium for transplantation was HAMC or eHAMC. B shows the spread of grafted cells exclusively in the parenchyma. C and D indicate the rostral and caudal spread of grafted cells separately. C corresponds to total cell spread and D to spread in the parenchyma. (E) Measurement of total cell spread (blue arrows) and spread in the parenchyma (yellow arrows). The dotted white line denotes the hemisection level. Error bars represent the SEM.

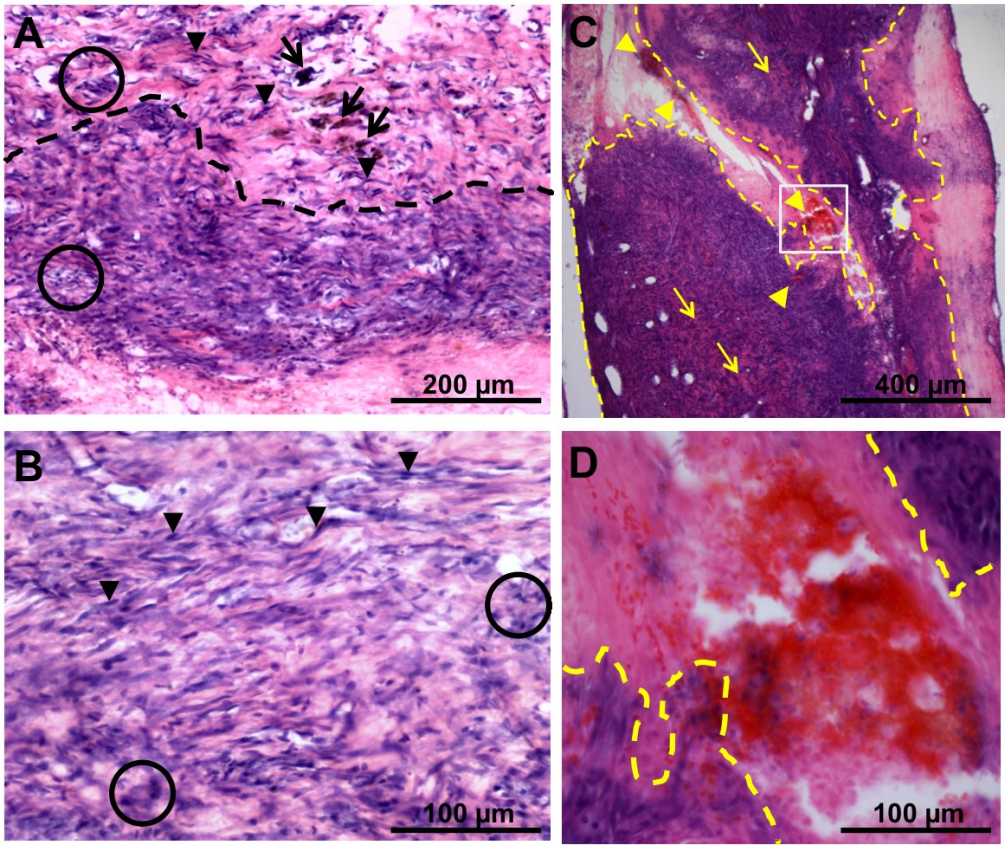

Figure 6. Adult SKP-SC growth exhibits morphological features characteristic of Schwannomas. Pictured here are H&E stained horizontal sections through a SKP-SC growth in the spinal cord. (A) Hypercellular Antoni A (below black dashes) and relatively sparse Antoni B regions (above black dashes) are apparent under microscopic examination. (A and B) As a whole, grafted cells display a spindle shape and nuclei with a slightly undulated contour and tapered or rounded ends (black arrow heads). However, there is some degree of nuclear pleomorphism (circles). Other features include the presence of hemosiderin laden macrophages (black arrows), indicating that the growth underwent hemorrhage. (C) Direct evidence of bleeding within and in the vicinity of the cell graft (yellow arrow heads). (C) There is also an absence of well-formed Verocay bodies due to hypercellularity (yellow arrows). The inset in C is magnified in D. (C and D) The yellow dashed lines demarcate the graft/spinal cord interface.

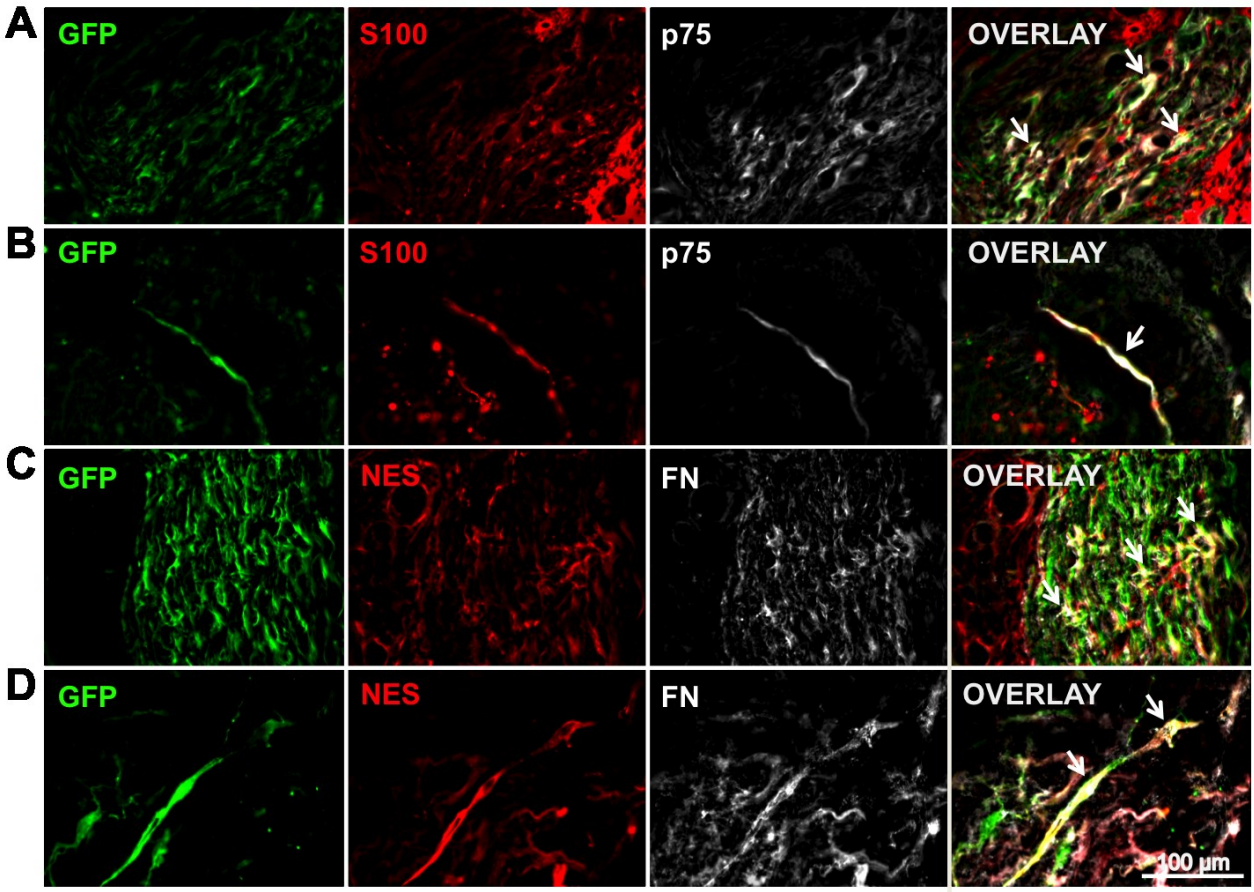

Figure 7. Adult SKP-SCs express immature Schwann cell markers 8 weeks post-transplantation into the injured rat spinal cord. (A and B) GFP^+ cells (green) showed a positive signal for the Schwann cell markers S100 (red) and p75 (white; arrows). (C and D) Further characterization revealed that some of the GFP^+ cells (green) expressed nestin (red) and fibronectin (white; arrows), identifiers of dedifferentiated Schwann cells.

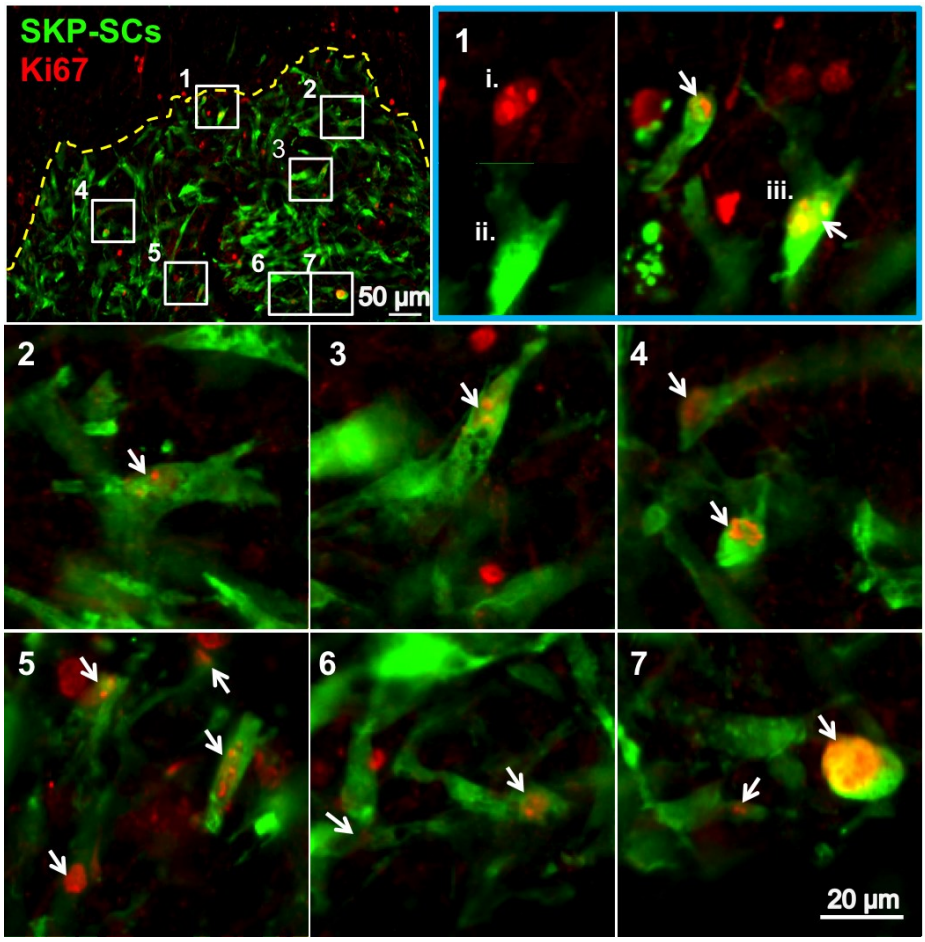

Figure 8. SKP-SCs express protein antigen ki-67, indicating continued cellular proliferation 8 weeks post-transplantation into the injured rat spinal cord. An overlay of GFP^+ SKP-SCs (green) and ki-67 (red) is shown in the top left. The yellow dashed line demarcates the graft/spinal cord interface. Insets 1-7 are magnified and labeled according to number designation. The magnification of inset 1 (outlined in blue) shows the ki67 (i.) and GFP (ii.) stains separately, and the overlap of the two stains (iii.). The white arrows point to ki-67 positive signal within the cell body of GFP^+ cells.

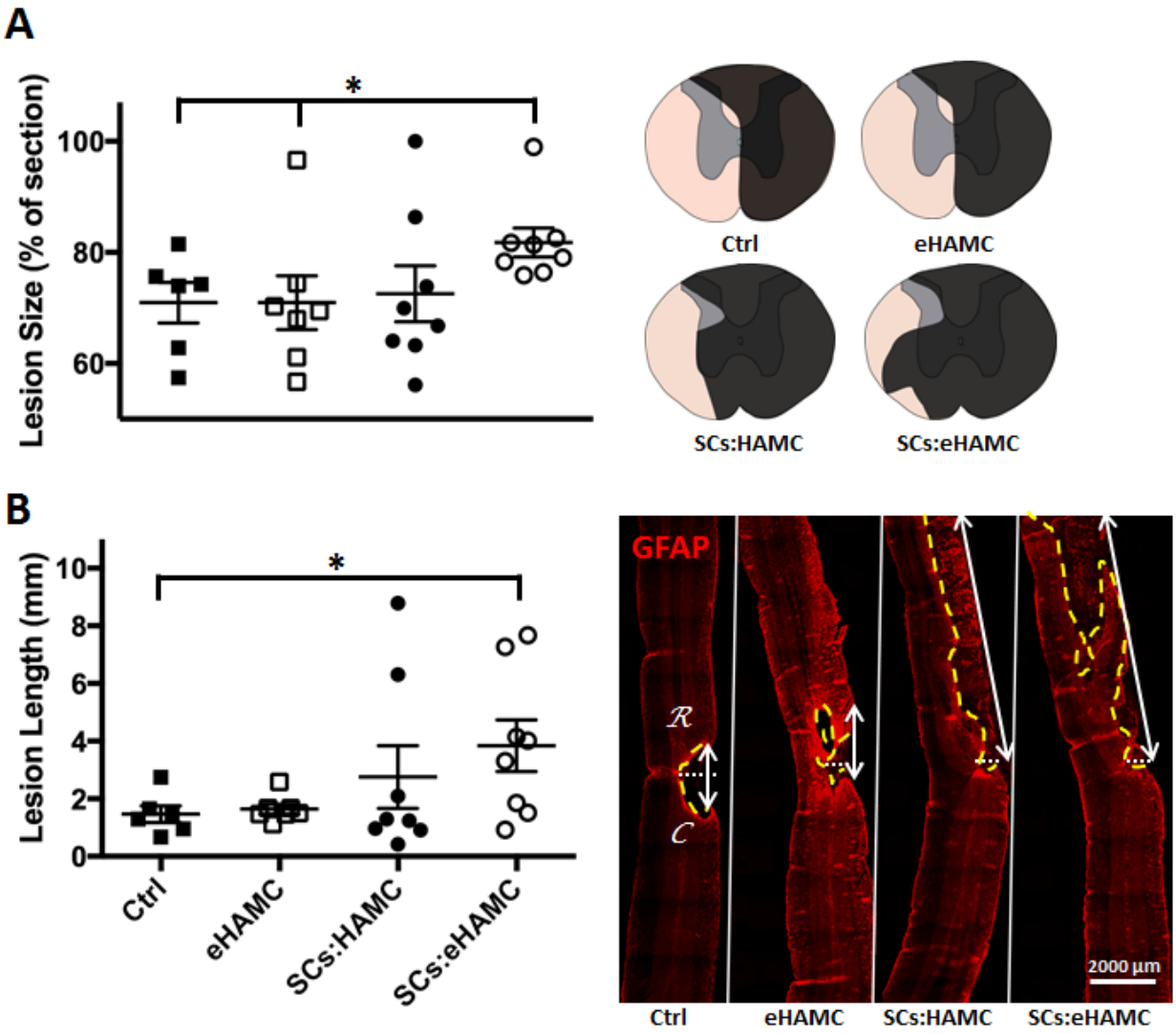

Figure 9. Lesion size and length were greater in graft-recipient rats that also received eHAMC. Lesion size as a percentage of cross-sectional area differed significantly between groups as analyzed by Kruskal-Wallis test ($p < 0.05$*). Dunn's multiple comparison test did not identify a difference. However, Mann-Whitney found a significant difference between ctrl vs SCs:eHAMC ($p < 0.05$*) and eHAMC vs SCs:eHAMC ($p < 0.05$*; A). Representative T8 cross-section schematics showing damaged tissue (black), spared white matter (pink), and spared grey matter (grey; A).The length of the SCI did not differ between groups according to Kruskal-Wallis test.

In contrast, analysis with Mann-Whitney revealed a difference between ctrl vs SCs:eHAMC ($p < 0.05$*; B). Horizontal tissue sections showing a typical lesion length (arrows) for each treatment group. Sections were stained for GFAP (red) to show the lesion borders (yellow dashes; B). Error bars represent the SEM.

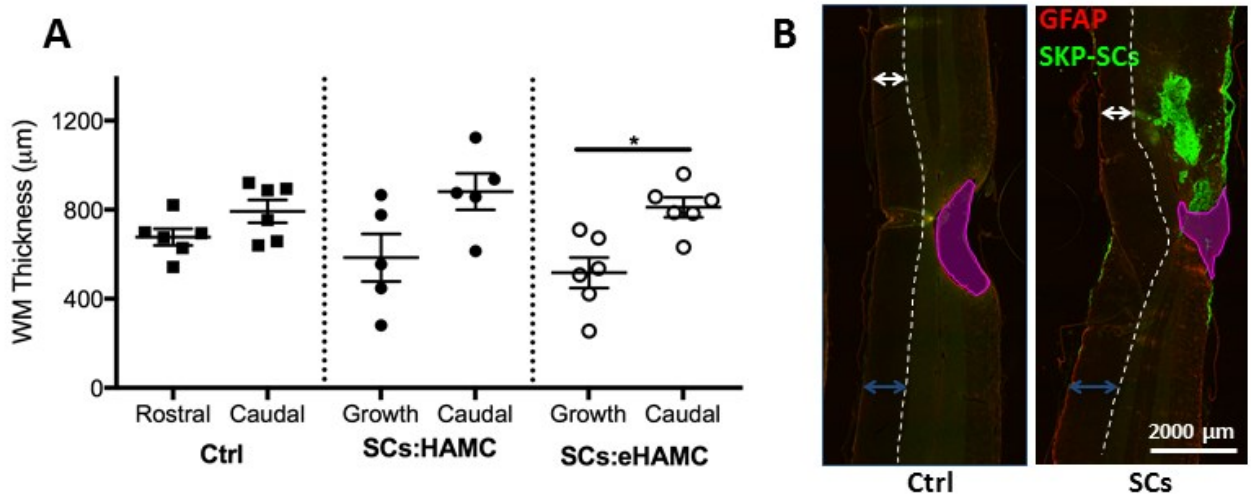

Figure 10. Spared white matter was compressed in rats that received SKP-SCs in eHAMC. (A) The points on the graph represent white matter thickness rostral to the SCI and caudal to the SCI in the lesion only control group. The points represent white matter thickness contralateral to the growth and caudal to the SCI in transplanted rats. The star indicates that rats that were grafted with SKP-SCs in eHAMC had significantly ($p < 0.05$*) thinner white matter contralateral to the growth compared to caudal to the SCI, which was not the case in control rats or rats that were grafted SKP-SCs in plain HAMC (B) Horizontal tissue sections showing examples of white matter thickness (arrows) for a control rat and a rat with a SKP-SC growth (green). Sections were stained for GFAP (red) to outline the lesion borders (magenta). The dotted white line denotes the grey/white matter spinal cord interface. Error bars represent the SEM.

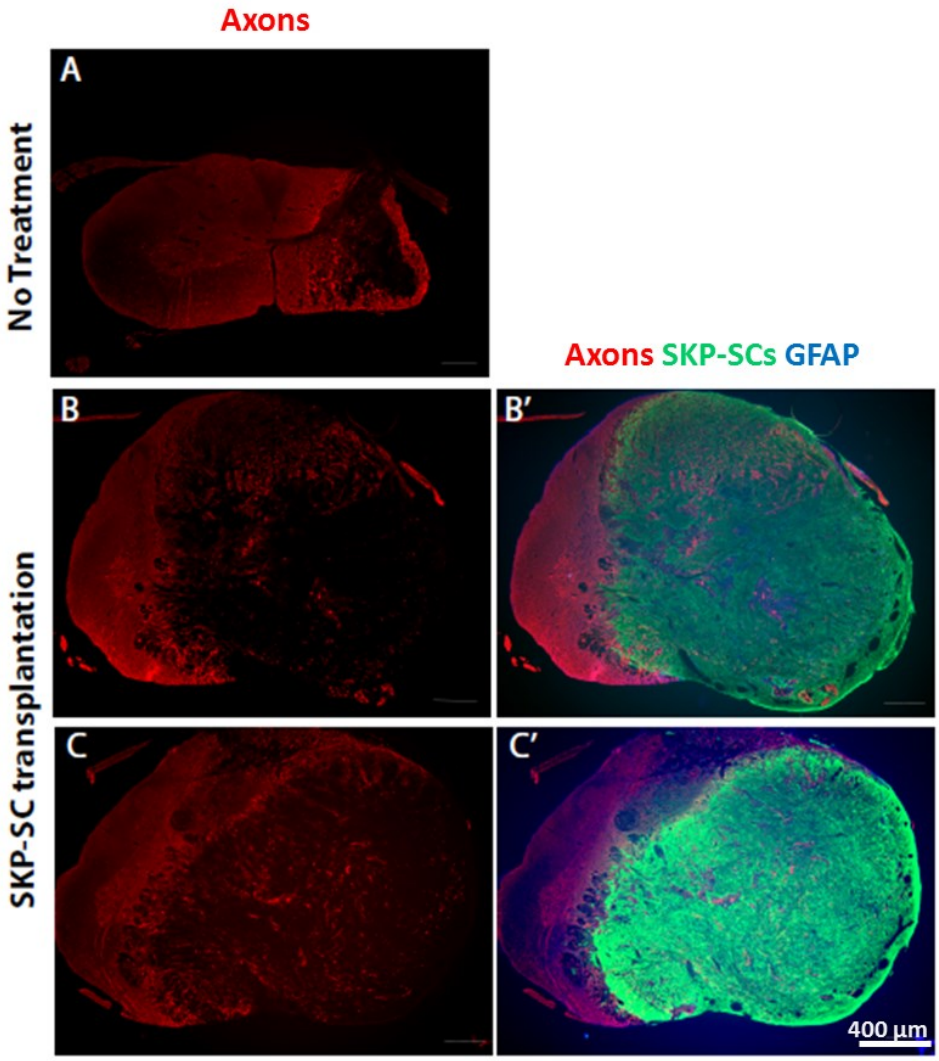

Figure 11. Adult SKP-SC growth formation occurs in the absence of a hydrogel matrix and immune suppression. In a separate experiment, GFP^+ SKP-SCs suspended in media only were transplanted in rats with a cervical SCI. No immunosuppressant was administered to the rats for the duration of the study. Cross-sections through the injury site were stained for NF200 and βIII-tubulin (axons; red), GFP^+ (green), and GFAP (blue). (A) Representative cross-section from a rat that received no treatment. Note that the injury is restricted to one hemicord. B and C show representative injuries from graft-recipient rats. B' and C' show a mass of GFP^+ SKP-SCs occupying the injured area.

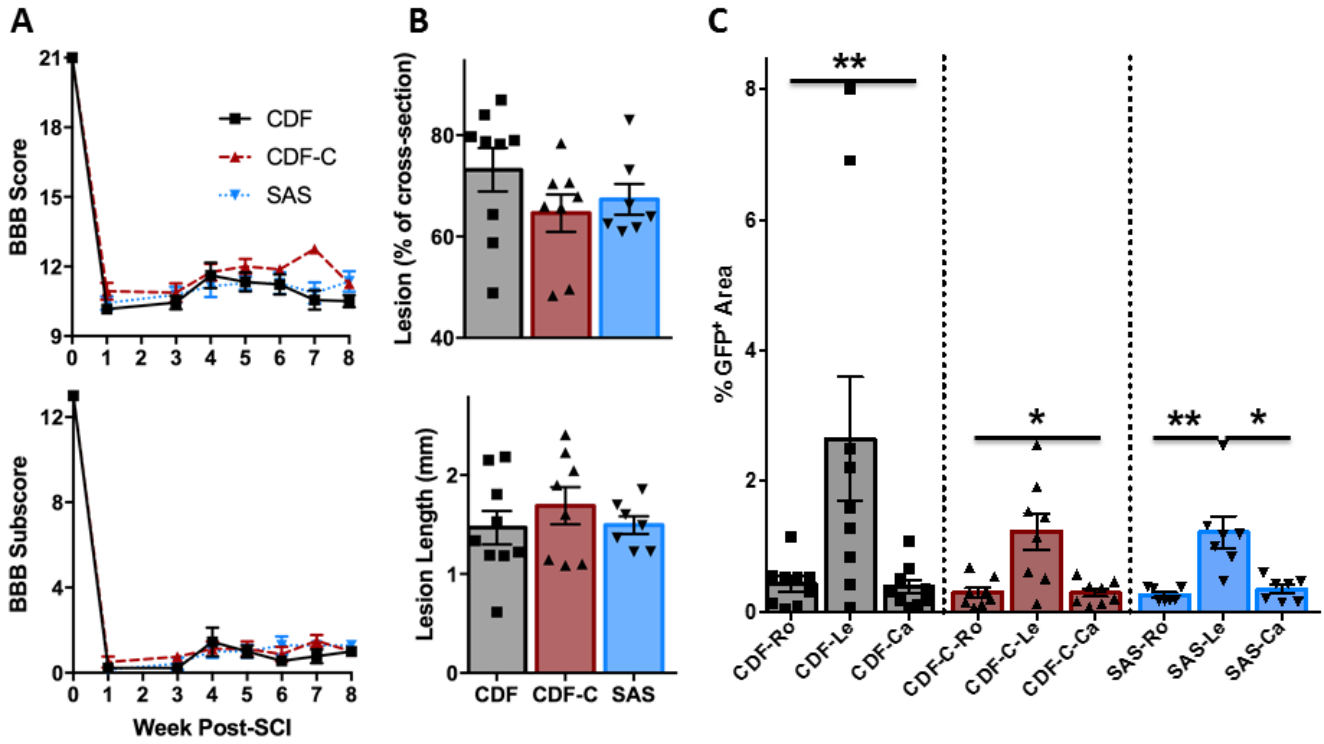

Figure 1. Locomotor ability, SCI severity, and SKP-SC survival were similar between immunosuppressed, immunocompetent, and sub-strain mismatched rats. (A) Points on the graphs represent average weekly group BBB and BBB sub-scale scores. (B) Bar graphs show the SCI cross-sectional size (%) and length (mm) for each group. (C) Bars show the average area (% of total area analyzed) covered by SKP-SCs at the SCI, and rostral and caudal to the injury for each group. Points on the bar graphs represent individual rat data. * indicates significant differences between the area covered by SKP-SCs at the SCI and rostral and caudal to the injury. $p<0.05$*, $p<0.01$**. Error bars represent the SEM.

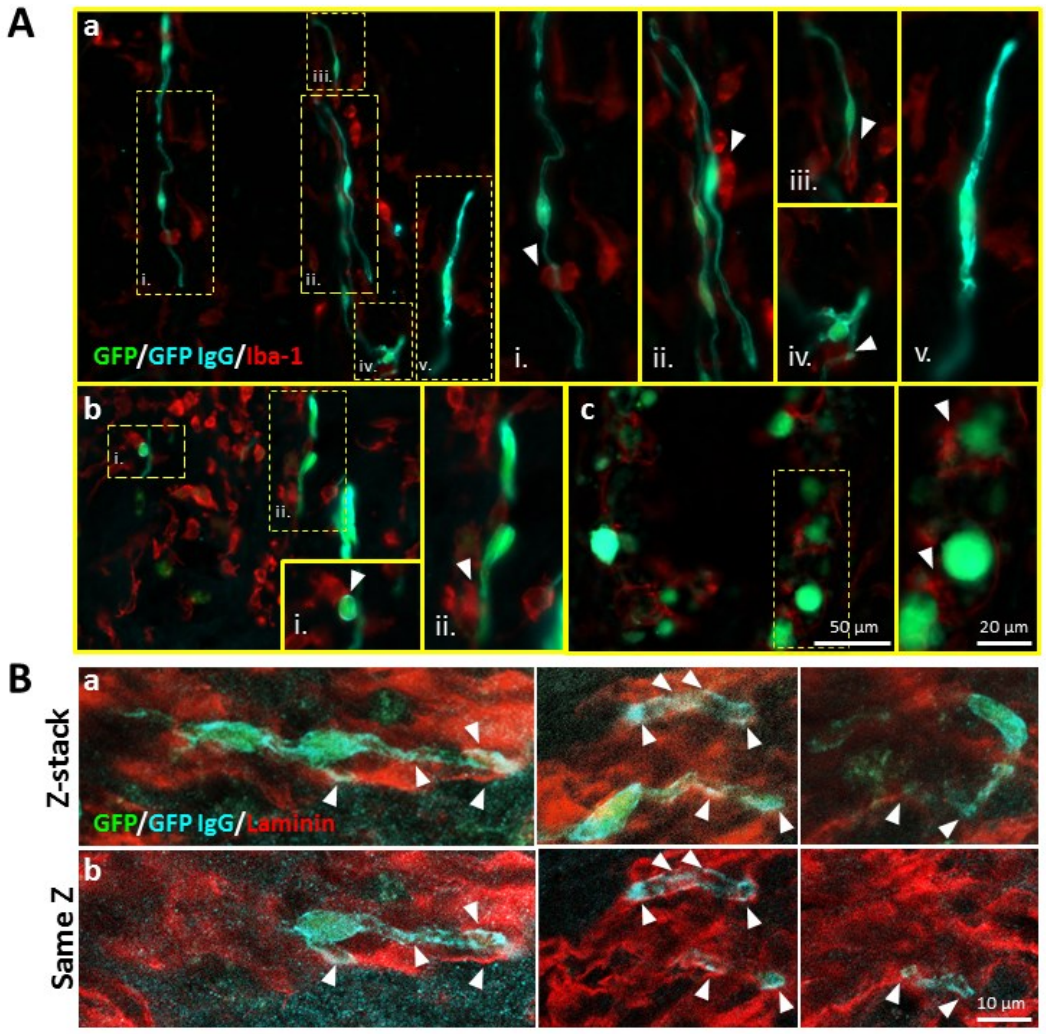

Figure 2. SKP-SCs were closely associated with Iba-1^{+} immune cells and laminin. (A). SKP-SCs (green/cyan) with varied morphologies showed proximity with Iba-1^{+} immune cells (red). a. Bipolar SKP-SCs with a central soma and a process on either end of the soma. b. SKP-SCs with either one process or none. c. Large spherical SKP-SCs surrounded by immune cells. Roman numerals indicate individual SKP-SCs. (B). a. SKP-SCs (green/cyan) contact laminin (red) in an image averaging the signal intensity of a confocal z-stack. b. SKP-SC contact with laminin is confirmed in images of the same z-plane.

6.3 Chapter 3

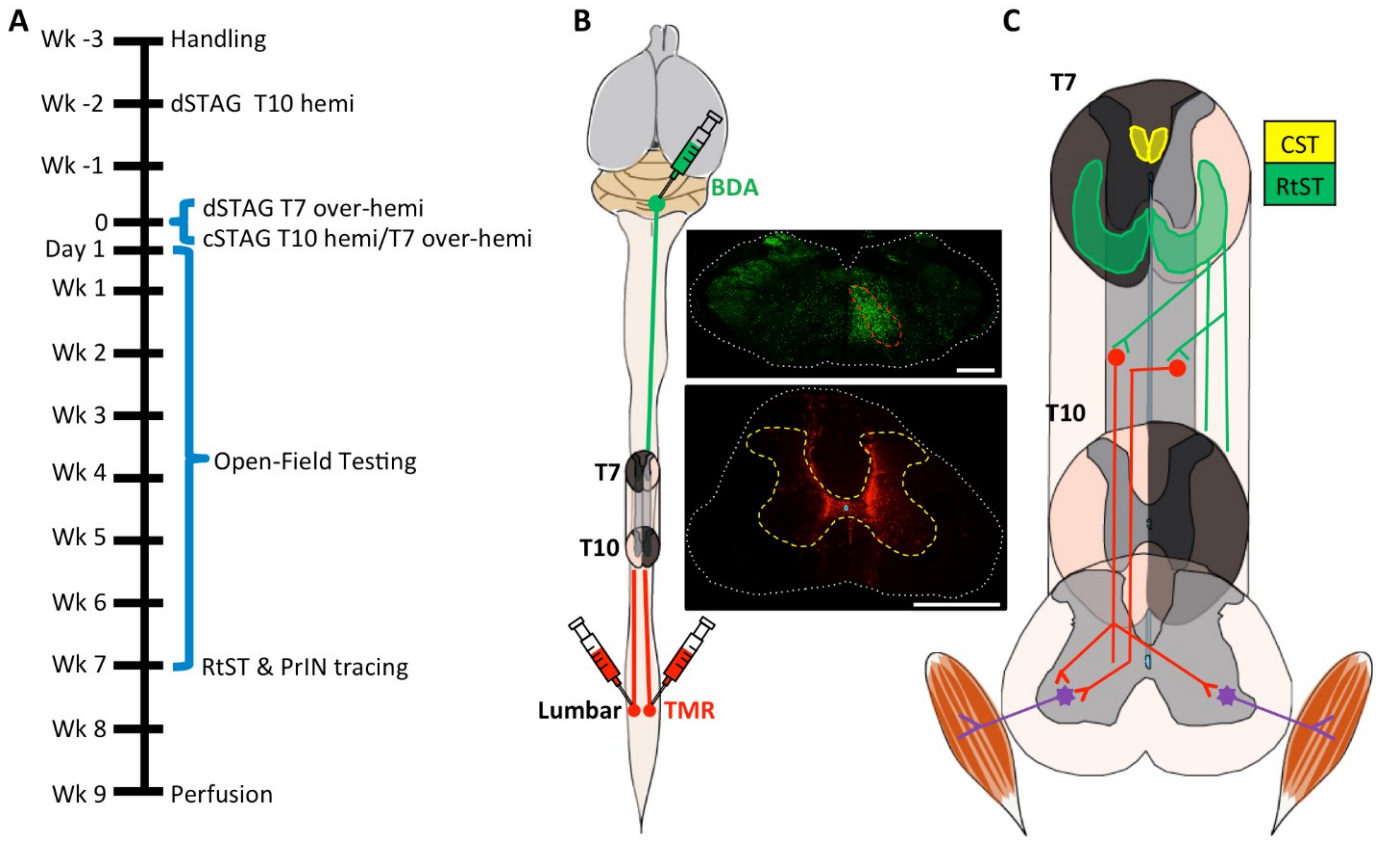

Figure 1. Experimental timeline and STAG SCI model. The timeline is shown in (A). The RtST was anterogradely traced with BDA and PrINs were retrogradely traced with TMR (B). C shows a more detailed view of the two SCIs and intact tissue bridge, and outlines some of the possible reticulo-propriospinal pathways that could circumvent the SCIs to allow descending input from the RtST to lumbar motor systems. Blackened areas of spinal cord correspond to the intended injuries. The CST and RtST appear in yellow and green respectively. Traced RtST axons are shown descending in the white matter of the unlesioned hemicord at T7 (green; C) and stopping once reaching the second injury at T10. We hypothesize that injured RtST axons could project collaterals into the grey matter and form contacts with PrINs (red; C) that would then carry the signal to motor neurons (purple; C) below the SCIs. White dashed line, outline of cross-section.

Red dashed line, gigantocellular reticular nucleus. Yellow dashed line, outline of lumbar grey matter. Scale bar = 1000 µm.

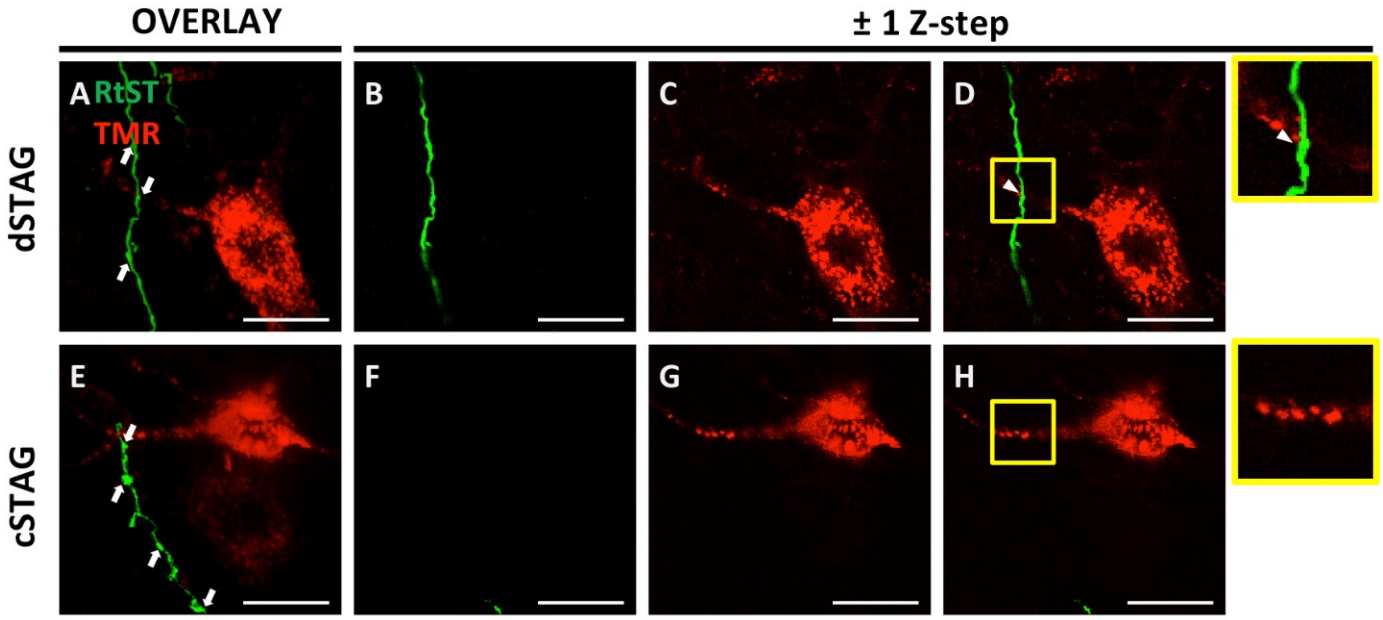

Figure 2. Close appositions between RtST boutons and PrIN neurons were considered contacts. Data from a dSTAG animal. RtST (green) and PrIN (red) channels (A-D). The arrows point to BDA stained RtST boutons on multi-step overlay of the two channels (A). RtST collateral (B) and PrIN soma (C) ± 1 Z-step of each other. Combining the channels reveals a contact between a RtST bouton and PrIN dendrite (D). Data from a cSTAG animal (E-H). The arrows point to axonal boutons on multi-step overlay (E). Green channel (F) ± 1 Z-step of PrIN soma (G). The combination image in H demonstrates an absence of RtST collaterals within close proximity of the PrIN. Therefore, the appositions shown in E were not considered contacts. 1 z-step = 0.76 µm. Scale = 20 µm.

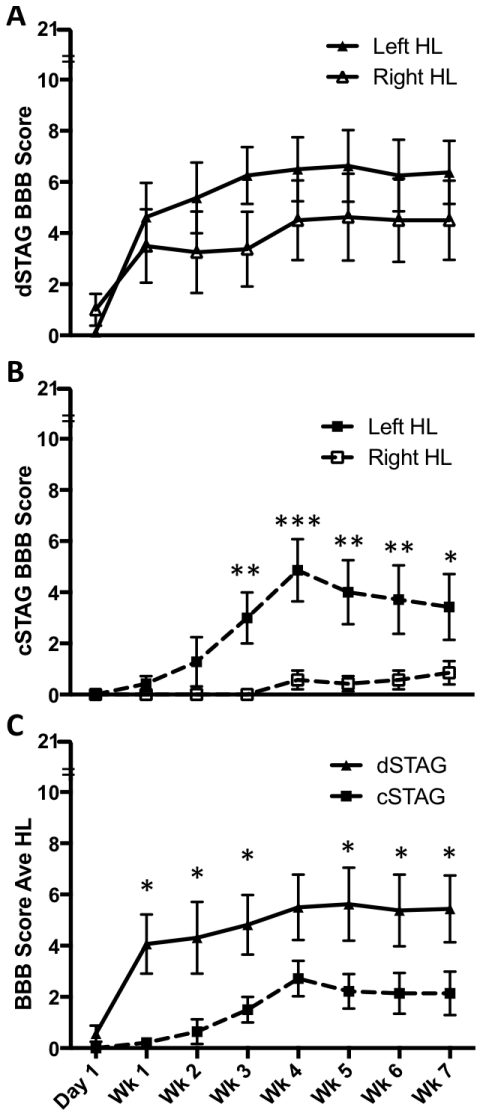

Figure 3. dSTAG animals displayed superior locomotor ability compared to cSTAG animals. Left and right hindlimb BBB scores of dSTAG rats were not significantly different (A), whereas left hindlimb scores of cSTAG rats were significantly higher than right hindlimb scores ($p < 0.05$*) as assessed by 2-way repeated measures ANOVA. Post-hoc testing showed the left hindlimb outperformed the right hindlimb of cSTAG animals at weeks 3 ($p < 0.01$**), 4 ($p < 0.001$***), 5 ($p < 0.01$**), 6 ($p < 0.01$**), and 7 ($p < 0.05$*). Average BBB score of the two hindlimbs was significantly greater for the dSTAG group compared to the cSTAG group (p

<0.05*) from weeks 1-3 and 5-7 (p <0.05*; C). Error bars represent the SEM.

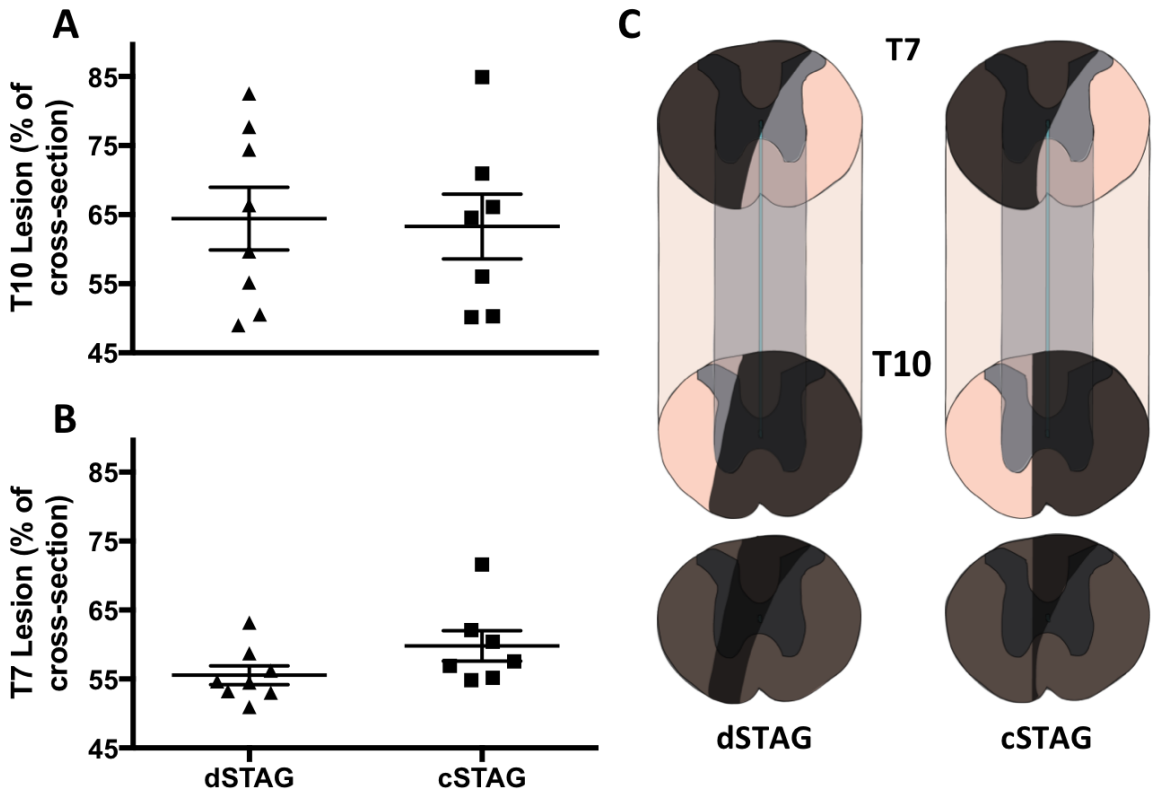

Figure 4. STAG SCI severity was unaffected by the inclusion of a time delay between injuries. The size of the T10 (A) and T7 (B) spinal lesions as a percent of the cross-sectional area were comparable between groups. Schematics of a spinal cord segments encompassing the lesions from representative dSTAG and cSTAG animals (C). Lesioned areas are blackened. White matter is spared ventrally at the level of the T7 lesion, but the T10 injury encroaches on the contralateral hemicord in both animals. Overlays of the T7 and T10 injuries are shown below the block schematics. When the two injuries are overlapped, the completeness of the lesion becomes evident. Error bars represent the SEM.

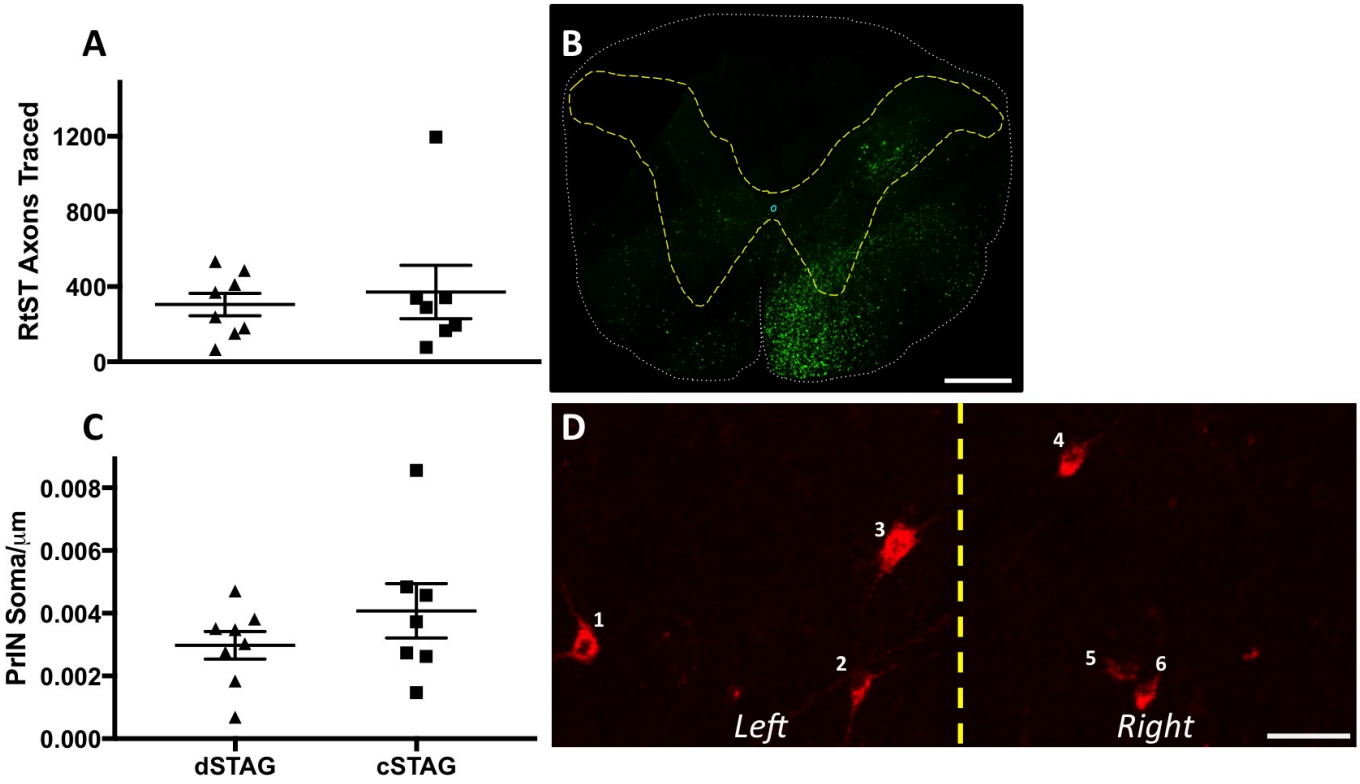

Figure 5. RtST traced axon and PrIN counts. No significant difference in the number of traced axons was found between groups (A). Representative C1 cross-section showing the BDA traced RtST (green; B). White dashed line, outline of cross-section. Yellow dashed line, outline of grey matter. Scale bar = 500 μm (B). No significant differences in the number of soma in the grey matter were found between dSTAG and cSTAG groups (C). Six PrIN cell bodies in the bilateral grey matter (D). Yellow dashed line, midline. Scale bar = 50 μm (D). Error bars represent the SEM.

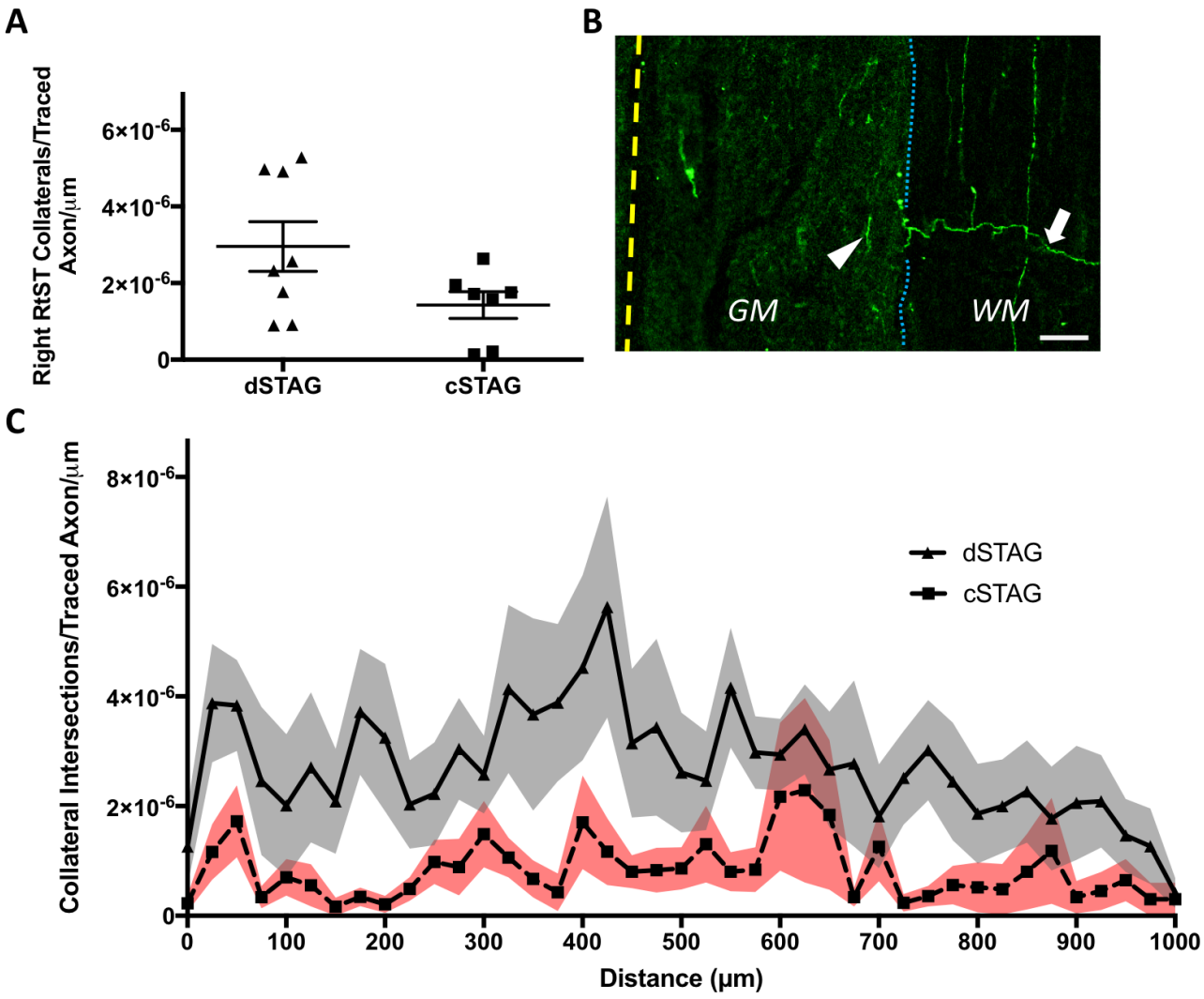

Figure 6. Traced RtST collateral counts and intersections at different distances from the grey/white matter border. Counts of traced RtST collaterals crossing into the grey matter did not differ significantly between groups (A). A right RtST collateral (arrow) is seen projecting across the grey/white matter (GM/WM) interface (dotted line). Scale = 50 μm (B). Line plot showing a greater number collaterals within the grey matter starting from the lateral grey/white matter border in the right spinal cord (0 μm) and continuing left to the lateral edge of the left grey/white border in the left spinal cord (1000 μm) for the dSTAG group. Grey and red areas represent the SEM (C).

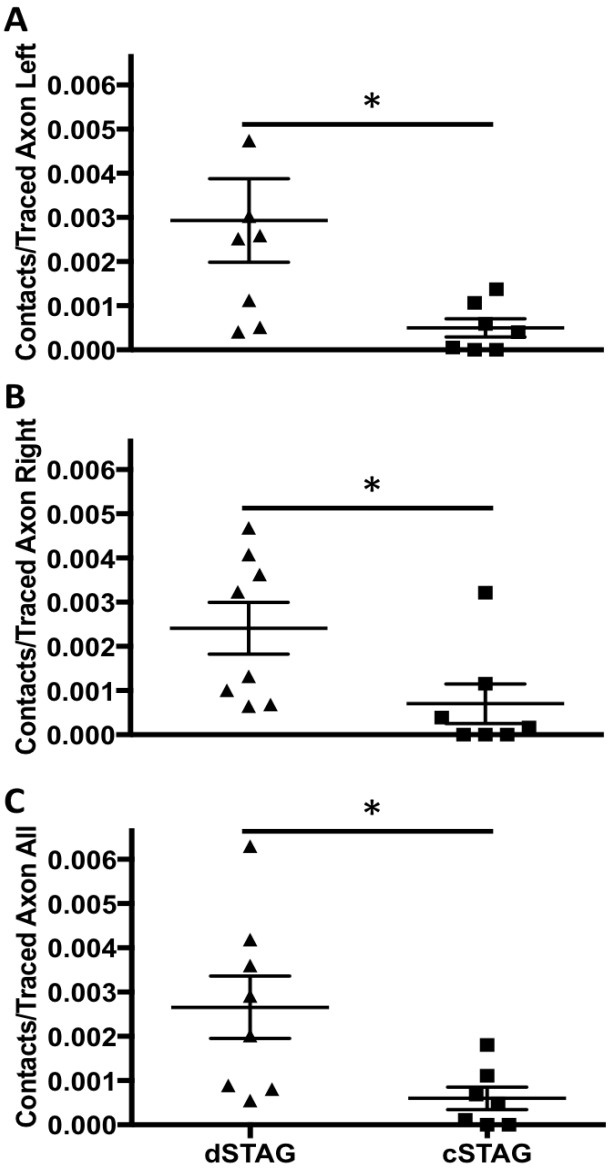

Figure 7. Higher numbers of reticulo-propriospinal contacts are found in dSTAG compared to cSTAG animals. dSTAG rats had significantly more reticulo-propriospinal contacts in the left (A; $p < 0.05$*), right (B; $p < 0.05$*), and bilateral grey matter of the spinal cord (C; $p < 0.05$*). Contact numbers were normalized to the total number of traced RtST axons in all cases.

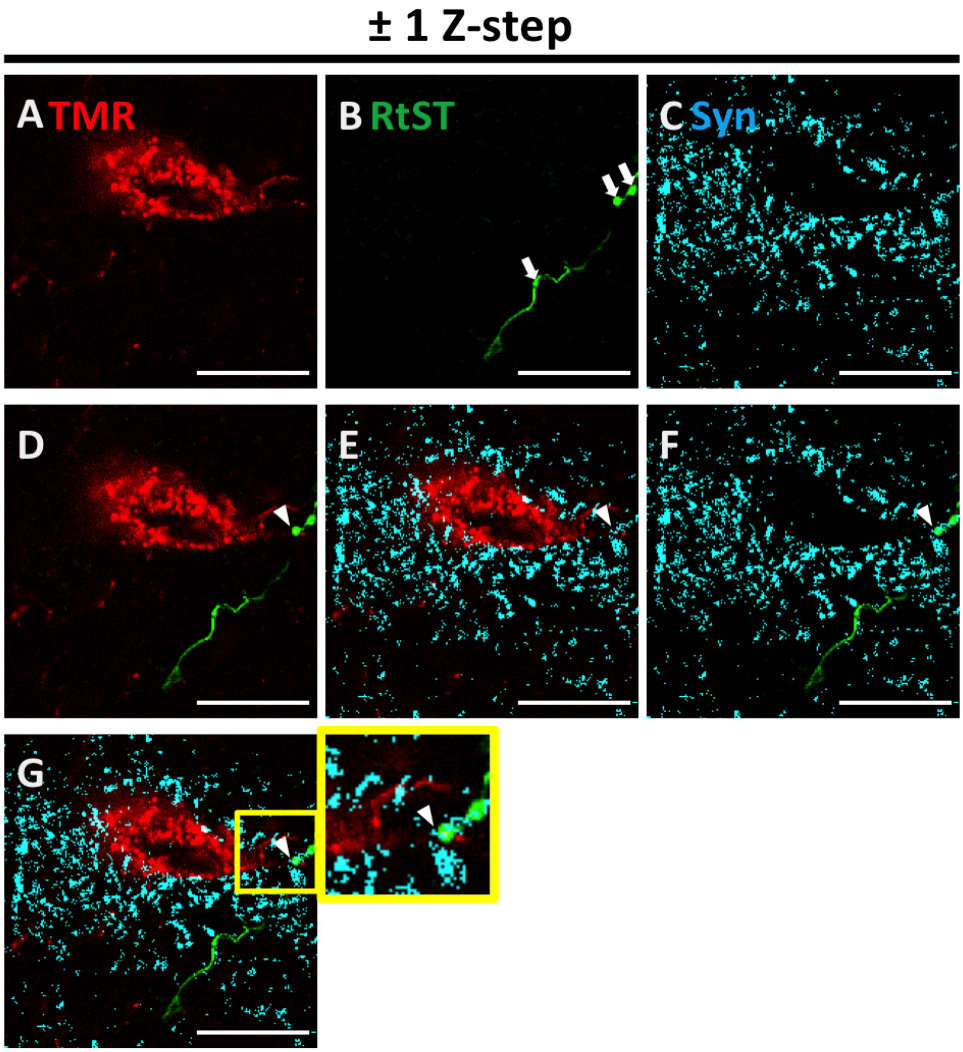

Figure 8. RtST boutons that form reticulo-propriospinal contacts contain synaptophysin. PrIN soma retrogradely labeled with TMR tracer (A) and RtST collateral (B). The white arrows point to BDA stained RtST boutons along the shaft of the axon. Synaptophysin staining outlines the shape of the PrIN cell body (C) shown in A. RtST bouton forms contact with PrIN cell body (arrowhead, D). Synaptic labeling is confirmed around the cell body (E). The RtST bouton is synaptophysin immunoreactive (F). Three channel overlay showing reticulo-propriospinal contact (G) at higher magnification (G inset). 1 z-step = 0.76 µm. Scale = 20 µm.

6.4 Chapter 4

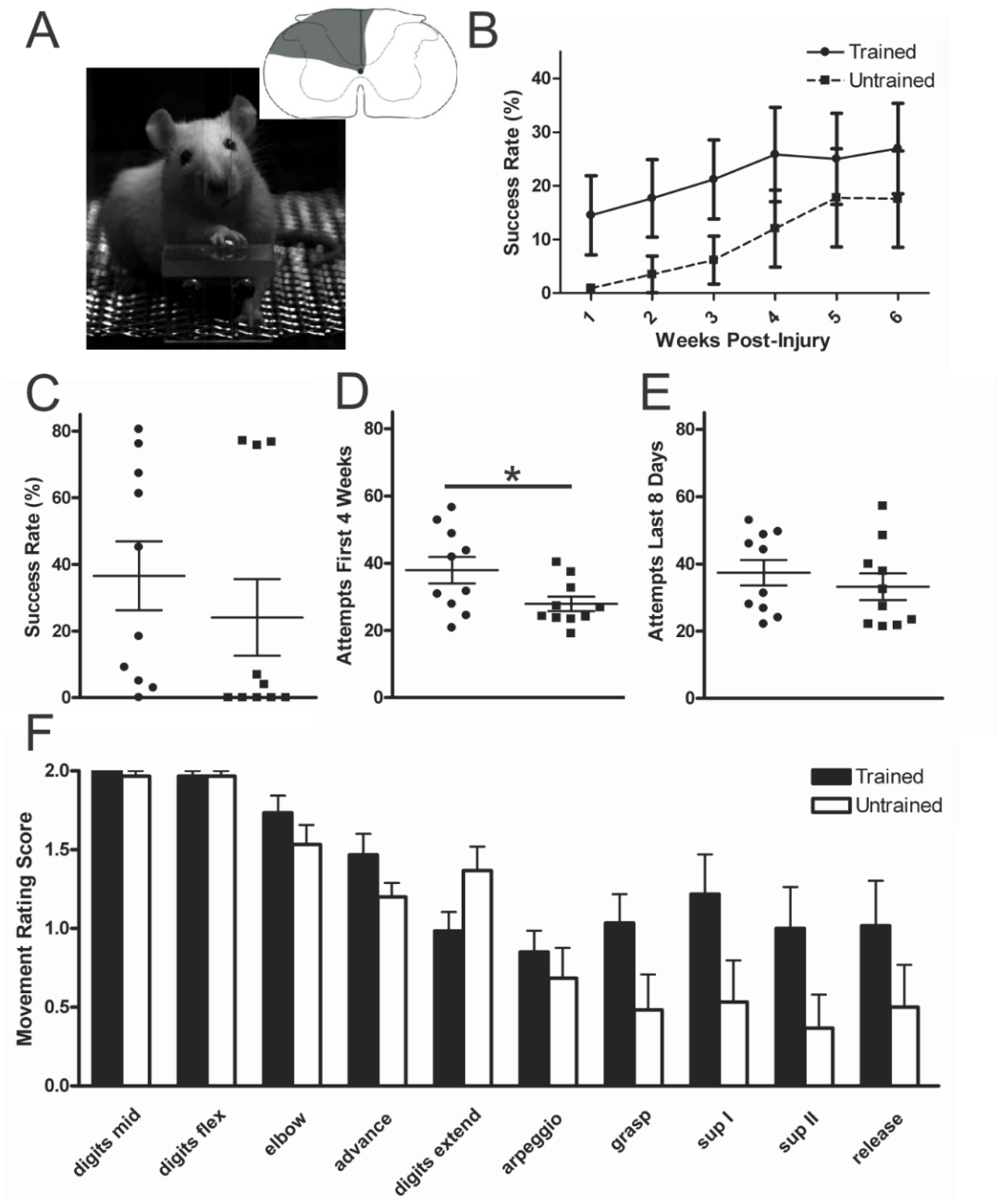

Figure 1. Pre-training in the single pellet grasping task (SPG) does not influence grasping ability in rats after a C4 dorsolateral quadrant (DLQ) spinal cord lesion. A DLQ lesion (A) abolishes the CST unilaterally and most of the RST, greatly diminishing grasping ability in rats. Weekly

grasping data (B) shows that there was a non-significant trend for pre-trained rats to successfully retrieve more pellets through a slot after an SCI than rats that were not trained before the injury (two-way repeated measures ANOVA P-value 0.204). When the best scores attained by the pre-trained and non-pre-trained group throughout the 6 weeks of rehabilitation were contrasted, a similar non-significant trend emerged (unpaired t-test two-tailed P-value 0.429; C). Pre-trained rats grasped significantly more pellets than non-pre-trained rats during the first 4 weeks of rehabilitation (unpaired t-test two-tailed $P < 0.05$; D), but this effect disappeared by the final days of rehabilitation (unpaired t-test two-tailed P-value 0.457; E). The detailed components of the grasping movement were analyzed 6 weeks after the DLQ lesion and rehabilitative training (E). Movements of pre-trained animals tended more towards normalcy (the scores were higher) than those of untrained rats, except for digit extension. However, no significant effects of pre-training were found on the 10 components of the grasping movement. In (F), Digits mid = digits turned toward body midline. Digits flex = digits flexed. Elbow = Elbow moved to midline. Advance = Forelimb advanced through the slot. De = Digits extend. Arpeggio = Paw pronates from digit 5 through to digit 2. Grasp = Paw closes over the pellet. Supination I = As the forelimb is pulled away, the paw is rotated 90˚. Supination II = Paw is rotated a further 45˚. Release = Pellet is released into the mouth. (* indicates $P < 0.05$). Error bars represent the SEM.

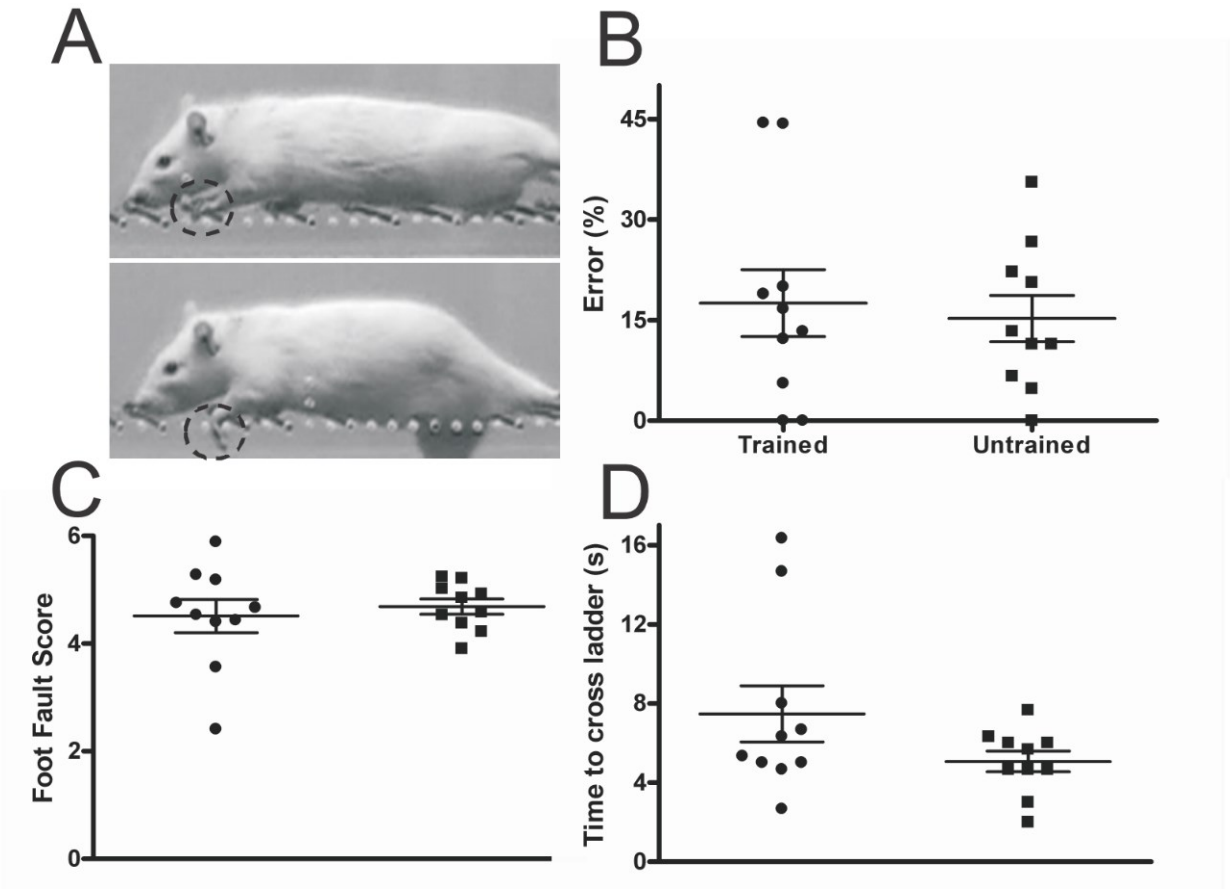

Figure 2. Performance on the horizontal ladder task is not affected by pre-training on the SPG task. In (A), a Lewis rat walks across the ladder. The dashed circle shows (top) correct paw placement and (bottom) a paw slip. Rats trained on pellet grasping did not make significantly more errors (rung misses or slips) than untrained rats when crossing the ladder (unpaired t-test unpaired t-test P-value 0.713; B). Performance on the foot fault scale was similar between groups (unpaired t-test P-value 0.606), with rats from both groups scoring close to the max score of 6 (C). A higher score is indicative of superior walking ability on the horizontal ladder task. Pre-trained rats took more time in (s) to cross the ladder than untrained rats (D), but this difference was not significant (unpaired t-test P-value 0.129). Error bars represent the SEM.

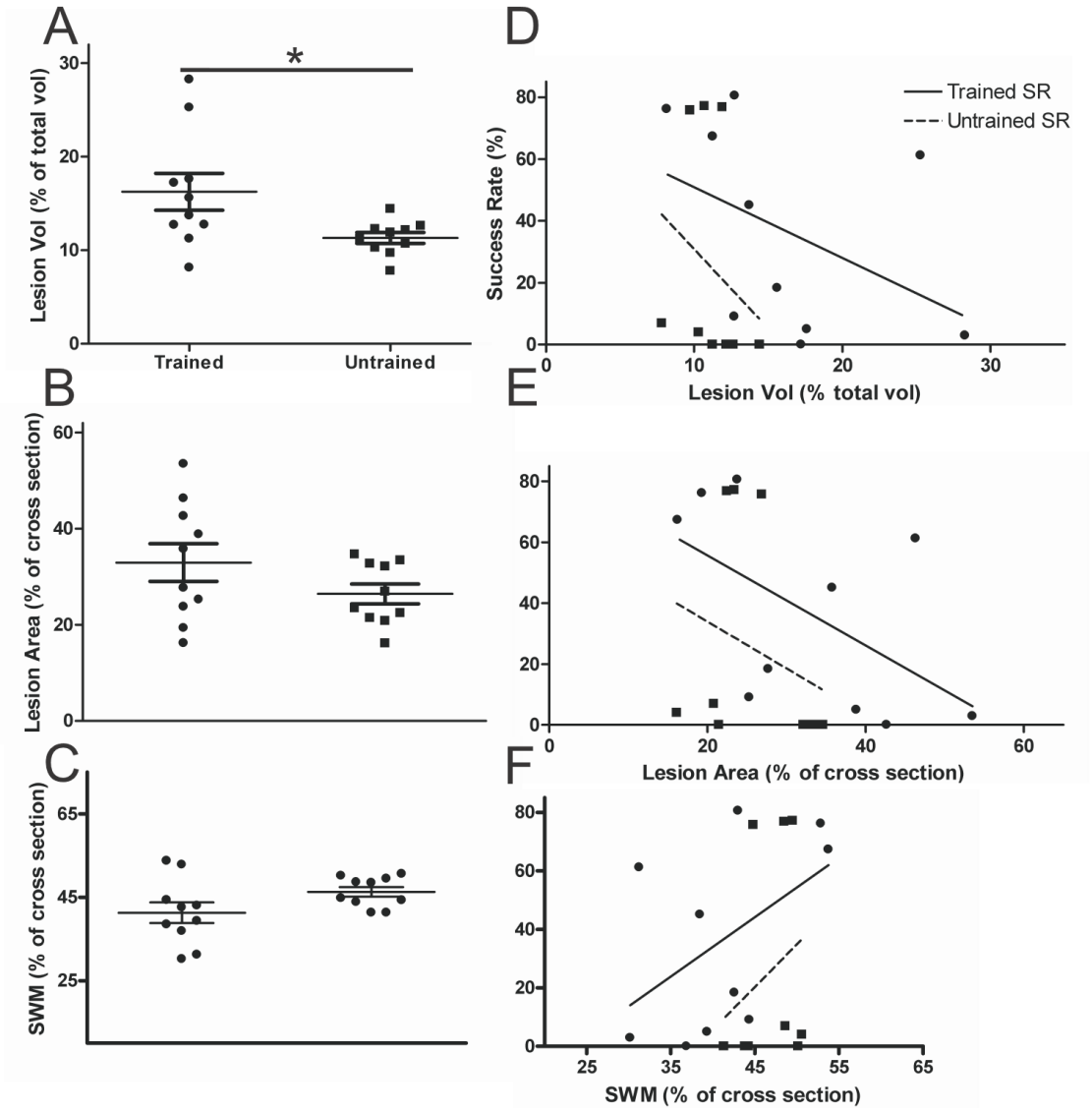

Figure 3. Lesion assessment and correlations of lesion and reaching success. Lesion volume was quantified using the Cavalieri method, and the lesion volumes of rats trained before the injury were found to be greater than those of rats that were not pre-trained (unpaired t-test $P < 0.05$; A). Using lesion reconstructions, lesion area and white matter sparing were also assessed. In this case, no group differences were found with regards to lesion size (unpaired t-test P-value 0.157; B) or white matter sparing (unpaired t-test P-value 0.083; C). Reaching success was not found to be correlated with the extent of injury in the rostral to caudal direction (D) for trained (Pearson's

r = -0.435) and untrained rats (Pearson's r = -0.257). Reaching success was not correlated with the extent of damage (E; pre-trained group Pearson's r = -0.557 and untrained group Pearson's r = -0.274) or with white matter sparing (F) in the two dimensional plane (pre-trained group Pearson's r = 0.488 and untrained group Pearson's r = 0.288). (*indicates P <0.05). Error bars represent the SEM.

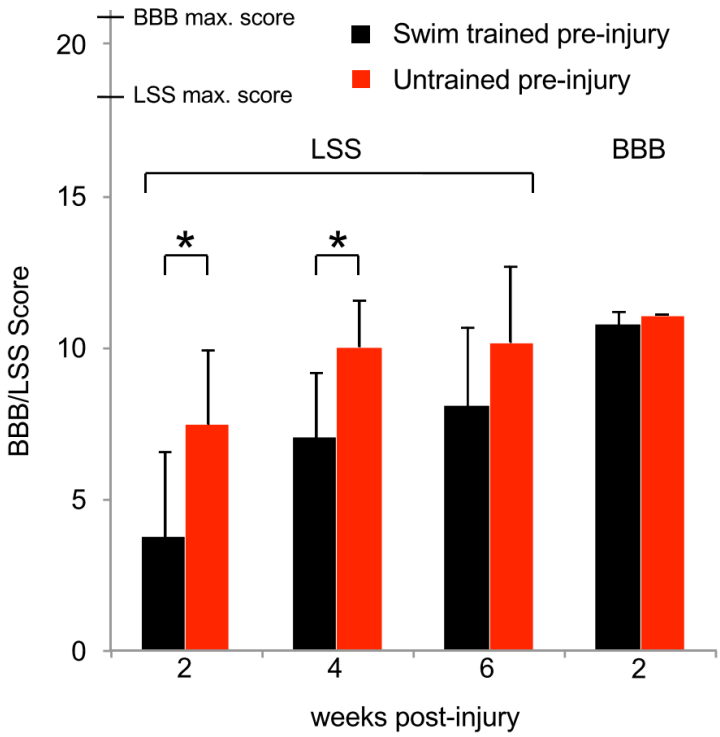

Figure 4. Shown are the Basso, Beattie & Bresnahan (BBB) open field locomotor scores and the Louisville Swim Scale (LSS) scores for the two experimental groups. The LSS, which has a maximum (normal baseline) score of 18, is shown for post-injury weeks 2, 4 and 6. The BBB, which has a maximum (normal baseline) score of 21, is shown for post-injury week 2. Data is shown as mean ± SD. Asterix shows significant difference for swim trained pre-injury animals compared to those that were untrained pre-injury. ANOVA and tukey post-hoc t-test, P <0.05. Error bars represent the SD.

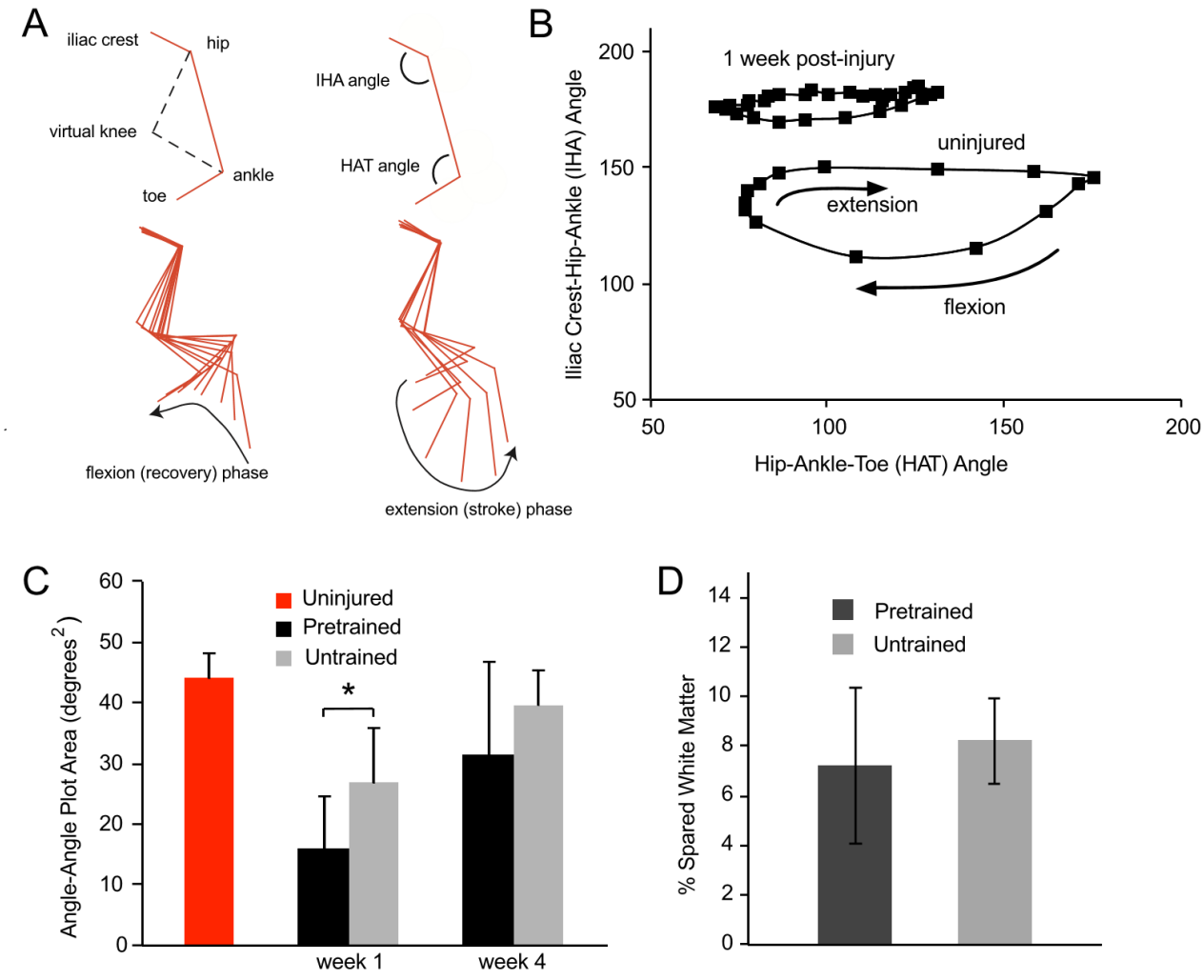

Figure 5. Shown in A are stylized examples of hindlimb stick figures for swimming to illustrate the iliac crest – hip – ankle and hip – ankle – toe angles. In B, these two angles are plotted against each other and the resulting ellipses show the angular excursions for single swimming strokes to illustrate an uninjured animal and an injured animal at 1 week post-injury. The ellipse areas, calculated using an elliptical fourier analysis, are shown in C. Pre-trained animals had a significantly lower angle-angle plot area (*, independent two-tailed t-test). D. Spared white matter, based on the cross sectional area of eriochrome cyanin stained compact white matter at the injury epicenter, is not different for the two experimental groups. Error bars represent the SD.

Appendix 1: Improved single pellet grasping using automated *ad libitum* full-time training robot

Keith K. Fenrich [a,b], Zacnicte May [a,b], Caitlin Hurd [a,b], Carolyn Boychuk [a,b], Jan Kowalczewski [a], David J. Bennett [a,b], Ian Q. Whishaw [c], Karim Fouad [a,b]

[a] Centre for Neuroscience, [b] Faculty of Rehabilitation Medicine, 3-88 Corbett Hall, University of Alberta, Edmonton, AB T6E 2G4, Canada, Department of Neuroscience,

[c] Canadian Centre for Behavioural Neuroscience, University of Lethbridge, 4401 University Drive West, Lethbridge, AB, T1K 3M4, Canada

Corresponding author:

Keith K. Fenrich

Faculty of Rehabilitation Medicine

3-88 Corbett Hall

University of Alberta

Edmonton, AB T6E 2G4

CANADA

Email: fenrich@ualberta.ca

Phone: +1 780 492 0938

Fax: +1 780 492 1626

Abstract

The single pellet grasping (SPG) task is a skilled forelimb motor task commonly used to evaluate reaching and grasp kinematics and recovery of forelimb function in rodent models of CNS injuries and diseases. To train rats in the SPG task, the animals are usually food restricted then placed in an SPG task enclosure and presented food pellets on a platform located beyond a slit located at the front of the task enclosure for 10-30 minutes, normally every weekday for several weeks. When the SPG task is applied in studies involving various experimental groups, training quickly becomes labor intensive, and can yield results with significant day-to-day variability. Furthermore, training is frequently done during the animals' light-cycle, which for nocturnal rodents such as mice and rats could affect performance. Here we describe an automated pellet presentation (APP) robotic system to train and test rats in the SPG task that reduces some of the procedural weaknesses of manual training. We found that APP trained rats performed significantly more trials per 24 hour period, and had higher success rates with less daily and weekly variability than manually trained rats. Moreover, the results show that success rates are positively correlated with the number of dark-cycle trials, suggesting that dark-cycle training has a positive effect on success rates. These results demonstrate that automated training is an effective method for evaluating and training skilled reaching performance of rats, opening up the possibility for new approaches to investigating the role of motor systems in enabling skilled forelimb use and new approaches to investigating rehabilitation following CNS injury.

Keywords: Single pellet grasp; Skilled motor task; Motor behaviour; Automated animal training; Rehabilitation

Abbreviations: Single pellet grasping (SPG), Automated pellet presentation (APP)

1. Introduction

Skilled motor tasks are effective research methods for studying the neural control of skilled movement and motor recovery after nervous system injury and disease (Bolton et al., 2006; Fouad et al., 2000; García-Alías et al., 2009; Kunkel-Bagden et al., 1993; Leblond et al., 2003; Montoya et al., 1991; Whishaw and Pellis, 1990). At the present time there are a number of manually administered reaching and stepping tasks available for the study of forepaw movement in rodents including the Montoya staircase test (Montoya et al., 1991; Nikkhah et al., 1998; Whishaw et al., 1997), the well-grasping test (García-Alías et al., 2009; Starkey et al., 2014), the Whishaw tray task (Whishaw et al., 1986), the horizontal ladder test (Bolton et al., 2006; Kunkel-Bagden et al., 1993; Metz and Whishaw, 2002), and the single pellet grasping (SPG) task (Whishaw and Pellis, 1990). However, it can be difficult and time consuming to train animals to perform many of these tasks. For example, the SPG task is a skilled motor task frequently used to evaluate rodent forelimb motor function (Whishaw and Pellis, 1990), and is an important method frequently used to assess motor recovery following various CNS injury models such as cervical spinal cord injury (García-Alías et al., 2009; Girgis et al., 2007; Krajacic et al., 2010), traumatic brain injury (Whishaw et al., 1991, 2004) and stroke (Alaverdashvili and Whishaw, 2010, 2013; Farr and Whishaw, 2002; Gharbawie et al., 2005; Gharbawie and Whishaw, 2006; MacLellan et al., 2006; Silasi et al., 2008).

There are a number of drawbacks to conventional use of manually administered reaching tasks. First, they can be procedurally time-consuming. In a conventional manually administered SPG task, a rat is placed within an SPG corridor task enclosure and must approach a narrow slit located in the wall at the front of the enclosure to grasp a food pellet located on a platform

beyond the slit. In this SPG protocol (Whishaw and Pellis, 1990), once the grasp attempt is complete the rat must return to the back of the enclosure before another pellet is placed on the platform.

Second, the SPG task can be considered a complex motor task given that success rates are well below 100% even in the most well trained rats (MacLellan *et al.*, 2006; Whishaw *et al.*, 2003), and success rates vary with the rat strain. As a result of its complexity, implementation of the SPG task requires extensive one-on-one researcher-to-rat manual training, especially in animals with CNS injuries (Alaverdashvili *et al.*, 2007). Despite the valuable forelimb motor function data that can be acquired using the SPG task, given the extensive training time required the SPG task is not well suited for high-throughput research such as drug screening studies.

Third, the extensive one-on-one researcher-to-rat training can be a source of variation between labs (MacLellan *et al.*, 2006; Whishaw *et al.*, 2003), and even from day to day within the same study (Fouad *et al.*, 2013). This variability is due, in part, to the methods of individual trainers, but could also be due to variability in the time of day or week training was performed. For instance, training is usually performed during the animals' light-cycle hours for experimenter convenience and thus conflict with the rodents' circadian cycle. A further contributor to success rate variability could be weekly training schedules. For instance, since training is rarely performed on weekends, success rates often follow a weekday cycle with lower success rates early in the week compared to later in the week (Fouad *et al.*, 2013). This weekly variation could be due to a variety of reasons, including the motivation of the animals that may have had *ad libitum* access to food for much of the weekend, or overall enthusiasm and motivation of the trainers at the beginning compared to the end of the week.

In a clinical setting it is well established that patients who receive intensive rehabilitation therapy after CNS injury have a more favorable prognosis of functional recovery compared to patients who receive minimal or no rehabilitation therapy. Thus, to study training related mechanisms in animal models, intensive training is a necessity. Intensive hind limb training (stepping) in animals can be accomplished using semi-automated devices such as training wheels within the home-cage (Engesser-Cesar *et al.*, 2005; Mandillo *et al.*, 2014). Intensive forelimb training, however, has proven difficult since (1) activity levels and motivation are low during the light-cycle in rats, (2) because of the extensive amounts of researcher time required to perform manual training and testing, and (3) the lack of appropriate automated devices for SPG training. These procedural drawbacks raise the question of whether the use of an automated procedure adapted to the rat circadian cycle might reduce methodological variability and enhance performance.

The purpose of the present study was to describe an Automated Pellet Presentation (APP) system to present pellets to rats 24 hours a day, 7 days a week. The effectiveness of the procedure was established by comparing APP trained rats to manually trained rats. Rats were successfully trained to perform the SPG task using the APP approach and had similar grasping movements to manually trained rats. We found that attempt rates were much higher during the dark-cycle using APP training, but there was no difference between light-cycle and dark-cycle success rates. Additionally, APP trained rats had higher and less variable attempt and success rates compared to manually trained rats, suggesting that APP training may be a useful high-throughput tool for modeling skilled forelimb movements.

2. Materials and methods

Forty-six female Lewis rats (Charles River Laboratories, Wilmington, MA, USA) weighing 200-240 g were trained either manually (n = 34 rats) or using APPRs (n = 12 rats) to perform the SPG task. All animals were housed in groups of 2 to 5 and kept on a 12/12 hour light/dark cycle. All procedures were approved by the Health Sciences Animal Care and Use Committee of the University of Alberta.

2.1 Manual SPG training

Manual SPG training followed the same training protocol as previously described (Girgis et al., 2007; Hurd et al., 2013). Briefly, upon arrival to the animal facility the rats had ad libitum access to rat chow and water. Several days prior to the start of SPG training the average food intake per rat per day was measured. On the day prior to each training session, food was restricted to 95% of the average food intake, usually between 9 and 11 g of food per rat per day, otherwise rats were fed *ad libitum*. Rats were weighed daily and their weight was maintained between 95 and 105% of start weight. Rats were provided one 20 minute training session on weekdays for 7 weeks.

To begin each training session, a rat was placed at the back of a standard acrylic SPG training chamber (45 cm long, 10 cm wide, 30 cm tall) with a 1 cm wide and 10 cm tall vertical slit in the front wall. Banana flavoured sugar pellets (45 mg, TestDiet, 5TUT sucrose tab, St. Louis USA) were placed on the pellet presentation shelf at the front of the chamber. Once the rat had approached the front of the chamber and had completed a grasp attempt, the trainer placed a sugar pellet at the back of the chamber to encourage the rat to return to the back of the enclosure. Once the rat had returned to the back of the enclosure, another pellet was placed on the pellet presentation shelf and the process was repeated for the entire session. Once the rat learned to

shuttle, pellets were no longer placed at the back of the enclosure. Following completion of each training session, the rat was returned to their home-cage.

2.2 Automated pellet presentation system

The APP system consists of an APP robot integrated within a modified SPG task enclosure, which is connected to the home-cage (Fig. 1A). The APP system was designed so that the rats had unrestricted access to their home-cage and the APP robot within the SPG enclosure 24 hours a day, 7 days a week, except during cleaning times. From within their home-cage, the rats had enrichment in the form of a PVC tube and a small cedar block 3 x 3 x 3 cm), and had *ad libitum* access to food and water. The home-cages were connected to the back of the task enclosures via a 5 cm diameter PVC tube. The task enclosures were 45 cm long, 10 cm wide, 30 cm tall, and made of clear acrylic sheets connected by right-angle joint fasteners. In the center of the front wall a 1 cm wide and 10 cm tall vertical slit was cut, through which the rats had access to the pellet platform. The enclosure floor was raised 10 cm above the base of the enclosure to accommodate the robotic machinery.

The APP robot was designed with three sections: a pellet retrieval and presenting system for positioning pellets on a platform beyond the enclosure slit, an adjustable barrier mechanism for limiting access to the pellet presentation platform, and sensors to determine whether a rat was located in the front of the enclosure (Fig. 1A,B). All electronic robotic components were purchased from Phidgets Inc. (Calgary, Canada), and robot-controller software written in Java using NeatBeans IDE 7.3. Motors were controlled using a PhidgetAdvancedServo 8-Motor controller board connected to a controller computer via USB. Sensor activity was monitored and LEDs were controlled using a PhidgetInterfaceKit 8/8/8 w/6 Port Hub connected to a controller

computer via USB. The robot frame was constructed of 20 mm extruded aluminum (Rocky Mountain Motion Control, Vancouver, Canada) and acrylic.

The pellet retrieval systems included a continuous rotation servo motor (3212_0 - SpringRC High Torque Servo Continuous Rotation (SM-S4315R)) coupled to a custom made pellet retrieval arm. The pellet retrieval arm had a 3 mm diameter loop at the distal tip, which we called the platform and could hold a single food pellet. In the initial testing phases of the APP system, we used the same sugar reward pellets as used for manual training, but due to high intake we switched to more nutritious banana flavoured grain-based food pellets (45 mg, TestDiet, 5TUM grain-based rodent tablet, St. Louis USA). To retrieve a pellet, the pellet arm motor was activated so the platform would pass through the pellet hopper and would continue to rotate until a pellet was detected on the pellet platform by the pellet sensor (1102_0 - IR Reflective Sensor 5mm), at which point a stop signal was sent to the pellet arm motor. The pellet retrieval process was repeated if the pellet sensor indicated the pellet had been removed from the pellet platform. Pellet retrieval arm speed was measured every 0.5 rotations using the pellet arm sensor (1102_0 - IR Reflective Sensor 5mm) and arm speed was adjusted by the controller software to maintain a rotational speed of about 0.2 Hz. As pellets were depleted from the hopper, the hopper was replenished from a pellet reservoir connected to the hopper near the pellet sensor. The location at which pellets were presented could be adjusted in 3D space (i.e., proximal-distal, medial-lateral, and up-down) relative to the slit opening by adjusting the position of the pellet retrieval system along the aluminum frame. Since each rat has a preference to use either their right or left paw to perform grasping tasks, manual SPG training enclosures typically have two fixed pellet presentation wells located about 0.5 cm left and 0.5 cm right relative to the center of the slit. Pellets are presented in the left well to rats with a right-paw preference, and pellets are presented

in the right well to rats with left-paw preference. With the APP system, presentation position was adjusted depending on the stage of training (see 2.3 Robot Training below) and the paw preference. Pellets were typically presented at a distance of 1.3 to 2 cm from the slit, up to 0.5 cm left or right of the center of the slit, and 2 cm up from the level of the enclosure floor.

Access beyond the slit was controlled by an adjustable barrier system. The barrier system consisted of a plastic barrier connected to a servo motor (3212_0 - SpringRC High Torque Servo Continuous Rotation (SM-S4315R) attached to the robot frame and located below the enclosure floor. Barriers had a spiral shape and were custom designed to block the slit to a height of 4.5 cm relative to the enclosure floor in the closed position, but only 2.0 cm in the open position to match the pellet presentation height. Barriers were ~3 mm thick, made of polylactic acid, and were fabricated on a homemade 3D printer. The position and velocity of the barrier was monitored using two proximity sensors (1102_0 - IR Reflective Sensor 5mm) located on either side of the enclosure, and the rotational speed of the barrier was maintained at 0.25 Hz.

Rat sensors were located in the front half of the enclosure and included two floor sensors located between a fixed base floor and a thin acrylic floating floor above the sensors held in place by four loosely fastened bolts. Pressure on the floating floor activated the floor sensors thus indicating the presence of a rat. The floating floor was removed and cleaned daily, and the space between the floating and fixed floors was cleared of all debris (e.g., bedding) daily to maintain the reliability of the sensor readings. Additionally, a proximity sensor (1103_1 - IR Reflective Sensor 10cm) was positioned in the middle of the enclosure to detect rats that were resting their forepaws on the floating floor (i.e., remained within the front half of the enclosure) without activating the floor sensors. Together, these sensors could effectively detect the presence of a rat

in the front half of the enclosure.

2.3 SPG task training using the APP system

SPG task training was divided into three stages (Fig. 1C). Stage 1 was designed to allow the rats to acclimatize to the pellet presentation system and to have easy access to the pellets. In Stage 1 the rat sensor system was deactivated and the pellets were presented very close to the slit opening (<15 mm) and aligned with the center of the slit. In this configuration, the rats had easy access to the pellets and were not required to return to the back of the enclosure for subsequent pellet presentation. All rats that had at least one day with ≥ 30 trials (n = 11 of 12) in Stage 1 were considered to have learned the location of the pellets and proceeded to Stage 2.

Given the closeness of the pellets in Stage 1 (<15 mm), a small number of rats (n = 3) preferentially obtained pellets by licking rather than grasping. Stage 2 was designed to promote forelimb grasping instead of licking and to train the rats to move to the back of the enclosure for each trial. To train the rats to move to the back of the enclosure, the barrier would remain closed until there was no rat detected by the rat sensors in the front half of the enclosure. Since a rat forepaw can reach through the slit further than an extended tongue, the distance of the pellet from the slit was gradually increased by 0.5-1 mm every 3-7d from <15 mm to as high as 20 mm, until the rats no longer attempted to obtain pellets by licking. In most cases licking ceased when the pellets were positioned at ~16 mm from the slit, but one rat (n = 1 of 12) made only lick attempts regardless of pellet distance and therefore did not proceed to Stage 3. The pellets were moved progressively more distal for all groups regardless of whether the group contained a rat that licked pellets.

In Stage 3 the rats were housed according to their preferred paw. Additionally, the APP

robot was setup so that the pellet presentation platform was located at 14.5-15 mm from the slit opening and aligned with the left edge of the slit for right-pawed rats or the right edge of the slit for left-pawed rats. In this configuration rats did not relapse into obtaining pellets by licking. The APP system remained in this configuration for the remainder of training.

2.4 Video recording and processing

Rats were video monitored 24 hours a day, 7 days a week using Blue Iris software (v. 3.5) and Foscam light/dark digital cameras (FI9821W) equipped with integrated infrared LEDs for dark-cycle recording. The cameras automatically activated the LED array and switched input gain and intensity during the dark-cycle. Video was continuously acquired using BlueIris software (v. 3.5; Perspective Software). To reduce video storage requirement and to optimize analysis, videos were saved using motion trigger software integrated into the BlueIris program. The motion detection zone was set as a 1 x 1 cm zone at the front of the enclosure. Whenever the rat was positioned to perform a grasp attempt, the motion detection trigger was activated. The motion detection trigger would remain active for 6 s unless retriggered. Upon triggering, the software saved a time-stamped video file that included the 3 s prior to triggering plus the entire time the trigger was activated. Video quality was set at 30 fps, with a resolution of 640 x 480.

High-speed video was acquired using an IMPERX (IPX-VGA210) camera and was used for grasp motion analysis.

2.5 Analysis

Videos were analyzed using BlueIris software. Analysis was performed on raw video and the outcome of each attempt to obtain a pellet. An attempt was defined as a clear forward motion

of the dominant forepaw beyond the threshold of the slit opening towards the pellet platform. Attempts were evaluated as pass, fail, or cheat.

Pass. A pass was scored when the rat successfully grasped a pellet from the pellet platform using their preferred forepaw and brought it back through the slit into the task enclosure.

Fail. A fail was scored when the rat made a grasp attempt, but failed to bring the pellet back through the slit.

Cheat. A cheat was scored when the rat tried to obtain a pellet using their tongue.

During some attempts, more than one rat was present in the enclosure at the same time. In cases where a rat made an attempt while another rat was located at the back of the enclosure and did not obstruct the movements of the attempting rat to move towards the slit and reach for the pellet, the trial was included in the study. If the other rat was located towards the front of the enclosure and obstructed access to the slit or the reaching movements of the attempting rat, the attempt was not considered a trial and was excluded.

For quantification purposes, each APP training session was considered as one light-dark cycle starting at lights-on. Rats were weighed daily partway through the light-cycle. Home-cage food consumption was measured daily and the average home-cage food per rat was calculated. For overall food consumption per rat, the number of food pellets obtained by the rat was multiplied by the weight of the food pellets (45 mg/pellet) and added to the average home-cage food consumed per rat.

Statistical analysis was performed using t-test and non-parametric tests including Mann-

Whitney-U test and Wilcoxon Signed-Rank test. Only training days with >5 trials were included for comparing SPG success rates. All averages are presented as mean ± SEM. Significance was set as $p < 0.05$.

3. Results

3.1 APP system for training rats to perform the SPG task

Our goals included to test whether rats have a higher SPG success rate during their dark-cycle compared to their light-cycle, and determine whether automated robotic *ad libitum* training of the SPG task resulted in less daily and weekly variation in SPG success rate than manually trained rats. For this we designed and built an APP system to automatically present pellets to train rats to perform the SPG task and test their overall SPG success rate once trained. Throughout the design process of the APP system we aimed for the device to be very well tolerated by the rats, safe, reliable, and require minimal maintenance. We found that APP trained rats tolerated the addition of the APP system to their home cage very well, continued to gain weight (Fig. 2A) and maintain food intake (average = 2.3 ± 0.2 g of pellet food and 10.2 ± 0.5 g of home-cage chow per rat per day) throughout all three stages of training (Fig. 2B).

Examples of performance are illustrated in (Fig. 3; Videos 1-3). The total number of trials evaluated for this study was n = 69,696 (average per rat = 7744 ± 827 SEM.), with 8,920 trials at Stage 1 (average per rat = 991 ± 219 SEM), 28,270 trials at Stage 2 (average per rat = 3,141 ± 637 SEM), and 32,506 trials at Stage 3 (average per rat = 3611 ± 499 SEM). Rats were housed and trained in groups of 2 (n = 2 rats), 3 (n = 6 rats), or 4 (n = 4 rats) per APP system. A total of 12 rats began training and 9 were successfully trained to perform the SPG task using the APP system. The greatest training success was observed with rats trained in groups of 2 (n = 2 of 2

trained), followed by groups of 3 (n = 5 of 6 trained), and groups of 4 (n = 2 of 4 trained). This progressive decrease in training success with increased number of rats per APP system was likely due to increased competition for access to the pellet platform in cages with higher rat-APP ratios, which resulted in reduced training by non-dominant rats.

3.2 Grasp kinematics are similar for manually trained and robot trained rats

To determine whether robot trained rats have altered grasp movements compared to manually trained rats, high-speed videos of grasp attempts were acquired. Frame-by-frame analysis of the videos showed that the grasp movements of APP trained rats were similar to those described for other albino rats (Whishaw et al., 2003). A representative example of a successful grasp attempt is shown in Fig. 4 and Video 4. Frame-by-frame motion analysis revealed that the APP trained rat began by sniffing the pellet (Frame 43). The grasping limb was then lifted and moved towards the midline with the digits flexed and closed (Frame 62). The aim movement occurred as part of the advance movement, with the digits extending during the advance (Frame 69). With the downward movement there was little to no pronation, but rather the paw came straight down with digits opening (Frame 74), and the food was caught between the second and third digit (Frame 76). As the limb was retracted there was little supination as the paw was dragged straight back to the edge of the shelf where it was contacted by the mouth (Frame 83). The food is eaten using both forepaws with full weight support on the hindquarters (Frame 112).

3.3 APP training stages

Training proceeded in three stages and behaviour of the rats varied as the rats progressed through the stages.

Stage 1. Stage 1 of training was designed to acquaint the rats with the APP system and to allow them to learn that pellets were present on a pellet platform beyond the slit in the front wall. It took the rats 3-6 d (average = 4.2 ± 0.5) to make at least 30 trials in a single light-dark cycle period. The number of trials per rat increased dramatically from as low as 0 trials per day at 0-4 d (average = 44.4 ± 14.6) up to 630 trials per training session at 5-7 d (average = 294.0 ± 35.6; Fig. 5A). As the number of trials increased there was a concomitant increase in SPG success rate from as low as 0% at 0-4 d (average = 14.4% ± 3.2) up to 63% at 5-7 d (average = 41.5% ± 3.1; Fig. 5A).

Stage 2. Stage 2 was designed to eliminate licking trials and to train the rats to return to the back of the enclosure at the end of each trial. Seven rats spent an average of 23 d in Stage 2, and the remaining 2 rats had 45 d of Stage 2 training. The time each group spent in this stage was dependent on the extent of cheating attempts, whereby a group of rats with a persistent cheater spent longer in the stage compared to groups without cheaters. Although most APP trained rats (n = 7 of 9) did not cheat, and therefore did not require Stage 2 training, these rats still received this training to maintain grouping arrangements. Compared to the final three days of Stage 1 training, in Stage 2 there was a considerable drop in attempt rate (average = 128.7 ± 7.7) and SPG success rate (average = 30.5% ± 1.4; Fig. 5B). Reduced motivation and grasping success rates in the first 1-2 d of Stage 2 training was likely because the rats had to learn to return to the back of the enclosure at the end of each trial. At later time-points the low attempt rates and grasping success rates were likely due to the progressive increases in pellet distance from the slit.

Stage 3. Stage 3 rats were housed according to their preferred paw and pellets were located close to the slit (14.5-15 mm) and offset to the edge of the slit opposite the preferred paw

for that group of rats. Rats spent 12-24 d in Stage 3 (average = 19 d ± 2). In this stage rats were skilled and efficient at performing SPG trials, often reaching attempt rates near the maximum presentation rate of the APP system (maximum pellet presentation rate of approximately 4 pellets per minute with the configuration used for this study). Most rats had immediate increases in SPG attempt and success rates at the start of Stage 3 compared to the end of Stage 2 (Fig. 5C). Both the number of trials per day (average = 177 ± 5.2) and daily SPG success rates (average = 45.5 % ± 1.2) were higher than Stage 2.

3.4 Performance as a function of circadian cycle

Since the APP trained rats were free to train at any point in the light-dark cycle, the attempt and SPG success rates were compared between training during the light-cycle and dark-cycle. Not surprisingly, attempt rates were significantly higher at dark for all stages (Fig. 6A). The proportion of dark-cycle attempt rates also increased for each training stage, with about 11:1, 15:1, and 20:1 dark- to light-cycle attempt ratios in stages 1, 2, and 3 respectively.

Given that rats are nocturnal, we hypothesized that SPG success rates would be higher during the dark-cycle compared to the light-cycle. However, only Stage 1 had a significantly higher SPG success rate during the dark- compared to light-cycles (Fig. 6B). To determine whether SPG success rates were dependent on the number of attempts we compared the average SPG% to average attempt rate per training session (i.e., 24 h cycle; Fig. 6C). There was a strong positive correlation between the average number of attempts and average SPG% per training session (Correlation coefficient = 0.807, Spearman Rank Order Correlation $p < 0.01$). Next, given the strong effect of training on success rates, to determine whether dark- and light-cycle training were independently correlated to SPG success rates, the average number of dark- and light-cycle

attempts was compared to the average dark- and light-cycle SPG% respectively. There was a strong positive correlation between the average number of dark-cycle attempts and average dark-cycle SPG% (Correlation coefficient = 0.795, Spearman Rank Order Correlation $p < 0.01$; Fig. 6D), but no significant correlation between the average number of light-cycle attempts and average light-cycle SPG% (Correlation coefficient = 0.167, Spearman Rank Order Correlation $p = 0.643$; Fig. 6E). Together, these data show that SPG success rates are dependent on the attempt rates, and since the majority of attempts are made during the dark-cycle, dark-cycle training is a key part of APP training.

3.5 Comparison of APP and SPG performance

To compare APP training to manual training, 34 rats were manually trained to perform the SPG task using a standard training protocol. Of these 34 rats, 31 were successfully trained to perform the SPG task and included in the study. Attempt rates for these rats increased slightly with time, with an overall average of 17.3 ± 0.5 trials per day (Fig. 7A). In the first 11 training sessions (from 0-14 d) the overall daily attempt rates were considerably lower than the overall rates (average = 7.3 ± 0.6). SPG success rates were also low in early training sessions (average = 8.8 ± 1.1 %), especially in the first 9 training sessions (0-12d) followed by a sharp upswing on training sessions 10 and 11 on days 13 and 14 respectively (Fig 7A, bottom). Considering the low attempt and success rates followed by a sharp upswing, days 0-14 of manual training were considered the 'learning' sessions, comparable to Stage 1 of APP training. Following the learning sessions, overall daily attempt rates were higher (average = 22.1 ± 0.6), and SPG success rates of manually trained animals remained fairly constant from days 15-44 (average = 30.4 ± 0.1 %), comparable to Stage 3 of the APP trained rats. When average attempt and SPG

success rates were compared between APP and manually trained rats, APP trained rats were found to perform significantly more trials with a higher SPG success rate than manually trained animals (Fig. 7B-C). However, given the large difference between APP and manual attempts rates, it is possible that on a per-trial basis, manual training may be more efficient. Comparison of the average number of cumulative trials required for each rat to attain an SPG% of 15, 20, 25, and 30% in a given training session revealed that manually trained rats require fewer trials to reach SPG% milestones than APP trained rats (Fig. 7D).

In comparison with APP training, where pellet presentation parameters remain constant, it is possible that manual training parameters could change from day-to-day depending on the status and motivation of the trainer (e.g., pellets are inadvertently presented more quickly towards the end of the week or trainer enthusiasm changes throughout the week), or that breaks in training (e.g., no training on weekends) could affect SPG% depending on the day of the week. To test whether this is the case, the normalized SPG success rates were grouped according to day of the week and compared between APP trained rats and manually trained rats (Fig. 7E). Average success rates remained within 6.3 ± 4.9 % of baseline for APP trained rats. The average grasping success rates of manually trained rats was significantly higher than baseline on both Thursdays (average = 124.7 ± 11.8% of baseline) and Fridays (average = 117.9 ± 9.6% of baseline; Fig. 7E-F). Next, to test if the SPG% varied significantly between training sessions, the absolute difference in SPG% for each successive training session was calculated for all APP Stage 3 and Manual Plateau Stage training sessions for each rat. For APP trained rats, the average difference in SPG% from one training session to the next (average = 10.5 ± 1.2 %) was significantly smaller than for manually trained rats (average = 15.1 ± 1.1 %; Fig. 7G).

Although APP trained rats have higher and less variable SPG success rates, given that they also perform significantly more trials per 24 h cycle and train over the weekends, it is possible that APP increases the overall amount of researcher time spent training each rat. To test whether this is the case, the amount of researcher time required to train each rat was calculated and compared between APP Stage 3 and Manual Plateau Stage training. As a first step, for APP trained rats the time required to analyze the videos of several hundred trials was measured and the average time required for each trial was calculated to be 2.5 s (Fig. 7H). Next, the amount of researcher time per rat per week was calculated by multiplying the average time trial evaluation time (n = 3 s/trial) by the average daily attempt rat (n = 177 trials/day) by the number of training days per week (n = 7), to yield an average of 52 min/rat/week (Fig. 7I). For manually trained rats, each rat performed an average of 22.1 trials per 20 min training session, resulting in an average of 54 s per trial (Fig. 7H), which is considerably slower than APP trial evaluation. The average amount of researcher time per week for manually trained animals was fixed at 20 min/d multiplied by 5d/week, to yield an average of 100 min/rat/week, which is roughly twice the time per week as APP trained rats (Fig. 7I). Collectively, these data suggest that APP trained rats have higher and less variable average success rates, and require less trainer time than manually trained rats.

4. Discussion

Skilled motor tasks such as the SPG task are important research tools for evaluating motor function and recovery from CNS injuries and other CNS pathologies (Alaverdashvili and Whishaw, 2010, 2013; Biernaskie et al., 2005; Bretzner et al., 2008; Gharbawie et al., 2005; Gharbawie and Whishaw, 2006; Girgis et al., 2007; Kanagal and Muir, 2007; MacLellan et al.,

2006; Silasi et al., 2008; Weishaupt, Li, et al., 2013; Weishaupt, Vavrek, et al., 2013; Whishaw et al., 1991, 2004). However, manual training is difficult and time-consuming, thus precluding the usefulness of the SPG task for high-throughput studies such as drug screening studies and rehabilitation studies that include multiple treatment groups. Here we describe an automated training technique that can extend the usefulness of the SPG task and reduce performance variability related to circadian cycles, food-deprivation related motivation, and other training-related variation. We show that rats can be trained to perform the SPG task using an automated *ad libitum* pellet presentation system, which significantly improved SPG success rates and reduced variability compared to manual training.

4.1 Practical advantages of APP training

To our knowledge, this is the first study to describe an automated method for training animals to perform the SPG task *ad libitum* for 24 hours a day, 7 days a week. From a practical perspective, although APP systems take longer and more technical skill to setup, once established training with the APP system provides several key advantages over manual training. For example, manual training requires researchers to be in close contact with rats for long periods of time on a regular basis. Rats are highly allergenic (Acton and McCauley, 2007; Bush et al., 1998; Seward, 1999, 2001), meaning that manual trainers are at high risk of suffering allergic responses as a result of training. APP training requires minimal contact with the animals thus reducing the risk of contracting rat allergies.

Rats learned to obtain pellets from the pellet platform in an average of 4.2 d and to move to the back of the enclosure for each pellet within 1-2 d thereafter, thus SPG training required about 5-6 d using the APP system compared to 14 d (11 training sessions) for manually trained

animals. Although APP trained rats achieved a higher overall SPG% with fewer training sessions, it required significantly more trials for APP rats to learn the task, suggesting that obtaining pellets using the APP system is more challenging than in manual task enclosures. This increased difficulty of the SPG task with the APP system is likely because slight grasping errors can result in the pellet being knocked from the pellet platform and lost, whereas the pellet presentation shelf of manual training enclosures may provide more tactile feedback (e.g., the fingers can form an arpeggio on the shelf beyond the pellet, thus orienting the fingertips) and allow the pellet to be slightly displaced without falling from the shelf. Furthermore, using APP training enforces grasping for pellets, as it does not allow sliding the pellet towards the enclosure. Moreover, rapid learning of the task in the APP system is partly offset by the few animals that licked the pellets from the platform and required Stage 2 training. Since only a few animals cheated, one possible approach for reducing training time would be to transfer all animals that do not cheat directly to Stage 3. An even simpler approach could be to simply transfer all animals directly from Stage 1 to Stage 3 since the pellets are left- or right-shifted to the edge of the slit away from the preferred paw in Stage 3, which may be sufficient to preclude licking. Regardless, even with Stage 2 the APP system greatly reduces the amount of researcher-time required to train rats to perform the SPG task, thus significantly reducing the cost of implementing the SPG task and making it more suitable for high-throughput studies.

With the APP system rats have *ad libitum* easy access to standard chow in their home cage meaning that they do not need to obtain pellets to achieve satiety, yet their attempt rates for obtaining pellets are remarkably high compared to food restricted manually trained animals. These high attempt rates suggest that rats are highly motivated to obtain the flavoured pellets offered by the APP system despite the extra effort required to obtain each pellet (i.e., to obtain a

pellet requires moving from the front to the back of the enclosure and includes the risk of not obtaining a pellet). The idea that the rats are motivated to interact with the APP system independent of a drive to reach satiety is further reinforced by the fact that the APP system uses less sweet grain-based food pellets instead of the highly palatable sugar reward pellets often used for manual training. Taken together, the APP system could be considered a form of housing enrichment.

4.2 Scientific advantages of APP training

APP training also has several scientific advantages over manual training. Importantly, APP trained rats have higher success rates with less weekly and daily variability than manually trained rats. The high variability with manual training could be due to virtually uncontrollable factors such as small changes in motivation and enthusiasm of the trainer from day-to-day, or a 'buildup' training effect throughout the week such that animals perform better later in the week following several days of daily training, but is lost over the weekend with no training. Less variability with APP training allows for the detection of more subtle changes in success and attempt rates compared to manual training. For example, changes in environment such as different enrichment in the home cage or changes in social networks such as new cage mates could be more easily detectable with APP training. Alternatively, APP training could be used as a high-throughput way to detect subtle effects of drugs on motivation or motor function.

For manually trained rats, there is a positive correlation between the amount of training and the overall success rate (Fouad et al., unpublished results), but the precise relationship between intense training and success rates remains poorly understood and a 'training-peak' has yet to be identified (i.e., the point at which increased training does not result in higher SPG

success rates). One way to explore the relationship between training intensity and success rates would be to increase the amount of training each rat receives. The APP system could be an important tool for precisely controlling training intensity levels for identifying training-peaks, optimizing the amount of training, determining minimum training thresholds for rehabilitation, and by maximizing training it would be easier to study mechanisms translating to plasticity. For example, the APP system could be programmed to present pellets more slowly or more quickly, or only at certain times of day to either increase or decrease attempt rates and thus control the amount of training.

To our knowledge, this is the first study to include dark-cycle training for the SPG task. Similar to the present study, rat training activity has been shown to increase during the dark-cycle when rats are permitted to train *ad libitum* (Engesser-Cesar et al., 2005; Mandillo et al., 2014; Starkey et al., 2014). Moreover, post-stroke rats trained to perform a reaching task during the light-cycle made roughly half as many reach attempts, show little functional recovery, and no evidence of elevated BDNF in the motor cortex compared to post-stroke rats trained during the dark-cycle (MacLellan et al., 2011). The low SPG success rates from manually trained rats may therefore be partly due to their being trained during the day-cycle. Whether manually training during the dark-cycle would improve attempt and success rates to that of APP trained rats remains to be tested. Interestingly, we found no difference in the light- and dark-cycle success rates despite a large difference in the training rates between these two times, suggesting that light-cycle success could be dependent on dark-cycle training. This was confirmed since both light- and dark-cycle success rates were positively correlated with the number of dark-cycle trials, whereas success rates were independent of the number of light-cycle trials. These data show that dark-cycle training is essential for achieving high success rates with the APP system.

Several other forelimb motor function testing methods exist, such as the Montoya staircase test (Montoya et al., 1991; Nikkhah et al., 1998; Whishaw et al., 1997), the isometric pull task (Hays et al., 2013), horizontal ladder (Bolton et al., 2006; Kunkel-Bagden et al., 1993; Metz and Whishaw, 2002), and the well-grasping test (García-Alías et al., 2009; Starkey et al., 2014), which have both advantages and limitations compared to the SPG task. In the case of Montoya staircase testing, the rats must reach through slits in the right and left side of an enclosure to obtain pellets located in bowls at different depths relative to the slit openings. This test is higher throughput than manual SPG training and has the advantage of being able to compare affected to unaffected paw separately when using CNS injury models. The Montoya staircase task is, however, a less complex task than the SPG task and it is difficult to differentiate between successes due to compensation and those due to motor recovery after CNS injury, (Whishaw et al., 1997), making it hard to decipher the mechanisms of recovery. Similar to the Montoya staircase test, the hole-grasping task requires the rat to reach down through a deep hole in the floor to obtain food rewards (García-Alías et al., 2009; Starkey et al., 2014). This test is comparatively simple and requires less training than manual SPG training, but it has had limited use compared to the other tasks and very little kinematic data can be acquired using this test. Horizontal ladder testing requires the rat to traverse a walkway in which the floor is replaced by a series of horizontal bars. Slips, forepaw missteps and kinematics are compared between treatment groups as a measure of forepaw motor function. Horizontal ladder requires less training than manual SPG training, but is not as specific a test for forelimb function because rat balance and slips from other limbs can have major effects on the forelimb of interest, especially in rats with CNS injuries. Finally, the isometric pull task requires the animal to grasp and pull a bar located beyond a slit, for which they receive an easily accessible food reward from a food

dispenser located next to the slit (Hays et al., 2013). The bar is attached to force sensors, which can measure the force generated by the grasp motion. This approach can provide important insight regarding the forces generated over time following CNS or peripheral injury, but since the bars do not move, it is impossible to know whether this form of training translates into improved pellet grasping and retrieval.

Given that these other forelimb tasks are well suited for testing a variety of forelimb motions and that all of these tests currently require manual training and testing for their implementation, it may be useful to adapt the APP system for training and testing rats in other tasks. For instance, the pellet presentation arm could be modified for easy pellet retrieval and moved to within a few millimeters of the slit opening, so the rats could obtain pellets by licking or knocking the pellets into the enclosure with nearly 100% success regardless of forelimb motor function. In this configuration, since the APP system is already designed to have the rat move to the back of the enclosure for each trial, it is possible to have the rat move across a variety of floor types (e.g., horizontal ladder) or through obstacle courses to obtain reward pellets. Alternatively, pellets could be presented at different depths through holes in the floor to automate the hole-grasping test, or at different depths below slit openings in the floor along the side edges of the enclosure to automate the Montoya staircase test. With these alternative devices it would also be possible to attach several APP training systems to a single home-cage for automated training and testing of a variety of motor function tasks simultaneously.

4.3 Significance for data quality, human studies, and high-throughput studies

The APP method has a much higher-throughput than manual SPG training. Reduced fine motor function can be a subtle but important side-effect of numerous drug treatments, and it is

important to identify these potential side-effects in early stages of drug development using animal models rather than in expensive drug trials. Large scale drug screening studies often have many treatment groups and thus require automation for cost- and time-effective implementation. The high-throughput advantage of APP training makes it suitable for testing skilled forelimb motor function as part of drug screening studies. However, once promising drug candidates are identified for human trials, it can be difficult to compare rodent behavioural results to human clinical tests. For more direct comparisons between animal experiments and human trials, this task could be automated for humans giving a parallel rodent human research methodology.

In a clinical setting, rehabilitation therapy is one of the most useful and universally prescribed treatment strategies for CNS injuries such as stroke, spinal cord injury, and traumatic brain injury, and can be important in the treatment of neurodegenerative diseases such as Parkinson's disease, multiple sclerosis, and dementia. Moreover, rehabilitation therapy is complimentary, and often necessary, for translating drug and cell treatments into meaningful functional recovery. Performing the SPG task is the equivalent of rehabilitation therapy for skilled forelimb motor function in the rat. Since CNS injury patients will almost certainly get rehabilitation therapy, it is important that all studies evaluating drug and cell treatment strategies include rehabilitation therapy to more fully mimic clinical approaches (Fouad and Tetzlaff, 2012). Moreover, drug and cell treatment studies often have multiple treatment groups, making it difficult to include rehabilitation therapy in these studies. The APP approach could be a time-effective and relevant approach for integrating rehabilitation therapy when testing the efficacy of drug and cell treatment strategies.

Taken together, APP training adds enrichment and reduced food stress on the animals, is

less work for researchers, more efficient, and allows one to explore training without time limitations or restrictions.

Acknowledgements

This work was supported by operating grants from the Canadian Institute for Health Research (CIHR) K.K.F. was supported by CIHR and Alberta Innovates Health Solutions (AIHS) Post-Doctoral Fellowships. We thank Arthur Prochazka for providing robot fabrication equipment and Michel Gauthier for technical assistance. The authors KKF, and KF have a provisional patent for the automated training robots used in this study.

References

Acton D, McCauley L. Laboratory animal allergy: an occupational hazard. AAOHN J. Off. J. Am. Assoc. Occup. Health Nurses 2007; 55: 241–244.

Alaverdashvili M, Lim DH, Whishaw IQ. No improvement by amphetamine on learned non-use, attempts, success or movement in skilled reaching by the rat after motor cortex stroke. Eur. J. Neurosci. 2007; 25: 3442–3452.

Alaverdashvili M, Whishaw IQ. Compensation aids skilled reaching in aging and in recovery from forelimb motor cortex stroke in the rat. Neuroscience 2010; 167: 21–30.

Alaverdashvili M, Whishaw IQ. A behavioral method for identifying recovery and compensation: hand use in a preclinical stroke model using the single pellet reaching task. Neurosci. Biobehav. Rev. 2013; 37: 950–967.

Biernaskie J, Szymanska A, Windle V, Corbett D. Bi-hemispheric contribution to functional

motor recovery of the affected forelimb following focal ischemic brain injury in rats. Eur. J. Neurosci. 2005; 21: 989–999.

Bolton DAE, Tse ADY, Ballermann M, Misiaszek JE, Fouad K. Task specific adaptations in rat locomotion: runway versus horizontal ladder. Behav. Brain Res. 2006; 168: 272–279.

Bretzner F, Liu J, Currie E, Roskams AJ, Tetzlaff W. Undesired effects of a combinatorial treatment for spinal cord injury--transplantation of olfactory ensheathing cells and BDNF infusion to the red nucleus. Eur. J. Neurosci. 2008; 28: 1795–1807.

Bush RK, Wood RA, Eggleston PA. Laboratory animal allergy. J. Allergy Clin. Immunol. 1998; 102: 99–112.

Engesser-Cesar C, Anderson AJ, Basso DM, Edgerton VR, Cotman CW. Voluntary wheel running improves recovery from a moderate spinal cord injury. J. Neurotrauma 2005; 22: 157–171.

Farr TD, Whishaw IQ. Quantitative and qualitative impairments in skilled reaching in the mouse (Mus musculus) after a focal motor cortex stroke. Stroke J. Cereb. Circ. 2002; 33: 1869–1875.

Fouad K, Hurd C, Magnuson DSK. Functional testing in animal models of spinal cord injury: not as straight forward as one would think. Front. Integr. Neurosci. 2013; 7: 85.

Fouad K, Metz GA, Merkler D, Dietz V, Schwab ME. Treadmill training in incomplete spinal cord injured rats. BehavBrain Res 2000; 115: 107–113.

Fouad K, Tetzlaff W. Rehabilitative training and plasticity following spinal cord injury. Exp.

Neurol. 2012; 235: 91–99.

García-Alías G, Barkhuysen S, Buckle M, Fawcett JW. Chondroitinase ABC treatment opens a window of opportunity for task-specific rehabilitation. Nat. Neurosci. 2009; 12: 1145–1151.

Gharbawie OA, Gonzalez CLR, Whishaw IQ. Skilled reaching impairments from the lateral frontal cortex component of middle cerebral artery stroke: a qualitative and quantitative comparison to focal motor cortex lesions in rats. Behav. Brain Res. 2005; 156: 125–137.

Gharbawie OA, Whishaw IQ. Parallel stages of learning and recovery of skilled reaching after motor cortex stroke: 'oppositions' organize normal and compensatory movements. Behav. Brain Res. 2006; 175: 249–262.

Girgis J, Merrett D, Kirkland S, Metz G a. S, Verge V, Fouad K. Reaching training in rats with spinal cord injury promotes plasticity and task specific recovery. Brain J. Neurol. 2007; 130: 2993–3003.

Hays SA, Khodaparast N, Sloan AM, Hulsey DR, Pantoja M, Ruiz AD, et al. The isometric pull task: a novel automated method for quantifying forelimb force generation in rats. J. Neurosci. Methods 2013; 212: 329–337.

Hurd C, Weishaupt N, Fouad K. Anatomical correlates of recovery in single pellet reaching in spinal cord injured rats. Exp. Neurol. 2013; 247: 605–614.

Kanagal SG, Muir GD. Bilateral dorsal funicular lesions alter sensorimotor behaviour in rats. Exp. Neurol. 2007; 205: 513–524.

Krajacic A, Weishaupt N, Girgis J, Tetzlaff W, Fouad K. Training-induced plasticity in rats with cervical spinal cord injury: effects and side effects. Behav. Brain Res. 2010; 214: 323–331.

Kunkel-Bagden E, Dai HN, Bregman BS. Methods to assess the development and recovery of locomotor function after spinal cord injury in rats. Exp. Neurol. 1993; 119: 153–164.

Leblond H, L'Esperance M, Orsal D, Rossignol S. Treadmill locomotion in the intact and spinal mouse. J Neurosci 2003; 23: 11411–11419.

MacLellan CL, Gyawali S, Colbourne F. Skilled reaching impairments follow intrastriatal hemorrhagic stroke in rats. Behav. Brain Res. 2006; 175: 82–89.

MacLellan CL, Keough MB, Granter-Button S, Chernenko GA, Butt S, Corbett D. A critical threshold of rehabilitation involving brain-derived neurotrophic factor is required for poststroke recovery. Neurorehabil. Neural Repair 2011; 25: 740–748.

Mandillo S, Heise I, Garbugino L, Tocchini-Valentini GP, Giuliani A, Wells S, et al. Early motor deficits in mouse disease models are reliably uncovered using an automated home-cage wheel-running system: a cross-laboratory validation. Dis. Model. Mech. 2014; 7: 397–407.

Metz GA, Whishaw IQ. Cortical and subcortical lesions impair skilled walking in the ladder rung walking test: a new task to evaluate fore- and hindlimb stepping, placing, and co-ordination. J. Neurosci. Methods 2002; 115: 169–179.

Montoya CP, Campbell-Hope LJ, Pemberton KD, Dunnett SB. The 'staircase test': a measure of

independent forelimb reaching and grasping abilities in rats. J. Neurosci. Methods 1991; 36: 219–228.

Nikkhah G, Rosenthal C, Hedrich HJ, Samii M. Differences in acquisition and full performance in skilled forelimb use as measured by the 'staircase test' in five rat strains. Behav. Brain Res. 1998; 92: 85–95.

Seward JP. Occupational allergy to animals. Occup. Med. Phila. Pa 1999; 14: 285–304.

Seward JP. Medical surveillance of allergy in laboratory animal handlers. ILAR J. Natl. Res. Counc. Inst. Lab. Anim. Resour. 2001; 42: 47–54.

Silasi G, Hamilton DA, Kolb B. Social instability blocks functional restitution following motor cortex stroke in rats. Behav. Brain Res. 2008; 188: 219–226.

Starkey ML, Bleul C, Kasper H, Mosberger AC, Zorner B, Giger S, et al. High-Impact, Self-Motivated Training Within an Enriched Environment With Single Animal Tracking Dose-Dependently Promotes Motor Skill Acquisition and Functional Recovery. Neurorehabil. Neural Repair 2014; 28: 594–605.

Weishaupt N, Li S, Di Pardo A, Sipione S, Fouad K. Synergistic effects of BDNF and rehabilitative training on recovery after cervical spinal cord injury. Behav. Brain Res. 2013; 239: 31–42.

Weishaupt N, Vavrek R, Fouad K. Training following unilateral cervical spinal cord injury in rats affects the contralesional forelimb. Neurosci. Lett. 2013; 539: 77–81.

Whishaw IQ, Gorny B, Foroud A, Kleim JA. Long-Evans and Sprague-Dawley rats have similar

skilled reaching success and limb representations in motor cortex but different movements: some cautionary insights into the selection of rat strains for neurobiological motor research. Behav. Brain Res. 2003; 145: 221–232.

Whishaw IQ, O'Connor WT, Dunnett SB. The contributions of motor cortex, nigrostriatal dopamine and caudate-putamen to skilled forelimb use in the rat. Brain J. Neurol. 1986; 109 (Pt 5): 805–843.

Whishaw IQ, Pellis SM. The structure of skilled forelimb reaching in the rat: a proximally driven movement with a single distal rotatory component. Behav. Brain Res. 1990; 41: 49–59.

Whishaw IQ, Pellis SM, Gorny BP, Pellis VC. The impairments in reaching and the movements of compensation in rats with motor cortex lesions: an endpoint, videorecording, and movement notation analysis. Behav. Brain Res. 1991; 42: 77–91.

Whishaw IQ, Piecharka DM, Zeeb F, Stein DG. Unilateral frontal lobe contusion and forelimb function: chronic quantitative and qualitative impairments in reflexive and skilled forelimb movements in rats. J. Neurotrauma 2004; 21: 1584–1600.

Whishaw IQ, Woodward NC, Miklyaeva E, Pellis SM. Analysis of limb use by control rats and unilateral DA-depleted rats in the Montoya staircase test: movements, impairments and compensatory strategies. Behav. Brain Res. 1997; 89: 167–177.

Figures

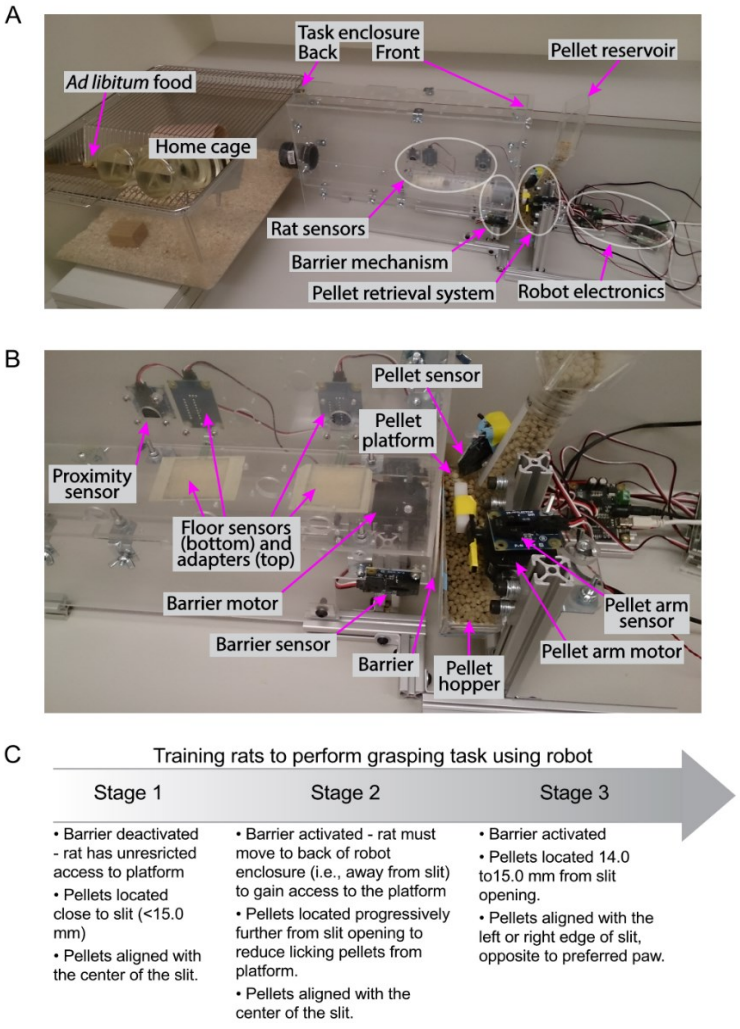

Figure 1. The APP system for automated continuous SPG training. A, Image of an APP system showing the home cage (left) connected to the task enclosure (middle), which is coupled to the APP robot (right). The robot includes an array of rat sensors at the front half of the enclosure, an adjustable barrier mechanism below the front wall of the enclosure, and a pellet retrieval system beyond the front wall of the enclosure. B, close-up photograph of the APP robot highlighting the locations of the specific sensors, motors, and other barrier and pellet retrieval components. C, time-line showing Stages 1-3 of training and the robot setup at each stage.

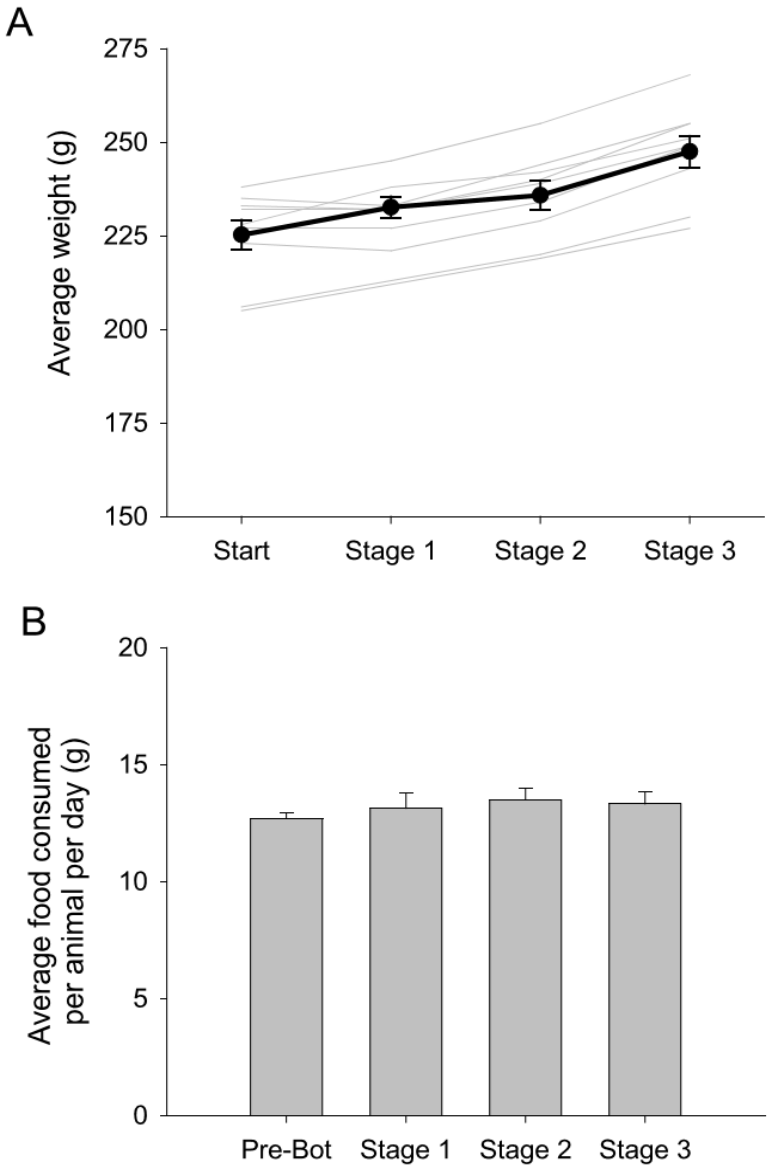

Figure 2. APP trained have a higher SPG success rate than manually trained rats. A, Plots showing average weight at the start of training and at each stage of training. Average (black line) and data from individual rats (grey lines). B, Bar graphs showing the average food consumed per animal per day in the several days prior to the start of training and at each stage of training. Error bars represent the SEM.

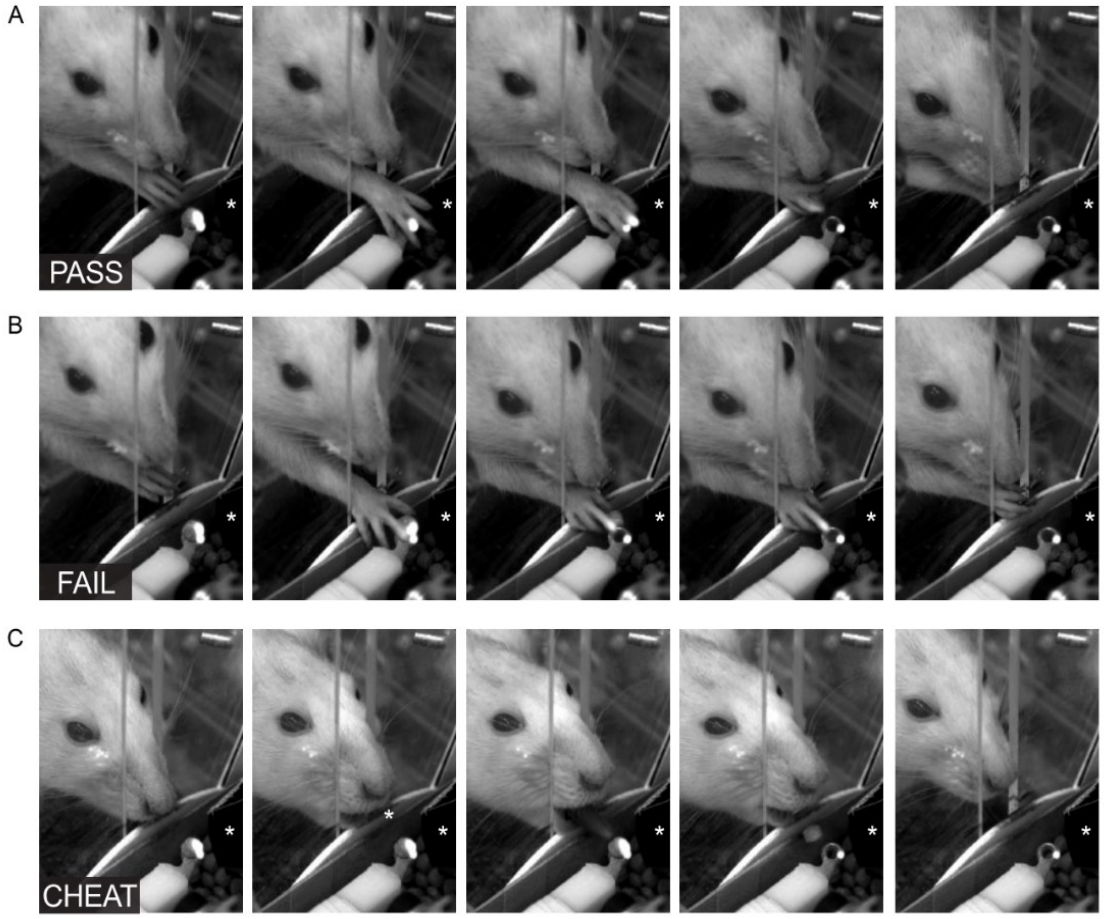

Figure 3. Trial evaluation with APP system. A-C, Image sequences from high-speed videos showing examples of a pass (A), fail (B), and cheat (C). The bright white spots on the right of the pellets in the first several frames and on the pellet platform in the later frames is the reflected infrared light emitted by the pellet sensor (asterisk), which is detected by the high-speed camera.

Figure 4. Grasping motions in APP system. Image sequence from a high-speed video showing the sniff (Frame 043), downward movement (Frame 073), retraction (Frame 080), and eating (frame 112) motions of a typical pass trial. See Video 4 for complete sequence of events.

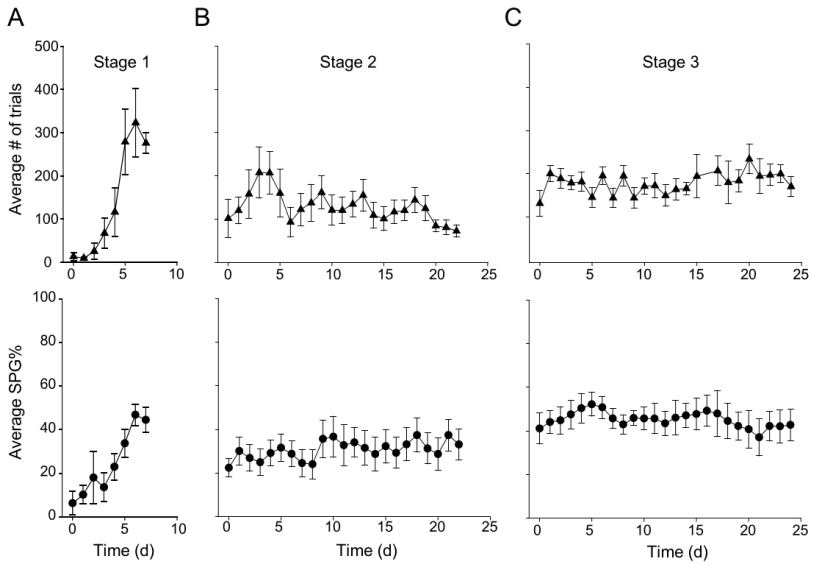

Figure 5. The stages of APP training. A-C, Plots showing the averages number of trials (top) and average grasping success rate (bottom) in Stage 1 (A), Stage 2 (B), and Stage 3 (C) of APP training. Error bars represent the SEM. n = 9.

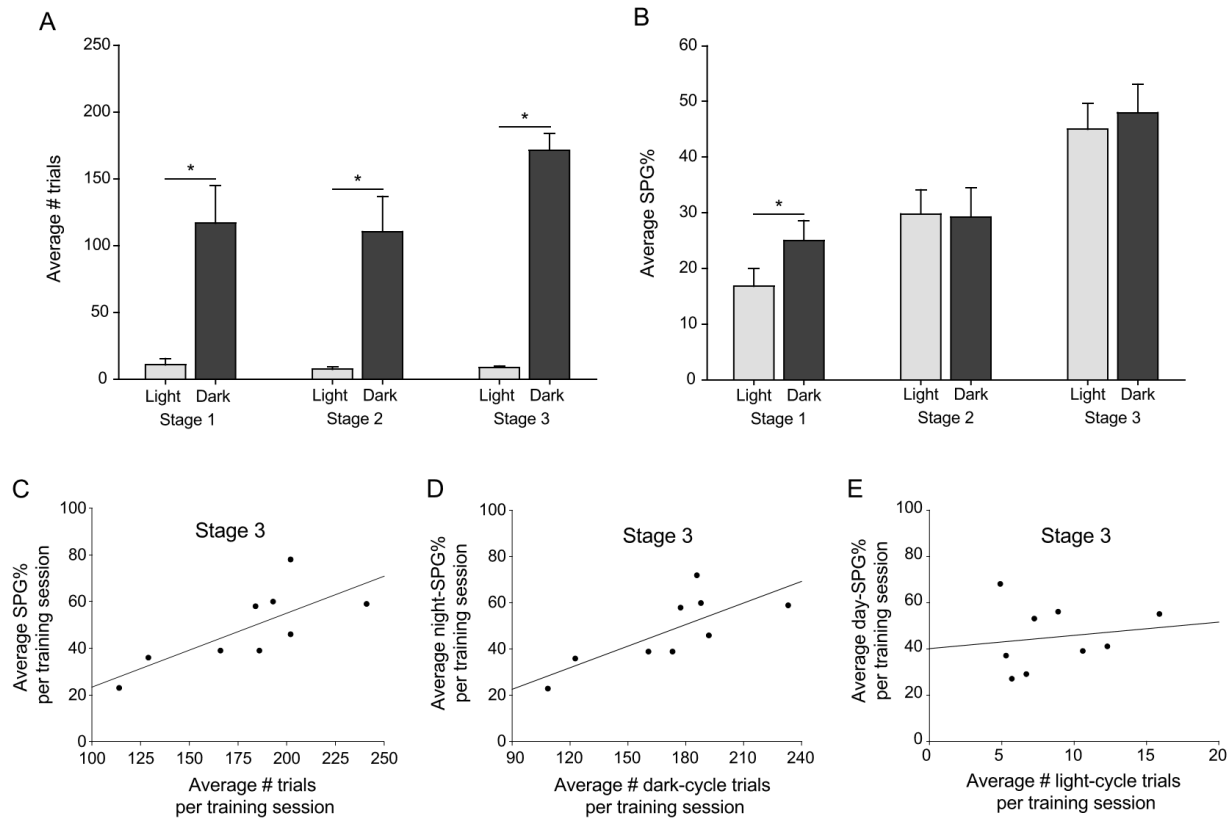

Figure 6. Dark-cycle training is essential for maintaining high light-cycle SPG grasping success. A, Bar graphs showing the average number of light- and dark-cycle trials per 24 hour period in each of the training stages. Error bars represent the SEM. *p <0.01, Wilcoxon signed-rank test. B, Bar graphs showing the average light-cycle and dark-cycle SPG success rates per 24 hour period in each of the training stages. Error bars represent the SEM. *p <0.01, Wilcoxon signed-rank test. C, Scatterplot with regression analysis showing a significant positive correlation between the average success rates and average attempts per training session per animal in Stage 3 training. p <0.01, Spearman rank order correlation. Correlation coefficient = 0.795. D, Scatterplot with regression analysis showing a significant positive correlation between the average dark-cycle success rates and average dark-cycle attempts per animal in Stage 3 training. p <0.01, Spearman rank order correlation. Correlation coefficient = 0.795. E, Scatterplot with

regression analysis showing no significant correlation between the average light-cycle success rates and average light-cycle number of trials per animal. $p = 0.643$, Spearman rank order correlation. Correlation coefficient = 0.167.

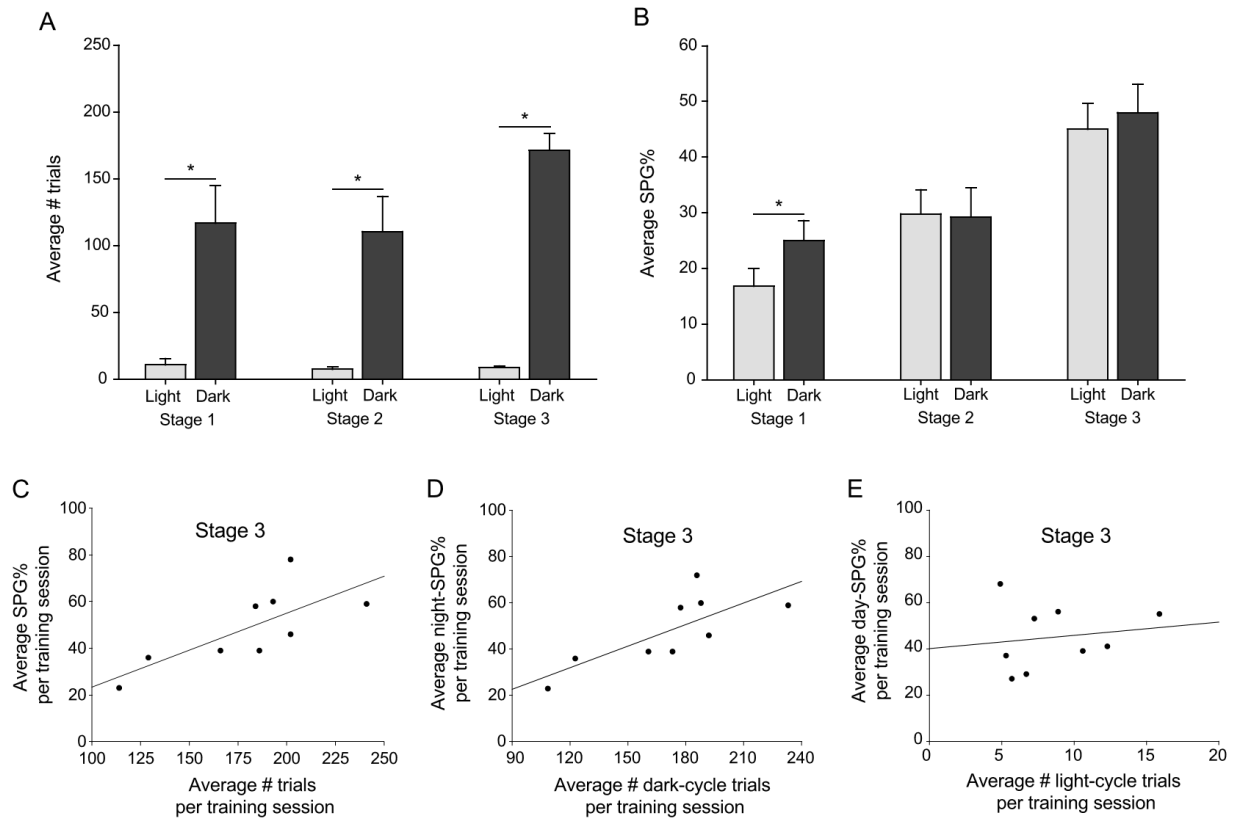

Figure 7. APP training improves attempt and success rates compared to manual training. A, Plots showing the averages number of trials (top) and average grasping success rate (bottom) throughout manual training. Each point represents a training session. Manual training is divided into two stages, the Learning stage (0-14d) and Plateau stage (15-44d). Error bars represent the SEM. B-C, Bar graphs showing the average number of trials (B) and average success rate (C) per training session in APP Stage 1, Manual Learning stage, APP Stage 3, and Manual Plateau stage. Error bars represent the SEM. *p <0.01, Mann-Whitney U-test. D, Plots showing the average cumulative number of trials to reach a training session with SPG% of ≥15, 20, 25, and 30% for APP trained rats (grey circles) and Manually trained rats (black triangles). Error bars represent the SEM. *p <0.05, Mann-Whitney U-test. E, Plots showing the average success rates of APP trained rats (grey circles) and manually trained rats (black triangles) grouped according to

weekday and normalized to Wednesdays. Error bars represent the SEM. *p <0.01, Student's T-test. F, Line graphs showing representative examples of daily variation throughout a one week cycle of a Stage 3 APP trained rat (grey circles) and a manually trained rat in the plateau stage of training (black triangles). Notice that the SPG% remains fairly constant for the APP trained rat, while there is a dramatic rise in SPG% towards the end of the week with manual training. G, Bar graphs showing the average difference in SPG% between each training session for APP Stage 3 and Manual Plateau stage rats. Error bars represent the SEM. *p <0.01, Mann-Whitney U-test. H-I, Bar graphs showing the average amount of researcher time required for each SPG trial (H) and average amount of researcher time for all SPG trials per rat per week (I) for APP Stage 3 and Manual Plateau stage rats.

Appendix 2: Single pellet grasping following cervical spinal cord injury in adult rat using an automated full-time training robot

Keith K. Fenrich [a,b], Zacincte May [a,b], Abel Torres-Espín [a,b], Juan Forero [a,b], David J. Bennett [a,b], Karim Fouad [a,b]

[a] Neuroscience and Mental Health Institute, [b]Department of Physiotherapy, Faculty of Rehabilitation Medicine, 3-88 Corbett Hall, University of Alberta, Edmonton, AB T6E 2G4, Canada

Corresponding author:

Keith K. Fenrich

Department of Physical Therapy

Faculty of Rehabilitation Medicine

3-88 Corbett Hall

University of Alberta

Edmonton, AB T6E 2G4

CANADA

Email: fenrich@ualberta.ca

Phone: +1 780 492 0938

Fax: +1 780 492 1626

Abstract

Task specific motor training is a common form of rehabilitation therapy in individuals with spinal cord injury (SCI). The single pellet grasping (SPG) task is a skilled forelimb motor task used to evaluate recovery of forelimb function in rodent models of SCI. The task requires animals to obtain food pellets located on a shelf beyond a slit at the front of an enclosure. Manually training and testing rats in the SPG task requires extensive time and often yields results with high outcome variability and small therapeutic windows (i.e., the difference between pre- and post-SCI success rates). Recent advances in automated SPG training using Automated Pellet Presentation (APP) systems allow rats to train *ad libitum* 24 hours a day, 7 days a week. APP trained rats have improved success rates, require less researcher time, and have lower outcome variability compared to manually trained rats. However, it is unclear whether APP trained rats can perform the SPG task using the APP system after SCI. Here we show that rats with cervical SCI can successfully perform the SPG task using the APP system. We found that SCI rats with APP training performed significantly more attempts, had slightly lower and less variable final score success rates, and larger therapeutic windows than SCI rats with manual training. These results demonstrate that APP training has clear advantages over manual training for evaluating reaching performance of SCI rats and represents a new tool for investigating rehabilitative motor training following CNS injury.

Keywords: Single pellet grasping; Spinal cord injury; Rehabilitation, Skilled motor task; Motor behavior; Automated animal training; Reaching; Grasping

Abbreviations: Single pellet grasping (SPG), Automated pellet presentation (APP), Spinal cord injury (SCI)

1. Introduction

It is widely acknowledged that task specific motor training is a key factor in recovery of fine motor function after CNS injury or disease. Skilled reaching tasks are important research tools for studying motor recovery in animal models of nervous system injuries such as spinal cord injury [SCI; 1,2–7] and stroke [8–11]. There are a number of manually administered reaching tasks used to study forepaw function and deliver forepaw rehabilitation in rodent models of CNS injury or disease including the Montoya staircase test [12,13], the Whishaw tray task [14], the isometric pull task [15], and the single pellet grasping (SPG) task [16]. However, because these reaching tasks rely on individual researcher interaction with animals they are subject to high degrees of variability between experiments, researchers, and laboratories. Moreover, these tests can be time consuming and tedious to administer (e.g., SPG, Montoya, and isometric pull tasks), especially in animals with forelimb dysfunction, and/or provide limited insight to kinematics and mechanisms of recovery from injury or disease (e.g., well-grasping, Whishaw tray, and isometric pull tasks).

The SPG task is frequently used to evaluate motor function and reaching motions before and after cervical SCI. It has several advantages compared to other reaching tests for evaluating forelimb motor function after cervical SCI. For example, SPG training and testing can be limited to the forepaw affected by injury and detailed analyses of reaching and grasping motions are possible. Moreover, the SPG task is a complex motor task and the SPG motions are not regularly performed in the home cage. As a result, changes in SPG performance can be attributed to training and testing within the enclosure rather than self-training in the home cage, which has been proven a problem for locomotor training [17]. Yet despite its advantages manual

administration of the SPG task requires extensive one-on-one researcher-to-rat training, which is time consuming and can be a source of variation between laboratories and from day to day within the same study. Also, manual training and testing of the SPG task before and after CNS injury or disease often results in small therapeutic windows (that is, the difference in SPG performance between pre-injury baseline and post-injury final scores), thus limiting the value to studies testing the effect of rehabilitative training or other treatments.

The role of rehabilitation training is growing in animal models partly because it is standard practice in the clinic, but also because there is mounting evidence drug and cell therapies are more effective when combined with rehabilitation therapy [2,18,19]. Given the limitations of current training methods there is a need for novel high-throughput and standardized training methods that accurately test the recovery of reaching and grasping function in animal models of CNS injury and disease.

We recently described an Automated Pellet Presentation (APP) system to present pellets to rats 24 hours a day, 7 days a week, which allowed APP trained rats to perform an automated version of the SPG task *ad libitum* [20]. Rats with APP training were successfully trained to perform the SPG task and employed similar grasping motions as manually trained rats. A key difference between the APP SPG task and the manual SPG task is that for the manual task pellets are presented from a small notch in a presentation shelf and can be scooped or dragged to the enclosure without grasping the pellet, whereas for the APP system there is a gap between the pellet presentation pedestal and the enclosure which precludes scooping or dragging pellets. Scooping and dragging is a common compensatory strategy used by rats with cervical SCI for obtaining pellets without grasping [21,22]. However, whether APP trained rats with SCI could

perform the SPG task without access to compensatory scooping or dragging and whether limiting compensation improves functional recovery remains unknown.

The purpose of the present study was to explore whether rehabilitative APP training would allow for a simplified and more standardized training of the SPG task, thus opening the door for systematic exploration of the effects of task specific rehabilitative motor training in rats with SCI. For this we tested whether rats could perform the SPG task using the APP systems following unilateral cervical SCIs that affected forelimb motor function. We found that rats with APP training were able to obtain pellets using the APP system after SCI, but with lower success and attempt rates than pre-injury baseline. Importantly, APP trained rats had larger therapeutic windows than manually trained rats, indicating that APP training will be a useful tool for identifying treatment effects that could not be detected using manual training approaches.

2. Materials and methods

Eighteen female Lewis rats (Charles River Laboratories, Wilmington, MA, USA) weighing 210-240 g were trained to perform the SPG task either manually (n = 10 rats) or using an APP system (n = 8 rats). All animals were individually marked on their tails and housed in groups of 2 to 5 and kept on a 12/12 hour light/dark cycle. Both manual and APP trained rats were housed in standard static home-cages with a PVC tube and small cedar block (~3x3x3 cm) for enrichment. Additionally, the static cages of the APP trained rats had a small hole with a tube connecting the home-cage to the APP task enclosure. All procedures were approved by the Health Sciences Animal Care and Use Committee of the University of Alberta.

2.1 Manual SPG training

Manual SPG training followed the same training protocol as previously described [21,22] and is consistent with similar training protocols for this task [1,2,5,7,16]. Briefly, upon arrival to the animal facility the rats had *ad libitum* access to rat chow and water. Several days prior to the start of SPG training the average food intake per rat per day was measured. On the day prior to each training session food was restricted to 95% of the average food intake, usually between 9 and 11 g of food per rat per day, otherwise rats were fed *ad libitum*. Rats were weighed daily and their weight was maintained at about 95% the weight of *ad libitum* fed animals (c.f., APP trained animals who were fed *ad libitum*; Fig. 1E) by adjusting the amount of home-cage food provided.

To begin each training session, a rat was placed at the back of a standard acrylic SPG training chamber (40 cm long, 12.5 cm wide, 45 cm tall) with a 1 cm wide and 10 cm tall vertical slit in the front wall. Since each rat has a preference to use either their right or left paw to perform grasping tasks, the manual SPG task enclosures had two fixed pellet presentation wells located about 0.5 cm left and 0.5 cm right relative to the center of the slit. In the first few training sessions banana flavoured sugar pellets (45 mg, TestDiet, 5TUT sucrose tab, St. Louis USA) were placed on both wells of the pellet presentation shelf at the front of the chamber. Once the rat had approached the front of the chamber and had completed a grasp attempt, the trainer placed a sugar pellet at the back of the chamber to encourage the rat to return to the back of the enclosure. The rat then returned to the back of the enclosure, another pellet was placed on the pellet presentation shelf, and the process was repeated for the entire session. Once the rat learned to shuttle, pellets were no longer placed at the back of the enclosure. Following completion of each training session the rat was returned to their home-cage. The preferred paw was determined by tracking which paw each rat used to obtain pellets. After a few training sessions, once paw preference was determined, pellets were presented in the left well to rats with a right-paw

preference, and vice versa.

All rats with manual training were trained to perform the SPG task for four weeks before SCI. One week following SCI, SPG training was continued for 6 weeks post-injury. For baseline and final scores in the reaching task the success rates of each animal were averaged for all training sessions in the final week before SCI and the final week of post-injury training respectively. With manual training SCI rats sometimes use compensatory strategies such as scooping or dragging the pellet to their mouth rather than grasping the pellet from the presentation shelf [21,23]. Since scooping is not possible with APP training, for this study scooped or dragged pellets observed during manual training were scored as a 'scoop' and counted as an attempt, but were not considered successful grasps.

2.2 Automated pellet presentation system

The same APP systems used for this study was used in a previous study [20]. Briefly, the APP systems consist of an APP robot integrated within a modified SPG task enclosure, which is connected to the home-cage. The APP system was designed so that the rats had unrestricted access to both their home-cage and the APP task enclosure (45 cm long, 10 cm wide, 30 cm tall) and the robot within the SPG enclosure 24 hours a day, 7 days a week, except during cleaning times. From within their home-cage, the rats had *ad libitum* access to food (standard rat chow) and water. Additionally, the APP trained rats could also obtain banana flavoured grain pellets (45 mg, TestDiet, 5TUM grain-based rodent tablet, St. Louis USA) from the APP system by successfully performing the SPG task (see below for details). In the center of the front wall a 1 cm wide and 10 cm tall vertical slit was cut, through which the rats had access to the pellet platform. All electronic robotic components were purchased from Phidgets Inc. (Calgary,

Canada), and robot-controller software written in Java using NeatBeans IDE 7.3. Motors were controlled using a PhidgetAdvancedServo 8-Motor controller board connected to a controller computer via USB. Sensor activity was monitored and LEDs were controlled using a Phidget Interface Kit 8/8/8 w/6 Port Hub connected to a controller computer via USB.

The APP system included a custom made pellet retrieval arm with a 3 mm diameter loop at the distal tip, called the platform, and could hold a single food pellet. To retrieve a pellet the pellet arm motor was activated so the platform would pass through the pellet hopper and would continue to rotate until a pellet was detected on the pellet platform by a pellet sensor, at which point a stop signal was sent to the controller to stop the pellet arm motor. The pellet retrieval process was repeated if the pellet sensor indicated the pellet had been removed from the pellet platform. The location at which pellets were presented could be adjusted in 3D space (i.e., proximal-distal, medial-lateral, and up-down) relative to the slit opening by adjusting the position of the pellet retrieval system along the aluminum frame. Since each rat has a preference to use either their right or left paw to perform grasping tasks, manual SPG training enclosures typically have two fixed pellet presentation wells located about 0.5 cm left and 0.5 cm right relative to the center of the slit. Pellets are presented in the left well to rats with a right-paw preference, and pellets are presented in the right well to rats with left-paw preference. With the APP system, presentation position was adjusted depending on the stage of training (see 2.3 SPG task training using the APP system below) and the paw preference. Pellets were typically presented at a distance of 1.3 to 2 cm from the slit, up to 0.5 cm left or right of the center of the slit, and 2 cm up from the level of the enclosure floor. Access beyond the slit was controlled by an adjustable barrier system.

Sensors to detect the presence of a rat were located in the front half of the enclosure. Two floor sensors were located between a fixed base floor and a thin acrylic floating floor above the sensors to indicate whether a rat was standing on the floating front floor. One proximity sensor was positioned in the middle of the enclosure to detect rats that were resting their forepaws on the floating floor (i.e., remained within the front half of the enclosure) without activating the floor sensors. Together, these sensors could effectively detect the presence of a rat in the front half of the enclosure.

2.3 SPG task training using the APP system

APP pre-injury training followed the same training protocol as previously described for uninjured rats [20]. Briefly, SPG training was divided into four stages; three pre-injury training stages (Stages 1-3) as described previously [20], followed by one post-injury stage (Stage 4; Fig. 1A). Stage 1 was designed to allow the rats to acclimatize to the pellet presentation system and to have easy access to the pellets. In Stage 1 the rat sensor system was deactivated and the pellets were presented very close to the slit opening (<15 mm) and aligned with the center of the slit. In this configuration the rats had easy access to the pellets and were not required to return to the back of the enclosure for subsequent pellet presentation. All rats that had at least one day with ≥ 30 attempts (n = 8 of 8) in Stage 1 were considered to have learned the location of the pellets and proceeded to Stage 2.

Given the closeness of the pellets in Stage 1 (<15 mm), a small number of rats (n = 3) preferentially obtained pellets by licking rather than grasping. Stage 2 was designed to promote forelimb grasping instead of licking and to train the rats to move to the back of the enclosure for each attempt. To train the rats to move to the back of the enclosure, the barrier would remain

closed until there was no rat detected by the rat sensors in the front half of the enclosure. Since a rat forepaw can reach through the slit further than an extended tongue, the distance of the pellet from the slit was gradually increased by 0.5-1 mm every 3-7d from <15 mm to as high as 20 mm, until the rats no longer attempted to obtain pellets by licking.

In Stage 3 rats were housed according to their preferred paw. Additionally, the APP system was setup so that the pellet presentation platform was located 14.5-15 mm from the slit opening and aligned with the left edge of the slit for right-pawed rats or the right edge of the slit for left-pawed rats. In this configuration rats did not relapse into obtaining pellets by licking. The APP system remained in this configuration for the remainder of training.

Stage 4 started 6-8 days after SCI and continued for 6 weeks post-injury for n = 7 animals. One animal performed an average of 4 attempts per 24 hour cycle in the first 6 days of Stage 4 training and zero attempts for the following 14 days of Stage 4 training. This animal was therefore removed from the APP system after only 4 weeks of post-injury training.

2.4 Video recording

Reaching attempts were video monitored 24 hours a day, 7 days a week using Blue Iris software (v. 3.5, Perspective Software) and Foscam light/dark digital cameras (FI9821W) equipped with an integrated infrared LED array for dark-cycle recording. The cameras automatically activated the LED array and switched input gain and intensity during the dark-cycle. Video acquisition was set at 30 fps with a resolution of 640 x 480 pixels.

2.5 Spinal cord injury

Following reaching training each rat received a dorsal lateral quadrant (DLQ) spinal

transection injury (see Fig. 5 for injury profiles) on the side of their preferred paw as established during reaching training. Rats were anaesthetized using isoflurane (2.5% in 50:50 air:oxygen mixture) and the dorsal neck was shaved and disinfected with 10% chlorhexidine digluconate. Buprenorphine was injected s.c., immediately post-op (0.03 mg/kg) and again 8-12 hours later (0.02 mg/kg). Body temperature was maintained with a heating blanket. The spinal cord between C4 and C5 was exposed with a small laminectomy of the caudal half of C4. The dura was resected from over the intended injury site and a custom-made blade was lowered 1 mm into the spinal cord at the midline and then moved laterally. The muscle layers were sutured, the skin closed with staples, and 4 ml of saline was injected s.c. to maintain hydration. Animals were kept on a heating blanket until fully awake. Post-operative pain was managed by s.c. injections of buprenorphine (0.05 mg/kg) every 12 hours for 2 days.

2.6 Histology and Lesion size quantification

Upon completion of post-injury training, rats were euthanized and perfused with saline followed by 4% formalin solution containing 5% sucrose. Spinal cords were dissected and post-fixed overnight then transferred to 30% sucrose in PBS for 3 days. Spinal cord cross-sections were cut at 25 μm on a cryostat. Tissue was dried for 30 min at 37 °C, rehydrated in TBS, then placed in 0.5% cresyl violet for 4 min. Tissue was rinsed 3 times in distilled water and then serially dehydrated in EtOH (50%, 75%, and 99%) for 2 min each. Finally, tissue sections were cleared in xylene for 2 min and coverslipped with Permount (Fisher Scientific, Canada).

Lesion sizes were evaluated using light microscopy. Lesion sites were considered as any part of the tissue section with intense cresyl violet staining and/or where tissue integrity was compromised. Lesion sizes were calculated as a percentage of the total cross-sectional area of the

tissue section using ImageJ (NIH, Bethesda Maryland, USA). Lesions were reconstructed on a schematic of a C4 spinal cord cross section based on a stereotaxic atlas [24]. Multiple tissue sections were evaluated for each animal and the tissue section with the greatest cross-sectional lesion area was used to calculate lesion size. Using ImageJ, the lesions were further analyzed to determine the extent of injury to specific spinal tracts such as the corticospinal tract (CST) and rubrospinal tract (RST) using reported projection sites [24–26]. For this, a C4 spinal cross-section diagram with the CST and RST superimposed over the diagram (Fig. 5A) was used to estimate the locations of the CST and RST in the injured spinal cords (Fig. 5B,C). The percentage of the CST and RST that was cut on the intended injury side was categorized as either 0, 25, 50, 75, and 100% cut for each spinal tract. In some animals the DLQ injury extended slightly beyond the midline thus resulting in damage to the contralateral CST. In these cases only the CST ipsilateral to the intended DLQ site was considered for CST injury analysis.

2.7 Analysis of APP video data

Videos were analyzed using BlueIris software. Most attempts required ~10 s of video and video playback rates were set at 4X normal speed, so each attempt required ~2.5s to analyze. The animal performing each attempt was determined based on tail markings and results were sorted by animal. An attempt was defined as a forward motion of the dominant forepaw beyond the threshold of the slit opening towards the pellet platform. Attempts were evaluated as pass or fail.

Pass. A pass was scored when the rat successfully grasped a pellet from the pellet platform using their preferred forepaw and brought it back through the slit into the task enclosure.

Fail. A fail was scored when the rat made a grasp attempt, but failed to bring the pellet

back through the slit.

Performance rates for each animal were calculated by dividing the number of passes by the number of attempts. Unlike with manual training, scooping or dragging pellets into the enclosure is not possible with the APP system because there is a gap between the pellet platform and the slit so that any scooped or dragged pellets would fall out of reach. Baseline performance before injury was calculated as the average success rate in the final week of training before injury.

During some attempts, more than one rat was present in the enclosure at the same time. In cases where a rat made an attempt while another rat was located at the back of the enclosure and did not obstruct the movements of the attempting rat to move towards the slit and reach for the pellet, the attempt was included in the study. On rare occasions another rat was located towards the front of the enclosure and obstructed access to the slit or the reaching movements of the rat reaching for a pellet. Since in these cases the reaching and grasping motions were compromised, the grasping motion was not considered an SPG attempt and was excluded.

For quantification purposes each APP training session was considered as one light-dark cycle starting at lights-on. Rats were weighed daily partway through the light-cycle. Home-cage food consumption was measured daily and the average home-cage food per rat was calculated. For overall food consumption per rat, the number of food pellets obtained by the rat was multiplied by the weight of the food pellets (45 mg/pellet) and added to the average home-cage food consumed per rat.

2.8 Statistical analysis

Statistical analysis was performed using non-parametric tests including the Mann-Whitney-U test, the Wilcoxon Signed-Rank test, and the two sample Kolmogorov–Smirnov test. All averages are presented as mean ± SEM. Significance was set as $p \leq 0.05$.

3. Results

3.1 APP system and manual training before and after SCI

Our primary goal was to explore whether full-time *ad libitum* APP training is effective after cervical SCI with the idea to simplify and standardize training and testing of the SPG task and thus allow for a systematic exploration of SPG training after SCI in rats. For this we tested whether rats with DLQ SCIs could perform the SPG task using a previously described APP system [20]. The results from the SCI rats with APP training (n = 8) were compared to those of SCI rats with manual training (n = 10) [22]. As a first step, rats were trained and tested in the SPG task using the APP system or using a manual training protocol as previously described [22]. Average baseline attempt rates for the final week of training before injury was higher for rats trained in the APP system (average = 194 ± 9 attempts/24 hours) compared to rats with manual training (Fig. 1B; average = 47 ± 3 attempts/24 hours; $p < 0.001$, Mann-Whitney test for two independent samples). There was, however, no significant difference in the baseline SPG success rates between rats with APP training (average = 48.8% ± 2.3) and manually trained rats (Fig. 1C; average = 43.7% ± 3.0; $p = 0.27$, Mann-Whitney test for two independent samples). One week following SCI, rats with APP training were re-introduced to the APP system for *ad libitum* full-time rehabilitative SPG training and rats with manual training were provided 10 minute of rehabilitative SPG training 5 days per week (n = 25 training sessions/rat) until 6 weeks post-injury. Average daily post-injury food intake of rats with APP training was higher throughout the

post-injury period compared to rats with manual training, likely because these rats were food restricted, which is typical of manual training, whereas rats with APP training were not (Fig. 1D). After SCI average body weight dropped by 13 ± 1 g for APP trained rats and 17 ± 2 g for manually trained rats, followed by steady gains for both groups consistent with normal rat growth (Fig. 1E). These results show that rats with APP training tolerated the APP system very well throughout the post-injury period.

Performance in the APP system was analyzed from digital video recordings of every attempt. Each attempt was evaluated as either a pass or fail. Examples of reaching by uninjured rats in the APP system have previously been shown [20]. Examples of pass and fail attempts of SCI rats are illustrated in Fig. 2 (Videos 1-2). The average amount of researcher time per rat per week to train and test SCI each rat using the APP system was calculated by multiplying the average time required to evaluate the outcome of each attempt (n = 2.5 s/trial) and multiplied by the average number of attempts per day (n = 70.7 trials/day) by the number of training days per week (n = 7) to yield and average of 21 min/rat/week. The average amount of research time per week for manually trained animals is fixed at 10 min/day multiplied by 5 days/week, to yield an average of 50 min/rat/week. Comparable to uninjured rats [20] post-injury training required less than half the researcher time per rat per week using the APP system relative to manual training.

3.2 Comparison of APP and manual training in attempt rates post-injury

Rats with APP training quickly resumed SPG training once reintroduced to the APP system post injury. Attempt rates for rats with APP training rose quickly and peaked at 10 days post-injury and slowly declined to a plateau at 30 days post-injury (Fig. 3A). Similarly, rats with manual training reached plateau levels at 13 days post-injury, but attempt rates remained fairly

constant thereafter (Fig. 3A). Pairwise comparison of baseline attempt and final score attempts rates showed that rats with APP training had lower attempts rates in the last week of training following SCI compared to baseline (Fig. 3B; final score average = 51 ± 2 attempts/24 hours; $p = 0.012$, Wilcoxon signed-rank test for paired samples). Conversely, baseline attempt and final score attempts rates were not significantly different for rats with manual training (Fig. 3B; final score average = 37 ± 2 attempts/24 hours; $p = 0.114$, Wilcoxon signed-rank test for paired samples). Despite the drop in number of attempts for rats with APP training, their average attempt rates were still higher than those of manually trained rats post-injury (Fig. 3C; $p = 0.05$, Mann-Whitney test for two independent samples). Moreover, similar to pre-injury APP training [20], most APP attempts were made during the dark cycle (Fig. 3D; $p = 0.006$, Wilcoxon signed-rank test for paired samples), whereas manual training was done exclusively during the light-cycle. Together these data suggest that standard manual training protocols do not provide adequate training time compared to APP training. Furthermore, comparison of the distributions of attempt rate final scores revealed that the attempt rates for rats with APP training were widely distributed ranging from 0 to 193 attempts per 24 hours, whereas the attempt rates for rats with manual training were closely grouped between 23 and 55 attempts per training session (Fig. 3E; $p = 0.031$, Two Sample Kolmogorov-Smirnov test). These data show that although rats with APP training generally have higher attempt rates: (1) rats with manual training are highly motivated to perform the SPG task as indicated by the relatively high minimum attempt rate of 23, likely due to food restriction and the use of sugar pellets for training rather than grain-based pellets as used for APP training; and (2) overall attempt rates with manual training is limited by restricted training times as indicated by the tight grouping of overall final score attempt rates near the maximum, further suggesting that rats with manual training less than most rats with APP

training.

3.3 Comparison of APP and manual training in SPG performance post-injury

At the start of post-injury training SPG success rates of rats with APP training followed a similar pattern as the attempt rates, with average daily SPG% increasing to peak levels at 7 days, two days after peak attempt rates, followed by a steady decline and to a plateau stage starting at about 27 days post-injury (Fig. 4A). Conversely, although the attempt rates for rats with manual training reached a plateau, SPG success rates slowly climbed throughout post-injury training with a short plateau period after 30 days post-injury (Fig. 4A). As a result of the steady increase in SPG success rate for manually trained rats there was no difference between baseline and final score results ($p = 0.093$, Wilcoxon signed-rank test for paired samples), whereas the SPG final score for rats with APP training was lower than baseline (Fig. 4B; $p = 0.036$, Wilcoxon signed-rank test for paired samples). Comparison of the final score results of rats with APP training and rats with manual training showed that rats with manual training had a higher average final score SPG% (Fig. 4C) and higher average final score SPG% when normalized to baseline (Fig. 4D) compared to rats with APP training, but the differences were not significant ($p > 0.05$, Mann-Whitney test for two independent samples). Moreover, although most APP attempts were made during the dark cycle, SPG final score success rates were the same during the light and dark cycles (Fig 4E; $p = 0.277$, Two Sample Kolmogorov-Smirnov test). Collectively, these results show that rats with APP training undergo a significant drop in success rates after SCI and have less variable final score success rates compared to rats with manual training.

3.4 SPG performance as a function of lesion severity and location

Possible explanations for why rats with APP training had lower final score SPG success

compared to baseline, whereas rats with manual training did not, could be because rats with APP training had more severe injuries than rats with manual training or because the APP SPG task is more difficult than the manual SPG task. To test if rats with APP training had more severe SCIs, lesions areas were evaluated and measured as a percentage of the cross section area of the caudal C4 spinal cord (Fig. 5A-C). Surprisingly, rats with APP training had injuries that were less severe than rats with manual training, yet rats with APP training had worse performance than manually trained rats (Fig. 5D,E; $p = 0.008$, Mann-Whitney test for two independent samples). The two APP trained animals with improved SPG% after SCI had lesion sizes near the average lesion size of the other APP animals with lower final score SPG%. Correlation analysis revealed that final score SPG% was negatively correlated with lesion area with correlation coefficient values of -0.405 and -0.730 for rats with APP and manual training respectively, but was significant only for manual training (Fig. 5E; $p = 0.405$ for APP training, $p < 0.013$ for manual training, Spearman Rank Order Correlation). Since certain spinal tracts such as the corticospinal tract (CST) and rubrospinal tract (RST) are important for rat forelimb function [21], these results raise the possibility that rats with APP training sustained more damage to these key spinal pathways than rats with manual training. Comparison of the transected cross sectional areas of CST and RST for the affected forelimbs of rats with APP and manual training showed no difference in the transected CST areas (Fig. 5F; $p = 0.421$, Mann-Whitney test for two independent samples), but rats with manual training had more severe RST lesions than rats with APP training (Fig. 5G; $p = 0.041$, Mann-Whitney test for two independent samples). Finally, it is also possible that since surgeons tend to have a preferred side, lesion severity may be different for animals with right-side lesions and animals with left-side lesions. To test this, the lesion sizes and final score SPG% for APP and manually trained animals were tested. There were no

significant differences between left- and right-paw preferred rats suggesting that there was no left-right bias in the lesions ($p > 0.05$, Mann-Whitney test for two independent samples; data not shown). Taken together, these results show that SCIs with modest severity can cause considerable reductions in SPG success rates for rats with APP training compared to rats with manual training and are consistent with the idea that the APP SPG task is more challenging than the manually trained SPG task.

3.5 SPG performance as a function of attempt rates

Following SCI, increasing the amount of manual rehabilitative training from 15 min/rat/day to 30 min/rat/day nearly doubles the SPG success rates (Fouad et al., unpublished results). However, unlike rats with manual training, the final score attempt and success rates of rats with APP training were lower than baseline. It is therefore possible that post-injury SPG success rates are not positively correlated with attempt rates as with manually trained rats. This was, however, not the case since correlation analysis revealed that final score SPG% was positively correlated with final score attempt rates with correlation-coefficient values of 0.74 and 0.83 for rats with APP and manual training respectively (Fig. 6A,B; $p = 0.029$ for APP training, $p < 0.001$ for manual training, Spearman Rank Order Correlation). Visual inspection of the SPG final score distributions in Figures 5A and 5B (also seen in Fig. 4B) suggests that SPG final scores were evenly distributed across the final score range, but rats with manual training seemed to be grouped into two categories: 'high-SPG achievers' and 'low-SPG achievers'. Distribution analysis of SPG final scores revealed that the final scores of rats with APP training were normally distributed ($p = 0.35$, Shapiro-Wilk test for normality) within a single group with a range of 0-40% (Fig. 6C). Conversely, the final scores of rats with manual training did not

follow a normal distribution ($p = 0.011$, Shapiro-Wilk test for normality), but rather formed two distinct groups; one with low-SPG final scores from 0-10% and the other with high-SPG final scores from 31-60% (Fig. 6D). This polarization of SPG success rates can lead to difficulties in performing statistical analysis and identifying treatment effects of manually trained rats [21], whereas the normal distribution of APP SPG final scores lends itself to simplified analysis and interpretation of results.

Given that success rate is negatively correlated with lesion size for manually trained animals, it is possible that the high-SPG achievers had less severe lesions than low-SPG achievers. Comparison of the lesion sizes between the high- and low-SPG achiever groups showed that although the average lesion sizes of high-achievers (28 ± 6% of spinal cord cross section) was less than low-achievers (38 ± 5% of spinal cord cross section), there was considerable overlap in lesion sizes between the two groups and the differences were therefore not significant (c.f., Fig. 5E; $p > 0.05$, Mann-Whitney test for two independent samples). Moreover, although manually trained high-achievers had considerably higher SPG% final scores (50.4 ± 4.4%) than APP trained rats (13.7 ± 4.8%; $p = 0.003$, Mann-Whitney test for two independent samples), manually trained high-achievers also had higher average lesion sizes (28 ± 6% of spinal cord cross section) than APP trained animals (18 ± 2% of spinal cord cross section), but this difference was not significant ($p > 0.05$, Mann-Whitney test for two independent samples). Taken together, these data are consistent with the idea that the APP SPG task is more challenging than the manually trained SPG task.

The fact that the APP SPG final scores of rats with manual training diverge into high- and low-success rate groups, whereas APP final score success rates are normally distributed, could

be linked to the way pellets are presented in the different SPG tasks. For instance, one key difference between rats with APP and manual training is that rats with manual training can obtain pellets by scooping them from the presentation shelf, whereas this is not possible for rats with APP training since pellets that are not properly grasped will drop from the pedestal and out of reach of the animal. It is therefore possible that scooping could influence grouping of SPG success rates. Comparison of SPG final scores of rats with manual training to the number of scoop attempts showed that manually trained rats from the high-SPG group made more scoop attempts than animals from the low-SPG group (Fig., 6E; $p = 0.038$, Mann-Whitney test for two independent samples). However, these results could be because the high-SPG group had a higher attempt rate. To determine if this was the case, the scoop rates between the groups were compared as a percentage of overall attempts, and again the high-SPG group made more scoops than the low-SPG group (Fig. 6F; $p = 0.030$, Mann-Whitney test for two independent samples). Furthermore, most scoop attempts occurred in earlier training sessions (Fig. 6G), which coincides with a period of steady increase in SPG success rates (c.f. Fig. 4A). This period of increasing SPG success rates is followed by a sharp reduction in scoop attempts (Fig 6G) and coincides with a period of plateaued SPG success rates (c.f. Fig. 4A). These data suggest that scooping could be an effective training strategy used by some manually trained rats to perform more successful grasp attempts later in training. Taken together, unlike manual training, APP SPG performance is not dependent on compensatory scooping strategies. This leads to more normalized results that are less variable over time, suggesting that rats with APP training would be highly useful for studying the effects of rehabilitation, drug, and cell therapies in rats with SCI.

Forelimb reaching and grasping tasks such as the SPG task are often used for testing therapeutic interventions to promote functional recovery of fine motor control after CNS injuries such as SCI [1–7] and stroke [8–11]. However, previous studies have highlighted the fact that following CNS injury manual implementation of the SPG task is time consuming and can yield highly variable results with success rates ranging from zero to better than baseline, which can lead to small treatment effect windows, and thus difficulties in identifying potentially useful treatment strategies [21]. Here we used an automated SPG task training technique, previously described for the training of uninjured rats [20], for task-specific reaching and grasping rehabilitation therapy after SCI. We showed that rats can be trained to perform the SPG task after SCI using the APP system, which increased treatment effect windows and reduced variability compared to manual training. Moreover, rats with APP training had an improved range of training intensities and few success rates of zero compared to rats with manual training, which allows us to test a full range of rehab intensities. On top of these advantages, the reduced researcher time required to train rats with APP training and the fact that compensatory strategies like scooping can be avoided, makes the APP system the preferred training and/or testing paradigm in forelimb reaching and grasping.

4.1 Treatment effect windows

Treatment effect windows in reaching and grasping tasks after SCI are the difference in baseline success rate before injury and the final score success rates post-injury [3,4,19,21]. Ideally, for animals that receive only post-injury task training (i.e., control animals), success rates should be high before injury, drop to low levels immediately following injury, and then rise to intermediate levels that remain significantly lower than baseline levels (Fig. 7). The rise in

success rates with progressive training can be attributed to post-injury rehabilitation therapy and/or spontaneous daily use therapy (e.g., using the affected limb for tasks such as locomotion and grooming). Although an idealized task would not fully model the large variability in reaching and grasping motor skills of SCI individuals, and robust treatment effects can be observed even with small therapeutic windows, large therapeutic windows remain desirable for scientific and practical purposes. For instance, identification of cell and/or drug treatment strategies with small beneficial effects are important since modest improvements can be considerably amplified when combined with rehab therapy [2,19]. Large therapeutic windows facilitate the identification of treatment strategies (e.g., drug or cell therapy) with small therapeutic effects. Moreover, the rate at which these changes occur can be measured to optimize the timelines of treatments.

Consistent with other studies [3,4,27] we found only small changes between average baseline and final scores of rats with manual training, with the average final scores being 72% ± 14 of baseline. This translates to a treatment effect window of 28%. Conversely, there was a decline in the SPG% for rats with APP training post-injury, with the average final scores at 39% ± 7 of baseline. This translates to a treatment effect window of about 60% for rats with APP training. The large treatment effect windows observed for APP trained animals might be due to an inadequate number of APP trained animals (n = 8), whereby a larger sample would have yielded a high- and low-achieving group as observed with the manually trained animals. However, this seems unlikely given that the final score success rates of manually trained animals were highly polarized with half (n = 5) of the animals having final score success rates close to or higher than baseline with the other half (n = 5) at or near zero. Conversely, APP final score success rates were more normally distributed with only two APP animals having final score

success rates near baseline and only one APP trained animal with a final score success rate of zero. Given the high attempt rates of APP trained animals it is possible that a study with a wide range of post-SCI APP training intensities would reveal a multi-modal relationship between training intensity and performance rates where progressively higher training intensities eventually leads to a performance plateau or reduced performance. Together, our results indicate that positive treatment effects would be easier to identify with the APP system and that SPG training and testing with the APP system yields results that more closely resemble an 'ideal' behavioral task than the manual SPG task.

4.2 SPG task difficulty and compensatory strategies

Our results show that manually trained rats achieve higher post-injury success rates, which suggests that manual training is more effective than APP training. One possible explanation for the significant drop in post-injury SPG success rates for rats with APP training is they had more severe lesions, since SPG success rates are inversely correlated with lesion severity [4,21]. Surprisingly, comparison of lesion cross-section areas showed that rats with APP training had less severe lesions than rats with manual training, suggesting that rats require more intact spinal circuitry to do the APP task than the manual task. Alternatively, the drop in APP success rates may be due to the concomitant drop in APP attempt rates after injury. However, rats with APP training had higher final score attempt rates than rats with manual training. Taken together, these results suggest that the APP SPG task is more difficult than the manual SPG task.

The increased difficulty of the APP task could be due to a variety of reasons. For instance, in the APP system rats can easily displace a pellet from the pedestal with a slight touch and fall out of reach prior to grasping [20]. As a result, more precise grasping motions are

required to obtain a pellet with the APP system. Conversely, in the manual enclosures pellets are presented within a small groove located on a shelf [16]. With this setup animals can displace the pellet from the groove without knocking it from the shelf, thus allowing more time and a greater margin of error for the grasping motion. Furthermore, the manual pellet presentation shelf can be used to guide the paw during the reaching/withdrawal motion or rest the paw/digits during grasping motions [16,28], especially after SCI [2,21], which is not possible with the APP system. Indeed, our results show that manually trained rats that scooped in the early stages of post-injury training made more attempts and had higher SPG final scores than manually trained rats that did not scoop. Scooping could therefore be a key training strategy to fine tune forelimb movements and achieve higher SPG success rates over time. Whether rats with APP training would employ the same strategy could be tested in future studies by adding a shelf that extends from the slit to the pellet presentation pedestal of the APP system, which would allow APP trained rats to scoop pellets with the high attempt rates possible with the APP system. Taken together, our data suggest that allowing and/or encouraging compensatory strategies may be a useful rehabilitation tool to encourage training and to promote functional recovery of fine motor control after SCI.

4.3 Attempt rates and food consumption

Two key differences between manual and APP training are access to food and access to training. Rats with APP training have unrestricted home-cage food and can train to grasp pellets *ad libitum* every day of the week, but rats with manual training have limited access to home-cage food and are restricted to short training sessions 5 times per week. Fixed manual training time limits the maximum number of attempts per session and thus reduces the effectiveness of rehabilitation therapy. Also, final score attempt rates were tightly distributed near the maximum

observed attempt rates suggesting that overall attempt rates of manually trained rats were limited by training time.

Following injury average attempt rates for rats with APP training decreased significantly. SCI typically results in pronounced changes in muscle physiology such as muscle atrophy [29], changes in muscle blood flow caused by vascular atrophy [30], and fiber type conversion [29,31,32], resulting in neuromuscular fatigue [29,31]. Fatigue is often a major limiting factor in motor function and motivation with rehabilitation training for SCI individuals [33,34]. It is possible that post-injury fatigue of the affected forelimb could explain the drop in attempt rates for rats with APP training. If true, training with the APP system could be considered a more clinically relevant fine motor task since it closely mimics the training fatigue experienced by individuals with SCI. Conversely, reduced attempt rates of rats with APP training after injury could also be due to diminished motivation. A reduction in motivation of the rats with APP training could be dictated by the *ad libitum* training schedule. For instance, the motivation of rats with APP training is higher during the dark cycle compared to light cycle, with over 92% of attempts made during the dark cycle, consistent with their nocturnal sleep-wake cycle. It is possible that overall activity of rats decreases post-SCI, which could reduce attempt rates, but this remains to be tested. Similar to uninjured animals [20], the increased dark-cycle attempt rates for post-injury rats with APP training did not result in increased dark-cycle SPG success rates. Instead, we found that final score attempt rates were a good indicator of final score SPG success rates for rats with APP training. Whether post-injury SPG success rates drop because of an inability to perform more attempts, or whether attempt rates drop because rats with APP training become frustrated with their poor SPG performance, or a combination of the two factors remains unknown. Motivation levels of rats with manual training are maintained with food

restriction and by training with sugar pellets rather than the grain-based pellets used for APP training. Either of these strategies may increase the motivation of rats with APP training. For example, in early trials with the APP system sugar pellets were used instead of grain-based pellets, which resulted in almost continuous training such that attempt rates were very high (>500 attempts per rat per 24 hour cycle; unpublished results). Presumably the use of sugar pellets and/or food restriction would also increase attempt rates post-injury. Collectively, our results suggest that standard manual training protocols likely do not provide adequate amounts of training to maximize both pre-injury baseline and post-injury final score success rates. The dramatic drop in attempt rates from baseline to post-injury for APP trained rats suggests that it is difficult for animals to maintain very high attempt rates after SCI. It is therefore possible that additional manual training could result in significantly more attempts before SCI followed by a considerable drop in post-injury attempt rates resulting in an improved therapeutic window, similar to APP trained rats. Whether manual training protocols with increased training frequency and session times improved functional outcomes and improved therapeutic windows for SCI in rats remains to be directly tested.

4.4 Significance for ad libitum training and translational studies

It is well established that repeated task rehabilitation therapy is one of the most effective treatments to improve fine motor function of the trained task following SCI. As robotic devices for rehabilitation therapy become more sophisticated and affordable, high-intensity repeated task rehabilitation will become more and more prevalent as part of rehabilitation in the clinic and at home. Though numerous animal studies have utilized various fine motor tasks to study the effects of rehabilitation therapy after SCI [e.g., 2,3,19], these studies limited the rehabilitation

time of the tested animals to short weekday training sessions. These approaches are not appropriate models for testing full time *ad libitum* rehabilitation therapy, as is now possible with home based therapies. Therefore, an upper limit for high-intensity rehabilitation therapy has yet to be identified in either animal models or individuals with SCI, and the cellular mechanisms underlying this limit remain unknown. It is important to understand the relationships between training intensity and functional outcomes using animal models since these studies will provide valuable insight regarding the cellular mechanisms underlying functional improvements as well as identifying potential risk factors associated with full time *ad libitum* training. For instance, previous studies using task-specific rehabilitation therapy have shown that intensive training of the rehabilitation task can adversely affect performance in other motor tasks [2,3].

Collectively, APP SPG training opens the door to studies with maximal training rates, will allow researcher to more easily identify the limitations of rehabilitation therapy, and can help to facilitate the study of the mechanisms underlying the benefits of rehabilitation therapy alone and in combination with other drug and cell therapies.

Acknowledgements

This work was supported by operating grants from the Canadian Institute for Health Research (CIHR; 201109MOP-257493-MOV-CBAA-118384). K.K.F. was supported by CIHR and Alberta Innovates Health Solutions (AIHS) Post-Doctoral Fellowships. We thank Arthur Prochazka for allowing the use of his fabrication equipment and Michel Gauthier, Jacques Bobet, and Taylor Nelson for technical assistance.

References

1. F. Bretzner, J. Liu, E. Currie, A.J. Roskams, W. Tetzlaff, Undesired effects of a combinatorial treatment for spinal cord injury--transplantation of olfactory ensheathing cells and BDNF infusion to the red nucleus, Eur. J. Neurosci. 28 (2008) 1795–1807. doi:10.1111/j.1460-9568.2008.06462.x.

2. G. García-Alías, S. Barkhuysen, M. Buckle, J.W. Fawcett, Chondroitinase ABC treatment opens a window of opportunity for task-specific rehabilitation, Nat. Neurosci. 12 (2009) 1145–1151. doi:10.1038/nn.2377.

3. J. Girgis, D. Merrett, S. Kirkland, G. a. S. Metz, V. Verge, K. Fouad, Reaching training in rats with spinal cord injury promotes plasticity and task specific recovery, Brain J. Neurol. 130 (2007) 2993–3003. doi:10.1093/brain/awm245.

4. A. Krajacic, N. Weishaupt, J. Girgis, W. Tetzlaff, K. Fouad, Training-induced plasticity in rats with cervical spinal cord injury: effects and side effects, Behav. Brain Res. 214 (2010) 323–331. doi:10.1016/j.bbr.2010.05.053.

5. E.J. Prosser-Loose, A. Hassan, G.S. Mitchell, G.D. Muir, Delayed Intervention with Intermittent Hypoxia and Task Training Improves Forelimb Function in a Rat Model of Cervical Spinal Injury, J. Neurotrauma. (2015) 150507115350005. doi:10.1089/neu.2014.3789.

6. O. Raineteau, K. Fouad, P. Noth, M. Thallmair, M.E. Schwab, Functional switch between motor tracts in the presence of the mAb IN-1 in the adult rat, Proc. Natl. Acad. Sci. U. S. A. 98 (2001) 6929–6934. doi:10.1073/pnas.111165498.

7. F. Streijger, W.T. Plunet, J.H.T. Lee, J. Liu, C.K. Lam, S. Park, et al., Ketogenic diet improves

forelimb motor function after spinal cord injury in rodents, PloS One. 8 (2013) e78765. doi:10.1371/journal.pone.0078765.

8. M. Alaverdashvili, I.Q. Whishaw, Compensation aids skilled reaching in aging and in recovery from forelimb motor cortex stroke in the rat, Neuroscience. 167 (2010) 21–30. doi:10.1016/j.neuroscience.2010.02.001.

9. T.D. Farr, I.Q. Whishaw, Quantitative and qualitative impairments in skilled reaching in the mouse (Mus musculus) after a focal motor cortex stroke, Stroke J. Cereb. Circ. 33 (2002) 1869–1875.

10. C.L. MacLellan, S. Gyawali, F. Colbourne, Skilled reaching impairments follow intrastriatal hemorrhagic stroke in rats, Behav. Brain Res. 175 (2006) 82–89. doi:10.1016/j.bbr.2006.08.001.

11. G. Silasi, D.A. Hamilton, B. Kolb, Social instability blocks functional restitution following motor cortex stroke in rats, Behav. Brain Res. 188 (2008) 219–226. doi:10.1016/j.bbr.2007.10.030.

12. C.P. Montoya, L.J. Campbell-Hope, K.D. Pemberton, S.B. Dunnett, The “staircase test”: a measure of independent forelimb reaching and grasping abilities in rats, J. Neurosci. Methods. 36 (1991) 219–228.

13. I.Q. Whishaw, N.C. Woodward, E. Miklyaeva, S.M. Pellis, Analysis of limb use by control rats and unilateral DA-depleted rats in the Montoya staircase test: movements, impairments and compensatory strategies, Behav. Brain Res. 89 (1997) 167–177.

14. I.Q. Whishaw, W.T. O'Connor, S.B. Dunnett, The contributions of motor cortex, nigrostriatal dopamine and caudate-putamen to skilled forelimb use in the rat, Brain J. Neurol. 109 (Pt 5) (1986) 805–843.

15. S.A. Hays, N. Khodaparast, A.M. Sloan, D.R. Hulsey, M. Pantoja, A.D. Ruiz, et al., The isometric pull task: a novel automated method for quantifying forelimb force generation in rats, J. Neurosci. Methods. 212 (2013) 329–337. doi:10.1016/j.jneumeth.2012.11.007.

16. I.Q. Whishaw, S.M. Pellis, The structure of skilled forelimb reaching in the rat: a proximally driven movement with a single distal rotatory component, Behav. Brain Res. 41 (1990) 49–59.

17. K.L. Caudle, E.H. Brown, A. Shum-Siu, D.A. Burke, T.S.G. Magnuson, M.J. Voor, et al., Hindlimb immobilization in a wheelchair alters functional recovery following contusive spinal cord injury in the adult rat, Neurorehabil. Neural Repair. 25 (2011) 729–739. doi:10.1177/1545968311407519.

18. Y. Ishikawa, S. Imagama, T. Ohgomori, N. Ishiguro, K. Kadomatsu, A combination of keratan sulfate digestion and rehabilitation promotes anatomical plasticity after rat spinal cord injury, Neurosci. Lett. 593 (2015) 13–18. doi:10.1016/j.neulet.2015.03.015.

19. N. Weishaupt, S. Li, A. Di Pardo, S. Sipione, K. Fouad, Synergistic effects of BDNF and rehabilitative training on recovery after cervical spinal cord injury, Behav. Brain Res. 239 (2013) 31–42. doi:10.1016/j.bbr.2012.10.047.

20. K.K. Fenrich, Z. May, C. Hurd, C.E. Boychuk, J. Kowalczewski, D.J. Bennett, et al., Improved single pellet grasping using automated *ad libitum* full-time training robot,

Behav. Brain Res. 281C (2014) 137–148. doi:10.1016/j.bbr.2014.11.048.

21. C. Hurd, N. Weishaupt, K. Fouad, Anatomical correlates of recovery in single pellet reaching in spinal cord injured rats, Exp. Neurol. 247 (2013) 605–614. doi:10.1016/j.expneurol.2013.02.013.

22. Z. May, K. Fouad, A. Shum-Siu, D.S.K. Magnuson, Challenges of animal models in SCI research: Effects of pre-injury task-specific training in adult rats before lesion, Behav. Brain Res. (2015). doi:10.1016/j.bbr.2015.04.058.

23. I.Q. Whishaw, S.M. Pellis, B.P. Gorny, V.C. Pellis, The impairments in reaching and the movements of compensation in rats with motor cortex lesions: an endpoint, videorecording, and movement notation analysis, Behav. Brain Res. 42 (1991) 77–91.

24. C. Watson, ed., The spinal cord a Christopher and Dana Reeve Foundation text and atlas, Academic, London, 2009.

25. M. Küchler, K. Fouad, O. Weinmann, M.E. Schwab, O. Raineteau, Red nucleus projections to distinct motor neuron pools in the rat spinal cord, J. Comp. Neurol. 448 (2002) 349–359. doi:10.1002/cne.10259.

26. L.T. Brown, Rubrospinal projections in the rat, J. Comp. Neurol. 154 (1974) 169–187. doi:10.1002/cne.901540205.

27. N. Weishaupt, C. Hurd, D.Z. Wei, K. Fouad, Reticulospinal plasticity after cervical spinal cord injury in the rat involves withdrawal of projections below the injury, Exp. Neurol. 247 (2013) 241–249. doi:10.1016/j.expneurol.2013.05.003.

28. I.Q. Whishaw, B. Gorny, A. Foroud, J.A. Kleim, Long-Evans and Sprague-Dawley rats have similar skilled reaching success and limb representations in motor cortex but different movements: some cautionary insights into the selection of rat strains for neurobiological motor research, Behav. Brain Res. 145 (2003) 221–232.

29. M.J. Castro, D.F. Apple, R.S. Staron, G.E. Campos, G.A. Dudley, Influence of complete spinal cord injury on skeletal muscle within 6 mo of injury, J. Appl. Physiol. Bethesda Md 1985. 86 (1999) 350–358.

30. J.L. Olive, G.A. Dudley, K.K. McCully, Vascular remodeling after spinal cord injury, Med. Sci. Sports Exerc. 35 (2003) 901–907. doi:10.1249/01.MSS.0000069755.40046.96.

31. R.K. Shields, Fatigability, relaxation properties, and electromyographic responses of the human paralyzed soleus muscle, J. Neurophysiol. 73 (1995) 2195–2206.

32. R.J. Talmadge, M.J. Castro, D.F. Apple, G.A. Dudley, Phenotypic adaptations in human muscle fibers 6 and 24 wk after spinal cord injury, J. Appl. Physiol. Bethesda Md 1985. 92 (2002) 147–154. doi:10.1152/japplphysiol.000247.2001.

33. V. Dietz, S. Grillner, A. Trepp, M. Hubli, M. Bolliger, Changes in spinal reflex and locomotor activity after a complete spinal cord injury: a common mechanism?, Brain J. Neurol. 132 (2009) 2196–2205. doi:10.1093/brain/awp124.

34. V. Dietz, R. Müller, Degradation of neuronal function following a spinal cord injury: mechanisms and countermeasures, Brain J. Neurol. 127 (2004) 2221–2231. doi:10.1093/brain/awh255.

Figures

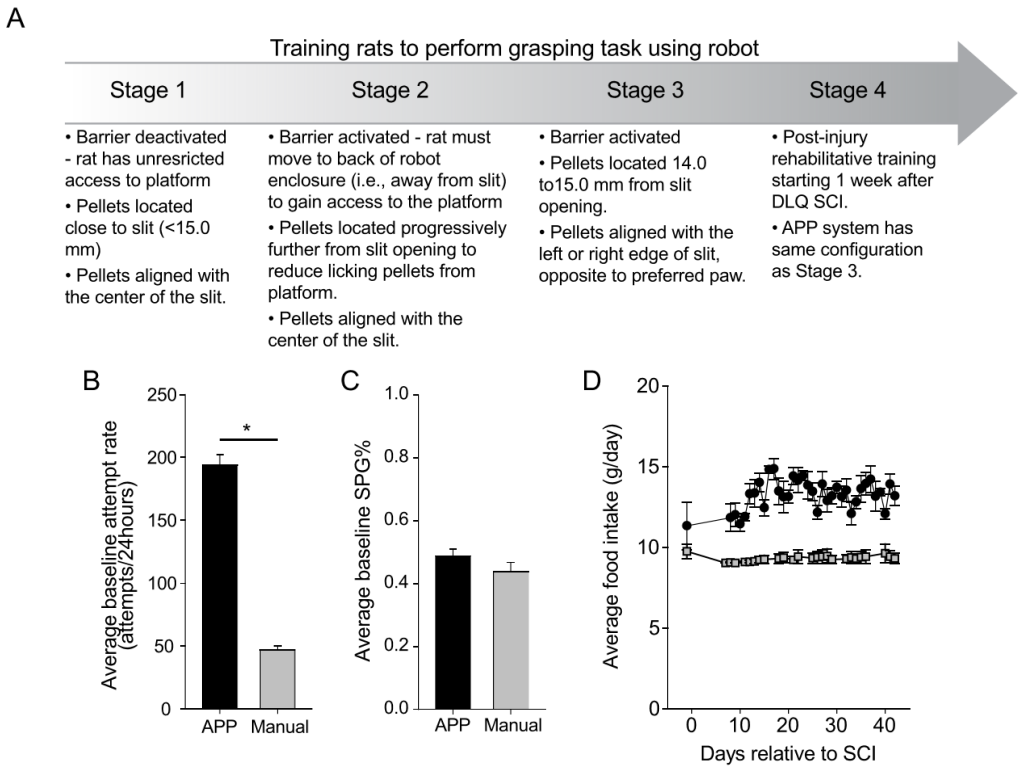

Figure 1. The APP system for automated continuous SPG training before and after SCI. (A) Time-line showing Stages 1–4 of training and setup of the APP system at each stage. (B, C) Bar graphs showing the baseline average number of attempts (B) and baseline average SPG% (C) per 24 h period for rats with APP training and rats with manual training. (D) Plots showing the average daily food consumed per animal immediately before SCI (arrow) and post-injury for rats with APP training (black circles) and rats with manual training (grey squares). *$p \leq 0.05$. Error bars represent the SEM.

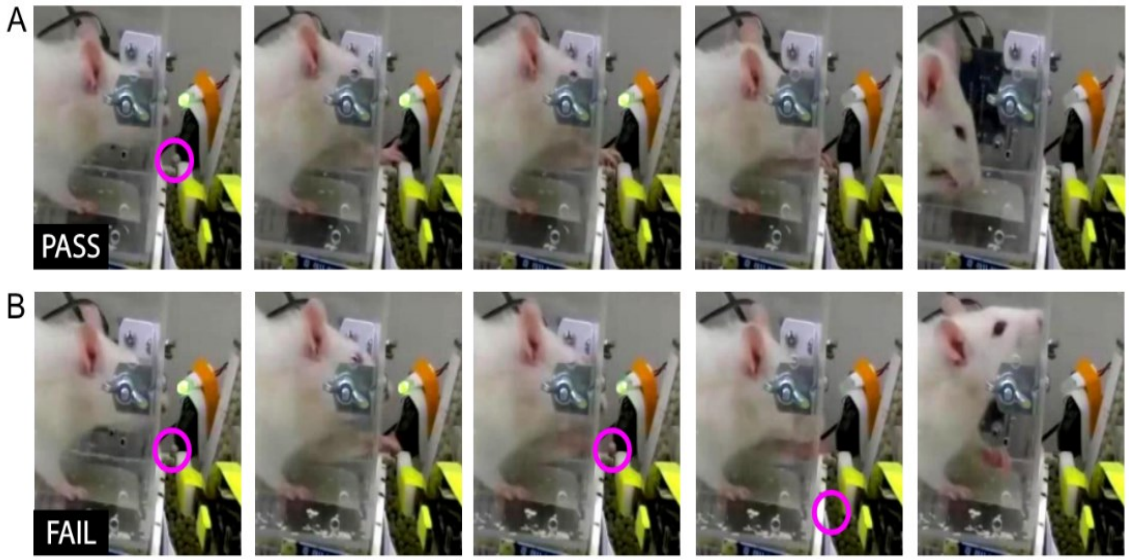

Figure 2. Trial evaluation with APP system. (A-B) Image sequences from analysis videos showing examples of a pass (A) and fail (B). Magenta circles in the first frames show pellet on pedestal before both the pass and fail attempts, and the circles in the third and fourth frame of B show the displaced pellet before it fell into the hopper following a failed attempt.

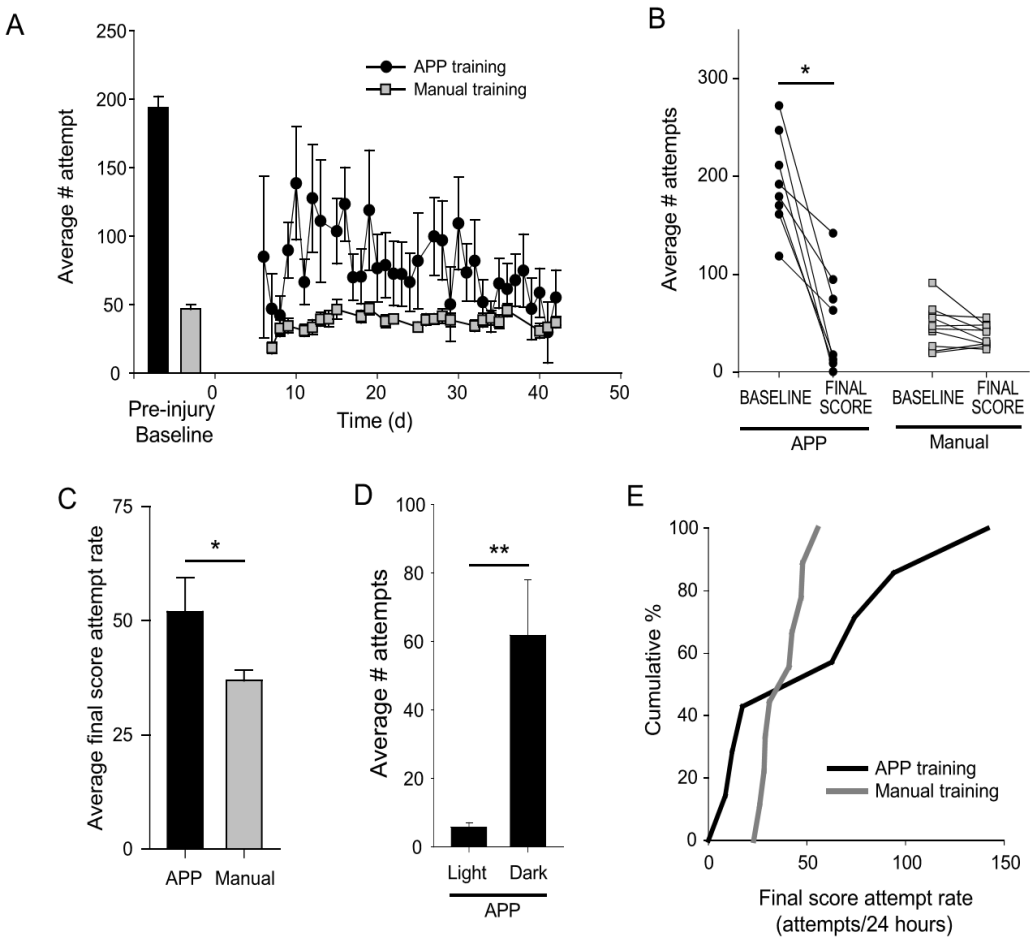

Figure 3. Attempt rates before and after injury. (A) Bar graphs and plots showing the average baseline attempt rates (bar graphs) and average daily post-injury attempt rates (plots) for rats with APP training and rats with manual training. (B) Plots showing baseline and final score attempt rates of individual rats with APP training and rats with manual training. (C) Bar graphs showing the average final score attempt rates for rats with APP training and rats with manual training. (D) Bar graphs showing the average number of attempts per light and dark cycle. (E) Plots showing the cumulative percentage of final score attempt rates for rats with APP training and rats with manual training. *$p \leq 0.05$, ** $p \leq 0.01$. Error bars represent the SEM.

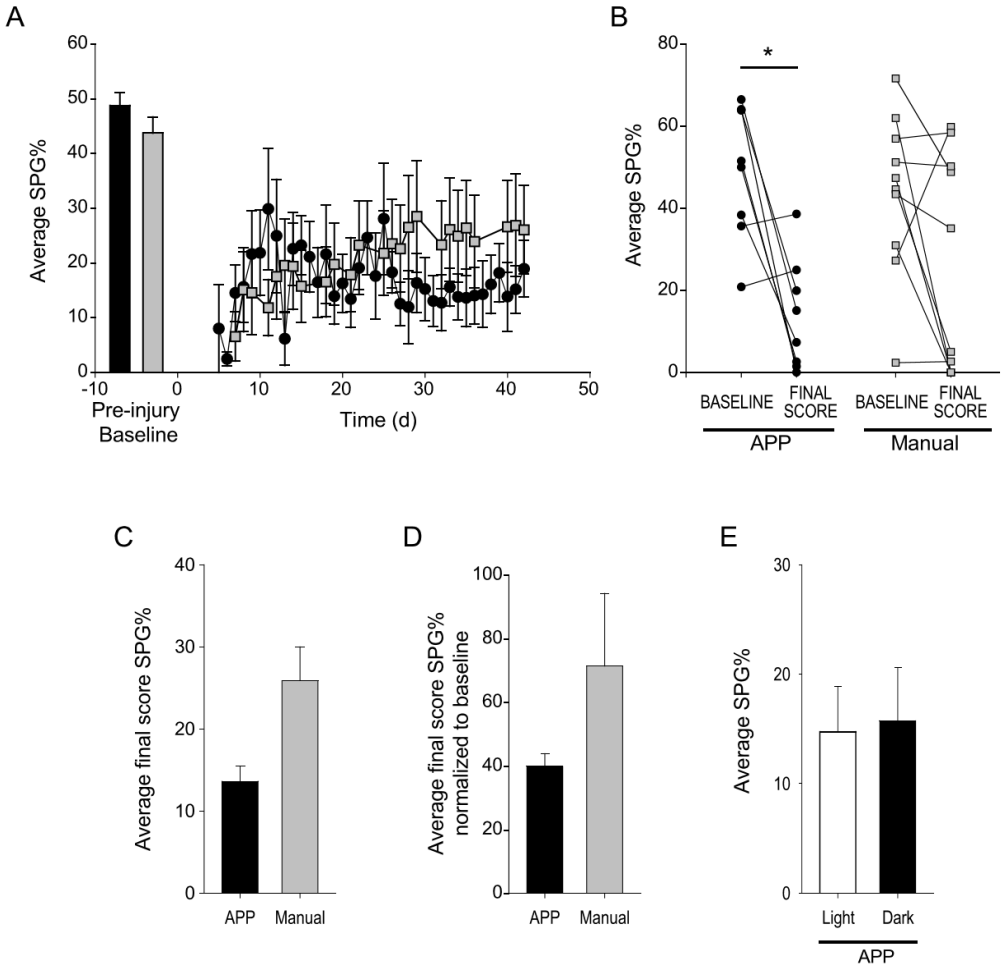

Figure 4. SPG success rates before and after injury. (A) Bar graphs and plots showing the average baseline SPG% (bar graphs) and average daily post-injury SPG% (plots) for rats with APP training and rats with manual training. (B) Plots showing baseline and final score SPG% of individual rats with APP training and rats with manual training. (C) Bar graphs showing the average final score SPG% for rats with APP training and rats with manual training. (D) Bar graphs showing the average final score SPG% normalized to baseline for rats with APP training and rats with manual training. (E) Bar graphs showing the average SPG% during the light and dark cycle. *$p \leq 0.05$. Error bars represent the SEM.

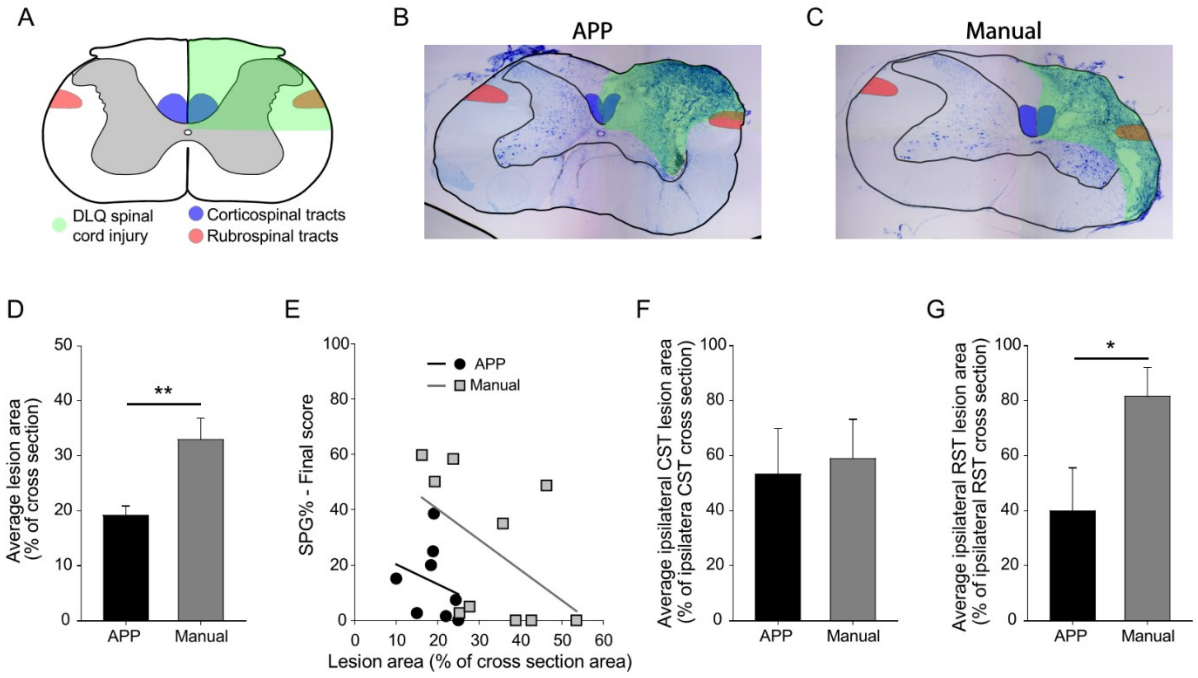

Figure 5. Lesion reconstruction. (A) Diagram of C4 cross section highlighting the intended location of the DLQ transections (pink), the corticospinal tracts (blue), and rubrospinal tracts (red). (B-C) Representative cresyl violet stained cervical (C4) cross sections demonstrating DLQ lesions from a rat with APP training (B) and a rat with manual training (C). Cross section and grey matter outlines shown with black lines, lesion site highlighted in green, estimated locations of CST highlighted in blue, and estimated locations of RST highlighted in red. Extent of CST and RST lesions in B were estimated as 100% and 50% respectively. Extent of CST and RST lesions in C were estimated as 100% and 100% respectively. (D) Bar graph showing the average lesion area at the lesion site as a percentage of total cross section area. (E) Scatterplots with linear-regression lines showing the average final score SPG% in relation to lesion area of rats with APP training and rats with manual training. (F) Bar graph showing the average ipsilateral CST lesion area as a percentage of total ipsilateral CST cross section area. (G) Bar graphs showing average ipsilateral RST cross section lesion area as a percentage of total ipsilateral cross section area. *$p \leq 0.05$, ** $p \leq 0.01$. Error bars represent the SEM.

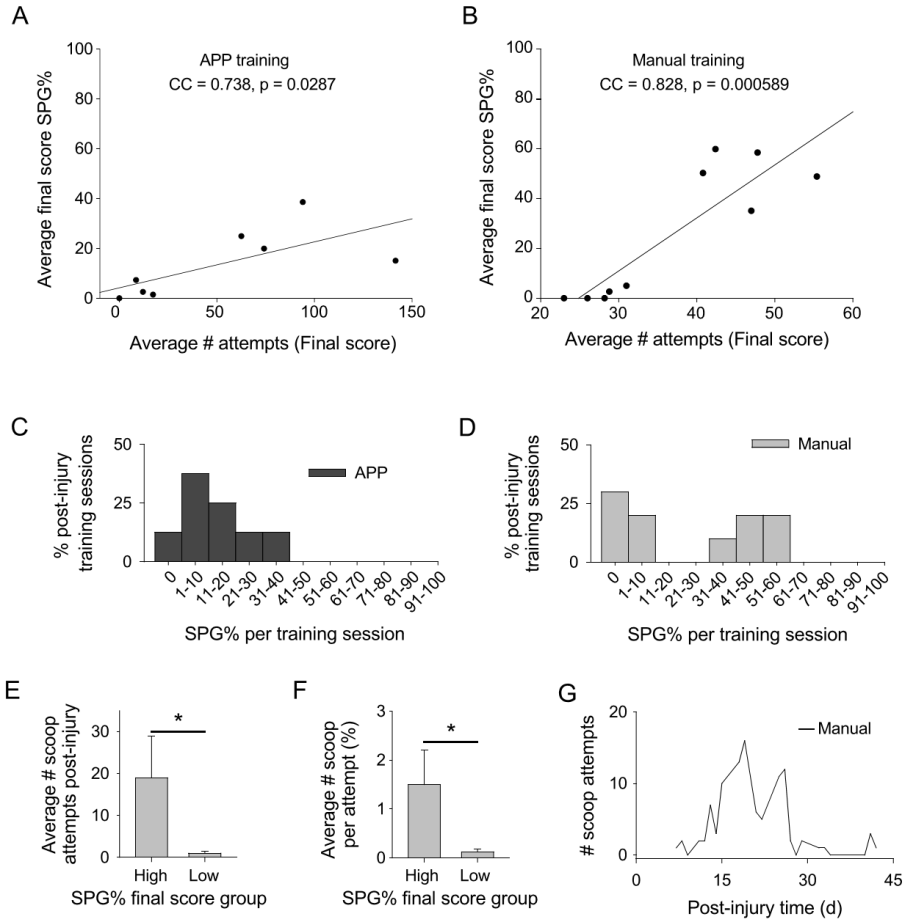

Figure 6. SPG performance and compensatory strategies. (A-B) Regression plots showing final score SPG% as a function of the average number of attempts per day in the last week of training for rats with APP (A) and manual training (B). (C-D) Bar graphs showing the percent of post-injury training sessions relative to the average SPG% per training session over the last week of training for rats with APP training (C) and rats with manual training (D). (E) Bar graphs showing the average number of scoop attempts per rat with manual training in the high-achiever group and low-achiever group. (F) Bar graphs showing the average number of scoop attempts as a percentage of total attempts per rat with manual training in the high-achiever group and low-achiever group. (G) Line plot showing the number of scoop attempts from the high-achiever rats with manual training relative to post-injury time. *$p \leq 0.05$. Error bars represent the SEM.

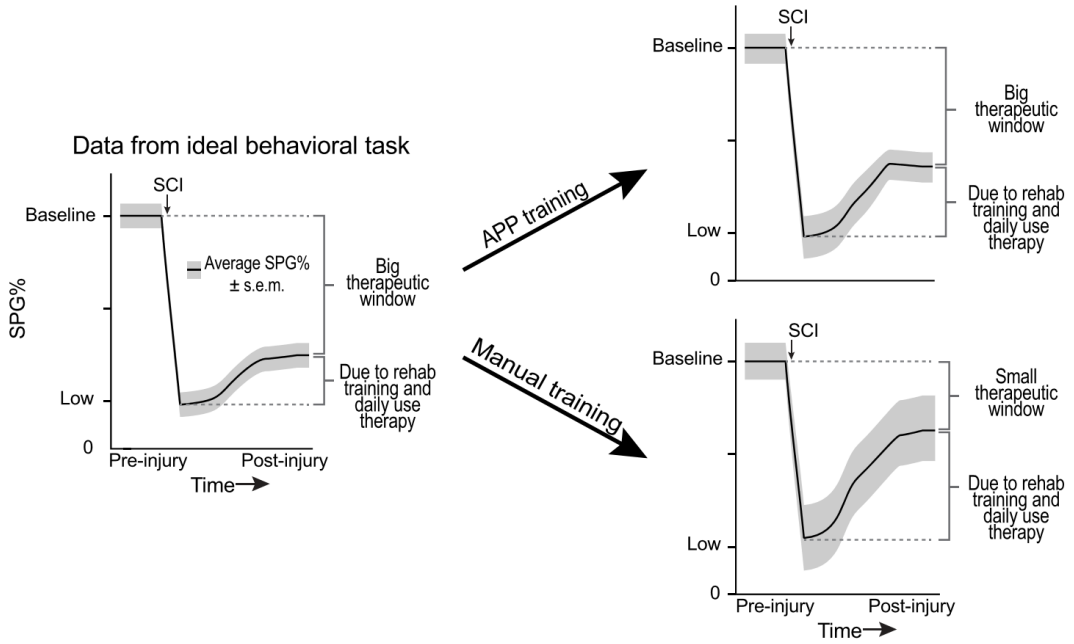

Figure 7. Schematic comparing performance of rats with APP training and rats with manual training to an idealized behavioral task. The average motor score and standard error of the mean are represented by black lines and the grey shaded areas, respectively, for both pre- and post-injury. The y-axis represents SPG% where up is a high score and down is a low score. The x-axis represents time before and after an SCI. In the ideal behavioral task there is a large drop in motor function after SCI, with a modest increase in motor function over time, thus resulting in a big therapeutic window. Our data suggest that rats with APP training have a considerable drop in SPG% after SCI followed by a modest increase in motor function over time resulting in a big therapeutic window. Conversely, rats with manual training have a similar drop in SPG% after SCI, but a more pronounced and highly variable recovery of motor function over time resulting in a comparatively small therapeutic window.